THE MOLECULAR AND CELLULAR IMPACT OF WAVE INTERACTIONS ON THE AGGRESSIVENESS OF PC-3 CELLS

by

Hoi Ping Weeks

Cardiff China Medical Research Collaborative

School of Medicine

Cardiff University

August 2014

Thesis submitted to Cardiff University for the degree of Doctor of Philosophy

Declaration

This work has not previously been accepted in substance for any degree and is not concurrently submitted in candidature for any degree.

Signed …… Date……

STATEMENT 1
This thesis is being submitted in partial fulfilment of the requirements for the degree of PhD.

Signed …… Date ……

STATEMENT 2
This thesis is the result of my own independent work/investigation, except where otherwise stated. Other sources are acknowledged by explicit references.

Signed …… Date ……

STATEMENT 3
I hereby give consent for my thesis, if accepted, to be available for photocopying and for interlibrary loan, and for the title and summary to be made available to outside organisations.

Signed …… Date ……

Dedication

I dedicate this PhD thesis to my loving grandmother.

Acknowledgements

My deepest gratitude goes to my two supervisors: Professor Wen Jiang and Professor Howard Kynaston for giving me the opportunity to pursue research with a focus towards bettering patient life. I am also extremely thankful to the Desna Robert Jones foundation for their financial funding that allowed this project to happen.

I have had the privilege of being affiliated with an incredibly hardworking research group who have encouraged me during my time there. My upmost thanks go to my mentor, Dr Andrew Sanders who throughout my time as a PhD student always found time to help me no matter how knees deep he was in helping other people. You are truly a master of problem solving and multi-tasking! I would also like to extend my sincerest thanks to Dr Tracey Martin, Dr Jane Lane, Dr Lin Ye, Fiona Ruge and all colleagues who have helped me incalculable times during my time at the institute. I am very grateful to Dr Jun Cai for proofreading my thesis and being very encouraging in the short time we have had the pleasure of knowing each other so far and Juliet Davies who has been seamless in helping me with all the administrative tasks that often get overlooked, I am so thankful. I consider myself extremely fortunate to have met so many lovely students and international fellows who have contributed to making my time at the institute an enjoyable and enriching experience.

I have never met a PhD student who has not been through the emotionally exhausting rollercoaster a doctorate entails. Whilst there are many ups, there are definitely more downs. Although my close friends and family may never understand how difficult these past few years have been for me, I am so thankful for their company and support.

Mum and dad, I hope I have made you incredibly proud. Your philosophy has always been that education is the most important thing someone can possess; no one can take knowledge away from you. I love you both very much.

To my mother-in-law, diolch yn fawr iawn for your warmth and kindness. To my father-in-law, I am exceptionally indebted to you for your boundless wisdom and inspiration.

I am and will always be eternally grateful to my beloved husband who always reminded me that there was light at the end of the tunnel. Thank you for your unconditional love and giving me the confidence to finish my PhD. You enrich my life. Dwi'n dy garu di.

Summary

The metastatic spread of cancer cells to distant sites in the body accounts for the majority of cancer-related death and significantly decreases patient survival. Whilst cell migration is a physiologically important process, when uncontrolled, it can be a contributing factor to the metastatic phenotype. Actin polymerisation enables the dynamic restructuring of the cytoskeleton which is fundamental to cell migration and is stimulated by the Arp (actin-related protein) 2/3 protein complex which in turn is activated by members of the WAVE (WASP Verprolin homologous protein) family.

WAVE1 and 3 expression was targeted separately in the PC-3 cell line utilising ribozyme transgene transfection. *In vitro* experiments revealed a reduction in cell growth and invasion following WAVE1 or 3 knockdown in PC-3 cells. These experiments were also repeated with small molecule inhibitors targeting the Arp2/3 complex, ROCK and N-WASP independently. This inhibitor work implicates Arp2/3 as a facilitator of cell proliferation through which WAVE regulates. Inhibition of Arp2/3, ROCK or N-WASP in WAVE1 knockdown cells increased cell invasion which may be attributed to the regulatory role of WAVE3 on MMP activity.

Co-localisation of WAVE1 and 3 with ARP2 and ROCK-I was observed in PC-3 cells whilst this affect was abolished with WAVE1 or 3 knockdown. Furthermore, WAVE3 and WAVE1 knockdown affected ARP2 and ROCK-II tyrosine phosphorylation, respectively.

These results suggest WAVE1 and 3 proteins are involved in several metastatic traits that characterise PC-3 cells. Furthermore, the contribution of WAVE in the networks that influence these traits may also involve association with Arp2/3 complex, ROCK-I and –II and N-WASP. Additionally, it sheds light on the similarities between these two related proteins and also highlights their subtle distinctions in PC-3 cells. The data outlined here provides justification to futher explore WAVE1 and 3 as potential contributors of prostate cancer progression.

Contents

List of Figures

Chapter 1:

Chapter 2:

Chapter 3:

Chapter 4:

Chapter 5:

Chapter 6:

List of Tables

Chapter 1:

Chapter 2:

Abbreviations

Abi - Abelson-interacting protein

ADF - Actin-depolymerizing factor

ADP - Adenosine diphosphate

ADT - Androgen deprivation therapy

APS - Ammonium Persulphate

ARF1 – ADP-ribosylation factor 1

Arp - Actin-related protein

ATP - Adenosine triphosphate

BP – Base pair

BPH - Benign prostatic hyperplasia

BRCA1- Breast cancer 1

BRCA2 - Breast cancer 2

BSA - Bovine serum albumin

BSS – Balanced salt solution

CAM - Cell adhesion molecules

Cdc2 - Cyclin-dependent kinase 1

CDC42 - Cell Division Cycle 42

Cdk5 - Cyclin-dependent kinase 5

cDNA – Complementary deoxyribonucleic acid

CRIB - Cdc42 and Rac interactive binding

CTC - Circulating tumour cells

CXCR4 - C-X-C chemokine receptor type 4

DEPC - Diethyl pyrocarbonate

DHT – Dihydrotestosterone

DMEM - Dulbecco's Modified Eagle's medium

DMSO - Dimethyl sulfoxide

DNA – Deoxyribonucleic acid

DRE - Digital rectal examination

DTT - Dithiothreitol

ECM - Extracellular matrix

EDTA - Ethylenediaminetetraacetic acid

EGF - Epidermal growth factor

EMT - Epithelial to mesenchymal transition

EVH1 - Drosphila enabled/VASP (vasodilator-stimulated phosphoprotein) homology 1

FAK – Focal adhesion kinase

GAP - GTPase activating proteins

GAPDH - Glyceraldehyde 3-phosphate dehydrogenase

GBD - GTPase binding domain

GDI - Guanine nucleotide dissociation inhibitors

GDP - Guanosine diphosphate

GEF - Guanine nucleotide exchange factor

GRB2 – Growth factor receptor-bound protein 2

GTP - Guanosine triphosphate

GTPase - Guanosine triphosphatase

GWAS - Genome wide association studies

HER2 - Human epidermal growth factor receptor 2

HIF-1 - Hypoxia-inducible factor-1

HPC1 - Hereditary prostate cancer 1

HSC - Haematopoietic stem cells

IGF-IR - Insulin-like growth factor type 1 receptor

IgSF - Immunoglobin superfamily

IRSp53 - Insulin receptor substrate p53

KCl – Potassium chloride

kDa – Kilodalton

KH_2PO_4 - Monopotassium phosphate

LB – Luria-Bertani

LDOC1 - Leucine Zipper, Down Regulated in Cancer 1

LHRH - Luteinising hormone releasing hormone

LIMK – LIM domain kinase

M - Molar

MAPK - Mitogen-activated protein kinase

MET - Mesenchymal-to-epithelial transition

Mg – Milli gram

$MgCl_2$ - Magnesium chloride

$MgSO_4$ – Magnesium sulphate

mL – Milli litre

mM – Milli molar

MMP - Matrix metalloproteinases

MRI - Magnetic Resonance Imaging

mRNA – Messenger RNA

Na_2HPO_4 - Disodium phosphate

NaCl – Sodium chloride

$NaHCO_3$ - Sodium bicarbonate

Nap1 – Nucleosome assembly protein 1

NP-40 - Nonidet P-40

NPF - Nucleation promoting factor

N-WASP – Neural-Wiskott-Alrich Syndrome Protein

PAK1 - p21-activated kinase 1

PAP - Prostatic acid phosphatase

PCR – Polymerase chain reaction

PDPN - Podoplanin

PIN - Prostatic intraepithelial neoplasia

PIP_2 - Phosphatidylinositol 4,5-bisphosphate

PIP_3 - Phosphatidylinositol (3,4,5)-trisphosphate

PMSF - Phenylmethanesulphonylfluoride

PS-1/γ – Presenilin 1

PSA - Prostate specific antigen

PSTPIP - Proline-serine-threonine phosphatase interacting protein

PTEN - Phosphatase and tensin homolog

QPCR – Quantitative polymerase chain reaction

Rac - Ras-related C3 botulinum toxin substrate 1

RhoA - Ras homolog gene family, member A

RNA - Ribonucleic acid

RNASEL – Ribonuclease L

ROCK - Rho-associated protein kinase

RPM – Revolutions per minute

RT-PCR – Reverse transcription polymerase chain reaction

SCAR - Suppressor of cAR

SDF-1 - Stromal cell-derived factor 1

SDS - Sodium dodecyl sulphate

SDS-PAGE - Sodium dodecyl sulphate polyacrylamide gel electrophoresis

SH3 - Src homology 3

SHD - SCAR homology domain

SNP - Single nucleotide polymorphisms

Sra1 – Steroid Receptor RNA Activator 1

SRD5A1 - Steroid-5-alpha-reductase 1

SRD5A2 - Steroid-5-alpha-reductase 2

TBE - Tris, Boric acid, EDTA

TBS – Tris-Buffered Saline

TIMP - tissue inhibitors of metalloproteinases

TNM - Tumour Node Metastasis

TRUS - Transrectal ultrasound

uPA - Urokinase-type plasminogen activator

uPAR - Urokinase-type plasminogen activator receptor

VEGF - Vascular endothelial growth factors

VPH - Verprolin-homology domain

WAS - Wiskott-Alrich syndrome

WASP - Wiskott-Alrich Syndrome Protein

WAVE - WASP verprolin homologous protein

WH1 - WASP homology 1

WH2 - WASP homology 2

WHD - WAVE homology domain

WIP - WASP-interacting protein

WISH - WASP-interacting SH3 protein

WRC – WAVE regulatory complex

WT – Wild type

Chapter 1

Introduction

1.1 Prostate cancer epidemiology

1.1.1 Prostate cancer incidence and mortality in the UK

Cancer of the prostate has long been recognised as a significant public health issue and is one of the major cancers to affect males worldwide (Globocan, 2012). Statistics from 2011 reported prostate cancer as the most prevalent cancer affecting men in the UK which accounted for approximately a quarter of all new male cancer diagnoses. There were 41,736 new prostate cancer cases recorded, followed by lung and bowel cancers which were the second and third most common male cancers with 23,770 and 23,171 cases, respectively (Cancer Research UK, 2014). However, prostate cancer mortality was responsible for only 13% of male cancer deaths making it the second most common cause of cancer death after lung cancer in the UK. In 2011, there were 10,793 prostate cancer related deaths in the UK (Cancer Research UK, 2014).

A strong correlation exists between incidence rates of prostate cancer and age. The mean age of patients at diagnosis with prostate cancer is 72-74 years (Gröenberg., 2003). Approximately three-quarters of prostate cancer cases are diagnosed in men aged 65 years and over with very few diagnoses made in men younger than 50 years old (Cancer Research UK, 2014) (Figure 1.1).

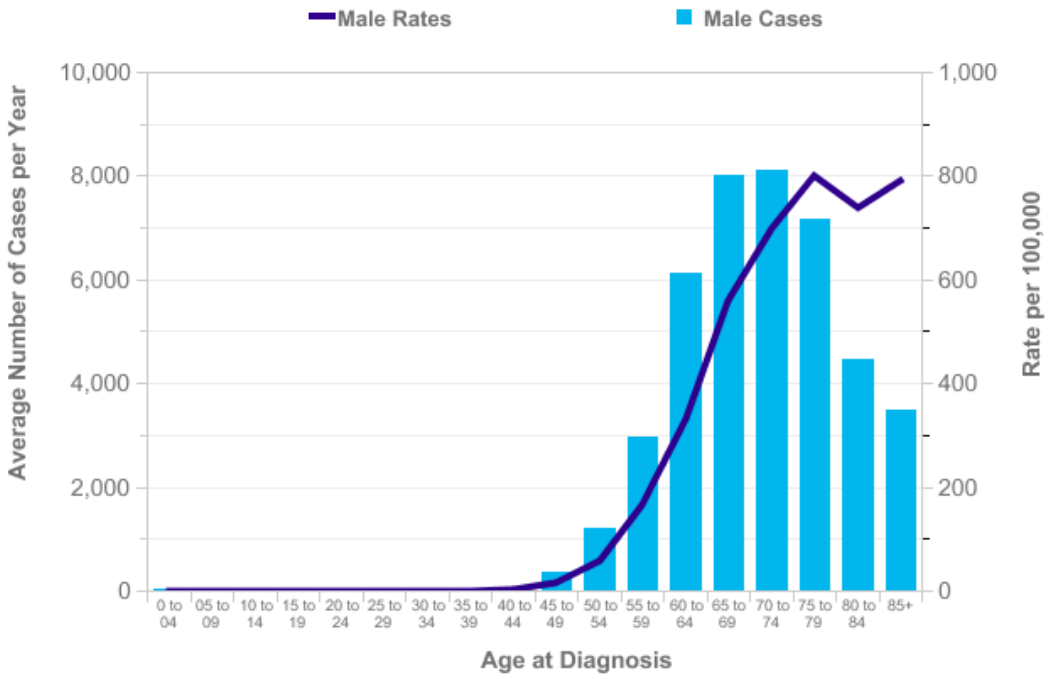

Figure 1.1 Relationship between prostate cancer incidence and age (Figure taken from Cancer Research UK, 2014)

Similarly, affected individuals show a strong trend of increased mortality with increasing age. Between 2009 and 2011 in the UK, affected individuals aged 65 years or older accounted for around 93% of all prostate cancer related deaths (Figure 1.2). Men beyond 85 years, have the highest number of prostate cancer deaths with 775 per 100,000 compared to 396.4 per 100,000 for the 80 to 84 year age group. Interestingly, an overwhelming majority of affected males are likely to die with, rather than as a result of prostate cancer (Kessler and Albertson., 2003). Nonetheless, it is evident that age is an important factor to consider when evaluating prostate cancer risk.

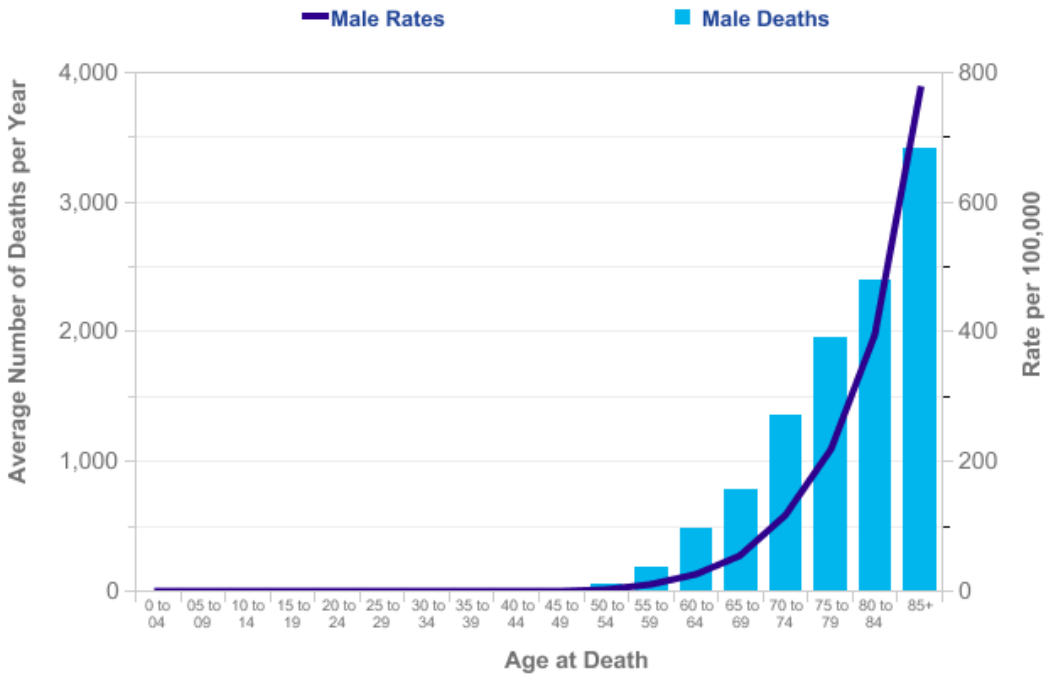

Figure 1.2 Relationship between prostate cancer mortality rates and age (Figure taken from Cancer Research UK, 2014)

1.1.2 Incidence within ethnic groups and geographical populations

The incidence of prostate cancer varies greatly when comparing different ethnic groups and geographical populations. Some of the lowest rates of disease are seen in Asia, for instance, 1.9 in 100,000 men per year in males from Tianjin in China are affected (Grönberg., 2003). In contrast, the highest rates are in North America and Scandinavia. Between 2004 and 2008, African-American males had a significantly higher incidence of the disease with 233.3 per 100,000 males per year compared to 149.5 per 100,000 in their white counterparts (DeChello *et al*., 2006; Quinn and Babb., 2002). Furthermore, these two ethnic groups have dissimilar aetiology and disease course/prognosis (Powell., 1998).

Multiple reasons have been put forward to explain the differences seen in incidence rates across different populations and ethnic groups. The fact that higher incidence rates are recorded in North America, Northern and Western Europe and Australia/New Zealand is largely attributed to a growing awareness of prostate cancer and the widespread availability of diagnostic procedures such as serum prostate specific antigen (PSA) testing and prostate biopsies (Potosky *et al*., 1995). Over two-thirds of registered prostate cancer cases in 2012 occurred in developed countries (Globocan, 2012). Even so, prostate cancer incidence rates are increasing in both high-risk and low-risk countries (Gröenberg., 2003).

1.1.3 Risk factors

1.1.3.1 Diet

Ethnic and geographical trends in prostate cancer incidence suggest numerous environmental and genetic factors may be responsible for the differences observed. Migration studies have demonstrated that when Japanese men emigrate from their native country, a region of low incidence, to North America, a country with a high incidence, prostate cancer frequency in this group of individuals is seen to increase. Despite this, the rate does not increase to even half of the levels seen for North Americans. These findings demonstrate a strong environmental impact on the disease but also an underlying genetic influence (Shimizu H *et al.*, 1991; Tominaga., 1985).

There is conflicting evidence regarding links between diet and cancer. However, there appears to be an increasing association between a diet comprising of higher levels of fat, meat and dairy products, characteristic of a Western lifestyle, with higher incidences of prostate cancer (Armstrong and Doll., 1975). In contrast, East-Asian populations report lower incidences of prostate cancer. In these regions, diets rich in isoflavones in soy and polyphenols in green tea, in addition to being low in red meat and dietary fat has been implicated as a preventative factor (Kim *et al*., 2008; Khan *et al*., 2009; Sim *et al*., 2005).

It has been suggested that selenium and vitamin E have potential preventative effects against prostate cancer, although many reports are conflicting (Venkateswaran and Klotz., 2010). However, the SELECT clinical trial reported that neither selenium nor vitamin E reduced the incidence of prostate cancer and that vitamin E was associated with a 17% increased prostate cancer risk compared to placebo (Nicastro and Dunn., 2013).

1.1.3.2 Genetic factors

A predisposition to prostate cancer has been linked to numerous genetic factors. Regardless of ethnicity, the risk of developing the disease is likely to increase two to three-fold if a first-degree relative is already affected. This risk increases with the number of affected relatives particularly when diagnosis is at a younger age (Whittemore *et al.*, 1995). Interestingly, males with an affected brother are more likely to develop prostate cancer than individuals with an affected father which may imply a recessive inheritance pattern or that it is X-chromosome linked (Monroe *et al*., 1995).

Genome-wide linkage studies have enabled the identification of susceptibility loci for prostate cancer. The disease was first mapped to the *Hereditary prostate cancer 1* (*HPC1*) locus in 1996 in a study examining high-risk families from Sweden and the USA (Smith *et al.*, 1996). Within the *HPC1* loci lies the *RNASEL* gene which has been proposed as a potential candidate gene, increasing the risk of developing prostate cancer. This gene is involved in the interferon-regulated 2-5A pathway and is implicated as a tumour suppressor gene due to its role in the regulation of cell proliferation and apoptosis (Liang *et al.*, 2006). Despite this, very few cases of familial prostate cancer have been linked to mutations in the *RNASEL* gene (Carpten *et al.*, 2002).

A comparison of gene expression profiles between African-American and Caucasian-American men revealed a significant number of genes showing differential expression between the two ethnic groups. Several metastasis-promoting genes were found to be expressed at higher levels in tumours from African-American relative to Caucasian-American patients (Wallace *et al.*, 2008).

Allelic differences in the *SRD5A1* and *2* genes which encode the 5α-reductase isoform 1 and 2, respectively, have shown interesting ethnic variation with some single nucleotide polymorphisms (SNPs) linked to prostate cancer risk (Makridakis *et al.*, 1999; Setlur *et al.*, 2010). These 5α-reductase enzymes are responsible for catalysing the conversion of testosterone to its active metabolite, dihydrotestosterone. This is essential for the development of the prostate gland and prostate cell growth but also necessary for the continued survival and growth of prostate cancer cells (Roy and Chaterjee., 1995).

Genome wide association studies (GWAS) have also identified numerous susceptibility loci associated with prostate cancer. Many of these SNPs are involved in the testosterone synthesis pathway and are found in regions which may hold potential clinical implications relevant to prostate cancer. These include a SNP found at a chromosomal location close to the *C-MYC* oncogene and another found upstream of microseminoprotein-β, a protein commonly found at lower levels in prostate cancer (Schkeutker., 2012; Goh *et al.*, 2012). Other deleterious genetic changes identified include germline mutations in the genes *BRCA1* and *BRCA2* (Castro and Eeles., 2012). These genetic variants have been associated with advanced prostate cancer with a poor prognosis.

1.2 Prostate biology

The human prostate is a walnut sized gland found solely in the male reproductive system. It surrounds the urethra proximal to the urinary bladder (prostatic urethra) and is anterior to the rectum. The prostate secretes a thick white alkaline fluid which comprises approximately a third of semen ejaculate that functions to neutralise the acidic environment in the female vagina and in turn protects and nourishes the sperm. This prostatic secretion also contains the enzyme prostate specific antigen (PSA) whose role is to liquefy semen to facilitate sperm motility in the vagina.

The prostate can be divided into four distinct glandular zones based on anatomic region, histologic appearance and disease susceptibility (refer to Figure 1.3). The central zone is a cone shaped region that surrounds the ejaculatory ducts extending from the seminal vesicle ducts and vas deferens to the verumontanum of the prostatic urethra. The peripheral zone, comprising approximately 70% of prostatic tissue, is located posterolaterally and surrounds the central zone and distal portion of the prostate urethra. This region houses the majority of prostatic glandular tissue where ducts secrete into the prostatic urethra. This zone, which comprises the greatest volume of the prostate, is also where the majority of prostate carcinomas originate (60-70%). The proximal urethra is surrounded by the transition zone which is found between the verumontanum and bladder (McNeal., 1988). Throughout life, this region enlarges and is responsible for benign prostatic hyperplasia which can obstruct the urethra and interfere with normal urine flow; a problem commonly seen in older men. Lastly, the anterior fibromuscular zone typically lacks glandular tissue and consists mainly of muscle and fibrous tissue.

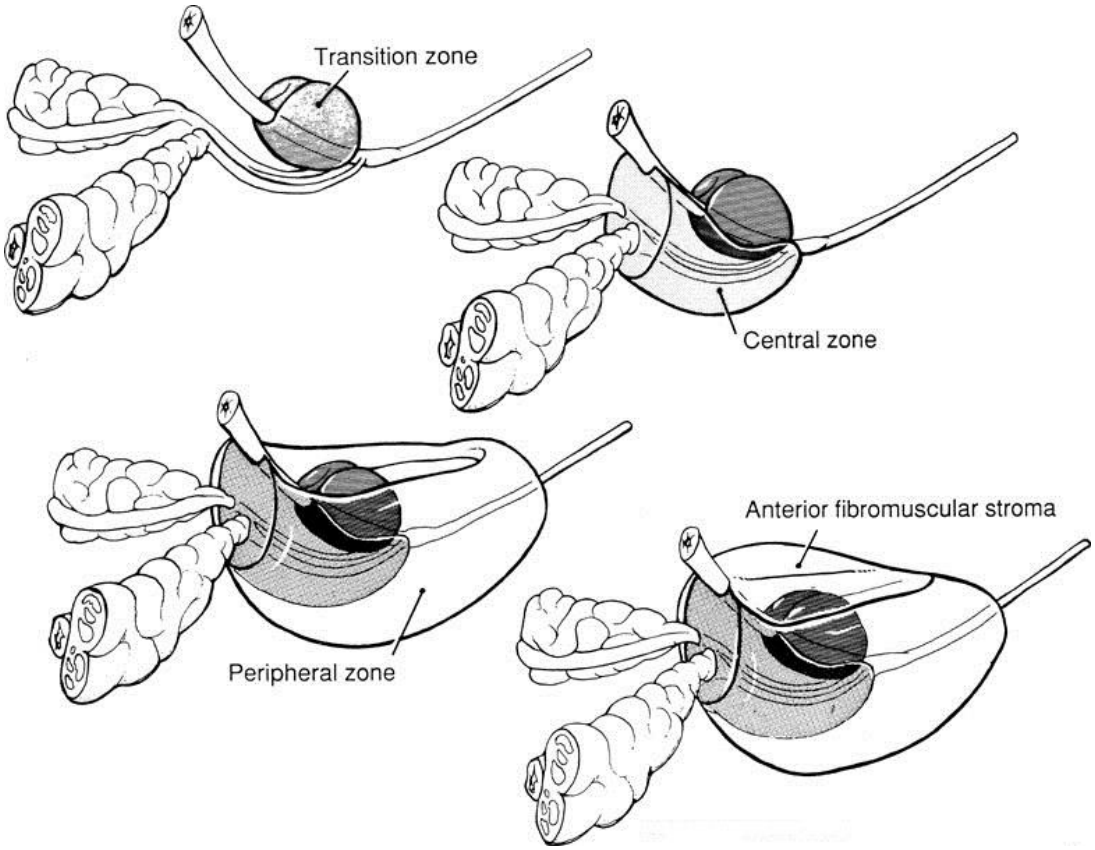

Figure 1.3 Anatomy of the prostate gland and the four main zones (Figure taken from Baylor College of Medicine, 1990).

Histologically, the human prostate contains pseudostratified epithelium which is comprised mainly of main differentiated cell populations (Schalken and van Leenders., 2003). The luminal epithelial cells form a continuous layer of polarised columnar cells and are responsible for protein secretions such as prostate specific antigen (PSA) and prostatic acid phosphatase (PAP) (McNeal., 1988). The basal cells are adhered to the basement membrane and located beneath the luminal epithelium.

The majority of prostate cancers are pathologically classified as adenocarcinomas (approximately 95%) and exhibit a luminal phenotype (Shen and Abate-Shen., 2010). Other subtypes of prostate cancer include: ductal carcinoma, mucinous carcinoma, signet ring carcinoma, neuroendocrine carcinoma and small cell carcinoma. It is widely accepted that adenocarcinoma of the prostate is preceded by prostatic intraepithelial neoplasia (PIN). At the histological level, PIN is characterised by the appearance of luminal epithelial hyperplasia, reduction in basal cells, enlargement of nuclei and nucleoli, cytoplasmic hyperchromasia and nuclear atypia (Shen and Abate-Shen., 2010). Even so, whether PIN is a true precursor of prostatic carcinoma is widely debated (DeMarzo *et al*., 2003). The metastatic progression of normal epithelium to adenocarcinoma in prostate cancer is shown in Figure 1.4.

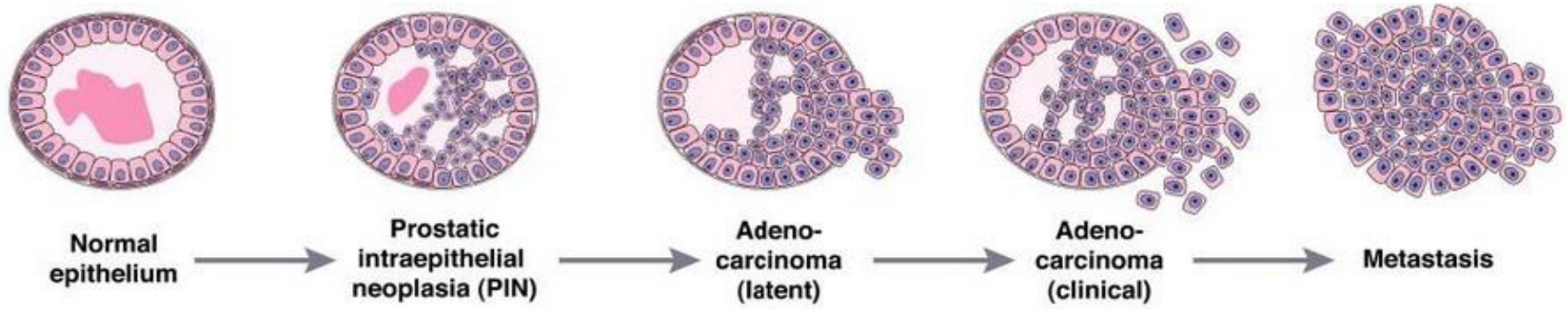

Figure 1.4 Prostate cancer progression at the histological level (Figure taken from Shen and Abate-Shen., 2010)

1.3 Detection and staging of prostate cancer

Prostate cancer is the most commonly diagnosed cancer in men in the UK. Being able to clearly determine disease progression for each individual is a major problem for prostate cancer management. Detection of prostate cancer in the early stages is crucial due to the well-known aggressive nature of the disease. Patients with symptoms such as haematuria (blood in urine) and pain in the bones usually indicate advanced prostate cancer and it is important to diagnose these patients and identify the best approach to treat the disease. Accurate staging of prostate cancer in affected individuals allows correct prognosis assessment and individualisation of treatment options.

1.3.1 Prostate cancer detection

1.3.1.1 Prostate specific antigen (PSA) testing

Prostate specific antigen (PSA) is a glycoprotein serine protease secreted by the epithelial cells of the prostate gland. It is present in small quantities in the serum of men with normal prostates but is usually elevated in men affected by prostate cancer (Haythorn and Ablin., 2001).

Screening PSA levels is a common clinical procedure and is relatively easy to conduct. PSA testing is a non-invasive blood test resulting in minimal patient discomfort relative to other detection methods available. PSA level thresholds are age-dependent: 2.5ng/ml for 40-49 years, 3.5ng/ml for 50-59 years, 4.5ng/ml for 60-69 years and 6.5 ng/ml for 70-79 years (Oesterling *et al.*, 1993; Prostate Cancer Risk Management Programme, 2013). These thresholds generally suggest an increased

risk of prostate cancer, whereas levels above 10ng/ml potentially indicate more advanced prostate cancer with possible metastasis (Schulz *et al.*, 2003). Despite being one of the most common methods to test for prostate cancer, its reliability is still a focus for debate and controversy. PSA is not a prostate cancer-specific biomarker as a high serum PSA level does not necessarily indicate a higher risk or aggressiveness of prostate cancer but can be attributed to an increase in prostate size as seen in non-malignant prostate diseases such as benign prostatic hyperplasia (BPH). In such cases, high serum PSA level can lead to a false positive result which may lead to unnecessary follow up tests (Ablin., 1997).

1.3.1.2 Digital rectal examination (DRE)

Digital rectal examination (DRE) was the first established method for detecting prostate cancer. This method involves the insertion of a gloved finger into the rectum to examine the prostate for any lumps or nodules. Due to the crude nature of this clinical procedure, it is limited in its ability to detect all prostate cancers as its accessibility is restricted to the area of the prostate most adjacent to the rectum (Spigelman *et al.,* 1986). In addition to this method being invasive to the patient, there is the possibility that any suspicious lumps detected via DRE could be aggressive cancers with the potential to metastasise. In these cases, therapeutic approaches are unlikely to be successful (Scardino *et al.,* 1992).

1.3.1.3 Transrectal ultrasound (TRUS)

Transrectal ultrasound (TRUS) is used to visualise and target prostate biopsies via an ultrasound probe inserted into the patient's rectum. Patients with an elevated level of PSA generally undergo TRUS guided prostate biopsies to confirm the diagnosis. An ultrasound image is created of the internal architecture of the prostate gland where any regions harbouring potential cancer abnormalities can be identified; doing so enables guided biopsies to be performed on these problematic areas. Despite the common use of this method, abnormal looking regions picked up via ultrasound imaging which could correlate to cancerous zones can in fact result from benign pathologies such as benign prostatic enlargement nodules. On the contrary, images which appear normal may actually be harbouring malignancies (Narain *et al*., 2002). To enable a thorough examination of the patient's prostate, it is important that biopsies are obtained from areas having both abnormal and normal appearance in a systematic manner with a recommendation that ten to twelve cores be obtained (National Institute of Health and Care Excellence guidelines CG175, 2014).

1.3.1.4 Magnetic Resonance Imaging (MRI)

Despite the plethora of detection options available for the patient, approaches such as PSA screening and random prostate gland biopsies often diagnose the patient with indolent or low-grade cancers that may remain asymptomatic. The use of Magnetic Resonance Imaging (MRI) has greatly improved the detection and staging of localised prostate cancer as well as metastases to distant sites in the body (Turkbey *et al.,* 2013). MRI is best suited for prostate cancer patients who are deemed at a high-risk of developing metastases, especially for bone metastases (Lecouvet *et al.,* 2007).

1.3.2 Prostate cancer staging

1.3.2.1 Tumour Node Metastasis (TNM) staging system

The TNM staging system considers the primary tumour (T), lymph node status (N) and metastasis (M) in order to stage the prostate cancer. It is the most widely used and accepted staging system at present which is regularly updated and revised (American Joint Committee on Cancer, 2009). However, there remains controversy and doubt over its application to predict disease progression and correct treatment selection. Despite lymph node status being used as an important prognostic factor, when using the TNM staging system in prostate cancer, clinical outcomes of patients with positive lymph nodes are highly variable (Adams and Cheng., 2011). A variety of physical examinations, imaging techniques, laboratory tests and pathology analyses allow the classification of each component in TNM staging which are described in Table 1.1 and Figures 1.5 and 1.6.

Table 1.1 The TNM staging system of the prostate (adapted from Borley *et al*., 2009)

Stage	Characterisation
Primary tumour (T)	
TX	Primary tumour cannot be assessed
T0	Primary tumour not evident
T1	Tumour clinically inapparent, not palpable or visible by imaging
T1a	Tumour (non-palpable) as incidental histological finding at transurethral resection of prostate in 5% tissue resected
T1b	Tumour (non-palpable) as incidental histological finding at transurethral resection of prostate in >5% tissue resected
T1c	Tumour (non-palpable) identified by needle biopsy (for elevated serum PSA) includes bilateral non-palpable tumour on needle biopsy
T2	Tumour confined within prostate (including prostatic apex and prostatic capsule) that is either palpable or visible on imaging, or (p-prefix) demonstrated in radical prostatectomy specimen
T2a	Tumour involving one-half of one lobe or less
T2b	Tumour involving more than one-half of one lobe or less
T2c	Tumour involving both lobes
T3	Tumour extends through prostatic capsule
T3a	Extra-capsular extension (ECE)
T3b	Invasion of seminal vesicle(s)
T4	Tumour fixed, or invades adjacent structures: bladder neck, external sphincter, rectum, levator muscles, and pelvic wall
Lymph nodes (N)	
NX	Regional lymph nodes cannot be assessed
N0	No regional lymph node metastases
N1	Regional lymph node metastases within true pelvis, below common iliac artery bifurcation, either unilateral or bilateral
Metastases (M)	
MX	Distant metastases cannot be assessed
M0	No distant metastases
M1a	Non-regional lymph node metastasis
M1b	Metastasis to bone(s)
M1c	Metastasis to other site(s)

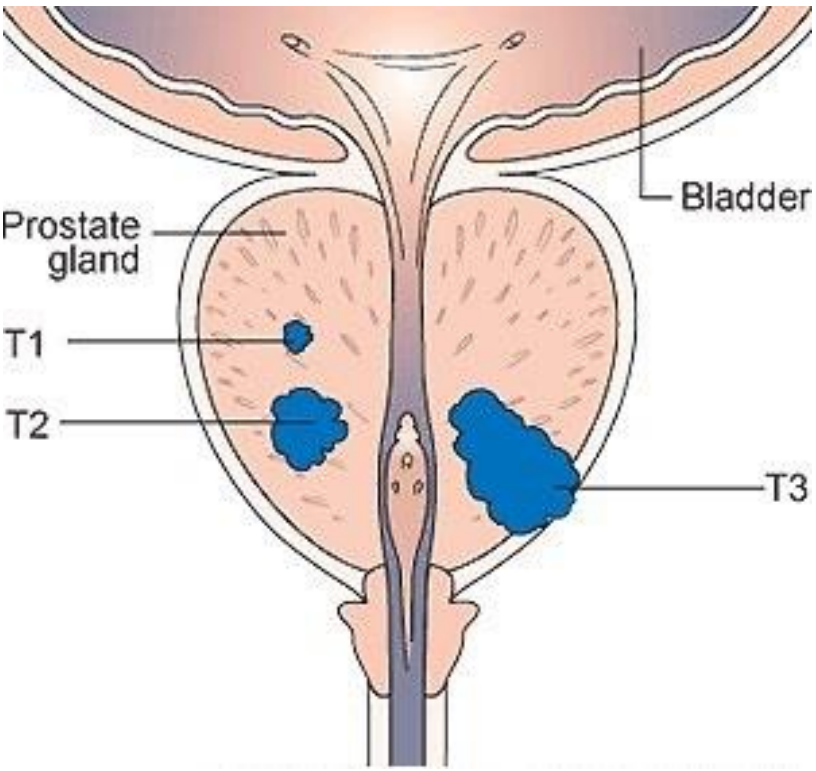

Figure 1.5 Coronal section through the prostate depicting stages T1-3 of prostate cancer (Image taken from Cancer Research UK).

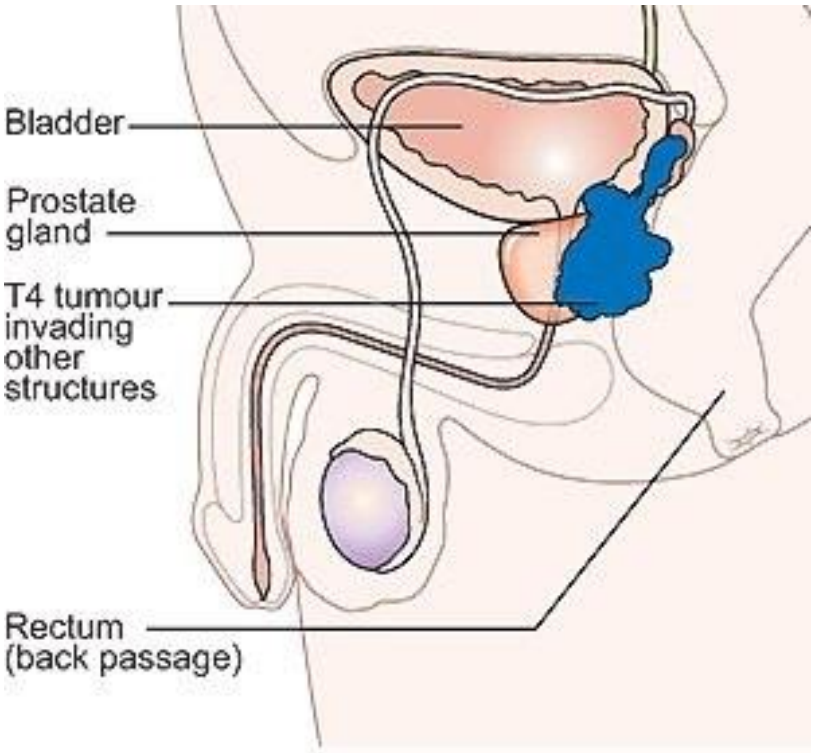

Figure 1.6 Sagittal cross section through the prostate depicting stages T3-4 of prostate cancer (Image taken from Cancer Research UK).

1.3.2.2 Gleason grading system

The Gleason grading system is used in conjunction with the TNM staging system to give a histological grade of prostate cancer status which also assists with prognosis. This platform for classification is based on the histological status of prostate cells to describe their distribution and growth patterns in prostatic sections, acquired from prostate biopsies or the whole organ, subsequent to radical prostatectomy. Following histological examination, the most common pattern discerned is assigned a score whilst the second most common pattern observed is assigned another. The sum of these two scores comprises the overall Gleason score given to the prostate cancer (Gleason, and Mellinger., 1974). A higher Gleason score is normally attributed to cancers exhibiting a more aggressive phenotype and poorer prognosis. An overall Gleason score of 6 or less is considered low risk; a score of 7 is regarded as moderate whilst a high grade Gleason score of 8 or above is deemed high risk. A comprehensive description of each score is given in Table 1.2 and Figure 1.7.

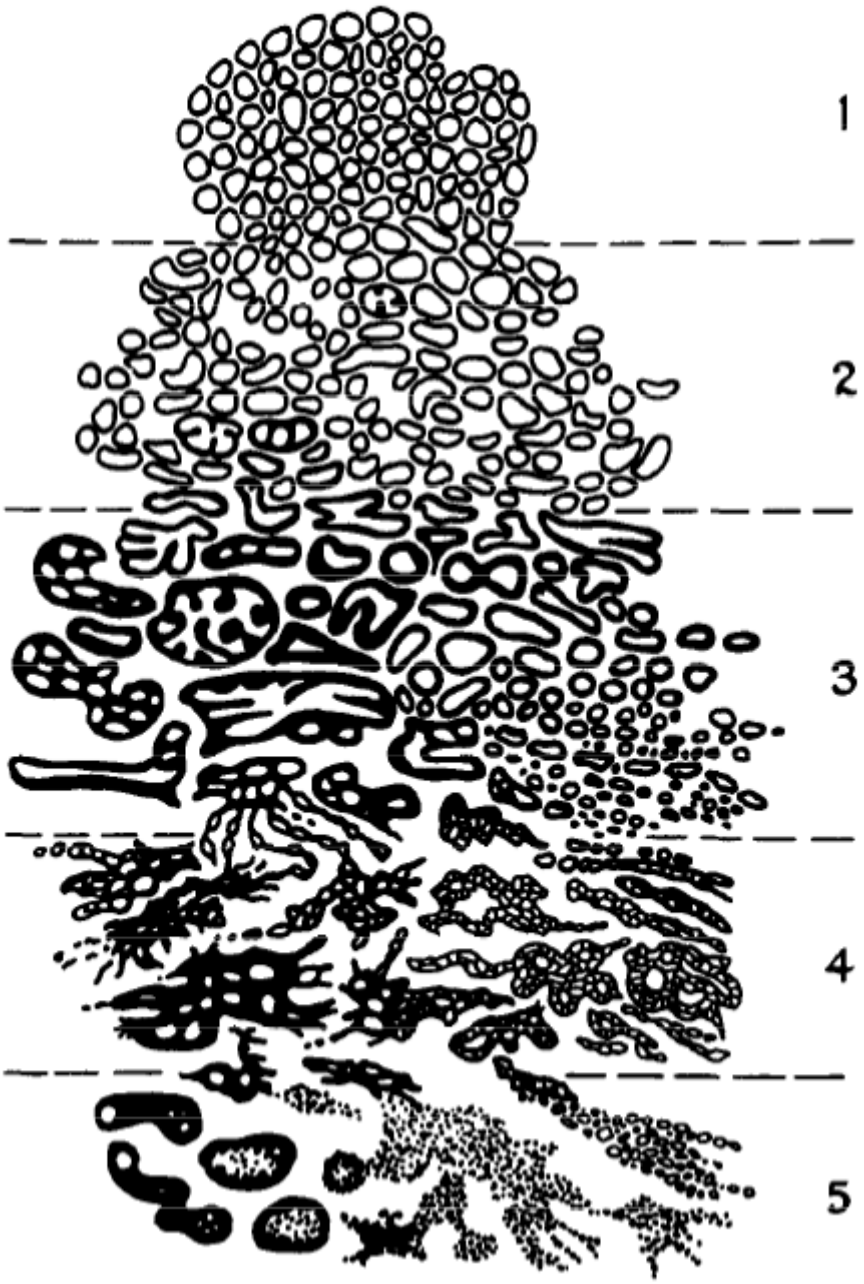

Figure 1.7 Gleason grade schematic for prostate cancer (Image taken from Gleason., 1992)

Table 1.2. Gleason grading system for prostate cancer (data adapted from Humphrey., 2004)

Score	Tumour shape	Stromal invasion	Tumour cell distribution	Gland size
1	Nodular with well defined smooth edges	Pushing	Single, oval and closely packed cells, but detached glands	Medium
2	Less defined and constrained masses	Some gland separation at tumour peripheries	Single, separated, loosely packed oval glands, with more variation in their size and shape	Medium
3A	Indefinable infiltrating edges	Irregular extension	Single, detached glands of variable shape and size, with elongated and twisted forms and wide stromal separation	Medium
3B	Indefinable infiltrating edges	Irregular extension	As with 3A except with smaller glands	Small to very small
3C	Masses and cylinders with smooth round edges	Expansile	Papillary and cribriform epithelium without necrosis	Medium to large
4A	Raggedly infiltrative	Disseminated and permeative	Amalgamated glands in masses, cords, or chains	Variable
4B	Raggedly infiltrative	Disseminated and permeative	As 4A, but cells have cleared cytoplasm (hypernephromatoid)	Variable
5A	Smooth and rounded cylinders	Expansile	Papillary, cribriform or solid masses with central necrosis (comedocarcinoma)	Variable
5B	Raggedly infiltrative	Disseminated and permeative	Masses and sheets of anaplastic carcinoma, with some tiny glands or signet cells	Variable

1.4 Prostate cancer treatments

A major problem faced by individuals affected by prostate cancer can be the indolent and latent nature of the disease. Symptoms of this disease can appear much later in life which usually indicates locally advanced or metastatic disease.

Prostate cancers deemed low risk and localised tend to be very slow growing or show no progression in growth at all. In such cases, these patients are offered active monitoring whereby the cancer is assessed over time and if the disease progresses, patients at risk can be quickly identified and treated appropriately. Due to the heterogeneity seen across prostate cancer cases, choosing a treatment best suited for a particular patient represents a difficult decision that requires careful consideration.

The D'Amico classification system for localised disease was designed for evaluating the risk of disease recurrence following primary prostate cancer treatment (D'Amico *et al.*, 1998). This risk assessment takes PSA level, Gleason score and tumour size (T stage) to classify this risk to patients as low, intermediate or high (refer to Table 1.3). This system aids an informed decision to select the most suitable treatment option.

Table 1.3. The D'Amico classification system for prostate cancer using PSA level, Gleason score and tumour size (T stage) to determine risk of disease recurrence

D'Amico risk classification	**PSA level**	**Gleason score**	**T stage**
Low	Less or equal to 10	Less or equal to 6	T1-2a
Intermediate	Between 10 and 20	Equal to 7	T2b
High	More than 20	More or equal to 8	T2c-3a

1.4.1 Radical prostatectomy

Surgical removal of the whole prostate, known as prostatectomy is a common procedure for prostate cancers at stage T1 or T2 when the tumour is confined within the prostate. For obvious reasons, this option is not suitable in cases where the cancer has metastasised to distant sites. The main technique used to surgically remove the prostate is radical prostatectomy which is an improvement on previous procedures as it involves sparing the neurovascular bundles adjacent to the prostate and therefore avoids impairing erectile function and sexual potency (Walsh *et al*., 1983). Refinements in the surgical technique have led to the development of laparoscopic and more recently robotic surgery for the surgical treatment of prostate cancer (Ali *et al.*, 2013).

1.4.2 Radiotherapy

Radiotherapy uses high doses of radiation to target cancer cells by promoting DNA damage induced apoptosis, a process to which cancer cells are more vulnerable than normal cells. This method is suitable for low-grade prostate cancers that are still confined within the prostate gland as well as cancers that have progressed to a locally advanced stage. Radiotherapy can help reduce tumour size and offers an element of relief for the patient. The two main types of radiotherapy available are brachytherapy and external beam radiotherapy. Brachytherapy involves the insertion of pellets comprised of radioactive elements such as iodine-125 or palladium-103 for low dose rate brachytherapy. These pellets are placed into thin needles which permits implantation directly into the prostate. These ‘seeds’ then expose the prostate to high

doses of radiation over a few months without being administered to the healthy tissues elsewhere in the body (Radge *et al.,* 2000).

Men opting for low dose rate brachytherapy require only a single treatment, making it the preferred choice for some patients compared to external beam radiotherapy where 30-35 treatment doses are administered over a period of 6-7 weeks at a frequency of 5 days a week. External beam radiotherapy directs high dose radiation beams from a linear accelerator to the prostate from outside the body. Like brachytherapy, this method spares the surrounding normal tissue from damage, however it is possible for patients to suffer from side effects including problems affecting the bowel and bladder regions such as diarrhoea, urinary incontinence and inflammation as well as erectile dysfunction (Mohan and Schellhammer., 2011).

1.4.3 Androgen deprivation therapy

The development of the prostate gland and prostate cell growth is stimulated by androgens. Such androgens include testosterone which is secreted from the testicles and is converted into dihydrotestosterone (DHT) in the prostate (Roy and Chaterjee., 1995). Despite being physiologically important, these hormones are also essential to the continued survival and growth of prostate cancer cells. Limiting androgen activity suppresses prostate cancer cell proliferation, triggers apoptosis and in *in vivo* models, a decrease in tumour size (Kyprianou *et al*., 1990).

Early research on prostate cancer focused on the androgen dependence of the disease which led to the suggestion that it was a hormone-dependent cancer (Huggins and Hodges., 1941). Androgen deprivation therapy (ADT) encompasses a wide variety of

drugs that either diminish circulating levels of androgens or block the androgen receptor as illustrated in Figure 1.8.

Luteinising hormone (LH) releasing hormone (LHRH) agonists and antagonists function by blocking the LHRH receptor which in turn reduces LH and thus causes a reduction in testosterone production in the testicles. This approach has replaced orchiectomy (surgical castration) due to patient preference and the flexibility this option offers to adapt treatment over the course of the disease (Stricker., 2001). In some patients, LHRH agents are used in conjunction with anti-androgens which inhibit the binding of testosterone or dihydrotestosterone to the androgen receptor. Doing so abolishes the testosterone negative feedback loop and thus stimulates the production of LHRH and therefore testosterone production (Denmeade and Isaacs., 2002). However, patients treated with androgen deprivation therapy often become resistant to these drugs and develop castration-resistant prostate cancer. Androgen insensitivity is commonly associated with advanced prostate cancer and contributes to the challenges faced in the treatment of this disease (Feldman and Feldman, 2001).

An adjuvant or neoadjuvant androgen deprivation therapeutic approach to radiotherapy is commonly used to improve outcome in patients presenting with locally advanced prostate cancer (Payne and Mason., 2011).

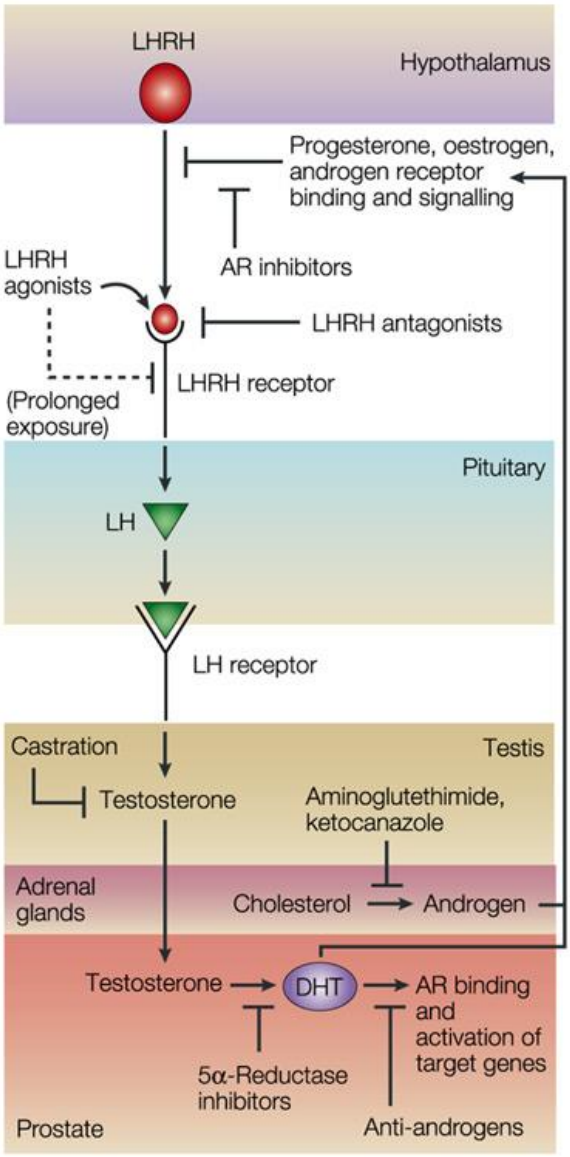

Figure 1.8 Androgen production and their regulation by therapeutic drugs. Luteinising hormone (LH) releasing hormone (LHRH) produced in the hypothalamus stimulates LH production in the pituitary gland. Activation of the the LH receptor stimulates testosterone production in the testicles and is converted to dihydrotestosterone. The mode of action elicited in this cascade described above is targeted by a variety of drugs to control and treat prostate cancer (Figure taken from Denmeade and Isaacs., 2002).

1.5 Cancer metastasis

The majority of prostate cancers are slow growing and asymptomatic. Even when considering aggressive cases, it is generally seen that prostate carcinomas remain confined to the prostate with very few cases progressing to metastasis. Despite this, cancer metastasis accounts for as much as 90% of cancer-related deaths. Even so, no definite preventative or curative treatments have yet been developed to target the metastatic cascade of cancer. It is hoped that ongoing dynamic research into this area of importance will yield an insight into the mechanisms underlying this complex multistage process and subsequently lead to the development of viable therapeutic approaches with the ability to prevent cancer metastasis.

1.5.1 Metastatic cascade

Cancer metastasis involves the establishment of cancer cells, originating from the primary tumour, to a distant site to form a secondary tumour. This complex process requires the coordination of several key events. The primary step involves the dissociation of cancer cells from the primary tumour which then proceed to locally invade surrounding tissue enabling entry into the circulatory system (intravasation). Successful passage into the bloodstream provides indiscriminate access for these cancer cells to distant sites within the body. Once a successful exit from the bloodstream (extravasation) has been achieved, the cancer cells will need to survive and proliferate in the distant tissue to establish a secondary tumour. This succession of events in the metastatic cascade is illustrated in Figure 1.9.

Instigation of the metastatic cascade occurs upon the acquisition of metastatic phenotypes by cancer cells in the primary tumour. A single point mutation has the

ability to transform a normal cell into a cancer cell and furthermore, an accumulation of genetic and/or epigenetic aberrations in a cancer cell at the primary site has the potential to confer aberrant characteristics such as increased motility, invasion and resistance to apoptosis which is ideal for metastasis.

Despite the aggressive nature of cancer metastases, accomplishing each stage of the metastatic cascade does not come without potential cell elimination along the way. With less than 0.1% of disseminated cancer cells from the primary tumour establishing secondary tumours at a distant site, this process is in reality very inefficient (Fidler., 1970). Even so, an appreciation of the molecular basis underlying each phase of the process will lead to a greater understanding of metastatic disease.

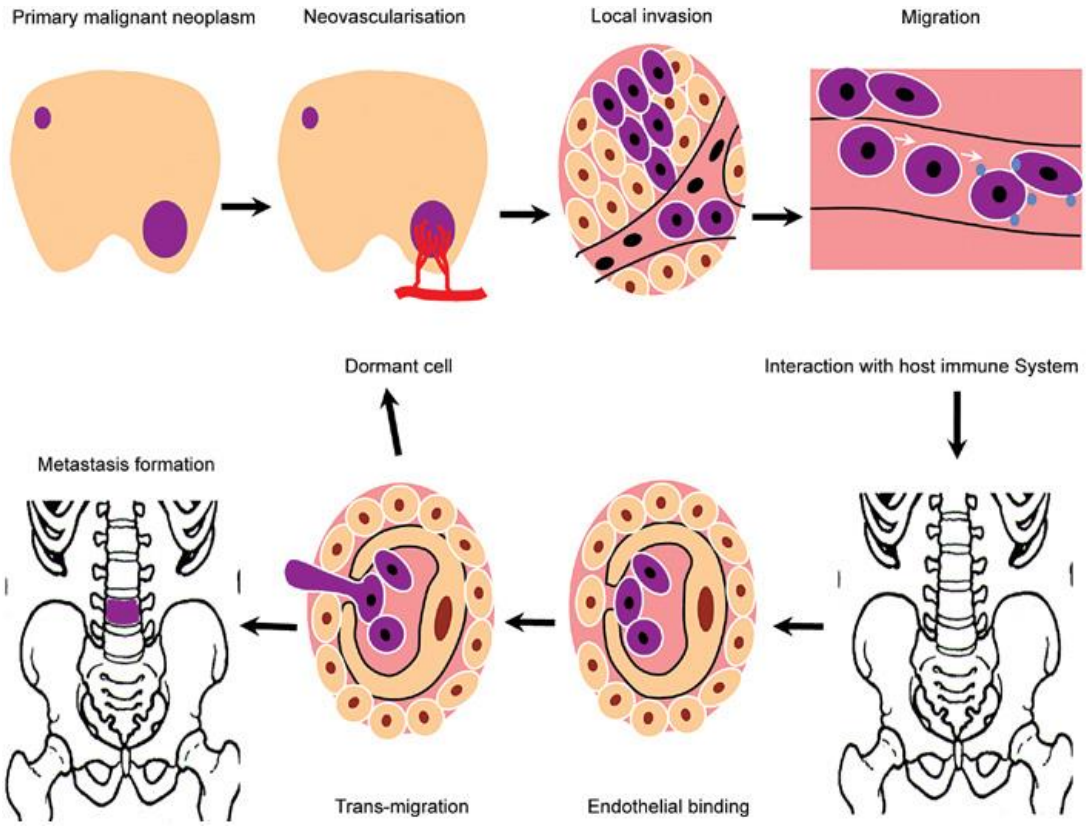

Figure 1.9 The metastatic cascade follows a sequence of steps: local invasion, intravasation, survival and migration in the vascular system, adhesion, extravastion ending with successful colonisation at the secondary site (Image taken from Clarke *et al*., 2009)

1.5.2 Local invasion

Dissemination of cancer cells from the primary site is the preliminary event that initiates the metastatic cascade, without which, there would be no possibility of these cells spreading elsewhere in the body. A vast spectrum of adhesion molecules including members of the immunoglobin superfamily (IgSF), cadherins, integrins, selectins, ephrins, claudins and occludin (Palmer *et al.,* 2011) play a cardinal role in regulating cell-cell and cell-matrix interactions. The establishment of dynamic interactions between adjacent cells and/or the extracellular matrix (ECM) is pivotal in regulating cell migration and invasiveness. In spite of this, the acquisition of metastatic traits can enable cancer cells to overcome the inhibitory effects inflicted by cell-cell and cell-matrix interactions, thus permitting cells to advance through the metastatic cascade. During metastasis, the architecture at the cell junctions can change, thus influencing cell-cell adhesion. Cell adhesion molecules (CAM) such as E-cadherin, N-cadherin and β-catenin are key elements in this metastatic transition.

Epithelial (E-) cadherin is a major component of adherens junctions in epithelial cells whereby cell-cell contacts are heavily mediated by its ability to co-ordinate with another E-cadherin molecule of a neighbouring epithelial cell. Furthermore, E-cadherin is able to associate intracellularly with members of the catenin family including β-catenin. The formation of cadherin-catenin complexes is a key link between adherens junctions and the actin cytoskeleton. Actin polymerisation factors have been suggested to be recruited by cadherin and catenin co-ordination to promote actin reorganisation to facilitate adherens junction assembly and formation of cell-cell contacts (Harris and Tepass., 2010). E-cadherin is regarded as a tumour/invasion suppressor due to findings of decreased expression levels in higher

grade carcinomas, thus implicating it as a potential biomarker for aggressive cancers (Rubin *et al.,* 2001).

Contemporaneously with decreased E-cadherin expression, an upregulation of mesenchymal markers such as vimentin and neural (N-) cadherin is associated with epithelial to mesenchymal transition (EMT). The loss of epithelial properties along with the gain of mesenchymal characteristics is indicative of EMT and is becoming increasingly recognised as a fundamental passage to metastasis. Increased N-cadherin levels induce cytoskeleton reorganisation via small GTPase signalling. This mediates the formation of cell protrusions such as stress fibres, filopodia and lamellipodia (Cavallaro and Christofori., 2004). Despite this cadherin switch being an inherent process in embryonic development, chronic inflammation and wound healing; aberrations of this operation are implicated as a defining development in conferring increased motile and invasive capacity in metastatic cancer cells.

Acquisition of a mesenchymal phenotype enables cancer cells to escape the confines of the primary tumour into the surrounding tissue. In the case of carcinomas such as prostate and breast cancer, which are epithelial in origin, invasion of these cells requires extracellular matrix (ECM) reconstruction to enable breach of the basement membrane. Cell-matrix contact is facilitated by adhesive proteins on the cancer cell surface and the ECM. The integrin family of proteins bind directly to structural components of the ECM. This action governs their crucial role in cell migration and invasion (Desgrosellier and Cheresh., 2010). These traits are facilitated by the ability of integrins to recruit proteases and regulate their activity which can assist cancer cells to cross tissue barriers by remodelling the surrounding matrix. Most prominent of these matrix degrading enzymes are the matrix metalloproteinases (MMPs) which

have the capacity to digest multiple ECM components including collagen, vitronectin, fibrinogen and laminin (Deryugina and Quigley., 2006).

1.5.3 Intravasation and survival in the vascular system

Angiogenesis is an essential process which orchestrates the formation of new blood vessels with the sole purpose of providing necessary nutrients and oxygen to tissue. However, as with the properties that characterise cancers, this normal physiological process is aberrantly upregulated in tumour growth and greatly facilitates the progression of cancer cell dissemination. As a tumour proliferates, its consumption of oxygen and nutrients grows. As the blood supply can become restricted, a state of oxygen starvation in these cancer cells results in the activation of pro-angiogenic factors such as hypoxia-inducible factor-1 (HIF-1). HIF-1 along with vascular endothelial growth factors (VEGF) can stimulate the generation of new blood vessels in their surrounding microenvironment (Jośko and Mazurek., 2004). Unsurprisingly, the formation of new blood vessels as a gateway for nutrients and oxygen is also an escape route for cancer cells, particularly cancer cells which have acquired migratory and invasive phenotypes.

Intravasation is the invasion of carcinoma cells into the circulatory or lymphatic system which enables cancer cells to reach distant organs (Gupta and Massaque., 2006). The blood of many patients presenting with advanced primary tumours harbour circulating tumour cells (CTCs). These cells represent metastatic intermediates advancing from their primary tumour origins to their uncertain destination. CTCs must overcome a multitude of challenges on this perilous journey, all of which could result in cell elimination.

Cancer cells face numerous hurdles which could hamper their translocation, one such hindrance being the large diameters of carcinoma cells (20-30μm) relative to the luminal diameter of capillaries (~8μm). Moreover, CTCs may travel as larger multi-cell clusters thus further restricting their movement. Considering the physical constraints of their surroundings, a large proportion of CTCs become trapped and destroyed. Moreover, CTCs can be subjected to attack by the immune system and the activation of apoptosis. Advantageously for CTCs, several mechanisms aid their survival in the circulatory system. The attributes acquired during EMT are not only limited to increased cell motility and invasion. Mesenchymal transformation also bestows stem cell properties, in particular, increased resistance to apoptosis and senescence and suppression of the immune system (Kallergi *et al.,* 2013). Furthermore, the production of chemokines, cytokines and growth factors by CTCs encourages the association of blood platelets. These platelet-coated tumour cells are thus 'cloaked' from attack by the immune system and provide an additional benefit to the cells which are shielded from potential damage inflicted by shear forces during transportation in the blood system (van Zijl *et al.,* 2011).

1.5.4 Extravasation

The mesenchymal phenotype of the cancer cells greatly benefits them in escaping from their primary tumour origins and in survival within the hostile environment of the circulatory system. Even so, this does not appropriately equip them for the latter stages of the process, namely, exit from the blood stream (extravasation) and colonisation at a distant site. However, the observation of an epithelial phenotype at the secondary tumour site and the close resemblance between the primary tumour

and the metastasised tumour at a distant site on a histopathological level has led to the suggestion that this is influenced by mesenchymal-to-epithelial transition (MET) (Gao *et al.,* 2012).

The acquisition of traits facilitating cancer cell progression through the metastatic cascade has already been established as a random series of events which benefit cell survival in an inefficient process. The colonisation of a secondary tumour on the other hand points towards a mechanism which is less accidental.

Prior to metastatic colonisation, CTCs need to escape the vascular system and arrest at distant organ sites. Evidence implicates the action of particular integrins to assist tumour cell adherence to the endothelium of the capillary bed at the target organ. Studies in mice have shown that β_4 integrin adhesion to the lung endothelial Ca^{2+}-activated chloride channel protein mCLCA1 is a mechanism that facilitates lung colonisation by B16-F10 cells (Abdel-Ghany *et al.,* 2002). Alternative *in vitro* studies have linked the integrin $\alpha_v\beta_3$ with assisting melanoma cell progression through a monolayer of human lung microvascular endothelial cells (Voura *et al.,* 2001). Besides integrins, the well-known cell adhesion molecule CD44 is known to form a complex with ezrin, a cytoskeletal anchoring protein. These properties support the notion of this complex's role in tumour-endothelium interaction (Martin *et al.,* 2003).

In other cases, CTCs may become lodged within capillary beds due to their large size relative to the smaller diameter of blood vessels, thus limiting their passage. Where this occurs in conjunction with cells that proliferate at a rapid rate, the cancerous lesion breaches through the confines of the vascular space into the neighbouring tissue (Al-Mehdi *et al.,* 2000).

The site of secondary tumours in patients diagnosed with a particular cancer is a complex issue. For example, prostate and breast cancer are the most common carcinomas to develop bone metastases whereas colorectal cancers have a tendency to metastasise to the liver (Lehr and Pienta., 1998; Kawada *et al.*, 2011). This apparent pattern observed for secondary sites of metastatic colonisation for specific cancers is unlikely to be attributable to chance. This observation was first documented and pioneered by Stephen Paget who established the 'seed and soil' hypothesis where he postulated that cancer cells with metastatic potential (the 'seed') would only go on to establish metastases if they settle at specific sites (the 'soil') (Paget., 1889).

The specificity of metastases in particular organs can be influenced by the capillary architecture of the tissues of these favoured organs, which can arrest CTCs at these sites as already mentioned. Furthermore, vascular flow patterns can contribute to metastatic specificity. For example, it is very common for colorectal cancers to form metastases in the liver due to cancer cells from the primary site being transported via the hepatic portal circulatory system and arriving directly at the liver (Chambers *et al.*, 2002). Additionally, the action of "homing signals" including chemokines and growth factors have also been implicated in organ-specific metastases (Langley and Fidler., 2011).

1.5.5 Metastatic colonisation

As with all stages of the metastatic cascade, colonisation at distant organs is an exceedingly inefficient process with the majority of CTCs undergoing apoptosis within 24 hours of extravasation (Chaffer and Weinberg., 2011). It is likely that the tissue microenvironment encountered by the extravasated tumour cells will differ from their primary tumour origins, thus making them poorly adapted. However, if cells successfully extravasate and are not terminated, these surviving tumour cells are postulated to exist in either a non-proliferative dormant state or in a state of rapid growth. Transition from quiescent mode to one that exhibits metastatic colonisation capacity is governed by the need for the cells to acclimatise to their new surroundings. Remodelling local microenvironments via Matrix metalloproteinases (MMPs), stimulation of integrins and recruitment of pro-angiogenetic factors such as VEGF have been implicated in this transition (Joyce and Pollard., 2008). Such remodelling, which has already been established, provides a portal for oxygen and nutrients in addition to an escape route for tumour cells with metastatic potential, allowing them to seed a secondary tumour elsewhere in the body.

1.6 Prostate cancer metastasis

According to worldwide statistics, prostate cancer has the second highest incidence rate. Despite this, mortality rates of this disease place it the sixth highest worldwide due to relatively few number of cases resulting in cancer-related death (Globocan, 2012). The vast majority of prostate cancer-related deaths are as a consequence of aggressive metastatic spread of the cancer cells to other sites within the body. Prostate cancer patients exhibiting localised tumours have approximately a 90% 5-

year survival rate which falls to 30% for patients presenting with metastases (Cancer Research UK, 2014). Metastatic lesions originating from prostate cancers most frequently occur in the bones. This is a trait shared with other leading cancer types including breast and lung. Mortality data indicate that over 80% of prostate cancer patient deaths exhibit bone metastatic lesions (Bubendorf *et al.,* 2000). Aside from the issue of mortality, symptoms experienced by individuals burdened by bone metastases often include chronic bone pain, hypercalcemia (elevated calcium levels in the blood), bone fractures and nerve compression (Gralow *et al.,* 2009). The development of bone metastases and the associated effects are indicative of poor prognosis. The processes that define the preference for prostate cancers to metastasise to the bone are poorly understood. Therefore, elucidating this mechanism will help understand this clinically significant disease and aid the development of therapies to inhibit and/or treat metastatic bone lesions.

The sequence of events in prostate cancer bone metastases follows those outlined in the previous section 'Cancer metastasis'. Before metastasis has initiated, it is generally observed, at the very early stages of prostate cancer, that the tumour cells to retain their epithelial traits and are well confined to the prostate. Their limited motility is due to stable adherence of these luminal basal cells to the basement membrane and to each other, thus forming a cell layer that coats the lumen. However, the influence of several molecular changes has the potential to disrupt these cell to cell and cell to matrix contacts which has therefore been linked to EMT in prostate cancer.

1.6.1 Cadherins and catenins

Maintaining contacts between cells and their matrix is managed by cell adhesion molecules (CAM). Downregulation of these fundamental interactions disrupts tissue architecture and is the prerequisite to developing an invasive phenotype in early metastasis. The CAMs encapsulate molecules of various classes and functions which include cadherins, integrins and the immunoglobin superfamily (IgSF).

As previously mentioned, loss of E-cadherin is linked with the acquisition of mesenchymal characteristics and this contribution to cancer metastasis has been well documented. Expression levels of E-cadherin are known to be lower in tumour specimens taken from patients presenting with higher-grade prostate cancers (Gleason score ≥8) compared to patients with a lower-grade (Umbras *et al.*, 1992). E-cadherin was also found to be down-regulated in several prostate cancer cell lines (Bussemakers *et al.,* 2000). Cadherins require an association with cytoplasmic proteins such as catenins to elicit their cell-cell adhesive properties. A well characterised complex formed from members of these protein families is comprised of E-cadherin and β-catenin. Interestingly, one study compared the expression levels of both proteins in primary prostate and bone metastases specimens, and observed both were down-regulated in the latter group (Bryden *et al.*, 2002). This finding implicates the dysfunction of this complex to be clinically relevant in prostate cancer. More recently, the significance of δ-catenin in prostate cancer progression was highlighted when it was demonstrated to influence E-cadherin processing via MMP and PS-1/γ-secretase which impacts β-catenin-mediated oncogenic signalling (Kim *et al.*, 2012).

1.6.2 Matrix metalloproteinases (MMPs) and other proteases

Degradation of the ECM carves a pathway for metastatic prostate cancer cells to breach the basement membrane. This is achieved via the enzymatic activity of several proteases which are able to digest the collagen, laminin and fibronectin ECM components. Matrix metalloproteinases are a family of zinc-binding enzymes able to cleave these ECM constituents whose activity is regulated by tissue inhibitors of metalloproteinases (TIMPs). These antagonistic protein groups are valuable in understanding cancer progression as an imbalance in their activity is a significant contributory factor to tumour cell invasion (Lokeshwar *et al.,* 1993).

Expression analysis comparing prostate cancer tissue to specimens from normal prostates found MMP-9 levels were significantly higher in the former group (Lichtinghagen *et al.,* 2002). Additionally, MT1-MMP, an activator of proMMP-2, was demonstrated to be up-regulated in the metastatic prostate cancer cell lines, PC-3 and DU-145 (Nagakawa *et al.,* 2000). The role of MMPs in prostate cancer metastasis was further demonstrated using RNAi to target MMP-12 expression in PC-3 cells with the consequence of reduced invasive capacity (Nabha *et al.,* 2008). The findings of this study were attributed to the action of MMP-12 in enhancing type I collagen degradation in the bone and highlights the contribution of MMPs in bone-related metastasis.

Serine proteases are another enzyme group able to degrade the ECM. These include trypsin, thrombin, plasmin, cathepsin G and urokinase-type plasminogen activator (uPA). Upon binding to its receptor, uPAR, uPA activity is greatly accelerated and is able to efficiently convert inactive plasminogen to a broad-spectrum protease plasmin which can cleave ECM components such as fibronectin, laminin, fibrin,

vitronectin and collagen. Furthermore, it has the ability to activate several proteases including procollagenases and MMPs (Li and Cozzi., 2007). This proteolytic enzyme has been studied at great length and is of much clinical interest due to findings that levels of uPA and uPAR are upregulated in prostate cancer tissues relative to those from benign lesions and normal prostate tissue (Gavrilov *et al.*, 2001). Additionally, uPA is secreted at higher levels by the metastatic prostate cancer cell lines PC-3 and DU-145 relative to LNCaP which exhibits comparatively low tumorigenicity (Hossein *et al.*, 1991).

Recognised worldwide as a diagnostic marker for the early detection of prostate cancer, PSA has also been implicated as a serine protease with the ability to aid prostate cancer cell invasion. Further to its primary role of liquefying semen during ejaculation, *in vitro* assays have demonstrated the ability of PSA to degrade fibronectin and laminin, main components of the ECM (Webber *et al.*, 1995).

1.6.3 Integrins

The integrins comprise a broad family of proteins with roles in cell apoptosis, angiogenesis, migration and adhesion (Desgrosellier and Cheresh., 2010). The diversity of the integrin family is reflected in the multiple downstream effectors it regulates including the focal adhesion kinase (FAK), phosphatase and tensin homolog (PTEN) and Ras/Mitogen-activated protein kinase (MAPK) pathway. It is therefore unsurprising that dysregulated integrin signalling is common in prostate cancer (Goel *et al.*, 2008; 2009). Whilst most α and β subunits that comprise integrin heterodimers are found to be downregulated in prostate cancers, overexpression of $\alpha_{6,}$ β_1, β_3 and β_6 are upregulated with the former two subunits linked with an increased

invasive capacity (Cress *et al.,* 1995). Cancer cells have been shown to utilise the β_1 integrin subunit in regulating insulin-like growth factor type 1 receptor (IGF-IR) localisation, expression and activity of which can promote cell proliferation and survival (Goel HL *et al.,* 2005). Similarly, the β_3 integrin subunit is of benefit to cancer cells because it increases levels of Cdc2 which results in promoted cell motility (Manes *et al.,* 2003).

As previously mentioned, cancer cells are subjected to an array of host immune responses once successful intravasation has occurred. It has been proposed that clumping with other cells particularly platelets, allows these cancer cells to overcome the hostile environment of the circulatory system. Integrins have been implicated as a possible mechanism to attract protective platelets to cancer cells as inhibiting platelet-cancer cell adhesion using antibodies to target αIIb-βIIIa-integrins reduced lung colonisation in mice injected with DU-145 cells (Trikha *et al.,* 1998).

Once circulating prostate cancer cells have survived the hostile environment in circulation, they need to attach to the vascular endothelium and extravasate. Due to the propensity of prostate cancer metastasis to establish in bone, this would suggest that the 'soil' referenced in Stephen Paget 'seed and soil' hypothesis is the bone marrow. Indeed, evidence implicates that prostate cancer cells adhere to human bone marrow endothelial cells with a higher affinity relative to other endothelial cells (Lehr and Pienta., 1998).

The mechanism that denotes endothelial cell type favouritism is not clear but several explanations have been postulated including the action of adhesion molecules on the surface of prostate cancer and endothelial cells, chemoattraction, paracrine interaction and growth factors (Cher., 2001). A model used to explain this specificity

is the ‘dock and lock’ mechanism which requires the aid of several adhesion molecules. For example, integrins including $\alpha_v\beta_3$, $\alpha_5\beta_1$ and $\alpha_3\beta_1$ mediate the ‘locking’ of prostate cancer cells with endothelial cells (Romanov and Goligorsky., 1999). Interestingly, $\alpha_v\beta_3$ is also expressed by osteoclasts; a major cellular component of bone (Nesbitt *et al.*, 1993). Moreover, the integrins facilitate the association of prostate cancer cells to extracellular matrix components to establish these cells at a distant site. The β_1 and β_4 integrins mediate binding to laminin and type IV and V collagen, whilst β_1 has also been shown to aid interaction with hyaluronan, fibronectin and type I collagen (Clarke *et al.*, 2009).

Together, the roles played by these integrin subunits within various signalling pathways permits an understanding as to how their aberrant expression can contribute to prostate cancer progression.

1.6.4 Prostatic bone metastasis

As previously stated, prostate cancers have a propensity to establish in the bone marrow and lymph nodes. Metastases can present as two types of lesions in the skeleton: osteoblastic or osteolytic. Imbalances in osteoblast activity (bone formation) and osteoclast activity (bone resorption) result in such skeletal irregularities. Although bone metastases associated with prostate cancer tend to be osteoblastic in nature, this is attributed to aberrations in both bone formation and resorption.

In addition to Paget’s ‘seed and soil’ hypothesis (Paget., 1889), an alternative theory was put forward by James Ewing who proposed that the pattern seen in different

cancers which favour metastases at particular sites was controlled by the direction of the vascular system (Fidler., 2003). This idea holds more validity when applied to certain cancers (e.g. colorectal cancer) however other mechanisms are implicated in the explanation of susceptibility of the bone to metastasis in prostate cancers. The presence of chemo-attractants in the eventual secondary site and the fact that it is an energy-rich source, can help to explain the homing phenomenon seen in cancers of the breast, lung and prostate.

Specificity for bone in prostate cancer was demonstrated when it was noted that the metastatic prostate cancer cell lines, PC-3 and DU-145 displayed increased invasiveness and chemotaxis when cultured with bone extracts in comparison to extracts taken from brain, kidney, liver, lung and splenic tissue (Jacob *et al.,* 1999). The chemo-attractant found in the bone was identified as osteonectin, a minor bone matrix protein and interestingly, this was also shown to upregulate MMP activity in prostate cancer cells.

Prostate cancer cells have been demonstrated to respond to certain growth factors which are expressed at sites where prostate cancers preferentially metastasise. Epidermal growth factor (EGF) which is expressed in the lymph nodes and bone stroma has been shown to increase chemo-migration of prostate cancer cells *in vitro* and treatment with an EGF blocking antibody interrupts this migratory effect (Rajan *et al.,* 1996) (Zolfaghari and Djakiew., 1996). Prostate cancer cells have also been shown to display increased migration in *in vitro* assays in response to insulin-like growth factor (IGF-) 1 and 2, both of which are produced by bone cells (Ritchie *et al.,* 1997).

The chemokine stromal cell-derived factor 1 (SDF-1) and its receptor CXCR4 facilitates the homing of haematopoietic stem cells (HSC) to the bone marrow. The fact that SDF-1 is expressed by bone marrow endothelial cells and osteoblasts supports this notion in addition to the finding that CXCR4 knockout cells are unable to engraft HSCs to the bone marrow (Aiuti *et al.*, 1999; Peled A *et al.*, 1999). This CXCR4-SDF-1 mechanism is known to influence bone metastasis in prostate cancer (Taichman *et al.*, 2002). Expression analysis of CXCR4 in prostate cancer patients revealed those affected by localised or metastasised cancers exhibited significantly upregulated SDF-1 and CXCR4 levels compared to individuals with normal or benign prostate tissue (Sun *et al.*, 2003). Furthermore, *in vitro* studies demonstrated increased migration in PC-3 and DU-145 cells in response to SDF-1 (Taichman *et al.*, 2002). As promising as these findings are, experiments blocking CXCR4/SDF-1 signalling did not inhibit the invasion of prostate epithelial cells towards bone marrow derivatives indicating that, despite being an important motility mechanism, other chemokine signalling cascades are involved (Hart *et al.*, 2005).

Along with chemokines at the eventual distant site, the presence of a rich energy source to attract metastasising cancer cells is important. The appeal of a lipid source to a cancer cell is clear when considering the aberrant levels of proliferation and migration commonly observed in cancer cells. Co-cultured adipocytes with PC-3 cells demonstrated that the proliferation of these cells was significantly higher compared to cells cultured alone (Tokuda *et al.*, 2003). The availability of lipids as a significant factor for prostate cancer metastasis was further exemplified when the high rates of migration observed by PC-3 cells in response to omega-6 lipids found in the bone marrow was suppressed by the competitive binding of omega-3 lipids (Brown *et al.*, 2006). The composition of bone marrow becomes increasingly

occupied by adipose tissue with age and is a frequent site for metastasising prostate cancer cells; these details along with the findings mentioned above provide a contributory explanation behind increased mortality rates associated with prostate cancer with increasing patient age. It also highlights another potential therapeutic target for affected individuals.

1.7 Cellular migration

Cell motility is a basic function underlying various physiological processes from tissue formation during embryogenesis to the migration of fibroblasts and vascular endothelial cells for wound healing and the deployment of leukocytes during an inflammatory response (Lambrechts *et al.*, 2004). Along with cell integrity, membrane trafficking and cell morphology changes; cell migration relies on the dynamic restructuring of the actin cytoskeleton.

A succession of four steps steer directional motility: protrusion of the cell leading edge, adhesion to the substrate, retraction, and de-adhesion of the tail. Extension of the cell's membrane at the leading edge can be accomplished via the formation of various cell protrusions. Filopodia are thin actin-rich membrane projections and act as sensory antennae for the cell to explore the surrounding environment. These structures are commonly found within or protruding from lamelliopodia. These flat sheet extensions are a characteristic feature at the leading edge and are proposed to be the motor pulling the cell forward during cell migration. The mechanism that directs the plasma membrane forward within filopodia and lamellipodia is actin polymerisation (Ridley., 2011). The cyclic progression of these cell migratory steps is depicted in Figure 1.10.

Cytoskeletal changes occur in response to extracellular stimuli and are coordinated via a multitude of signalling factors comprising G-protein-coupled membrane receptors, Rho-GTPase family proteins and protein kinases. The precise mechanisms linking these signalling factors to actin reorganisation at the leading edge of the cell remains obscure. Even so, downstream cytoskeletal targets which play a cardinal role in actin polymerisation, resulting in cell motility and morphology changes, are well documented and encompass proteins involved in specific actin polymerisation stages.

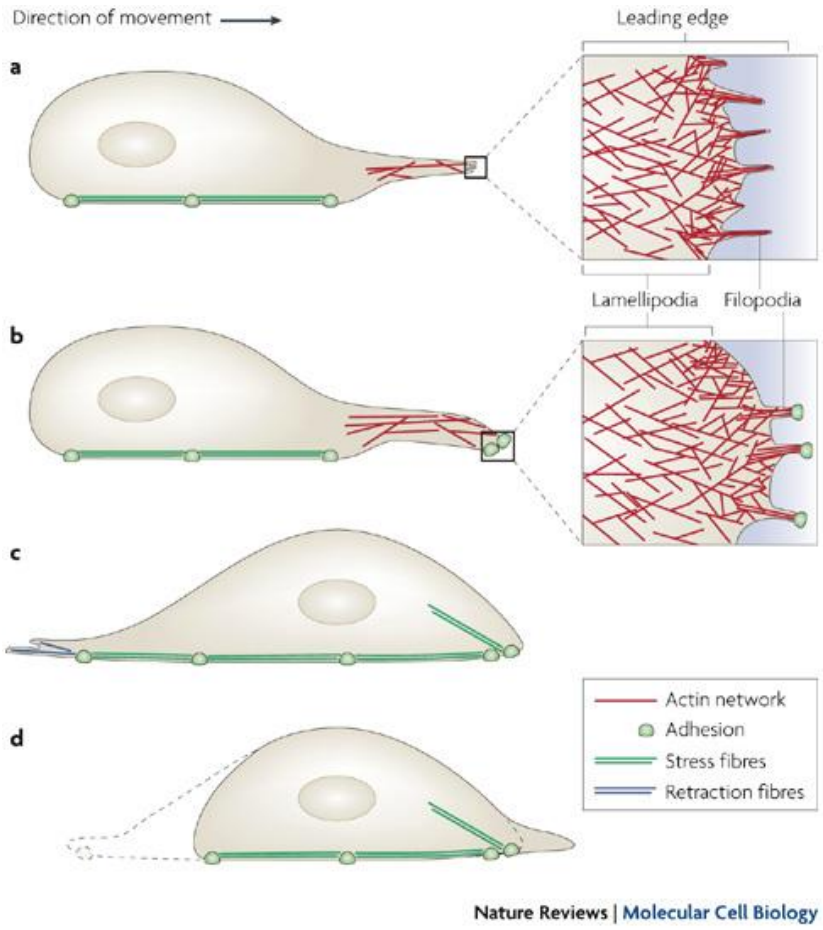

Figure 1.10 Cell migration is driven by cyclic steps dependent on cytoskeletal reorganisation. (a) Protrusive structures such as filopodia and lamellipodia at the leading edge extend out in the direction of movement (b) The leading edge adheres to the substrate (c) (d) The tail end of the cell is detached and retracted (Image taken from Mattila and Lappalainen., 2008).

1.8 Rho GTPases

The Rho family of guanosine triphosphatases (GTPases) are a group of small GTP-binding proteins which are a subgroup of the Ras superfamily. They are small proteins (21-25kDa) which share structural homology (40-95%) and become activated upon GTP association. The participation of Rho GTPases in processes such as cell polarity, gene transcription, cell proliferation, cell polarity and apoptosis highlights the immense versatility and complexity of these proteins. This diversity is attributed to the existence of numerous Rho GTPase family members and their targets as well as the ability of these proteins to become post-translationally modified by isoprenoid lipids at their C-terminal, influencing subcellular localisation and interaction with cellular structures (Parri and Chiarugi., 2010).

Mammalian cells express 22 Rho GTPases with the best characterised members of this GTPase subgroup being three Rho isoforms (A, B and C), three Rac isoforms (1, 2 and 3) and Cdc42. Despite their ability to catalyse the same chemical reactions and share many cellular targets, the roles played by these small GTPases are also distinctly different. Characteristically, Rho activation through Rho-associated protein kinase (ROCK) influences stress fibre and focal adhesion formation, whilst Rac and Cdc42 are involved with lamellipodia and filopodium formation, respectively (Katoh *et al.,* 2001; Ridley *et al.,* 1999).

The cell protrusive effects elicited by these proteins emphasises their pivotal role in cytoskeletal organisation which is perhaps the best characterised process associated with the Rho GTPase family. Like all GTP-binding proteins, these protein family members contain a sequence motif required for GDP and GTP binding with high affinity. The distinguishing structural feature of Rho GTPases is the Rho insert

domain present between a β and α helix within the GTPase domain (Zong *et al*., 2001).

The importance of these GTPases in regulating a plethora of downstream signalling pathways lies in them being sensitive molecular switches which are either in an inactive GDP-bound form or an active GTP-bound form (refer to Figure 1.11). The switch between active and inactive forms in Rho GTPases is orchestrated by three classes of GTPase regulatory proteins: guanine nucleotide exchange factors (GEFs), GTPase activating proteins (GAPs) and guanine nucleotide dissociation inhibitors (GDIs).

GEFs catalyse the conversion of GDP to GTP and are therefore key in activating Rho GTPases which will subsequently interact with a multitude of various effectors of different signalling pathways (Schmidt and Hall., 2002). As the human genome encodes over 60 GEFs, and these proteins are the target for numerous extracellular signals, it is not surprising that with so many different effectors, Rho GTPases have the capacity to engage with such a diversity of cellular functions. Fine tuning specific Rho GTPase activity is achieved through tissue specific GTPase effectors and directing specific intracellular localisation via different lipid modifications as well as phosphorlyation by a variety of different kinases (Etienne-Manneville and Hall., 2002; Ellerbroek *et al.*, 2003).

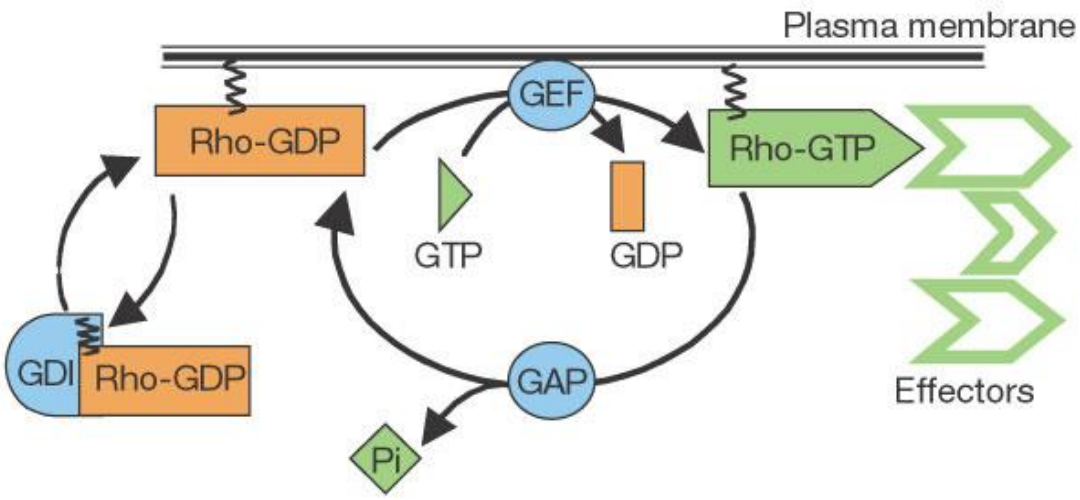

Figure 1.11 The cyclic transition between an active GTP-bound state and inactive GDP-bound state of Rho GTPases facilitated by guanine nucleotide exchange factors (GEF); GTPase activating proteins (GAP) and guanine nucleotide dissociation inhibitors (GDI). Pi denotes a phosphate group which is released upon GTPase hydrolysis (Figure taken from Etienne-Manneville and Hall., 2002).

Rho GTPases exhibit intrinsic GTPase activity, with the ability to hydrolyse GTP to GDP and therefore provide a mechanism for self inactivation. Even so, levels of GTPase activity displayed by these proteins are insufficient to account for the rapid conversion of active GTPases to an inactive form and are instead attributed to GAPs. The GAP family comprises a vast number of members with the human genome encoding approximately 100 GAPs. As with GEFs, GAPs can be induced by several factors due to this protein group manifesting a multitude of protein structures and functions (Etienne-Manneville and Hall., 2002).

The mode of action of GDIs differs from that described by GEFs and GAPs as this class of proteins does not regulate Rho GTPases through their GDP/GTP state. In contrast, GDIs maintain Rho GTPases in an inactive form by suppressing GDP dissociation and hinder activation by GEFs. Additionally, GDIs are able to associate with GTP-bound Rho GTPases; this inhibits GTP hydrolysis both intrinsically and by GAPs, but more importantly prevents activated Rho GTPases from interacting with downstream targets. Furthermore, the ability of GDIs to sequester Rho GTPases in the cytosol means that Rho proteins are unable to associate with the plasma membrane and become activated by GEFs (Hart *et al.,* 1992) (Leonard *et al.,* 1992) (Oloffsson., 1999). Together these points affirm a multifaceted inhibitory function by GDIs to control Rho GTPase activity.

1.8.1 Rho GTPases in cancer

The plethora of physiological processes requiring Rho GTPases reflects their considerable contribution and importance in normal cell function. Unsurprisingly, these proteins are also known to contribute to various stages of cancer progression including cell migration and invasion; traits well established as early stages of metastasis. The motile ability of cancer cells is dependent on cell adhesion and dynamic cytoskeletal restructuring, both of which are regulated by the Rho GTPase family. Whilst activating mutations in the proto-oncogene family Ras are well documented in human solid tumours, Rho GTPase mutations are rarely associated with such tumours. Conversely, aberrant expression and elevated GTPase activity is frequently observed in human tumours (Gomez del Pulgar *et al*., 2005). Such traits in isoforms belonging to the subgroups Rho, Rac and Cdc42 of the Rho GTPase family have been associated with cancer advancement. Elevated RhoA and RhoC expression is commonly seen in human tumours whilst RhoB is downregulated; such observations can be explained by the different roles of these Rho isoforms in the cell. Cell-cell contact and cell polarity in epithelial cells is maintained by RhoA, however, disruption of these integral measures by RhoA aberrance is a prerequisite of tumour progression. Additionally, *in vitro* studies have revealed an ability of constitutively active RhoA to induce malignant transformation (Vega *et al*., 2008). The contribution of Rho GTPases to cancer progression is emphasized by the interaction of these proteins with pathways which direct cadherin-dependent cell-cell contacts and the finding that the production of MMPs is also regulated by Rho GTPases, thus emphasising the interplay of these proteins in cell adhesion and migration (Lozano *et al*., 2003). In addition to transformation, it appears RhoA also has the ability to influence cancer metastasis. A study demonstrated how perturbing the RhoA

pathway in prostate cancer cells significantly inhibited cell migration across the bone marrow endothelial barrier with some influence on changes in MMP expression and their associated inhibitors, tissue inhibitor of metalloproteinase (TIMPs) (Montague *et al.,* 2004).

Conversely, the role played by RhoC in cell invasion and migration suggests this influences cancer metastasis as opposed to transformation upon its atypical expression. A study demonstrated EMT coincided with elevated RhoC expression and activity in colon cancer cells. Moreover, RhoC expression and poor patient outcome was observed in colorectal cancer patients (Bellovin *et al*., 2006). The clinical significance of RhoC has also been observed in breast and lung cancer and melanoma metastasis (Ma *et al*., 2007; Clark *et al*., 2000). Additionally, a correlation was shown between nodal involvement and metastasis with raised levels of RhoC, in breast tumour tissue and significantly higher levels of RhoC in patients with advanced breast cancer (Jiang *et al*., 2003). Further investigation revealed that eliminating the expression of RhoC by ribozyme technology in MDA-MB-231 breast cancer cells reduces their *in vitro* invasiveness compared with wild type MDA-MB-231 cells (Lane *et al*., 2010). The contributory value of RhoC to the metastatic potential of cancer cells is further emphasised by findings that it is involved in angiogenesis (Merajver *et al*., 2005). In contrast, RhoB is commonly found to be downregulated in human cancers and has a potential role as a tumour suppressor due to its apparent ability to hinder cell migration and invasion in addition to exhibiting pro-apoptotic capacities (Huang and Prendergast., 2006).

Similarly, the three Rac isoforms Rac1, Rac2 and Rac3 are commonly overexpressed in various human cancers (Gomez del Pulgar *et al.,* 2005; Abraham *et al.,* 2001; Mira *et al.,* 2000). Even so, it is interesting that in addition to aberrant Rac1

overexpression, mutations in this gene are observed in some human tumours (Hwang *et al.,* 2004). The Rac isoforms display some distinct differences in the cancers with which they are associated in addition to the mechanisms with which they are associated. For example, Rac1 and Rac2 are both involved with macrophage migration, however, cell invasion is governed solely by Rac1 (Wheeler *et al.,* 2006). Moreover, *in vivo* studies demonstrated a specific role for Rac3 in the development of Brc-Abl-induced lymphomas and not Rac1 nor Rac2 (Cho *et al.,* 2005).

As for Cdc42, correlation between its expression state and contribution to cancer progression suggests some tissue specificity due to the demonstration of upregulated expression in some cases of breast cancer, whilst Cdc42 knock-out targeting the liver revealed increased cancer advancement (Fritz *et al.,* 1999; van Hengel *et al.,* 2008). In normal epithelial cells, Cdc42 regulates cell polarity and motility, thus, any aberrations in its mode of action are likely to influence these cell traits and contribute to the metastatic potential of cancer cells.

The great impact of the Rho GTPase family on normal cell function is reflected by their interplay with a wide variety plethora of proteins, both upstream and downstream, in multifaceted signalling pathways. As previously mentioned, many of these cell traits directed by the Rho GTPases are associated with their ability to manipulate cell cytoskeletal reorganisation. Pathways via which these proteins elicit these effects are through direct interaction with members of the Wiskott-Alrich Syndrome Protein (WASP) family which stimulates structures such as lamellipodia and filopodia. Although cell protrusions at the leading edge are essential for cell migration, if unregulated could easily become a precursor to cell metastasis.

1.9 Arp2/3 complex and activation

Actin polymerisation is orchestrated by a plethora of proteins, but without the action of actin nucleating factors it cannot proceed at a rate that cell migration necessitates. Motile ends at the leading edge of cells have been shown to be rich in the Actin-related protein (Arp) 2/3 protein complex, implicating its role in cell migration (Schafer *et al*., 1998).

The Arp2/3 complex was first purified from *Acanthamoeba castellanii* and subsequently isolated from humans, *Xenopus laevis* and *Saccharomyces cerevisiae* (Machesky and Gould., 1999). The Arp2/3 complex is comprised of seven closely associated polypeptides which include a stable assembly of two Arps (actin-related proteins), Arp2 (ACTR2) and Arp3 (ACTR3) in addition to five proteins; ARPC1, ARPC2, ARPC3, ARPC4 and ARPC5 (Beltzner and Pollard., 2002; Blessing *et al*., 2004).

The Arp2/3 complex cannot work alone and is intrinsically inactive which was demonstrated when purified Arp2/3 complex was shown to not (or poorly) stimulate actin nucleation (Pollard and Beltzner., 2002). Stimulation by nucleation promoting factors (NPFs) is able to activate Arp2/3 by inducing a conformational change whereby the activated protein complex configuration results in the subunits Arp2 and Arp3 being brought within close proximity to each other creating an actin pseudo-dimer (Higgs and Pollard, 1999). As previously mentioned, spontaneous actin polymerisation from actin monomers is kinetically unfavourable (Mullins *et al.*, 1998). However, the formation of an actin dimer or trimer provides a kick start platform for rapid actin reorganisation. Generating an actin pseudo-dimer mimics a free barbed end and, through this mechanism, allows Arp2/3 to nucleate new filaments.

1.9.1 Arp2/3 complex in cancer

The Arp2/3 complex is an essential driving force in cell migration through the formation of cell protrusions at the cell leading edge via actin polymerisation. Whilst its role in this normal physiological process is irrefutable, emerging evidence has also identified a potential contribution of the Arp2/3 complex in human cancer.

In one breast cancer study, an association was established between breast cancer cells exhibiting HER2 gene amplification and higher expression of Arp2/3 bound to one of its nucleation promoting factors, WASP verprolin homologous protein (WAVE) 2. This Arp2/3-WAVE2 signal was weaker in breast cancer cells lacking HER2 gene amplification. The link between HER2 and Arp2/3-WAVE2 was further emphasised when cell lines devoid of HER2 gene amplification were transfected with HER2 leading to an increase in lamellipodia formation and cell migration. Both of these traits were suppressed in HER2 amplified breast cancer cells when treated with a HER2 targeted drug. Moreover, immunohistochemical analysis of breast cancer sections showed a correlation between HER2 overexpression and Arp2/3-WAVE2 co-expression (Yokotsuka *et al.*, 2011).

Another study focused on the significance of Arp2/3 in pancreatic cancer. Here the expression status of all subunits comprising the Arp2/3 complex were analysed in pancreatic cancer cell lines. Whilst ARPC3 was demonstrated to be one of the most highly expressed subunits, ARPC2 was one of the component members to be expressed at low levels. Each subunit was targeted by siRNA individually and this revealed that silencing ARPC4 reduced cell migration at the most significant levels (Rauhala *et al.*, 2013).

The prognostic potential of Arp2/3 in human cancer was also highlighted whereby the expression of Arp2 and Arp3 was immunohistochemically investigated in a large cohort of colorectal tumours. A correlation was discerned between increased Arp2 and Arp3 expression and tumours exhibiting an aggressive invasive phenotype (Otsubo *et al.,* 2004).

As cell motility is mediated by actin polymerisation, which is itself promoted by Arp2/3, it is not unreasonable to implicate a role for this protein complex as a contributory factor in cancer cell invasion and metastasis when aberrantly expressed or exhibiting enhanced activity.

1.10 Actin polymerisation

The generation of polarised projections of the cytoplasm at the cell's leading edge via the formation of cell protrusions such as lamellipodia and filopodia assemble the prerequisite elements underlying cell locomotion. It has long been known that actin polymerisation is important for lamellipodia and filopodia formation. The driving force behind these cell protrusions and therefore cell motility is actin polymerisation (Ridley *et al.,* 2003).

Actin filaments (F-actin) constitute much of the dynamic branched framework at the extension of cell protrusions found at the leading edge of the cell. These filaments are orientated with their rapidly polymerising ends facing outwards in the direction of extension. Actin filaments are assembled via the reversible polymerisation of globular monomeric actin (G-actin) into polarised double helical polymers. These filaments exhibit two biochemically distinct ends where polarity reflects the rate of polymerisation and consequently the direction of the plasma membrane extension.

In the cell, the addition of ATP-bound actin monomers are favoured at the plus end where rapid actin polymerisation occurs. It is also referred to as the barbed end due to the association of myosin giving it an arrowhead appearance. In contrast, rates of actin polymerisation are much slower at the minus end where ADP-bound actin monomers dissociate, alternatively called the pointed end (Pollard., 1986). With the plus end orientated towards the plasma membrane in the cell, rapid actin polymerisation at this terminal gives rise to the cell membrane protrusions at the leading edge during cell motility.

The dynamics of actin assembly at the plus and minus ends of actin filaments relates to their different critical concentrations. This describes the dissociation equilibrium constant for G-actin binding at the filament terminal. As the rate of actin polymerisation is dependent on the concentration of G-actin, all actin above the critical concentration polymerises. Owing to a lower critical concentration at the barbed end relative to the pointed end, the barbed end is the fast growing terminal of the actin filament.

The spontaneous assembly of pure actin monomers into filaments is kinetically unfavourable due to the relative instability of actin dimers and trimers, making this the rate-limiting step in actin polymerisation. However, beyond the formation of an actin trimer, known as the nucleus, into what is essentially a free barbed end, filament elongation proceeds quickly with the rapid addition of actin monomers at the plus end. Actin monomer diffusion is responsible for the rate of filament growth and is dependent on subunit collision at the plus end with only 2% of collisions successful in incorporation of subunits in the correct orientation (Drenckhahn and Pollard., 1986). However, diffusion alone cannot account for the behaviour of highly motile cells.

The process of actin addition at the barbed end is transient and the polymerisation of actin filaments does not continue infinitely as the pool of unpolymerised actin is not limitless and the action of capping proteins at the barbed end terminates filament elongation. To overcome the problem of finite actin monomer availability, they are recycled from the pointed end and can be re-used at the barbed end to enable cell migration in the desired direction. The dendritic nucleation/array treadmilling model is used to understand actin assembly and dissociation at the leading edge of the cell and is depicted in Figure 1.12. Cells contain a pool of actin monomers bound to sequestering proteins such as profilin or thymosin-β4. This acts as one of many mechanisms to moderate actin polymerisation. In response to nucleation signals, actin is added to an existing free barbed end. Upon polymerisation, rapid ATP hydrolysis occurs with a half time of approximately 2 seconds (Carlier *et al.*, 1988), whilst release of the resulting phosphate group is slow and can remain bound to ADP-actin for a much longer period with a half-life of about 350 seconds (Carlier and Pantaloni., 1986). Consequently, these half-lives result in newly assembled actin filaments comprised mainly of ADP-P_i-actin intermediates which exist for a comparatively lengthy duration.

The eventual dissociation of the phosphate group is responsible for actin filament disassembly by inducing the action of ADF (actin-depolymerizing factor)/cofilin which promotes the dissociation of ADP-actin from the filament pointed end. Severing ADP-actin from the pointed end can also be brought about by the action of ADF/cofilin as a mechanism of removing ADP-actin from the filament ends. The dynamic turnover in this process is facilitated by the additional role played by profilin as a nucleotide exchange factor for actin. ADP-bound actin is converted into

ATP and is returned to the pool of ATP-bound actin sequestered to profilin for the next cycle of actin assembly at the barbed end (Pollard and Borisy., 2003).

All actin polymerisation is dependent on free barbed ends. At present, there exist three proposed mechanisms to explain the generation of free barbed ends in the cell. Firstly, capping proteins such as gelsolin, are able to associate with the barbed end to inhibit actin polymerisation and therefore provide a mechanism to regulate this process. The involvement of membrane phosphoinositides have been shown to prevent the action of capping proteins and therefore expose the free barbed end of actin filaments to allow filament elongation to proceed (Hartwig., 1995).

Alternatively, the action of ADF/cofilin family of proteins severs pre-existing filaments to produce free barbed ends (Ichetovkin, *et al*., 2002). Providing there is a sufficient concentration of unsequestered G-actin, ADF/cofilin can rapidly facilitate the rate of actin polymerisation at the barbed end.

In addition to these two mechanisms is *de novo* nucleation. As previously mentioned, spontaneous assembly of actin filaments is kinetically unfavourable. Despite this, the involvement of proteins such as the Arp2/3 complex has been shown to accelerate actin polymerisation by acting as the nucleation template and creating a nucleation core.

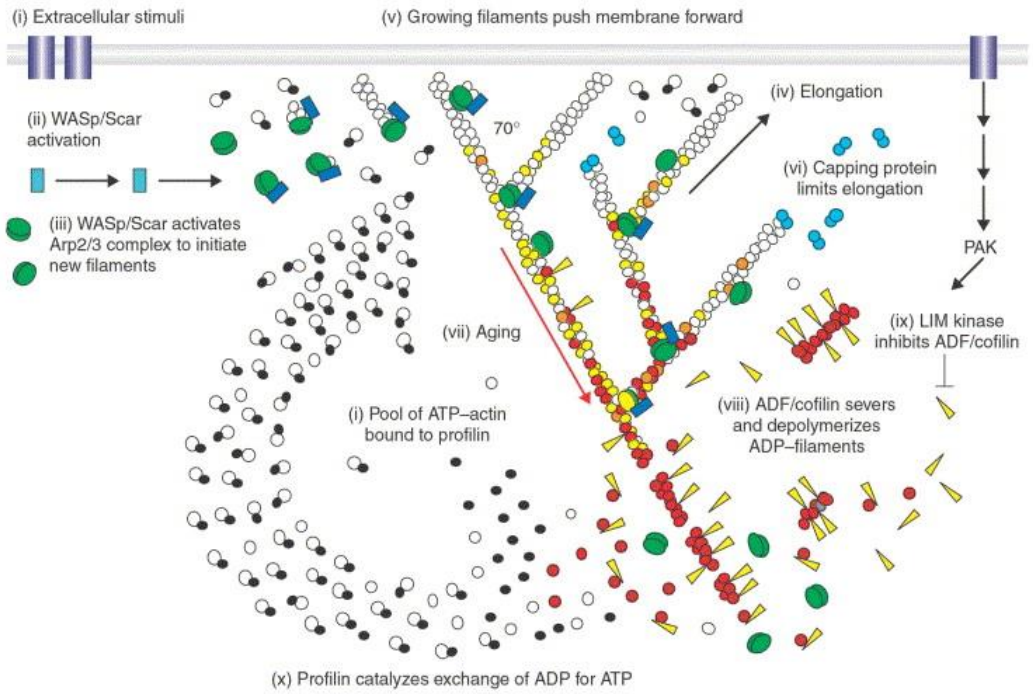

Figure 1.12 Dendritic nucleation model which depicts the assembly and disassembly of actin filaments at the cell's leading edge. The chronological sequence of events during this process is described numerically (Image taken from Pollard and Beltzner., 2002).

1.11 Wiskott-Aldrich Syndrome Protein (WASP)

The human family of Wiskott-Alrich syndrome proteins (WASP) currently includes five members: WASP, N-WASP, WAVE1, WAVE2 and WAVE3. The first member of this protein family to be isolated was WASP in 1994, through linkage studies which associated the mutated gene to Wiskott-Alrich syndrome (WAS), an X-linked recessive disorder defined by immunodeficiency, thromocytopenia, ezcema as well as an increased risk of malignancies (Derry *et al*., 1994; Thrasher., 2009). The human WASP gene is located at Xp11.22-p11.23 which spans over 1Mb and is expressed exclusively in haematopoietic cell lineages. This fact underlies the WAS inheritance pattern and the immunodeficiency and platelet function defects seen in affected individuals as well as the observation of defective cell migration in several patient cell lineages including macrophage, dendritic, T and B lymphocytes and haematopoietic stem cells (Binks *et al.,* 1998; Burns *et al.,* 2001). A 137 bp region upstream of the transcription start site is responsible for the restricted expression of WASP to haematopoietic cells (Petrella *et al.*, 1998).

Analysis of the WASP cDNA sequence identified a region rich in proline residues which is proposed to act as a ligand for Src homology 3 (SH3) domains. Following proteomic searches for proteins that interact with SH3 domains, a novel 65 kDa protein was identified and named neural (N-) WASP as it was first isolated in the brain, although it is now established to be ubiquitously expressed. The N-WASP gene is localised to chromosome region 7q31.3 (Miki *et al*., 1996).

Although both proteins contain regions implicated in SH3 domain association, more important is the carboxyl (C-) terminus which contains protein domains cardinal to their role during actin polymerisation. Characteristic of this protein family, they contain a WH2 (WASP homology 2) sequence alternatively named the verprolin

homology (V) domain, followed by a short central (C) sequence, also known as the cofilin homology domain and finally an acidic (A) sequence. Collectively, they comprise the VCA region where each domain orchestrates their functional roles to confer actin polymerising properties to the protein. The WH2 domain binds to an actin monomer whilst both the cofilin homology domain and acidic region work together to interact with the actin polymerisation activator, Arp2/3 protein complex. Only N-WASP contains two WH2 domains and accordingly exhibits a much higher nucleation rate associated with the VCA region in contrast to the other members within the mammalian WASP protein family (Yamaguchi *et al.,* 2000).

The proline rich region of these proteins allows the binding of SH3 containing proteins such as Ash/Grb2 (Miki *et al.,* 1996; She *et al.,* 1997), Nck (Rivero-Lezcano *et al.,* 1995) and proline-serine-threonine phosphatase interacting protein (PSTPIP) (Wu *et al.,* 1995). This stretch of residues separates the C-terminus from the amino (N-) terminus. At the N-terminus is the WH1 (WASP homology 1) domain which is known to be related to the EVH1 [Ena (Drosphila enabled)/VASP (vasodilator-stimulated phosphoprotein) homology 1] domain seen in members of the Ena/VASP protein family. The WH1 domain facilities association with WIP (WASP-interacting protein) which is implicated in protecting WASP from protease degradation (Ramesh *et al*., 1997; de la Fuente *et al.,* 2007). Adjacent to this region is a basic stretch which is involved with phospholipid PIP_2 (phosphatidylinositol 4,5-bisphosphate) interaction and is postulated to coordinate with Cdc42 to drive actin polymerisation (Prehoda *et al*., 2000). Proximal to this basic stretch, and integral to the role played by WASP and N-WASP in actin polymerisation, is the presence of the CRIB (Cdc42 and Rac interactive binding) domain alternatively named GBD (GTPase binding domain). This region allows Cdc42 binding, a GTPase involved with filopodium

formation and cell polarity (Higgs and Pollard., 2000; Miki *et al.*, 1998). The presence of these domains in WASP and N-WASP defines the N-terminus of these proteins as being essential for protein regulation.

1.11.1 WASP activation

WASP and N-WASP are intrinsically inactive due to intramolecular interactions between the VCA region and the CRIB domain at the C-terminal and N-terminal, respectively. This folded conformation masks the VCA region and therefore prevents the C and A domains from activating the Arp2/3 complex (Kim *et al*., 2000). Disrupting intramolecular interactions relieves the inhibited state of the protein and can be brought about via the competitive binding of various ligands such as the Rho GTPase, Cdc42 and phosphatidyl inositol 4.5-bisphosphate (PIP2) which can associate with the GBD and basic-rich region of the protein, respectively and exposes the VCA region for subsequent Arp2/3 activation (Rohatgi *et al.,* 2000; Kim *et al*., 2000; Prehoda *et al.*, 2000).

Other mechanisms of protein activation include the binding of proteins containing SH3-domains to the proline-rich region of WASP and N-WASP. Such proteins include Nck, whose actin nucleation activity is further stimulated by PIP2; Ash/Grb2 which cooperates with Cdc42 to enable full WASP/N-WASP activation, whilst WASP-interacting SH3 protein (WISH) stimulates optimal WASP/N-WASP activity independent of Cdc42 (Carlier *et al.*, 2000; Rohatgi *et al*., 2001; Fukuoka *et al*., 2001).

Serine and tyrosine residues within WASP and N-WASP are subject to phosphorylation by numerous kinases which are able to influence their activity and localisation. For instance, it has been shown that releasing WASP and N-WASP intramolecular interactions occurred following protein phosphorylation by the Src family of tyrosine kinases adjacent to the CRIB region (Cory *et al.*, 2002). Additionally, focal adhesion kinase (FAK) phosphorylates tyrosine residue 256 of N-WASP which affects its nuclear localisation and promotes cell migration (Wu *et al.*, 2004). A potential explanation for this link between FAK and N-WASP is that activated FAK recruits Cdc42 which promotes N-WASP activation thus stimulating Arp2/3 and promoting actin polymerisation, a necessary step in cell motility (Sanchez *et al.*, 2010). The equivalent conserved tyrosine residue described in WASP is at position 291 in N-WASP and is also subject to tyrosine kinase phosphorylation which leads to subsequent actin polymerisation and filopodium formation (Cory *et al.*, 2002). Furthermore, two serine residues found in the VCA domain of WASP are targeted by casein kinase 2. Phosphorylation of these serine residues dramatically increases VCA domain and Arp2/3 interaction which significantly influences actin nucleation (Cory *et al.*, 2003).

Described above are two main mechanisms through which WASP and N-WASP can be released from their intrinsically inactive state. However, these two modes of activation are not independent of each other as some interplay has been discovered. Coupling protein phosphorylation with Cdc42 intervention was found to have an enhanced effect on WASP activation (Torres and Rosen., 2003). Another study demonstrated how Cdc42 was able to recruit WASP to the plasma membrane where it was subjected to phosphorylation by Lyn and Btk (Guinamard *et al.*, 1998).

1.11.2 WASP and human disease

Discovery of the WASP gene stemmed from the identification of mutations in the gene in patients affected by Wiskott-Alrich syndrome (WAS). Affected individuals present a broad spectrum of symptoms and severity, with some patients exhibiting the full triad of clinical manifestations with poor survival rates compared to those with a milder phenotype and who survive to adulthood. The genetics underlying WAS have been linked to several hundred mutations in the *WASP* gene with some evidence of a genotype to phenotype relationship (Imai *et al.,* 2003). For example, missense mutations within the first three exons of the *WASP* gene are associated with individuals displaying mild symptoms whilst those with nonsense, frameshift, splice site, insertion or deletion mutations in the *WASP* gene are linked with symptoms of a more aggressive nature (Orange *et al.,* 2004). On a molecular level, such mutations within the *WASP* gene would result in a defective protein product and could cause a decline in WASP activity. Alternatively, mutations within important domains of *WASP* could disrupt its specified function. For instance, amongst the missense mutations identified in the *WASP* gene, the vast majority of these are found within the regions that encode the WH1 domain. Aberrations within this protein domain could potentially interfere with WIP interaction.

In addition to platelet abnormalities, immunological defects and eczema being commonly observed in affected individuals, many WAS patients are at an increased risk of developing malignancies, especially those presenting with autoimmune disorders (Sullivan *et al.,* 1994). Accordingly, the majority of these malignancies are lymphoreticular in origin and such malignant tumours can establish at a young age, although the frequency at which they occur is higher in adolescents through to adulthood. Statistics from a North American group of WAS patients found

malignancies were present in 13% of the cohort with a mean age of onset of 9.5 years. The most common malignancy reported is B-cell lymphoma testing positive for Epstein-Barr virus (Sullivan *et al.,* 1994).

Beyond the human malignancies associated with the WAS clinical phenotypes, the WASP family of proteins have also been linked to other cancers. Using immunohistochemical approaches, N-WASP expression was demonstrated to be lower in breast tumour tissue compared to normal mammary epithelial cells. The same study also revealed a link between tumours from patients with a poor prognosis and significantly lower N-WASP levels compared to those with a good prognosis. Forced expression of N-WASP was induced in the breast cancer cell line MDA-MB-231 which displayed significantly reduced invasiveness and motility (Martin *et al.,* 2008). Another study using the metastatic breast cancer cell line, MTLn3 revealed the use of either dominant negative N-WASP cells or treatment of cells with shRNA targeting N-WASP considerably decreased the ability of invadopodia formation, fundamental cell protrusions for cell invasion (Gligorijevic *et al.,* 2012). Despite the contradicting conclusions drawn from these studies, it would be logical to associate WASP abnormalities with human cancer due to their role in actin polymerisation, a driver of cell motility, a contributory trait to cancer progression upon its aberration.

1.12 WASP family verprolin homologous (WAVE) protein family

A novel WASP-related protein was identified following database searches using the verprolin-homology (VPH) domain sequence due to its sequence conservation between WASP and N-WASP and its actin polymerising properties (Machesky *et al*., 1998; Miki *et al.,* 1998). This newly identified protein was subsequently named

WASP-family verprolin-homologous (WAVE) protein. Following this discovery, two additional WAVE proteins were identified, thus the original protein is now known as WAVE1 (alternatively named suppressor of cAR; SCAR1) and the latter two as WAVE 2 and WAVE 3 (Suetsugu *et al.*, 1999). The *WAVE1* gene is located at chromosomal region 6q21 and encodes a gene product of 80,186 bp. The translated protein is 559 amino acids long and whilst there is evidence that it is widely expressed, it is expressed particularly strongly in the brain. At the chromosomal region 1p36.11 resides the *WAVE2* gene which encodes a product of 85,940 bp. The corresponding protein is 498 amino acids long and is ubiquitously expressed but more so in peripheral blood leukocytes. The remaining protein of this subfamily is WAVE 3 whose gene, found at chromosomal region 13q12.13, encodes a product of 131,246 bp which when translated into a protein of 502 amino acids is found expressed mainly in the ovary and brain (GeneCards, 2014; UniProt, 2014; Kurisu and Takenawa., 2009).

WAVE homologs of those defined in human are evident in a diverse variety of eukaryotes. WAVE1 is known also as Scar1 due to the initial discovery that it was a mammalian homologue of SCAR in *Dictyostelium discoideum* (Machesky and Insall., 1998). WAVE homologs have also been identified in *Caenorhabditis elegans* (WVE-1), *Drosophila melanogaster* (SCAR) and *Arabidopsis thaliana* (*SCAR1-4*), *Mus musculus* (WAVE1-3) and *Pongo abelii* (WAVE1) (Kurisu and Takenawa., 2009; UniProt, 2014). Evidence of WAVE homologs in a wide diversity of eukaryotes exemplifies their importance in controlling actin polymerisation in cytoskeletal reorganisation.

All WAVE proteins share a common carboxyl- (C-) terminus comprised of the verprolin homology domain (V) also known as WASP homology 2 (WH2) domain,

central/cofilin homology sequence (C) and an acidic region (A) which together comprise the VCA region which is homologous with and serves the same purpose as the WASP and N-WASP C-terminal in actin monomer and Arp2/3 complex interaction. Moreover, the similarity seen in protein domains of all five WASP and WAVE members extends to the presence of a highly basic region and a long proline region between the amino- (N-) terminus and C-terminus of these proteins. The distinguishing factor between the WASP and WAVE proteins is the WH1 and GBD domains characteristically seen at the N-terminus of WASP proteins which is absent in the WAVE proteins. In contrast, the N-terminus of WAVE proteins possesses the WAVE homology domain/SCAR homology domain (WHD/SHD). The conserved WAVE protein domains are shown in Figure 1.13.

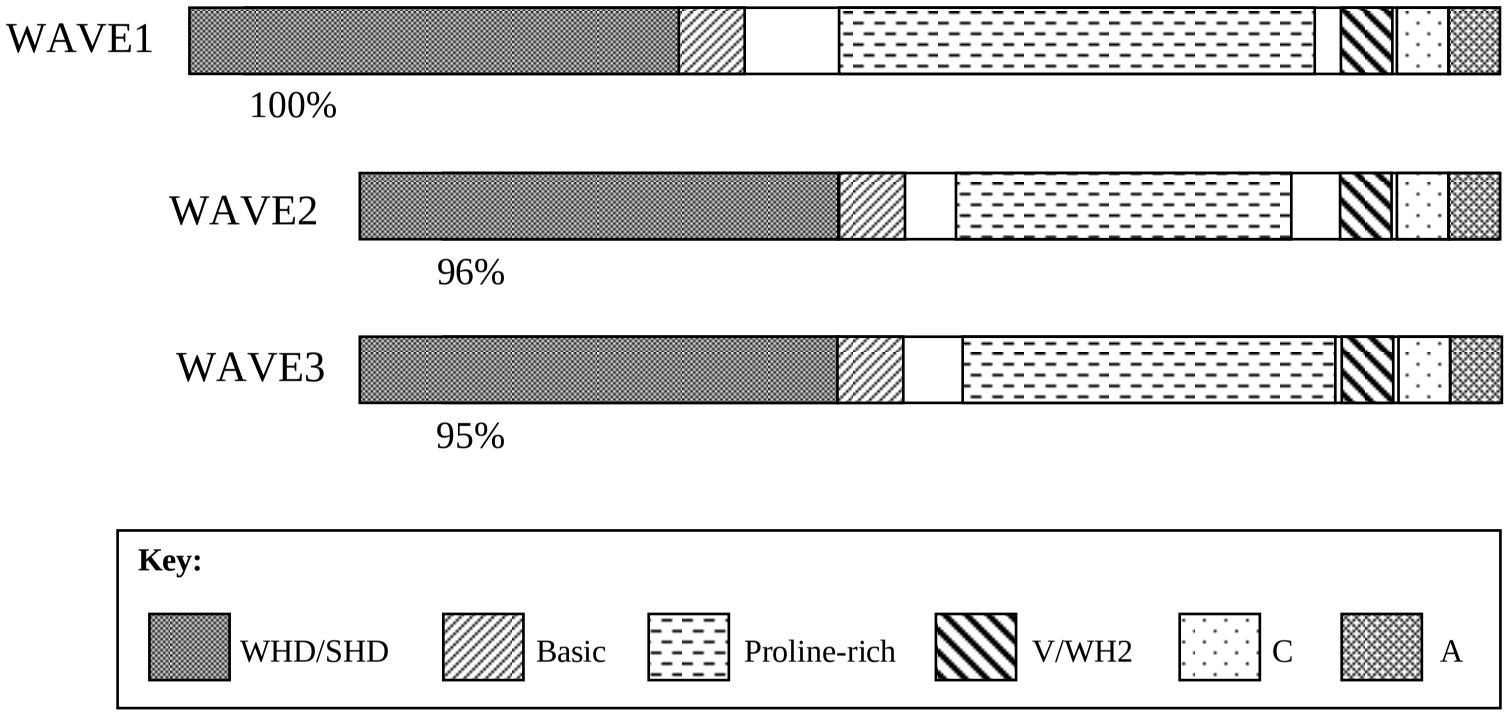

Figure 1.13 Human WAVE protein domain structure. Key denotes conserved domains. The percentage shown below the WHD/SHD domain indicates the amino acid similarity of that domain. (Figure modified from Kurisu and Takenawa., 2009).

1.12.1 WAVE activation

Unlike the WASP proteins which exist independently in cells, each WAVE protein needs to associate with four additional proteins via its WHD to form the WAVE regulatory complex (WRC) and it is only in this arrangement that WAVE is able to confer its actin polymerising capacity. The components of this 400kDa pentameric heterocomplex are Abi (Abelson-interacting protein), Nap1/Hem-2, Sra1/Cyfip1 and HSPC300/Brick1 (Eden *et al.*, 2002). In this complex, Abi and HSPC300 bind directly to the WHD domain of the WAVE proteins and stabilise WRC formation. Abi links WAVE to Nap1 which is itself linked to Sra1 (Takenawa and Suetsugu., 2007). As mentioned previously, WAVE proteins lack a GBD but can be activated indirectly via the association of Sra1 with the Rho GTPase Rac leading to WRC activation (Kobayashi *et al*., 1998). Additionally, proteins comprising the WRC have shown the ability to become phosphorylated at various residues with some modifications showing enhanced signalling activity of the complex (Ardern *et al.*, 2006; Leng *et al.*, 2005; Sossey-Alaoui *et al*., 2007). Figure 1.14 demonstrates the configuration of WRC components and the principle behind WRC activation for subsequent actin polymerisation.

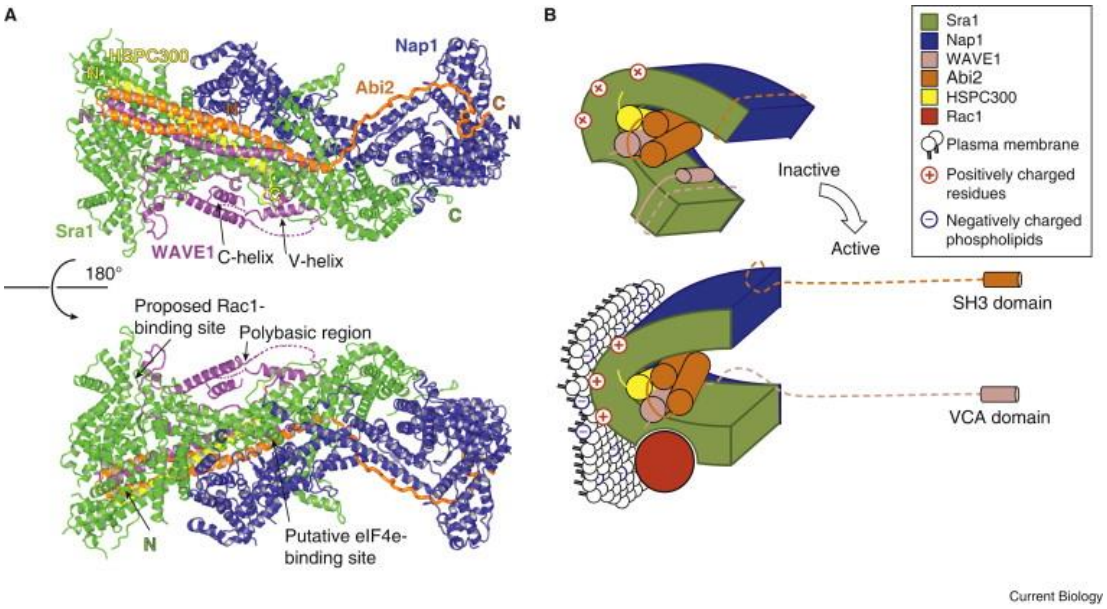

Figure 1.14. WAVE regulatory complex (WRC) structure and regulation. (A) Structure of WRC. Sra1 (green), Nap1 (blue), HSPC300 (yellow), WAVE1 (magenta) and Abi2 (orange). The WAVE proline rich domain has been replaced with a short linker (dashed line) whilst the Abi2 SH3 domain has been removed. This image is taken from Chen et al, 2010. (B) Simplified schematic demonstrating protein interactions between components of the WRC in addition to mode of activation. The WAVE VCA region is sequestered by WRC components in its inactive state. Upon Rac1 association with Sra1, WRC is recruited to the plasma membrane and the VCA is released whereby interactions with the negatively charged phospholipids at the plasma membrane induce the VCA domain into the correct orientation for actin polymerisation at the cell leading edge (This image is taken from Davidson and Insall., 2011).

Integration of the WAVE protein with other subunits to create a protein conglomerate is also an intra-complex mechanism to inhibit WAVE. Within the WRC, the V and C regions of WAVE1 are sequestered by Sra1 as a way to block WAVE activation. Actin-binding residues of the V region are concealed by Sra1 binding making it impossible for monomeric actin to associate. Coupled with a combination of inter-protein contacts within the WAVE1 structure, the V region is rendered inactive and the WRC is induced into a configuration which is incompatible with actin association and therefore suppresses actin polymerisation. Studies have shown how mutations of certain Sra1 residues, important for actin V region binding, enable WRC association with the Arp2/3 complex and consequently stimulates actin filament branching. Moreover, the effects of mutations at particular residues within the C region have been found to reduce WRC activity towards the Arp2/3 complex (Chen *et al.*, 2010).

The WRC is constitutively inactive without intervention by Rac GTPases, phosphatidylinositols and/or kinases. Recruitment of the WAVE proteins to the plasma membrane is facilitated by Rac GTPases. However, WAVE proteins are unable to interact directly with Rac in the same way WASP and N-WASP do with Cdc42. Alternatively, WAVE relies on components of the WRC to elicit these effects. RNA interference studies have shown how the removal of either Sra-1 or Nap1 prevented the ability of cells to produce Rac-dependent lamellipodia (Steffen *et al.*, 2004). Whether Rho GTPase dependent activation of WASP or WAVE is direct or not, regulating their activity is controlled via the competitive binding of GTPases.

The competitive binding of Cdc42 which disrupts intramolecular interactions between the CRIB domain and VCA region, induces WASP out of its intrinsically inactive state. In a similar way, deletion of the VCA region of WAVE was found to

increase the affinity between WRC and Rac1 as VCA deletion released Sra1 for Rac1 binding (Chen *et al*., 2010). This could explain previous findings that certain *Sra1* mutations impeded Arp2/3 complex activation by WRC; this is likely to be due to reduced affinity of Rac1 for WRC.

Although the relationship between Rac and WAVE in cell motility has been long established, it would seem that Rac is not the sole GTPase activator of the WRC. *In vitro* approaches have demonstrated the affinity of Rac1 for WRC interaction was relatively low as was the case for WRC activation by Arf1 GTPase alone. However, upon the coordinated efforts of Rac1 and Arf1 together, WRC recruitment and activity at the plasma membrane were greatly enhanced (Koronakis *et al*., 2011). Although not a GTPase, the Src homology 2 and 3 domain (SH2 and SH3, respectively) containing adaptor protein Nck, has been shown to facilitate actin polymerisation by perturbing trans-inhibition within the WRC (Eden *et al*., 2002). The relationship between Rac and WAVE appears to be indirect, presumably mediated through auxiliary proteins to the WRC. For example, Rac was discovered to associate with the N-terminus of IRSp53 whilst the SH3 domain of IRSp53 binds to WAVE2 and IRSp53 knockdown suppressed lamellipodia formation (Miki *et al*., 2000; Suetsugu *et al*., 2006). Furthermore, these protein interactions were promoted by phosphatidylinositol (3,4,5) trisphosphate (PIP_3) containing liposomes. The recruitment of WAVE to the plasma membrane has been demonstrated to be mediated by PIP_3 which binds to the basic domain of WAVE2 (Oikawa *et al*., 2004). These negatively charged lipids at the plasma membrane are proposed to bind to the positive face of WRC and orientate the complex in a configuration that positions the VCA region extending into the cytoplasm where it promotes actin polymerisation (Davidson and Insall., 2011).

Phosphorylation of residues within regions of WAVE has been shown to be an influential factor in WRC activity with the potential to facilitate actin polymerisation (Sossey-Alaoui *et al*., 2007). It has been proposed that specific phosphorylation modifications could affect the stability of helix structures of the VCA motif and thus Sra1 interaction. WAVE1 phosphorylation of serine residues by cyclin-dependent kinase 5 (Cdk5) suppresses its ability to activate actin polymerisation through the Arp2/3 complex (Kim *et al.*, 2006). However, phosphorylation of WAVE1 at tyrosine residue 125 by the non-receptor tyrosine kinase Src was shown to enhance both Arp2/3 complex association and activity *in vitro* and *in vivo* (Ardern *et al.*, 2006). Likewise, phosphorylation of the tyrosine residue 150 in WAVE2 by Ableson (Abl) non-receptor tyrosine kinase was found to be essential in actin polymerisation and cytoskeletal remodelling, as Y150 mutations hindered these effects (Leng *et al.*, 2005). Furthermore, Abl-mediated WAVE3 phosphorylation was shown to phosphorylate four tyrosine residues in WAVE3 (Y151, Y248, Y337 and Y486) and promoted lamellipodia formation and cell motility (Sossey-Alaoui *et al.*, 2007).

1.12.2 WAVE and cancer

Identification of the WAVE1/Scar1 protein by two independent research groups revealed it to be a downstream effector of the Rac GTPase and for itself to target the Arp2/3 complex with the result of promoting actin polymerisation (Machesky and Insall., 1998; Miki *et al.*, 1998). With this discovery came a flourish of interest surrounding members of the WAVE protein subfamily and their influence on lamellipodia formation with regards to their importance in cell migration as an essential physiologically relevant process. Migrating cells form cytoplasmic protrusions rich in actin at their leading edge comprised of protrusive structures such

as lamellipodia, filopodia and microspikes. Aberrations in upstream molecular signalling which regulate actin polymerisation can result in abnormal invasive phenotypes such as invadopodia, fundamental perquisites to cancer cell metastasis. With this logic, it became apparent that aberrations in WAVE activity were linked to invasive and metastatic cell phenotypes. This was highlighted in a study which demonstrated higher levels of WAVE1 and WAVE2 expression in addition to increased Rac activity in malignant B16F10 mouse melanoma cells which exhibit invasive and metastatic potential compared to parental B16 cells which lack both of these traits. WAVE2 knockdown demonstrated a dramatic reduction in membrane ruffling, cell motility and invasion in addition to suppression of B16F10 cell metastasis (Kurisu *et al*., 2005).

The prognostic importance of WAVE2 in human disease has been further emphasised whereby immunohistochemical approaches revealed that co-expression of WAVE2 and ARP2 was significantly higher in lung adenocarcinoma sections from patients presenting with lymph-node metastasis compared to those with bronchioalveolar carcinoma which lacked these metastatic traits. Sections from patients who had a shorter disease-free survival time and overall survival time also revealed cancer cells that stained for both WAVE2 and ARP2 (Semba *et al*., 2006). These findings were mirrored in a report from the same research group detailing WAVE2 and ARP2 immunohistochemical status of specimens from colorectal cancer patients, with tissue blocks from the primary tumour in addition to liver sections from patients who exhibited metastatic spread to the liver. Co-localisation of WAVE2 and ARP2 was apparent in approximately 36% of the cancer cohort whilst a distinct absence of co-localisation was observed when staining for these proteins in normal epithelial cells. This study concluded that WAVE2 and ARP2 co-localisation

was a risk factor for colorectal cancer derived liver metastasis (Iwaya *et al*., 2007). Previous to this study, the clinical relevance of WAVE2 in liver cancer was explored whereby 112 samples from hepatocellular carcinoma patients were analysed using reverse transcription PCR, Western blotting and immunhistochemistry. The majority of cases displayed significantly increased WAVE2 expression in addition to a correlation with characteristics associated with more aggressive cancers such as higher Edmondson-Steiner grade and reduced median survival time (Yang *et al*., 2006).

The clinical importance of WAVE3 was first documented by Sossey-Alaoui's research team whereby WAVE3 was identified as a potential tumour suppressor gene in a ganglioneuroblastoma case study. The affected patient was discovered to harbour a truncation within the WAVE3 gene and thus rendering it inactivate. Since this work, Sossey-Alaoui's research group has focused heavily on the role of WAVE3 in cell motility and cancer metastasis as well its prognostic value in human cancer (Sossey-Alaoui *et al*., 2002).

Subsequent work by Sossey-Alaoui's research group screened WAVE3 levels in breast tumour specimens from a spectrum of breast cancer stages and grades. Whilst normal breast tissue and grade I tumours showed little or no levels of WAVE3, in contrast, specimens derived from grade III tumours demonstrated higher levels of WAVE3 by approximately threefold. With a potential link between elevated levels of WAVE3 and advanced breast cancer tissues, they proceeded to investigate the effects of WAVE3 expression knockdown in the MDA-MB-231 cell line. Doing so revealed the suppression of *in vitro* cell invasive capabilities and accordingly, injection of these cells into a xenograft mouse model not only reduced the rate of tumour growth at the primary site but also inhibited the metastatic spread of the cells to distant

organs as is normally seen in mice implanted with MDA-MB-231 cells (Sossey-Alaoui *et al.*, 2007).

Another study analysing WAVE and its association with breast cancer demonstrated an overall trend of elevated expression in all three isoforms in the breast tumour tissues relative to normal breast tissue. This pattern of expression was also evident for patients who died from breast cancer with WAVE2 levels showing statistical significance. Furthermore, node-positive specimens and moderately and poorly differentiated tumours exhibited significant WAVE2 overexpression (Fernando *et al*., 2007).

The clinical significance of WAVE in cancer was further implicated by Fernando *et al* who demonstrated higher expression levels of WAVE1 and WAVE3 in the metastatic prostate cancer cell lines, PC-3 and DU-145 in comparison to epithelial prostate cancer cells. Accordingly, immunohistochemistry techniques revealed stronger staining for WAVE1 and WAVE3 in prostate tumour specimens compared to normal prostate specimens. WAVE1 expression knockdown in PC-3 and DU-145 cells revealed a significant reduction in growth rate and invasive capacities of the cells whilst the same approaches were utilised to knockdown WAVE3 expression which showed a significant decrease in cell invasion (Fernando *et al*., 2008; Fernando *et al*., 2010). An independent research group also demonstrated suppression of *in vitro* cell invasion following *WASF3* gene inactivation in metastatic prostate cancer cells, PC-3 and DU-145. Furthermore, they were able to show a reduction in cell motility as well as decreased proliferative abilities which contrast with findings published by Fernando which showed no significant change in cell growth. The same group also evaluated the *in vivo* effects by injecting WAVE3 knockdown prostate cancer cells into the flanks of mice. Tumour growth rate was

significantly reduced with no evidence of metastatic spread to the lungs in mice injected with WAVE3 knockdown cells compared to the control group (Teng *et al*., 2010). These findings mirror those of breast cancer *in vivo* and the effects of WAVE3 knockdown mentioned previously (Sossey-Alaoui *et al*., 2007). The relationship between WAVE and their associated cancer are listed in Table 1.4.

Table 1.4 The relationship between WAVE aberrations and their associated cancers

Molecule	**Aberration**	**Associated cancer**	**Reference**
N-WASP	Decreased expression	Breast cancer	Martin *et al*., 2008
WAVE1	Increased expression	Breast cancer	Fernando *et al*., 2007
		Prostate cancer	Fernando *et al*., 2008
WAVE2	Co-expressed with ARP2	Lung adenocarcinoma	Semba *et al*., 2006
	Co-localised with ARP2	Colorectal cancer	Iwaya *et al*., 2007
	Increased expression	Liver cancer	Yang *et al*., 2006
		Breast cancer	Fernando *et al*., 2007
WAVE3	Increased expression	Breast cancer	Sossey-Alaoui*et al*., 2007
			Fernando *et al*., 2007
	Increased expression	Prostate cancer	Fernando *et al*., 2010

Whilst WAVE proteins are heavily implicated in cell motility, it is interesting to note their invasive potential may result from the regulation of downstream targets. WAVE3 knockdown experiments in the breast cancer cell line MDA-MB-231 displayed cell motility and invasion inhibition. Expression analysis revealed a reduction of MMP-1, MMP-3 and MMP-9 coupled with decreased p38 MAPK levels (Sossey-Alaoui *et al*., 2005). The association between WAVE3 and MMP-9 was investigated more recently in a large cohort of colorectal cancer samples whereby their mRNA and protein levels were analysed using quantitative PCR and immunohistochemistry, respectively. Both approaches revealed over-expression of WAVE3 and MMP-9 in the colorectal cancer tissues compared to their corresponding normal mucosa (Zhang *et al*., 2012). These findings reveal an insight into the WAVE signalling pathway which appears to function through the p38 MAPK pathway to regulate MMP activity, giving rise to the motile and invasive phenotypes commonly attributed to cancer cell metastasis.

1.13 Aims and Objectives

The importance of the WAVE family of proteins as a signal messenger between Rac GTPase and the actin polymerisation promoter Arp2/3 in cell migration is well established. Linking this knowledge to the wealth of literature surrounding uncontrolled migratory potential of cells as a contributory factor in cancer metastasis, has led to the WAVE proteins being a focus of interest in cancer research. Whilst a clear association between aberrant expression of different WAVEs and certain human cancers has been made, the wider picture, encapsulating the molecular mechanisms underlying WAVE mode of action in cell migration, is still poorly

understood. Cell motility is a complex process involving a vast array of proteins influencing different signalling cascades in addition to pathway interplay. Identifying interactions between proteins which impact cell motility will provide insights into the network in which WAVE influences cell function in cancer metastasis. Moreover, due to functional differences between the WAVE isoforms, which may reflect why different WAVEs are linked with pathogenesis of certain cancers, it is important to discern differences in their modes of action and protein cooperation. As a clear link has been made between WAVE1 and 3 with prostate cancer these two isoforms were investigated. With these objectives in mind, the aims of this study are to:

1) Establish WAVE1 and WAVE3 knockdown prostate cancer cell lines to ensure replication of previously published cell function findings
2) Elucidate potential pathways through which WAVE interacts by conducting cell function assays using small molecule inhibitor treatments and utilising confocal microscopy approaches
3) Determine any influence on phosphorylation states of proteins involved in cell motility following WAVE1 or WAVE3 knockdown

Chapter 2

Materials and Methods

2.1 Standard solutions and reagents

All standard chemicals and reagents, unless otherwise stated, were obtained from Sigma-Aldrich (Dorset, UK).

2.1.1 Solutions for cell culture work

0.05M EDTA

One gram KCl (Fisons Scientific Equipment, Loughborough, UK), 5.72g Na_2HPO_4, 1g KH_2PO_4, 40g NaCl and 1.4g EDTA (Duchefa Biochemie, Haarlem, The Netherlands) were dissolved in distilled water to make a final volume of 5L. The solution was adjusted to pH 7.4 before autoclaving and storing for use.

Trypsin (25mg/ml)

Five hundred milligrams trypsin were dissolved in 20ml 0.05M EDTA. The solution was mixed and filtered through a 0.2μm Minisart Syringe filter (Sartorius, Epsom, UK), distributed into 10ml aliquots and stored at -20˚C. When required for cell detachment, one 5ml aliquot was diluted in 100ml of 0.05M EDTA.

Antibiotic and antifungal mix for tissue culture

An antibiotic and antifugal mixture for tissue culture were made consisting of 5g streptomycin, 3.3g penicillin and 12.5mg amphotericin B (2ml of 6.25mg/ml amphotericin B in DMSO). These components were fully dissolved topped up to a total volume of 500ml with BSS, filtered through a 0.2μm Minisart Syringe filter (Sartorius, Epsom, UK) and pipetted into 5ml aliquots. When a 5ml aliquot of this 100x concentrated mix was added to 500ml medium the concentrations of the

antibiotics and antifugal agents were as follows: 100U/ml penicillin, 0.1mg/ml streptomycin and 0.25µg/ml amphotericin B.

Balanced Saline Solution (BSS)

Seventy nine point five grams NaCl, 2.2g KCl, 2.1g KH_2PO_4, and 1.1g Na_2HPO_4 were dissolved in distilled water to make a final volume of 10L. The pH was adjusted to 7.2 before use.

2.1.2 Solutions for cloning work

LB agar

Ten grams of tryptone, 5g yeast extract, 10g NaCl and 15g agar were dissolved in distilled water to a final volume of 1L, the pH adjusted to 7.0 and the solution autoclaved. When required, the solution was heated to yield a liquid state and cooled slightly before adding selective antibiotic (if required). The solution was then poured into $10cm^2$ petri dish plates (Bibby Sterilin Ltd., Staffs, UK), allowed to cool and solidify then inverted for storage at 4˚C until required.

LB broth

Ten grams of tryptone (Duchefa Biochemie, Haarlem, The Netherlands), 5g yeast extract (Duchefa Biochemie, Haarlem, The Netherlands) and 10g NaCl were dissolved in distilled water to a final volume of 1L and the pH adjusted to 7.0. This was autoclaved and allowed to cool before adding selective antibiotic (if required) and stored at room temperature.

2.1.3 Solutions for use in RNA and DNA molecular biology

DEPC water

Two hundred and fifty microlitres diethyl pyrocarbonate (DEPC) were added to 5ml distilled water. This solution was then autoclaved before use.

5x Tris, Boric acid, EDTA (TBE)

Five hundred and forty grams of tris-Cl (Melford Laboratories Ltd., Suffolk, UK), 275g Boric acid (Duchefa Biochemie, Haarlem, The Netherlands) and 46.5g of disodium EDTA were dissolved in distilled water, made up to a final volume of 10L and stored at room temperature. When required, the solution was diluted 1:5 in distilled water prior to use in agarose gel electrophoresis.

SYBR®Safe DNA Gel Stain

A 1:10,000 dilution of SYBR®Safe DNA Gel Stain (Invitrogen, Life Technologies Ltd, Paisley, UK) was used to stain DNA in the agarose gel following electrophoresis as specified by manufacture's intructions.

2.1.4 Solutions for protein work

2X Lysis Buffer

A mixture of solutions comprising one hundred and fifty millimolar NaCl (8.76g/l), 50mM Tris (6.05g/l), 0.02% sodium azide (200mg/l), 0.5% sodium deoxycholate (5g/l) and 1.5% Triton X-100 (15ml/l, v/v) was diluted in 1L distilled water and stored at 4˚C until required.

2X Inhibitor buffer

Five millimolar Na_3VO_4 (919.5mg/l), 1µg/ml aprotinin (1mg/L) and 1µg/ml leupeptin (1mg/L) were dissolved in 1L distilled water and kept at 4˚C until required.

Phenylmethanesulphonylfluoride (PMSF)

Five millilitres of phenylmethanesulphonylfluoride (10mg/ml) were dissolved in 495ml isopropanol to obtain a concentration of 100µg/ml.

Dithiothreitol (DTT)

Five millilitres of DTT (10mM) were diluted in 495ml distilled water to yield a final concentration of 100µM.

10% Sodium dodecyl sulphate (SDS)

One gram of sodium dodecyl sulphate was dissolved in 10ml of distilled water and stored at room temperature until required.

10% Ammonium Persulphate (APS)

One gram of ammonium persulphate was dissolved in 10ml of distilled water and stored at 4˚C until required.

10x Running buffer

Three hundred and three grams Tris, 1.44Kg Glycine and 100g SDS were dissolved in distilled water to a final volume of 10L. The solution was further diluted to 1X strength before use.

Transfer buffer

Seventy two grams of glycine, 15.15g Tris and 1L Methanol (Fisher Scientific, Leicestershire, UK) were dissolved in distilled water to a final volume of 5 litres.

10X TBS

One hundred and twenty one point one grams of Tris and 400.3g NaCl were dissolved in distilled water, made up to a final volume of 5L and adjusted to pH 7.4.

2.2 Cell line work

2.2.1 Cell line

Cell lines used throughout this thesis were cultured under conditions listed in section 2.2.4. The PC-3 cell is derived from bone metastases of a grade IV prostatic adenocarcinoma from a 62 year old male. PC-3 cells are adherent and epithelial in morphology. The cell line is androgen insensitive and is highly tumorigenic. The PC-3 cell line was obtained from the American type culture collection (ATCC, Rockville, Maryland, USA).

2.2.2 Preparation of cell medium

Cells were routinely cultured in Dulbecco's Modified Eagle's medium (DMEM / Ham's F12 with L-Glutamine), pH 7.3 containing 2mM L-glutamine and 4.5mM $NaHCO_3$ supplemented with streptomycin, penicillin, amphotericin B and 10% heat inactivated foetal calf serum. Cell lines transfected with the pEF6 plasmid were

cultured in blasticidin S (Melford Laboratories Ltd, Suffolk, UK) selection medium at a concentration of 5μg/ml for at least 7 days and subsequently in a blasticidin S maintenance medium at a concentration of 0.5μg/ml (according to manufacturer's recommendation and routine protocol in the research laboratory).

2.2.3 Revival of cells from liquid nitrogen

When cells were required, cryotubes (Greiner Bio-One Ltd, Gloucestershire, UK) containing the desired cells were removed from storage in liquid nitrogen and revived for culture using the following steps. Cells were thawed rapidly following their removal from liquid nitrogen before the transfer of contents into a universal container containing 10ml of pre-warmed medium to immediately dilute the DMSO present in the storage medium. This was then centrifuged at 1,800 RPM for 10 minutes to form a cell pellet. The medium was aspirated to remove any traces of DMSO, the cell pellet resuspended in 5ml of pre-warmed medium, placed into a fresh 25cm^2 tissue culture flask (Greiner Bio-One Ltd, Gloucestershire, UK) and incubated for 4 - 5 hours. Following examination under a microscope to determine adherence of cells to the flask, the medium was changed to remove dead cells and residual DMSO then returned to the incubator.

2.2.4 Maintenance of cells

Cells were maintained in supplemented DMEM medium prepared as described in Section 2.2.2, and routinely sub-cultured upon reaching 60-80% confluency as described later in Section 2.3.5. Confluence was assessed by visualising the

approximate coverage of cells over the surface of the tissue culture flask using a light microscope. Cells were maintained and grown in either $25cm^2$ or $75cm^2$ tissue culture flasks (Greiner Bio-One Ltd, Gloucestershire, UK), in an incubator at 37°C, 5% CO_2 and 95% humidity. All tissue culture techniques were carried out following aseptic techniques using autoclaved and sterile equipment inside a Class II laminar flow cabinet which had been cleaned prior to and following use with 70% ethanol.

2.2.5 Detachment of adherent cells and cell counting

Upon reaching approximately 60-80% confluency, medium was aspirated and adherent cells were detached from the tissue culture flask by incubating with 1-2ml of trypsin/EDTA for several minutes. Once detached the cell suspension was placed in a 30ml universal container (Greiner Bio-One Ltd, Gloucestershire, UK) and centrifuged at 1,800 RPM for 10 minutes to form a cell pellet. The cell pellet was typically resuspended in 1ml fresh medium to allow a determination of cell density. Cells were counted in a haemocytometer counting chamber (Hawksley, Sussex, UK) using an inverted microscope (Ceti Microscopes; Medline,Oxon, UK) under 10 x 10 magnification. Each 16 square area of the haemocytometer counting chamber measuring 1mm x 1mm x 0.2mm allowed calculation of the number of cells per millilitre using the following equation:

$$\text{Cell no. / ml} = (\text{number of cell in 16 square area} \div 2) \times 10^4$$

Two 16 square areas of the haemocytometer counting chamber were counted and the mean was used to calculate cell number per millilitre which was then used to

calculate volume of resuspended cells for use in the appropriate *in vitro* cell function assays.

2.2.6 Storage of cell stocks in liquid nitrogen

Stocks of low passage cells were stored in liquid nitrogen. Cells were first detached from their flasks using EDTA/Trypsin as described in Section 2.2.5 and pelleted in a centrifuge at 1,800 RPM for 10 minutes. These cells were resuspended in the required volume (dependent on the number of samples to be frozen) of a protective medium consisting of 10% dimethyl sulphoxide (DMSO) in normal growth medium. Following resuspension, cells were aliquoted into pre-labelled 1.8ml cryotubes (Greiner Bio-One Ltd, Gloucestershire, UK), in 1 ml volumes, wrapped loosely in tissue paper and stored overnight at -80°C in a deep freezer. Cells were later transferred to liquid nitrogen tanks for long term storage.

2.3 Generation of mutant PC-3 cell lines

2.3.1 Production of ribozyme transgenes

Ribozyme transgenes were designed to specifically target and cleave either WAVE1 or WAVE3 messenger RNA transcripts to down regulate their expression. These ribozyme constructs were developed previous to this study by Fernando *et al* (2008; 2010) however the steps are outlined here. The secondary structure of the WAVE 1 and WAVE 3 transcript was initially predicted using Zuker's RNA mFold software (Zuker, 2003) (Predicted structures shown in Figures 2.1a and 2.1b). Doing so allowed identification of loop structures which are unpaired regions and are less

stable than paired stemmed regions and therefore make them good ribozyme targets. Suitable GUC or AUC ribozyme target sites were selected from the predicted secondary structure loop structures and a ribozyme was designed for that region, allowing it to specifically bind to the sequence surrounding the target GUC or AUC codon regions. Doing so, allowed the hammerhead catalytic region of the ribozyme transgene to interact with and accurately cleave the mRNA transcript of interest at the specific GUC codon sequence. The secondary structure of the hammerhead ribozyme is shown in Figure 2.1c whilst its mode of action is depicted in Figure 2.2.

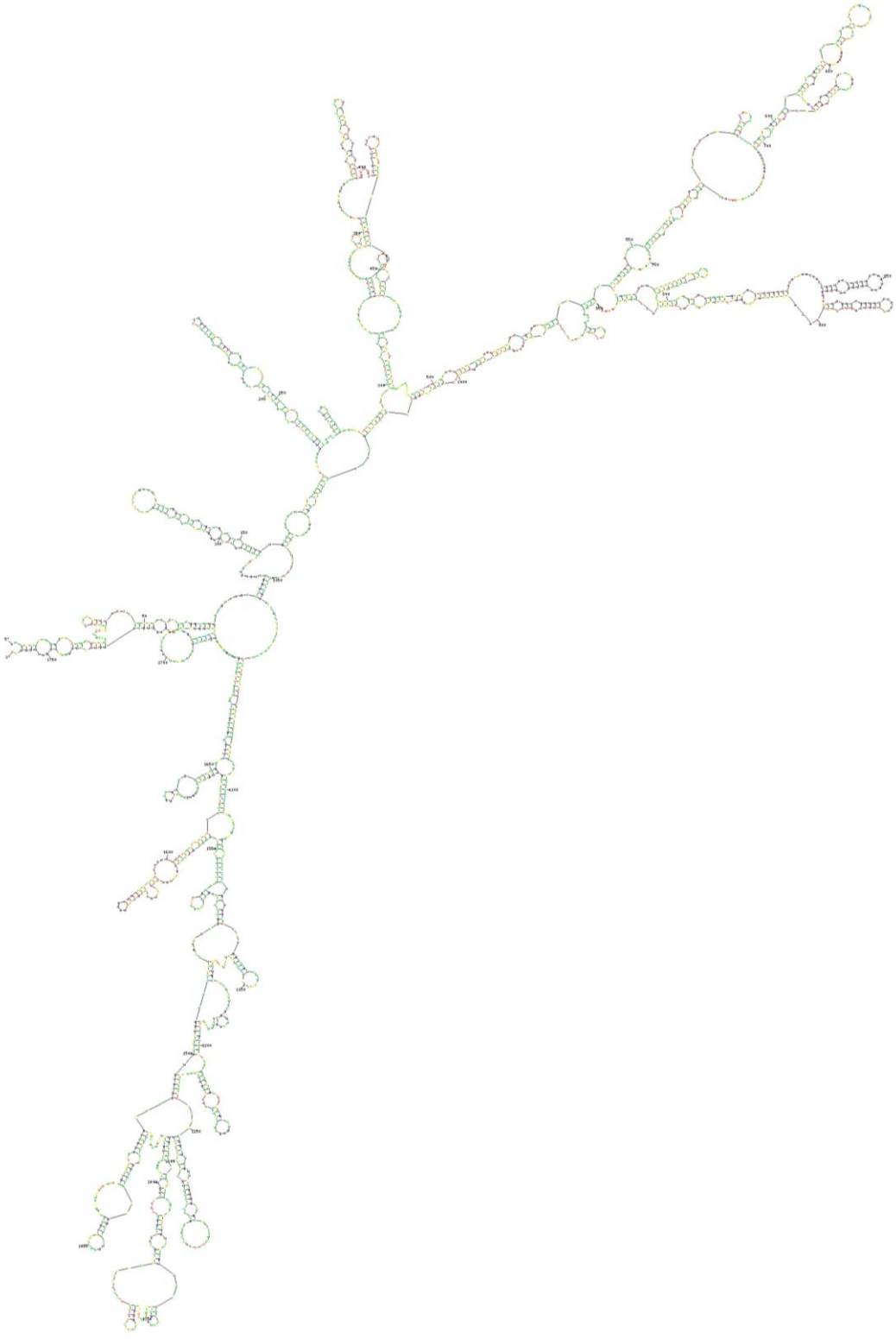

Figure 2.1a. Secondary structure of human WAVE1 mRNA based on the Zuker programme

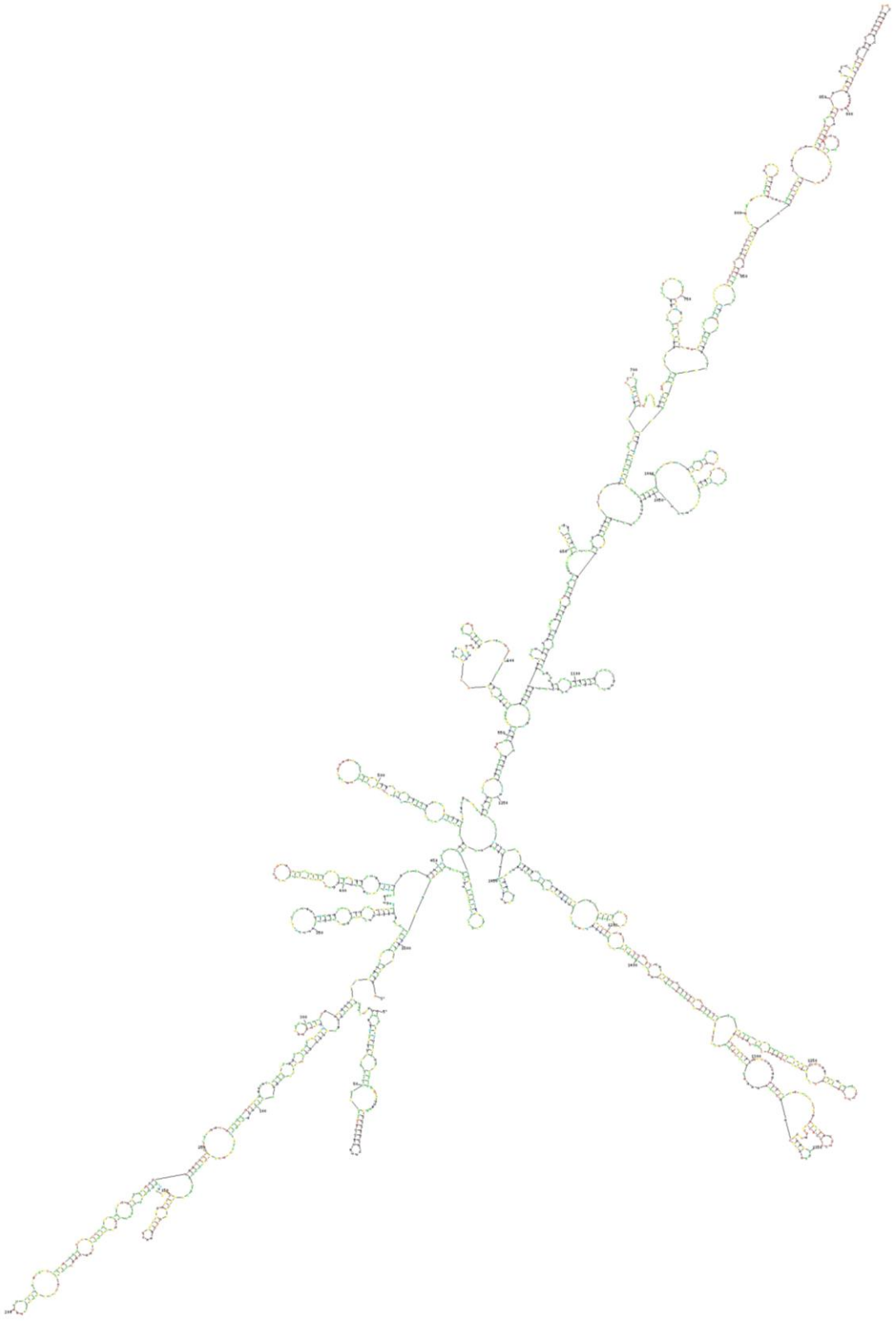

Figure 2.1b. Secondary structure of human WAVE3 mRNA based on the Zuker programme

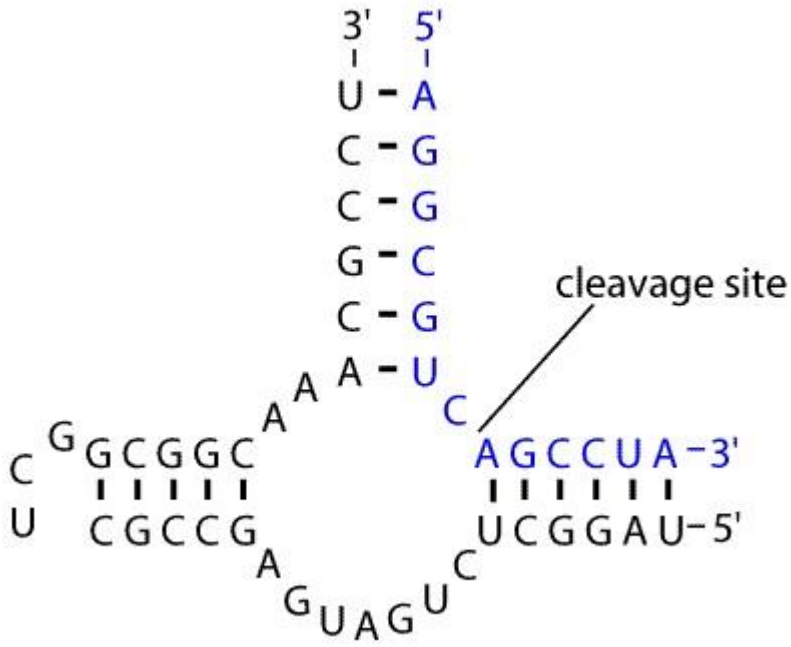

Figure 2.1c. Representative diagram of the secondary structure of a hammerhead ribozyme and its associated substrate (Figure taken from Shaw *et al*, 2001)

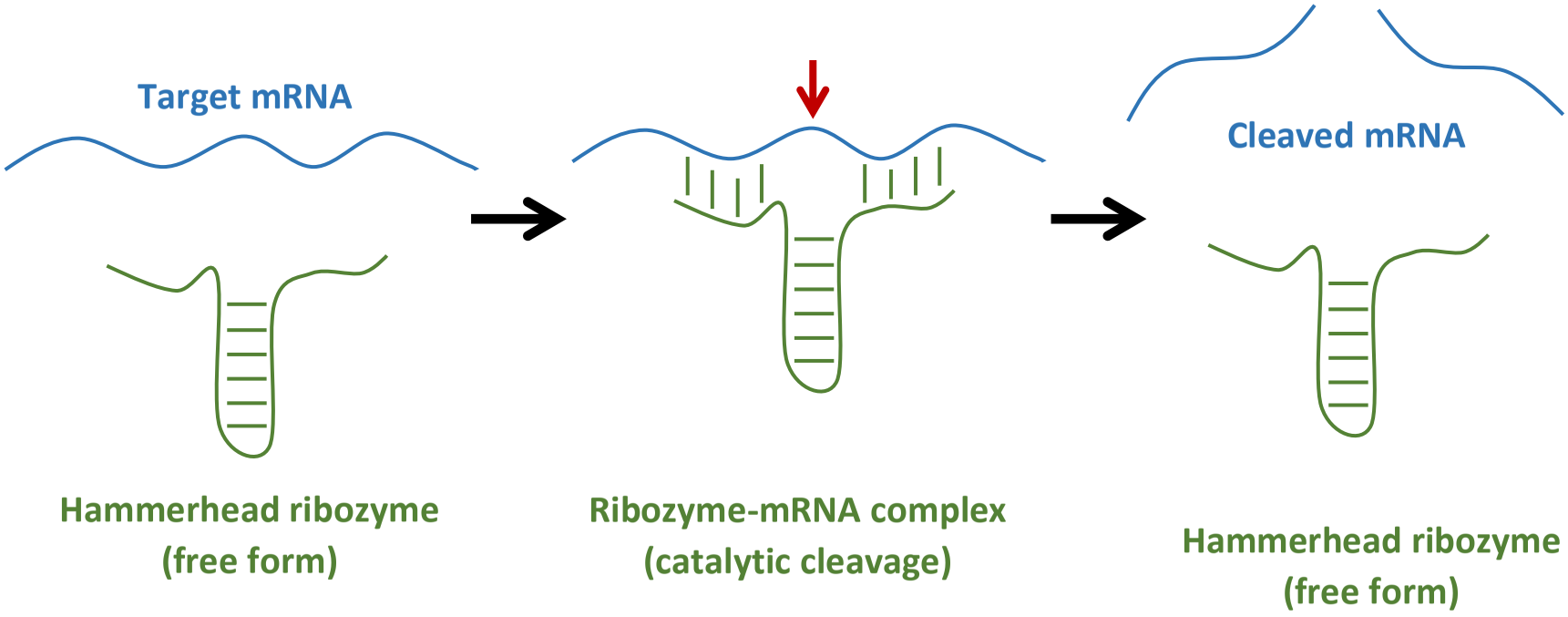

Figure 2.2 Schematic representation of the mode of action elicited on target mRNA by their specifically designed hammerhead ribozymes. The ribozyme hybridises to the substrate and enzymatically cleaves at the target site. Dissociation from the substrate sees the release of the cleaved product (Figure adapted from Mulbacher et al, 2010).

Once designed, the oligo sequences for the ribozyme transgene were synthesised by Invitrogen as sense/antisense strands (ribozyme transgene sequences are shown in Table 2.1). Incorporation of these strands into the transgene was achieved using touchdown PCR. The touchdown PCR parameters were as follows:

• Step 1: Initial denaturing period – 94°C for 5 minutes

• Step 2: Denaturing step – 94°C for 10 seconds

• Step 3: Various annealing steps – 70°C for 15 seconds, 65°C for 15 seconds, 60°C for 15 seconds, 57°C for 15 seconds, 54°C for 15 seconds and 50°C for 15 seconds.

• Step 4: Extension step – 72°C for 20 seconds

• Step 5: Final extension period – 72°C for 7 minutes

Step 2 – 4 was repeated over 48 cycles, each different annealing temperature comprising 8 cycles.

Once combined, the transgenes were electrophoresed on a 2% agarose gel to confirm presence and correct size before being inserted into the pEF6 plasmid in the TOPO cloning reaction, as described in a later section.

Table 2.1. Ribozyme transgene sequences used for the TOPO cloning step

Target gene	**Ribozyme**	**Ribozyme sequence 5'-3'**
WAVE1	WAVE1Rib1F	CTGCAGCATCATCTTCAGCCAGCTCTGCTGATGAGTCCGTGAGGA
	WAVE1Rib1R	ACTAGTTGGCAGAAGCTGGCCCAAGTTTCGTCCTCACGGACT
	WAVE1Rib2F	CTGCAGTTCATGAGGAAGATCTACTGATGAGTCCGTGAGGA
	WAVE1Rib2R	CTAGTCATGACAGGCAGAAAAATTTCGTCCTCACGGACT
WAVE3	WAVE3Rib1F	CTGCAGTTGTAAATATCAGCAACAGCTGATGAGTCCGTGAGGA
	WAVE3Rib1R	ACTAGTTTCAAAGAACAGCATTCCTAATTTCGTCCTCACGGACT
	WAVE3Rib2F	CTGCAGCCCCCTCTGGGGCCTGAGGGGCTGATGAGTCCGTGAGG
	WAVE3Rib2R	ACTAGTCAGCCGCCCCCCCGGCGTTTCGTCCTCACGGACT

2.3.2 TOPO cloning reaction

Cloning of all ribozyme transgene sequences was achieved using the pEF6/V5-His TOPO TA Expression Kit (Invitrogen, Life Technologies Ltd , UK) following the manufacturer's protocol provided described here. This kit allows fast effective cloning of *Taq* polymerase amplified products for expression in mammalian cells. The following TOPO cloning reaction was set up in a pre-labelled eppendorf tube for each ribozyme transgene sequence used:

- PCR product (ribozyme transgene) – 4µl
- Salt solution – 1µl
- TOPO vector – 1µl

This reaction was gently mixed and incubated at room temperature for 30 minutes and stored in ice before proceeding to One Shot Chemical Transformation.

2.3.3 Transformation of chemically competent *Escherichia coli*

A 5µl volume from the TOPO cloning reaction outlined in Section 2.3.2 was added to a vial of One Shot TOP10 Chemically Competent *E. coli* and gently mixed by stirring the mixture in the eppendorf tube using the pipette tip as opposed to pipetting up and down to avoid damage to the bacteria. The vial was placed in ice for 30 minutes, exposed to heat-shock treatment at 42˚C for 30 seconds and immediately placed back into ice. To each tube, 250µl of SOC medium (2% Tryptone, 0.5% yeast extract, 10nM NaCl, 2.5mM KCl, 10mM $MgCl_2$, 10mM $MgSO_4$ and 20mM glucose) at room temperature were added followed by shaking at 200 RPM on a horizontal

orbital shaker (Bibby Stuart Scientific, UK), at 37°C for 1 hour. Following this incubation period, the contents of the tube were spread at a high and low seeding density onto two separate selective agar plates containing 100μg/ml ampicillin (Melford Laboratories Ltd., Suffolk, UK) and allowed to grow overnight at 37˚C in an incubator. As the pEF6 plasmid contains two antibiotic resistance genes that allow cells containing the plasmid to grow in the presence of ampicillin and blasticidin S selection, any colonies successfully growing on these plates should theoretically contain the pEF6 plasmid (refer to Figure 2.3).

2.3.4 Selection and orientation analysis of positive colonies

Confirmation of correct insertion and orientation of the ribozyme sequence in the pEF6 plasmid was analysed to ensure whether transcription of the sequence would generate the transcript of interest. The colonies were tested using polymerase chain reaction (PCR) using primers specific to either the plasmid or the ribozyme sequence. To check the orientation of the ribozyme sequences a combination of T7F vs RbToP and T7F vs RbBMR were used (refer to Table 2.2). RbToP and RbBMR recognise and bind to sequences within the ribozyme transgene that are common to all of the ribozymes used. There are approximately 90bp between the T7F promoter and the beginning of the insert. Thus, correct orientation and ribozyme size (based on approximate ribozyme size of 50bp), would be confirmed by a band of approximately 140bp in the T7F vs RbBMR reaction. Likewise, a band of approximately 140bp in the T7F vs RbToP would indicate incorrect orientation of the sequence.

Table 2.2 Plasmid/ribozyme specific primers

Primer name	**Primer sequence**
T7F	TAATACGACTCACTATAGGG
RbBMR	TTCGTCCTCACGGACTCATCAG
RbToP	CTGATGAGTCCGTGAGGACGA

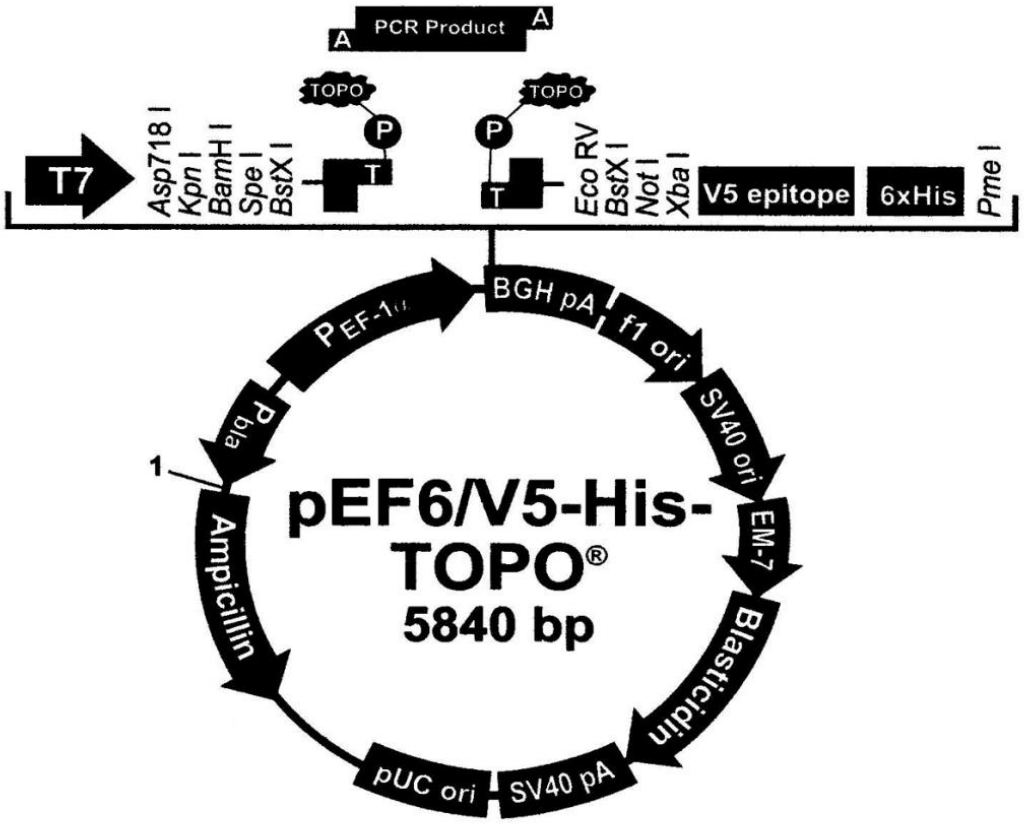

Figure 2.3 Schematic diagram of the pEF6 plasmid used during cell transfection. Figure was taken from the pEF6/V5-His TOPO TA Expression Kit protocol (Invitrogen, Life Technologies Ltd, UK)

Following overnight incubation, the plates were examined for colony growth. Colonies were selected for orientation analysis and labelled on the Petri dishes. Two PCR reactions were carried out for each selected colony using the following parameters (full primer sequences are given in Table 2.3 shown in the RT-PCR Section 2.4.4):

Ribozyme orientation reaction 1

• 8µl – 2x GoTaq Green Master mix (Promega, Dorset, UK)

• 1µl – T7F plasmid specific forward primer

• 1µl – Ribozyme specific forward primer (RbToP)

• 6µl – PCR water

Ribozyme orientation reaction 2

• 8µl – 2x GoTaq Green Master mix (Promega, Dorset, UK)

• 1µl – T7F plasmid specific primer

• 1µl – Ribozyme specific reverse primer (RbBMR)

• 6µl – PCR water

In order to test the orientation of the inserted ribozyme sequence present in the colonies, a sample was picked from the plate using a sterile pipette tip and inoculated into both mixes before the addition of the specific primers. Each reaction mix was then placed in a thermal cycler and subjected to the following conditions:

• Step 1: Initial denaturing period – 95˚C for 10 minutes

• Step 2: Denaturing step – 94˚C for 1 minute

• Step 3: Annealing step – 55˚C for 1 minute } 34 cycles

• Step 4: Extension step – 72˚C for 1 minute

• Step 5: Final extension period – 72˚C for 10 minutes

The mixture was run on a 2% agarose gel and visualized under ultra violet light. Colonies showing correct orientation of the insert were picked off the plate, used to inoculate 10ml of ampicillin selective LB broth and incubated overnight whilst being horizontally shaken at 225 RPM.

2.3.5 Plasmid extraction, purification and quantification

Plasmid extraction was undertaken using the Sigma GenElute Plasmid MiniPrep Kit according to the manufacturer's protocol. Five millilitres of the LB broth, previously inoculated with the correct colony and cultured overnight, were centrifuged at 3,000 RPM for 10 minutes to obtain a pellet of bacteria. The supernatant was discarded and the bacterial pellet was resuspended in 200µl of resuspension solution (containing RNase A) and mixed through repetitive pipetting. Two hundred microlitres of lysis solution were then added to the container and inverted 5 - 6 times. This stage was completed within 5 minutes before adding 350µl of the neutralisation solution, inverting 4 – 6 times and centrifuging at 12,000 RPM in a microcentrifuge. Plasmid DNA was bound to the column by transferring the cleared lysate to a Mini Spin Column placed inside a collection tube, spinning at 12,000 RPM for 30 seconds to 1 minute and discarding the flow through. Seven hundred and fifty microlitres of wash solution (containing ethanol) were added to the column before spinning at 12,000 RPM for 30 seconds to 1 minute and again discarding flow through. The column was spun at 12,000 RPM for 30 seconds – 1 minute to remove any remaining flow through before transferring the Mini Spin Column to a fresh collection tube.

Plasmid DNA was eluted by the addition of 100µl of elution solution and spinning the column at 12,000 RPM for 1 minute. The eluted plasmid solution was then

electrophoresed on a 0.8% agarose gel to confirm presence and correct size of the plasmid.

2.3.6 Transfection of mammalian cells using electroporation

Following plasmid purification and quantification (quantification carried out utilising protocol as described for RNA quantification in Section 2.4.2 with a configuration to detect double stranded DNA and DEPC water substituted for elution solution) 1-10µg of the extracted plasmid was used to transform the PC-3 prostate cancer cell line. Confluent PC-3 wild type cells were detached from tissue culture flasks using trypsin/EDTA, pelleted and resuspensed in the required volume of medium. Six hundred microlitres of this cell suspension was added to an electroporation cuvette (Eurgenetech, Southampton, UK) together with the purified plasmid. This was mixed briefly before being subjected to an electrical pulse of 290V and 1500 capacitance from an electroporator (Easyject, Flowgene, Surrey, UK). Following this pulse, the cell and plasmid suspension was quickly transferred into 10ml of pre-warmed medium and placed in an incubator to allow any surviving cells to fully recover from the electroporation process.

2.3.7 Establishment of stably transformed PC-3 prostate cancer cell lines

The pEF6 plasmid used to transform the cells, encodes two antibiotic resistance genes. As previously described, the ampicillin resistance gene allows initial selection of bacterial cells containing the plasmid. The plasmid also contains a blasticidin S resistance gene. Blasticidin S is a potent microbial antibiotic that inhibits protein

synthesis in both prokaryotes and eukaryotes and is used to specifically select for mammalian cells containing the pEF6 plasmid. The use of two antibiotic resistance genes allows an accurate selection of plasmid containing cells throughout the cloning process. Following overnight incubation, the cells were subjected to an initial intense selection period of 7 days. During this 7 day period, the cells were incubated in medium that had been supplemented with 5μg/ml of the blasticidin S antibiotic (Melford Laboratories Ltd., Suffolk, UK) to kill all cells that did not contain the pEF6 plasmid. After this initial intense selection the cells were maintained in maintenance medium containing 0.5μg/ml of blasticidin S, this maintains a selection pressure on the cells to retain the plasmid and results in long term transformation of the cells.

All cells were tested initially and following routine use, to estimate the efficacy and stability of both the transformation and the ribozyme transgene or expression sequence using RT-PCR and Western blot analysis. This methodology for altering the expression levels of various proteins within mammalian cells is well established within our research group.

2.4 Synthesis of complementary DNA for use in PCR analysis

2.4.1 Total RNA isolation

RNA isolation was completed using the TRI Reagent RNA Isolation Reagent and protocol. Cells were cultured until 60-80% confluent; the medium was aspirated prior to the addition of 1ml TRI Reagent which aids the detachment of the cell monoloayer and induces cell lysis. After approximately 5 minutes at room

temperature, a cell scraper was used to physically remove the cell monoloayer into the TRI Reagent allowing transfer of the cell lysate into an Eppendorf tube. After the addition of 200µl chloroform to the cell lysate, the Eppendorf was shaken vigorously, inverted multiple times for 15 seconds and then centrifuged in a refrigerated centrifuge at 4-5°C (Boeco, Germany) for 15 minutes at 12,000 RPM. After centrifugation, the homogenate separates into three phases: the lower pink organic phase contains protein, the murky inter phase contains DNA whilst the upper aqueous phase contains RNA. This upper aqueous layer was transferred to a fresh Eppendorf tube containing 500µl isopropanol and left at room temperature for 10 minutes before centrifugation at 12,000 RPM for 10 minutes at 4˚C. Due to the insolubility of RNA in isopropanol, this step precipitates RNA out of the solution and forms a visible pellet at the bottom of the Eppendorf tube. The supernatant was discarded, 1ml 75% ethanol (3:1 ratio of ethanol to DEPC water) added to the pellet and the mixture was then centrifuged at 7,500 RPM for 5 minutes at 4˚C. The ethanol was removed leaving the pellet which was dried in a drying oven (Techne Hybridiser, UK) at 55˚C for 5-10 minutes. The remaining RNA pellet was dissolved in 40-60µl DEPC water (dependent on pellet size) via repetitive pipetting and vortexing for subsequent RNA quantification. The inclusion of histidine-specific alkylating agents in DEPC water inhibits the action of RNases which would otherwise affect RNA sample quality and concentration.

2.4.2 RNA quantitation

Concentration of isolated RNA was determined using a UV1101 Biotech Photometer (WPA, Cambridge, UK) set to read absorbance measurements at 260nm wavelength and was configured to detect single stranded RNA samples at a 1:10 dilution. Prior to RNA sample quantification, the photometer was normalised with DEPC water. All samples and blanks were pipetted into a glass cuvette (StamaBrand, Optiglass Limited, UK).

2.4.3 Reverse transcription-polymerase chain reaction (RT-PCR) of RNA

RNA was used as template for reverse transcription to complementary DNA (cDNA) using High Capacity cDNA Reverse Transcription Kit (Applied Biosystems, Life Technologies Ltd, UK) following the manufacturer's protocol as described here. The quantified RNA was prepared with PCR water to provide a final concentration of 250ng in 10µl which was added to 10µl of 2xRT master mix in a thin-walled 200µl PCR tube (ABgene, Surrey, UK). This was placed into an ABi 2720 Thermal cycler (Applied Biosystems, Life Technologies Ltd, UK) and the following parameters applied:

- 25°C for 10 minutes
- 37°C for 120 minutes
- 85°C for 5 minutes

The newly generated cDNA was diluted 1:4 with PCR water and stored at -20°C until required.

2.4.4 Polymerase chain reaction (PCR)

Polymerase chain reaction (PCR) is a method devised for detecting and amplifying a specific target DNA sequence. PCR was carried out using GoTaq Green Master mix (Promega, Dorset, UK). PCR reactions were set up for each cDNA sample with a total reaction volume of 16µl containing the following reagents:

- 8µl – 2x GreenTaq ReadyMix PCR Reaction mix
- 1µl – Specific forward primer
- 1µl – Specific reverse primer
- 5µl – PCR water
- 1µl – cDNA

Primers were designed using the Beacon Designer programme (Palo Alto, California, USA) and were synthesised by Invitrogen (Paisley, UK). These are listed in Table 2.3. Primers were diluted to a concentration of 10pM before being used in the PCR reaction. The PCR reaction was set up in a 200µl PCR tube (ABgene, Surrey, UK), mixed briefly and centrifuged before being placed in an ABi 2720 Thermocycler (Applied Biosystems; Life Technologies Ltd, Paiseley, UK) and subjected to the following temperature parameters:

- Step 1: Initial denaturing period – 94°C for 5 minutes
- Step 2: Denaturing step – 94°C for 40 seconds

• Step 3: Annealing step – 55°C for 40 seconds

• Step 4: Extension step – 72°C for 40 seconds

• Step 5: Final extension period – 72°C for 10 minutes

Steps 2 – 4 were repeated for typically 34 cycles. Primer binding sites and predicted product sizes were verified using the Primer3 (v.0.4.0) software available online (http://frodo.wi.mit.edu/). RT-PCR products which corresponded with this predicted size following electrophoresis (refer to Section 2.4.5) and staining were taken as being accurate. A negative control which replaced cDNA with PCR water was also included to assess any contamination.

Table 2.3 Primer used for polymerase chain reaction. Primers listed 'ZR' include Z sequences designed for quantitative PCR WAVE1 and 3 primers were previously published (Fernando et al 2008; 2010).

Gene	**Primer**	**Primer sequence 5'-3'**
WAVE1	WAVE1F11	CCTCCTCCACCACCTCTTC
	WAVE1R11	GCACACTCCTGGCATCAC
WAVE3	WAVE3F11	TACTCTTGCCGCTATCATACG
	WAVE3R11	TGCCATCATATTCCACTCCTG
ARP2	ARP2F1	ATTGAGCAAGAGCAGAAACT
	ARP2ZR	ACTGAACCTGACCGTACATTCTGGTGCTTCAAATCTCT
ARP3	ARP3F1	AGAAGTAGGAATCCCTCCCTCCAG
	ARP3ZR	ACTGAACCTGACCGTACATTAATCCATTTTGACCCATC
N-WASP	NWASPF8	AGTCCCTCTTCACTTTCCTC
	NWASPR8	GCTTTTCCCTTCTTCTTTTC
ROCK-I	ROCK1F1	ATGGAAGAGAATGTGACTGG
	ROCK1ZR	ACTGAACCTGACCGTACAGCTGTAAGTTCCAACCAAAG
ROCK-II	ROCKF1	CATATGGACAAAAAGGAGGA
	ROCK2ZR	ACTGAACCTGACCGTACACTGCTTCTGTAGAATTTGC
GAPDH	GAPDHF8	GGCTGCTTTTAACTCTGGTA
	GAPDHR8	GACTGTGGTCATGAGTCCTT
PDPN	PDPLF8	GAATCATCGTTGTGGTTATG
	PDPLZR	ACTGAACCTGACCGTACACTTTCATTTGCCTATCACAT

2.4.5 Agarose gel electrophoresis

The amplified PCR product outlined in the previous section was separated according to product size using agarose gel electrophoresis. Generally, PCR product sizes were approximately 500bp, thus a 0.8% agarose gel was used. For PCR products amplified using primers designed for quantitative PCR (QPCR), these were typically 100-200bp and therefore a 2% agarose gel was used. Powdered agarose (Melford Laboratories Ltd., Suffolk, UK) was added to 1xTBE solution and heated to fully dissolve the agarose. The molten solution was poured into an electrophoresis cassette (Scie-Plas Ltd., Cambridge, UK) prepared with plastic combs creating loading wells once the gel had set. The set agarose gel was placed into the electrophoresis tank and submerged in 1xTBE buffer before the loading of 8µl PCR product and a 100bp DNA ladder (GenScript, New Jersey, USA) after the removal of the combs. The samples were electrophoretically separated at 95 volts for approximately 30 minutes (depending on the degree of separation required) by connecting a power pack to the electrophoretic tank (Gibco BRL, Life Technologies Inc.).

2.4.6 DNA staining and visualisation

Following the separation of PCR products electrophoretically, the agarose gel was placed in SYBR® SAFE (Invitrogen, UK) diluted in 1xTBE buffer at a dilution of 1:10000. The gel was left to stain for approximately 20 minutes with constant agitation to ensure even staining of the gel before visualisation under blue light using the U-Genius3 gel imaging system (Syngene, Cambridge, UK). Images were captured with the integrated camera imaging system, and printed with a SONY thermo printer (SONY UK, London, UK) or saved as a TIFF file. If insufficient

staining was found, the gel was returned to in the SYBR® SAFE solution for further staining or distilled water to destain the gel if it was observed to show too much background staining. Alternatively, 5µl SYBR® SAFE solution was added to 50ml molten agarose before pouring. Following electrophoresis, the gel was visualised under blue light.

2.4.7 Quantitative RT-PCR (Q-RT-PCR)

Q-RT-PCR is a sensitive technique that is capable of detecting very small quantities of cDNA within a sample and also allows an accurate determination of template copy number or gene expression. This technique is based on the principle of a sequence-specific DNA based fluorescent reporter probe which allows the quantification of DNA templates containing the probe sequence (refer to Figure 2.4).

The Q-PCR protocol used in this study utilised the Amplifluor™ Uniprimer™ Universal system (Intergen company®, New York, USA) to quantify transcript copy number. The amplifluor probe carries a 3'region which is complementary to the Z-sequence (ACTGAACCTGACCGTACA) which has been incorporated into one of the primers included in the QPCR reaction. This is used at a 1/10 concentration of the other primer and the amplifluor probe. In addition to the Z sequence specific region found at the 3' end of the probe is the presence of a 5'hairpin structure labelled with a fluorophore tag (FAM). In this hairpin structure the fluorophore tag associates with an acceptor moiety (DABSYL) which quenches fluorescence and therefore produces no signal. During PCR, the specificity of the amplifluor's 3' region to the Z sequence present in the PCR primer generates PCR products with an incorporation of the amplifluor. This sequence itself acts as a template for subsequent

steps in DNA polymerisation resulting in the disruption of the hairpin structure causing fluorescence which can be detected and quantified. The fluorescent signal emitted during QPCR reaction is compared to a range of standards of known transcript copy number thus allowing the calculation of transcript copy number within each sample. The same samples are also run in parallel using primers specific for the gene *GAPDH* whose transcript copy numbers are used to standardise and normalise the calculation of transcript copy number for the gene of interest in the samples.

The cDNA for use in Q-RT-PCR was generated as described in the sections above; this cDNA was then used in the following Q-PCR reaction mix:

Component	**Volume**
iQSupermix (Bio-Rad, UK)	5µl
Forward primer (10pmol/µl)	0.3µl
Reverse Z primer (1pmol/µl)	0.3µl
Probe Ampifluor (10pmol/µl)	0.3µl
PCR water	2.1 µl
cDNA	2µl

Each sample was placed into a 96-well plate (BioRad laboratories, Hemel Hampstead, UK) in parallel with the standards mentioned previously (copy numbers ranging from 10^1 to 10^8) which would permit quantitation of samples (refer to Figure 2.5). The standards used for this purpose were amplified using primers targeting the *PDPN* gene (Podoplanin). Sample cDNA was amplified and quantified over a large number of shorter cycles using an iCycler IQ thermal cycler and detection software (Bio-Rad, UK) and experimental conditions as outlined below:

- Step 1: Initial denaturing period – 95°C for 7 minutes
- Step 2: Denaturing step – 95°C for 10 seconds
- Step 3: Annealing step – 55°C for 35 seconds
- Step 4: Extension step – 72°C for 20 seconds

Step 2 – 4 was repeated over 90 cycles. The camera used in this system was set to detect fluorescent signals during the annealing stage. The calculation of sample copy number depends on the point at which the sample crosses threshold (CT) in comparison to the standards, automatically generated by the instrument software.

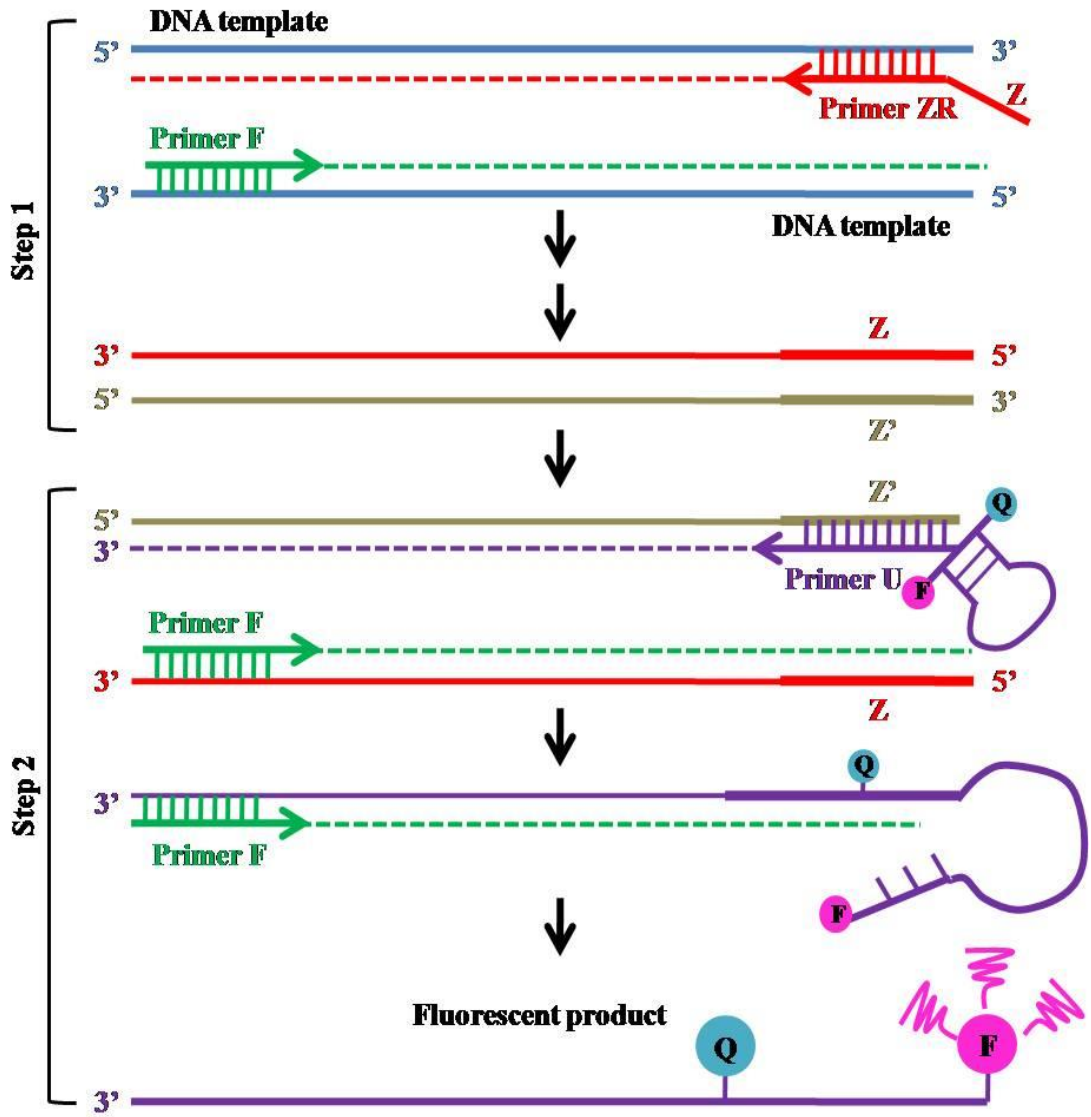

Figure 2.4 Schematic diagram depicting the key steps underlying quantitative PCR when using the uniprimer fluorescent probe

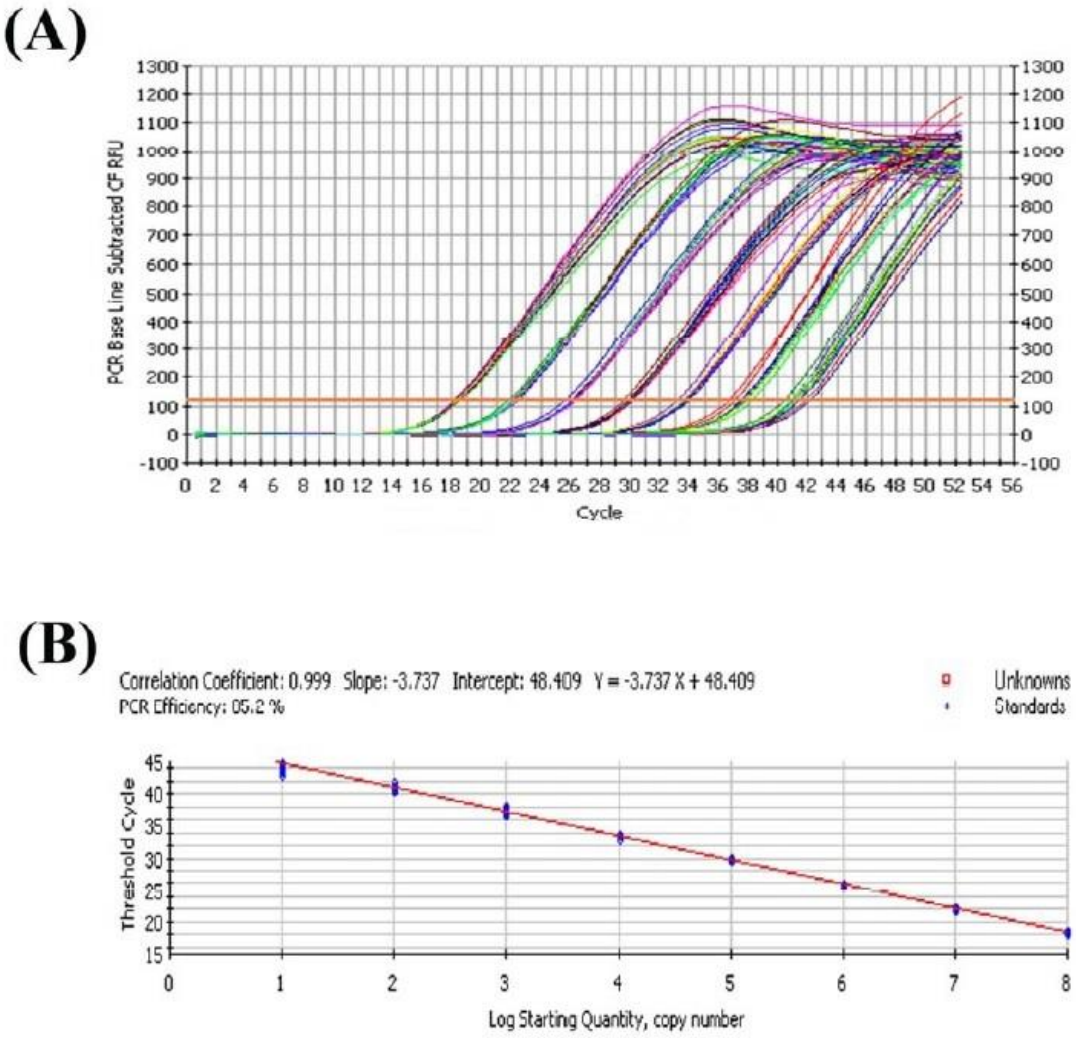

Figure 2.5 Standardisation of transcript copy number (A) Qunatitative PCR was carried out on a series of standard samples ranging from 10^1 to 10^8 (B) A standard curve was generated from the standard samples and was used to determine copy number in tested samples

2.5 SDS-PAGE and Western blotting

2.5.1 Cellular lysis and protein extraction

Upon a cell monolayer reaching sufficient confluency, medium was aspirated from the flask and the cells washed with BSS. A small volume of BSS was added to the flasks for the detachment of the cell monolayer using a sterile cell scraper. Both the detached cells and BSS were transferred to a universal container. The cell suspension was centrifuged at 2,000 RPM for 20 minutes to form a cell pellet. Following centrifugation, BSS was aspirated and the cells were lysed in 200 – 250µl (depending on pellet size) of either SDS or NP40 lysis buffer (depending on application). SDS lysis buffer was made by mixing 4.85ml 2x lysis buffer, 4.85ml 2x inhibitor buffer, 100µl PMSF, 100µl DTT and 100µl SDS (10%), whilst NP40 lysis buffer was made with the same quantities and components but substituting SDS with NP40. Protein extraction using lysis buffer containing SDS totally disrupts the cell membrane and protein:protein interactions. For applications such as immunoprecipitation techniques, where protein interaction is being investigated, SDS lysis buffer is thus not suitable. Alternatively, lysis buffer containing NP40 does not disrupt these protein interactions.

The cell lysate was transferred into a 1.8ml Eppendorf tube (Greiner Bio-One Ltd, Gloucestershire, UK) and placed on a Labinco rotating wheel (Wolf laboratories, York, UK) for approximately 1 hour in a refrigerator (4-5°C). The lysis solution was then spun at 13,000 RPM in a microcentrifuge for 15 minutes to pellet insoluble material. The subsequent protein concentration of the aspirated supernatant was determined as described in Section 2.5.2.

2.5.2 Protein quantification

Prior to their use in Western blotting, determination of protein concentration in the samples were quantified using a Bio-Rad DC Protein Assay kit (Bio-Rad, UK) following the 96-well plate protocol as described here. Bovine serum albumin (BSA) at a concentration of 100mg/ml was used to make serial standard dilutions in lysis buffer ranging from 50 mg/ml to 0.02 mg/ml. Five microlitres of either the sample or standard was pipetted into an empty well before adding 25µl of 'working reagent A' followed by 200µl of reagent B. 'Working reagent A' was prepared by combining each millilitre of reagent A with 20µl of reagent S which was used for detergent containing samples. Following addition of reagent B, samples were mixed briefly and then left for approximately 45 minutes to allow the colorimetric reaction to fully occur. Absorbance of samples and standards at 620nm was then measured using an ELx800 plate reading spectrophotometer (Bio-Tek, North Star Scientific, Leeds, UK). A standard curve was constructed based on the absorbance of the BSA standards which allowed determination of the protein sample concentrations. All samples were normalised to the desired final concentration of between 1.0 and 1.5mg/ml by dilution in an appropriate amount of lysis buffer (as described in section 2.5.1) and further diluted at a 1:1 ratio with 2x Lamelli sample buffer concentrate. Samples were then boiled at 100°C for 5 minutes and stored at -20°C prior to use.

2.5.3 Immunoprecipitation

When assessing protein interactions, immunoprecipitation techniques were utilised prior to the subsequent steps outlined in Sections 2.5.4 to 2.5.7. In this case, proteins were first extracted with a lysis buffer free of SDS but substituted with NP40. After

protein quantification, the samples were standardised to a final concentration of 1-2mg/ml via dilution with lysis buffer in a total volume of 100µl in an Eppendorf tube. An additional protein sample was prepared at the same concentration but to a final volume of 30µl, this comprised the raw lysate for subsequent use. A 100µl volume of antibody specific for the initial protein of interest was added to the 100µl protein volume tube at a dilution of 1:5 and was then placed on a rotating wheel for 1-2 hours at 4°C. The antibodies used for this step are listed in Table 2.4. After this time, 20µl of Protein AG agarose immunoprecipitation reagent beads (Santa Cruz Biotechnology, California) were pipetted into each tube and returned to the rotating wheel for at least 2 hours. The Eppendorfs tubes were centrifuged at 8,000 RPM for 5 minutes after which the supernatant was removed for the addition of 300µl lysis buffer to the tube and centrifuged again at 8,000 RPM for 5 minutes. This step was repeated to provide a total of three washes. After the final wash, the supernatant was removed for the addition of 50µl of 1x Laemmli buffer and boiled for 5 minutes. The raw lysate samples were also boiled for 5 minutes following the addition of an equal volume of 2x Laemmli buffer. These samples were then stored at -20°C until required for SDS-PAGE.

2.5.4 Sodium dodecyl sulphate polyacrylamide gel electrophoresis (SDS-PAGE)

SDS-PAGE was used to detect the presence, or absence, of specific proteins. SDS-PAGE was undertaken using an OmniPAGE VS10 vertical electrophoresis system (Cleaver Scientific, Warwickshire, UK). Resolving gels of a particular acrylamide percentage (depending on the predicted size of the protein of interest) were made up in a universal container and added in-between glass plates held in place in a loading

cassette. Typically, proteins ranging from approximately 50-100kDa were separated with an 8% resolving gel whilst a 10% resolving gel was prepared for proteins of approximately 20-90kDa. The components and their quantities for making these gels at a total volume of 15ml (sufficient for two gels) are as follows:

Resolving gel component	**10% acrylamide gel**	**8% acrylamide gel**
Distilled water	5.9ml	6.9ml
30% acrylamide mix	5.0ml	4.0ml
1.5M Tris (pH 8.8)	3.8ml	3.8ml
10% SDS	150µl	150µl
10% APS	150µl	150µl
TEMED	6µl	9µl

Once the resolving gel had set, the stacking gel was prepared and added to the top of the resolving gel. A plastic comb was placed in the unset stacking gel and the mixture was left to harden. The components and quantities required to prepare 5ml of stacking gel solution (enough for two gels) are as follows:

Stacking gel component	**Volume**
Distilled water	3.4ml
30% acrylamide mix	830µl
1.5M Tris (pH 6.8)	630µl
10% SDS	50µl
10% APS	50µl
TEMED	5µl

Once both resolving and stacking gels had set, the loading cassette was placed into an electrophoresis tank and submerged in 1x running buffer. The combs were removed for the addition of 10µl of broad range marker whilst a volume of 10-18µl of protein sample was added to separate wells (volume loaded dependant on protein concentration). The proteins were then electrophoretically separated according to molecular weight at 100V, 50mA and 50W for approximately 2.5-3 hours (dependent on protein size and acrylamide gel percentage).

2.5.5 Western blotting

Following PAGE of the protein samples the bands were transferred to a nitrocellulose membrane using Western blotting. Gels were removed from the electrophoretic tank and unclipped from the loading cassette; the stacking gel was cut away and the resolving gel placed on top of UltraCruz™ Nitrocellulose Pure Transfer Membrane with a 0.45µM pore size (Santa Cruz Biotechnology, California) which had been pre-soaked in 1x transfer buffer and assembled in a SD10 SemiDry Maxi System blotting unit (SemiDRY, Wolf Laboratories, York, UK). The arrangement of 3 sheets of pre-soaked 3mm chromatography paper (Whatman International Ltd., Maidstone, UK) as filter paper, the acrylamide gel and nitrocellulose membrane within this blotting platform is depicted in Figure 2.6. Electroblotting was undertaken at 15V, 500mA, 8W over a 1 hour period. Once complete, the membranes were carefully removed for subsequent steps.

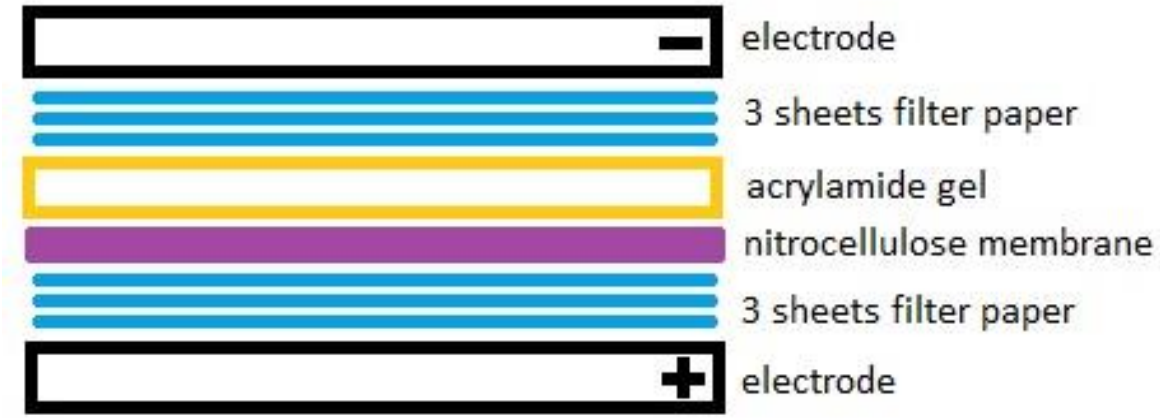

Figure 2.6 Schematic diagram of the arrangement of components for transferring proteins separated during SDS-PAGE in acrylamide gels onto nitrocellulose membrane utilising Western blotting

2.5.6 Staining of proteins

2.5.6.1 Nitrocellulose membrane staining

Membranes were stained prior to probing with specific antibodies to confirm successful transfer or to aid in the sectioning of the membrane. Membranes were placed in Ponceau S solution for several minutes to allow visualisation of protein bands on the membrane, the membrane was then cut into the required number of sections before washing off the stain several times in distilled water.

2.5.6.2 Detection of proteins using specific antibody probing

Membranes were probed with protein specific antibodies utilising the SNAP i.d. Protein Detection System (Merck Millipore, Darmstadt, Germany). This vacuum-driven platform incorporates the blocking, antibody incubation and washing steps which can all be completed within 30 minutes. Prior to these steps, distilled water was used to wet the membrane layer of the blot holder before placing the nitrocellulose membrane protein side down. A membrane roller was used to remove air bubbles before placing a blot spacer on top and rolled again. The blot holder was clipped shut and then placed and secured into the chamber of the SNAP i.d. system with the protein side up. A volume of 30ml blocking buffer comprised of 0.2% milk (Marvel dried skimmed milk), 0.1% TWEEN 1xTBS was added to the wells of the blot holder and vacuum was applied. Following passage of blocking buffer, 3ml primary antibody at a 1:350 dilution was added to the well with the vacuum switched off to allow the antibody to incubate for 10 minutes at room temperature. A list of the primary antibodies used are outlined in Table 2.4. Following this incubation, the

vacuum was applied and wash buffer (0.1% TWEEN 1x TBS) was passed through the membrane three times. Once the well was empty, 3ml secondary antibody at a 1:350 dilution was added to the well with the vacuum turned off and left to incubate for a further 10 minutes at room temperature before three washes with wash buffer. The secondary antibodies that were used are listed in Table 2.5.

Table 2.4 Primary antibodies used for probing proteins following transfer onto nitrocellulose membrane , immunoprecipitation and confocal microscopy setup

Primary antibody	**Molecular weight (kDa)**	**Supplier**	**Product code**	**Application**
Goat anti-WAVE1	84	Santa Cruz Biotechnology	SC-10388	WB/IP
Goat anti-WAVE3	70	R&D Systems	AF5515	WB
Mouse anti-ARP2	43	Santa Cruz Biotechnology	SC-137250	WB/IP
Goat anti-ARP3	53	Santa Cruz Biotechnology	SC-10130	WB/IP
Goat anti-N-WASP	65	Santa Cruz Biotechnology	SC-10122	WB/IP
Mouse anti-ROCK-I	160	Santa Cruz Biotechnology	SC-17794	WB/IP
Rabbit anti-ROCK-II	160	Santa Cruz Biotechnology	SC-5561	WB/IP
Mouse anti-GAPDH	37	Santa Cruz Biotechnology	SC-32233	WB/IP
GOAT anti-WAVE3	70	Santa Cruz Biotechnology	SC-26499	IP
Mouse anti-Phosphotyrosine (PY20)	Dependent on protein	Santa Cruz Biotechnology	SC-508	IP
Mouse anti-phosphotyrosine (PY99)	Dependent on protein	Santa Cruz Biotechnology	SC-7020	IP

Table 2.5 Secondary antibodies used for probing the appropriate primary antibodies listed in Table 2.4 following the steps outlined in Section 2.5.6.2

Secondary antibody	**Molecular weight (kDa)**	**Supplier**	**Product code**
Rabbit anti-mouse (whole molecule) IgG peroxidise conjugate	Dependent on primary	Sigma-Aldrich Ltd, Dorset, UK	A-9044
Goat anti-rabbit (whole molecule) IgG peroxidise conjugate	Dependent on primary	Sigma-Aldrich Ltd, Dorset, UK	A-9169
Rabbit anti-goat (whole molecule) IgG peroxidise conjugate	Dependent on primary	Sigma-Aldrich Ltd, Dorset, UK	A-5420

2.5.7 Chemiluminescent detection of antibody-antigen complex

Following antibody incubation and buffer washes, the membrane was carefully removed from the blot holder and placed into a weighing boat for the addition of 1ml Luminata Forte Western HRP Substrate (Merck Millipore, Darmstadt, Germany) which was left to incubate for 5-10 minutes at room temperature away from light exposure. Excess substrate was removed before placing the membrane into the UVITec imager (UVItec Limited, Cambridge, UK). The image was captured by a camera in the imager which also includes an illuminator. Membranes were subjected to various exposure times and captured images were analysed on a connected computer using UVIprochem software (UVItec Limited, Cambridge, UK).

2.6 Tumour cell functional assays

2.6.1 *In vitro* tumour cell growth assay

Cells were detached from the culture flask and cell density (per millilitre) was established as described previously. Cells were then seeded into a 96 well plate (Greiner Bio-One Ltd, Gloucestershire, UK) at a seeding density of 3,000 cells in 200µl of normal medium. Triplicate plates were set up to obtain a cell density reading following 24, 72 and 120 hour incubation periods. Following the appropriate incubation period, the medium was removed and cells were fixed in 4% formaldehyde in BSS for at least 5 minutes before rinsing and staining in 0.5% (w/v) crystal violet in distilled water for 5 minutes. The stain was then extracted from the cells using 10% acetic acid and cell density determined by measuring the absorbance at 540nm on an ELx800 plate reading spectrophotometer (Bio-Tek, North Star

Scientific, Leeds, UK). The sensitivity of crystal violet staining as a method to quantify cell number is shown in Figure 2.7. Cell growth was presented as percentage increase and calculated by comparing the absorbances obtained for each incubation period using the following equation:

Percentage increase = ((day 3 or 5 absorbance) – day 1 absorbance / day 1 absorbance) X 100

Six replicate wells were set up for each experiment and the entire experiment was repeated at least three times. The *in vitro* cell growth assay outlined here has previously been described and is well established in our research group (Fernando *et al*., 2008).

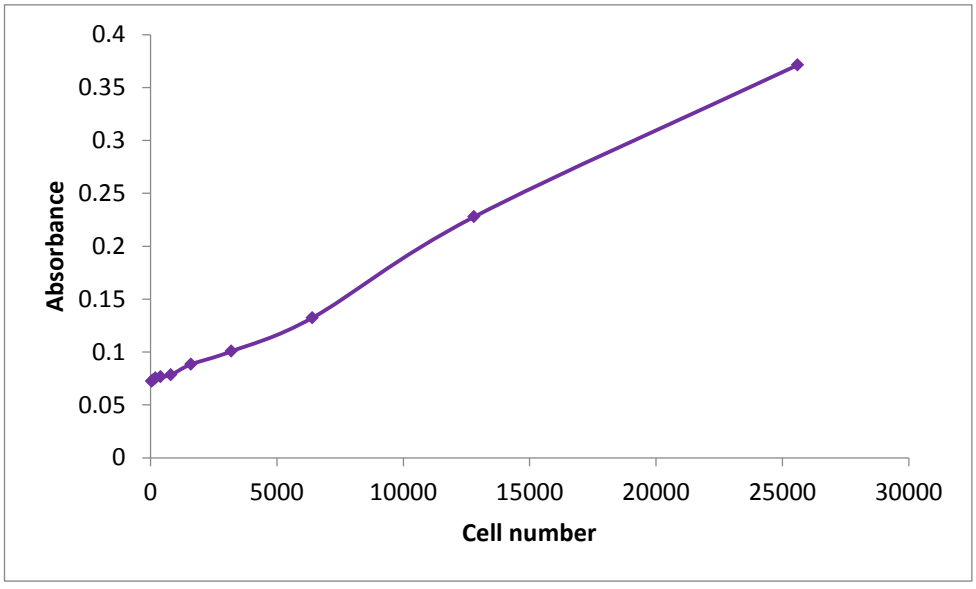

Figure 2.7 Sensitivity of crystal violet assay Graph shows level of absorbance for crystal violet staining and relationship with number of cells

2.6.2 *In vitro* tumour cell Matrigel invasion assay

The invasive capacity of the cells used in this study was determined using an *in vitro* Matrigel invasion assay. This assay measures the cells ability to degrade and invade through an artificial basement membrane and migrate through 8μm pores. Cell culture plate inserts (BD Biosciences, Oxford, UK) containing 8.0μm pores were coated in 50μg of Matrigel (BD Biosciences, Oxford, UK). The working concentration of Matrigel at 500μg/ml was made up in serum free medium where 100μl was added to each insert and allowed to set in a HB-1D Techne Hybridiser drying oven (Techne, Staffordshire, UK). Once dried, these inserts were placed into sterile 24 well plates and the artificial membrane was rehydrated in 200μl of serum free medium for approximately 40 minutes. Once rehydrated, the serum free medium was aspirated and 1ml of normal medium was added to the well containing the insert in order to sustain any cells that may have invaded through the insert. Twenty thousand cells in 200μl of normal medium were then added to the insert over the top of the artificial basement membrane. The arrangement of this invasion assay is depicted in Figure 2.8.

The plate was then incubated for 72 hours at 37˚C, 5% CO_2 and 95% humidity. After 72 hours, the inserts were removed from the plate and the inside of the insert (which was initially seeded with cells) was cleaned thoroughly with tissue paper to remove Matrigel and non-invaded cells. Any cells which had invaded through the membrane and passed to the underside of the insert were fixed with 4% formaldehyde (v/v) in BSS for 5 minutes before being stained with 0.5% crystal violet solution (w/v) in distilled water. Excess crystal violet was washed away and the inserts were left to dry. These cells were then visualised under the microscope under x20 objective magnification and the random fields captured using Motic Plus 2.0 imaging software

(Motic, Wetzlar, Germany). Three random fields per insert were counted and the experimental procedure was repeated a minimum of three times. The *in vitro* cell invasion assay outlined here has previously been described and is well established in our research group (Fernando *et al*., 2008).

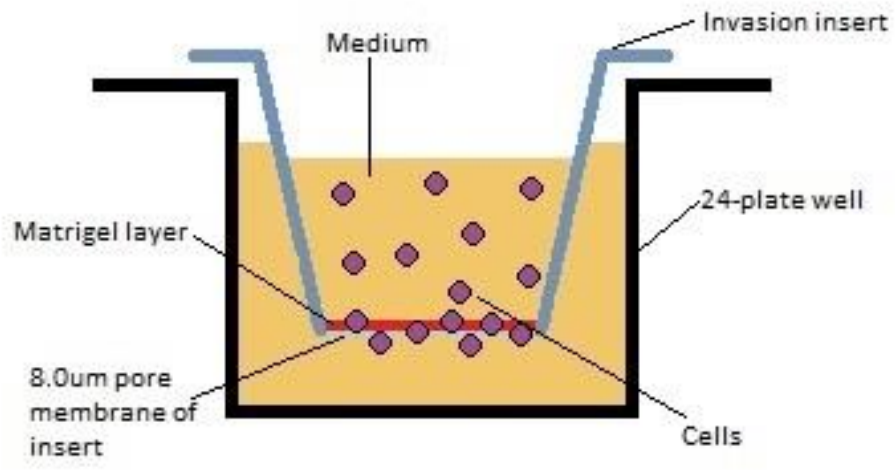

Figure 2.8 Schematic diagram showing the setup of the invasion insert in a 24-well plate. Invasive cells would invade through the Matrigel layer and the 8.0µm pores of the insert membrane.

2.6.3 *In vitro* tumour cell Matrigel adhesion assay

The ability of tumour cells to adhere to an artificial Matrigel basement membrane was examined using an *in vitro* Matrigel adhesion assay. A working concentration of Matrigel at 50µg/ml was made in serum free medium whereby 100µl were pipetted into each well of a 96-well plate and placed into an oven to dry to form an artificial basement membrane. This membrane was then rehydrated in 100µl of serum free medium for 40 minutes before cell seeding. Forty five thousand cells were seeded onto the Matrigel basement membrane in 200µl of normal medium and incubated for 45 minutes. Following this incubation period, the medium was removed and the membrane washed five times with BSS to remove non- and loosely attached cells. Adherent cells were then fixed with 4% formaldehyde (v/v) in BSS for 5 minutes before being stained with 0.5% crystal violet solution (w/v) in distilled water. Adherent cells were then visualised under the microscope under x20 objective magnification and random fields captured using Motic Plus 2.0 imaging software (Motic, Wetzlar, Germany). Three random fields per insert were counted, with 6 replicate wells each run and the experimental procedure was repeated a minimum of three times. The *in vitro* cell adhesion assay outlined here has previously been described and is well established in our research group (Fernando *et al*., 2008).

2.6.4 *In vitro* tumour cell motility assay

Cellular motility was assessed using a cytodex-2 bead motility assay whereby one million cells for each cell type were incubated in 10ml of growth medium containing 100µl of cytodex-2 beads (GE Healthcare, Cardiff, UK) overnight to allow the cells to adhere to the beads. The beads were then washed twice in 5ml of normal growth

medium to remove non-adherent or dead cells. After the second wash the beads were resuspended in 1ml of growth medium. One hundred microlitres of this solution were then added to a 96-well plate containing a further 100µl of normal medium and incubated for 4 hours. Following incubation, any cells that had migrated from the cytodex-2 beads and adhered to the base of the well were fixed with 4% formaldehyde (v/v) for 5 minutes and stained with 0.5% crystal violet (w/v). The stain was then extracted from the cells using 10% acetic acid and density of migrated cells was determined by measuring the absorbance at 540nm on an ELx800 plate reading spectrophotometer (Bio-Tek, North Star Scientific, Leeds, UK). Each experimental run included at least triplicate repeats and the entire experiment protocol was repeated at least three times. The *in vitro* cell motility assay outlined here has previously been described and is well established in our research group (Davies *et al*., 2008).

2.7 Confocal microscopy

Confocal microscopy was used to investigate protein co-localisation and cell morphology. A volume of 400µl medium containing 30,000 cells was added to each well of a Millicell® EZ Slide (Merck Millipore, Darmstadt, Germany) before incubation overnight. The following day, the cells were fixed with 4% formaldehyde before rehydration in BSS for 20 minutes at room temperature. Cells were permeabilised with 0.1% TritonX100 prepared in BSS for 5 minutes for subsequent blocking using a diluent consisting of BSS/5-10% horse serum for 20 minutes. The wells were washed three times with BSS for the addition of 100µl of each primary antibody at 1:100 dilution made up in the diluent (one primary antibody of different

species for each protein being investigated for protein co-localisation) then incubated at room temperature for 1 hour (The primary antibodies used are outlined in Table 2.4). Each well was washed three times with BSS for the addition of 100µl of each appropriate FITC or TRITC secondary antibodies at 1:250 dilution made up in the diluent and left to incubate at room temperature for 1 hour (one secondary antibody for each appropriate primary antibody used in prior steps; all secondary antibodies used are listed in Table 2.6). Each well was washed three times with BSS. The plastic frame was removed from the Millicell® EZ Slide for a coverslide to be mounted using FluorSave Reagent (Merck Millipore, Darmstadt, Germany) before storage in a refrigerator. Cells were visualised using the Olympus Fluoview FV10i confocal laser-scanning microscope under X60 magnification and analysed with the accompanying manufacturer's software (Olympus, Southend-on-Sea, UK).

2.8 Statistical analysis

Statistical analysis was performed using SigmaPlot 11.0 statistical software (Systat Software Inc, London, UK). Data was analysed using a two-sample, two-tailed t-test. Normality of data to perform these parametric tests was assessed by the Sigmaplot software and if deemed non-parametric, Mann-Whitney was performed. Each assay was performed at least three times. P-values < 0.05 were considered statistically significant.

Table 2.6 Fluorescent tagged secondary antibodies used for probing the appropriate primary antibodies listed in Table 2.4 during following the confocal microscopy protocol.

Secondary antibody	**Supplier**	**Product code**
Anti-Goat IgG (whole molecule)-FITC antibody produced in rabbit	Sigma-Aldrich Ltd, Dorset, UK	F7367
Anti-Mouse IgG (whole molecule)-TRITC antibody produced in goat. IgG fraction of antiserum	Sigma-Aldrich Ltd, Dorset, UK	T5393
Anti-Rabbit IgG (whole molecule)-FITC antibody produced in goat	Sigma-Aldrich Ltd, Dorset, UK	T6778

Chapter 3

The effects of WAVE1 and WAVE3 knockdown in PC-3 cells

3.1 Introduction

As discussed in Chapter 1, the WASP family of proteins contains five members, of which three form a subgroup referred to as the WAVE protein family. The pivotal role of WAVE proteins in cell motility through their interactions with a network of proteins is well documented (Fernando et al., 2009).

The ability of a cell to migrate is dependent on the formation of protrusions at the cell leading edge. Dynamic rearrangement of the actin cytoskeleton is a major mechanism driving the formation of cell protrusions and is dependent on the Arp2/3 protein complex (Figure 3.1). The association between cell motility and the Arp2/3 complex is related to the well known ability of this protein complex to stimulate actin polymerisation (Welch, 1999). The assembly of actin filaments by Arp2/3 at the cell leading edge results in the generation of polarised projections of the cytoplasm, an essential step in cell locomotion.

Despite the ability of Arp2/3 to elicit these actin polymerising effects, it is unable to do so without firstly becoming activated by members of the WAVE family. Arp2/3 activation is stimulated by WAVE which induces the complex into a conformational change which causes the two subunits, Arp2 and Arp3 to be brought into close proximity (Higgs and Pollard, 1999). In this configuration, these two subunits mimic an actin dimer which is able to induce rapid actin polymerisation. However, prior to this interaction between WAVE and Arp2/3, it is necessary for WAVE itself to become activated which occurs indirectly between the Sra1 subunit component of the WAVE regulatory complex and Rac, a member of the Rho GTPase family. It is now understood that WAVE acts as a ‘middle man’ between Rac GTPases and the Arp 2/3 protein complex.

Cell migration is an essential mechanism that underlies a plethora of normal cellular processes including wound healing, immune response and tissue formation during embryonic development. Whilst the migration of normal, healthy cells is physiologically important to ensure such mechanisms function properly, it also has the potential to drive the migration of abnormal cells. When uncontrolled, cell motility has the ability to contribute to the aggressive spread of cancer cells and is recognised as a promoting factor of cancer metastasis (Wang *et al.,* 2005).

This link between aberrant cell migration and its influence on cancer metastasis has long been established (Liotta, 1986). An *in vivo* study comparing the gene expression profiles of invasive tumour cells to the primary tumour cell population in a xenograft tumour model discovered an up-regulation of genes involved in pathways central to cell motility including actin polymerisation. Up-regulated genes included subunits comprising the Arp2/3 complex (Arp2 and Arp5) as well as Cdc42, an upstream stimulator of Arp2/3 known to regulate N-WASP (Wang *et al.,* 2007) (Refer to Figure 3.1).

Although work in this field has heavily focused on the relevance of the Rho GTPases in cancer metastasis through their role in cell motility (as outlined in Chapter 1), the significance of their downstream proteins has been explored to a lesser extent. With links between several proteins implicated in cell motility and the findings of their up-regulated expression and/or activity in aggressive and metastatic cancers, it is logical to explore the potential contribution of WAVE proteins in cancer metastasis.

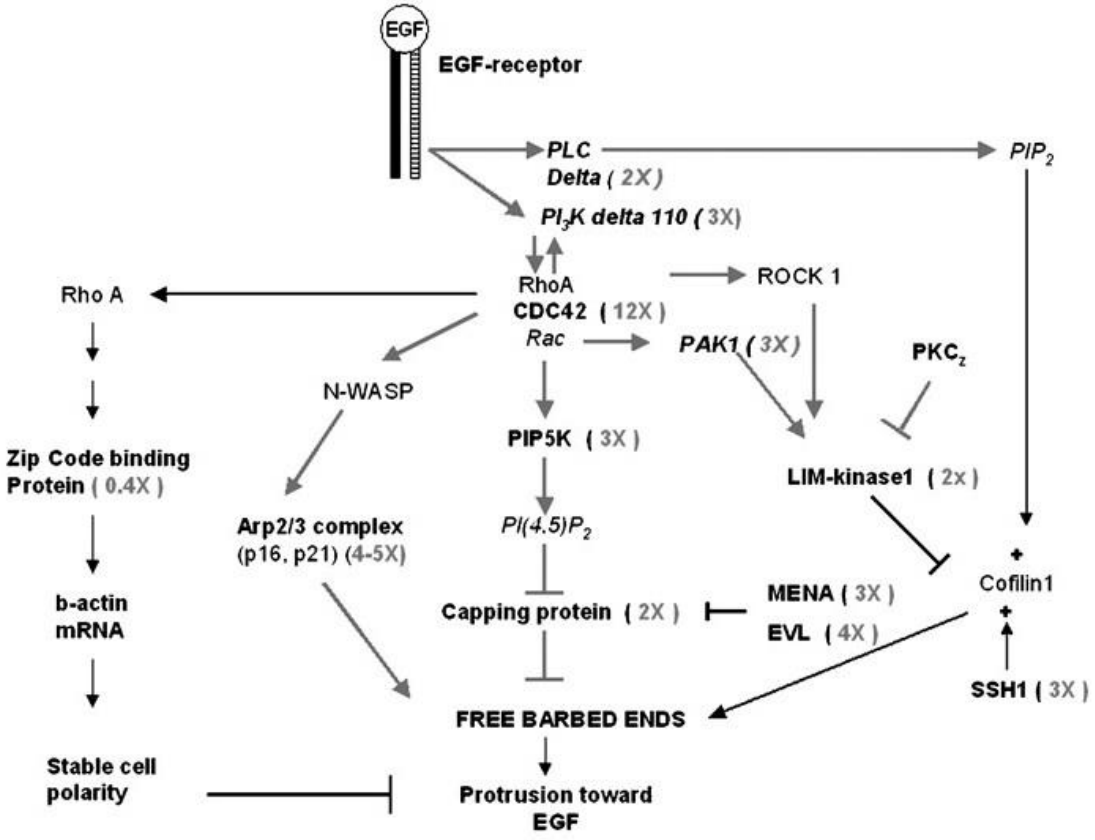

Figure 3.1 Cell motility pathways outlining the protein interaction networks which regulate the Arp2/3 complex, capping protein and cofilin pathways. All these pathways have implications on actin polymerisation at the cell leading edge and therefore regulate cell locomotion.

The relevance of the WASP protein family in human disease has been well documented with particular interest focusing on the WAVE proteins and their significance in cancer metastasis. An association between aberrant WAVE expression and several metastatic cancers has been identified (Kurisu *et al.,* 2005; Iwaya *et al*., 2007; Sossey-Alaoui *et al.*, 2007). In line with these findings is the suggestion of a potential contribution of WAVE1 and WAVE3 to prostate cancer metastasis (Fernando *et al*, 2008; Fernando *et al*, 2010). The expression levels of WAVE1 and 3 were found to be up-regulated in the metastatic prostate cancer cell lines, PC-3 and DU-145 compared to non-cancerous prostatic epithelial cell lines. Knockdown of WAVE1 and 3 was independently carried out in the metastatic prostate cancer cell lines, PC-3 and DU-145 with the aim to determine the effects of knockdown on several cell functions in relation to cancer metastasis. This research described a decrease in cell invasive and growth capabilities in both cell lines with WAVE1 knockdown, whilst WAVE3 knockdown was only shown to reduce cell invasion but no effect on proliferation. Neither WAVE1 nor 3 knockdown was shown to affect cell adhesive ability.

These findings implicate aberrant WAVE expression as a potential contributor to the metastatic traits seen in aggressive prostate cancer cell lines. This chapter aims to firstly independently reproduce the findings of Fernando *et al* (2008; 2010) and to supplement the initial study by investigating the effect of WAVE1 or 3 knockdown on cell motility. Given the role of WAVE1 and 3 in cell motility, expression knockdown of either isoform in the PC-3 cell line should see suppression in their cellular motile potential.

3.2 Methods and materials

3.2.1 Cell lines

PC-3 cells were cultured as outlined in Chapter 2.

3.2.2 Generation of WAVE 1 and 3 knockdown PC-3 cell lines

Ribozyme transgenes that specifically target and cleave WAVE 1 or 3 mRNA were generated and cloned into the PC-3 prostate cancer cell line. The full protocol followed to generate ribozymes, insertion into the plasmid vector, amplify the plasmid in *E.coli*, plasmid extraction and electroporation to introduce the plasmid into PC-3 cells are outlined in Section 2.3. Ribozyme sequence data are displayed in Table 2.1 in Section 2.3.

3.2.3 Synthesis of complementary DNA and reverse transcription polymerase chain reaction

This is fully described in Section 2.4.3. RNA was isolated from wild type PC-3 cells and its plasmid transfected equivalents. Complementary DNA (cDNA) was generated from the standardised RNA extractions using reverse transcription polymerase chain reaction (RT-PCR) for subsequent expression analysis using conventional and quantitative PCR using primer sequences shown in Table 2.3 of Section 2.4.4.

3.3 Results

3.3.1 Generation of WAVE 1 and WAVE 3 ribozyme transgene pEF6 plasmids

In order to generate WAVE 1 and WAVE 3 ribozyme transgenes, ribozymes were designed to target a specific site on the predicted secondary structure of the WAVE 1 and 3 mRNA transcripts. This was achieved using a predictive mRNA folding software programme as described in Section 2.3.1. Initial synthesis of WAVE 1 and 3 ribozyme transgenes was carried out following the touchdown PCR parameters as outlined in Section 2.3.1. Following plasmid integration and amplification in *E.coli*, these plasmids were extracted for subsequent analysis. Ensuring the ribozyme transgenes were integrated into the plasmid vector in the correct orientation is crucial, therefore orientation checks were carried out with PCR and electrophoresis. Bands of approximately 140 bp resulting from a T7F vs RbBMR reaction indicated correct orientation whereas a 140bp band from a T7F vs RbToP reaction demonstrated incorrect orientation of the ribozyme transgene insert.

As Figure 3.2 demonstrates, colonies 4 and 7 display bands of 140bp for T7F and RbBMR PCR reactions for WAVE1 ribozyme 1 samples which indicates correct orientation of the ribozyme insert into the plasmid vector. Therefore these colonies were chosen to be used for plasmid amplification, purification and transfection into the PC-3 cell line. Similarly, colonies 2 and 6 were identified as colonies carrying ribozyme 2 for WAVE1 whilst colonies 1 and 4 were selected for WAVE 3 ribozyme 1 and colony 8 was chosen for WAVE 3 ribozyme 2.

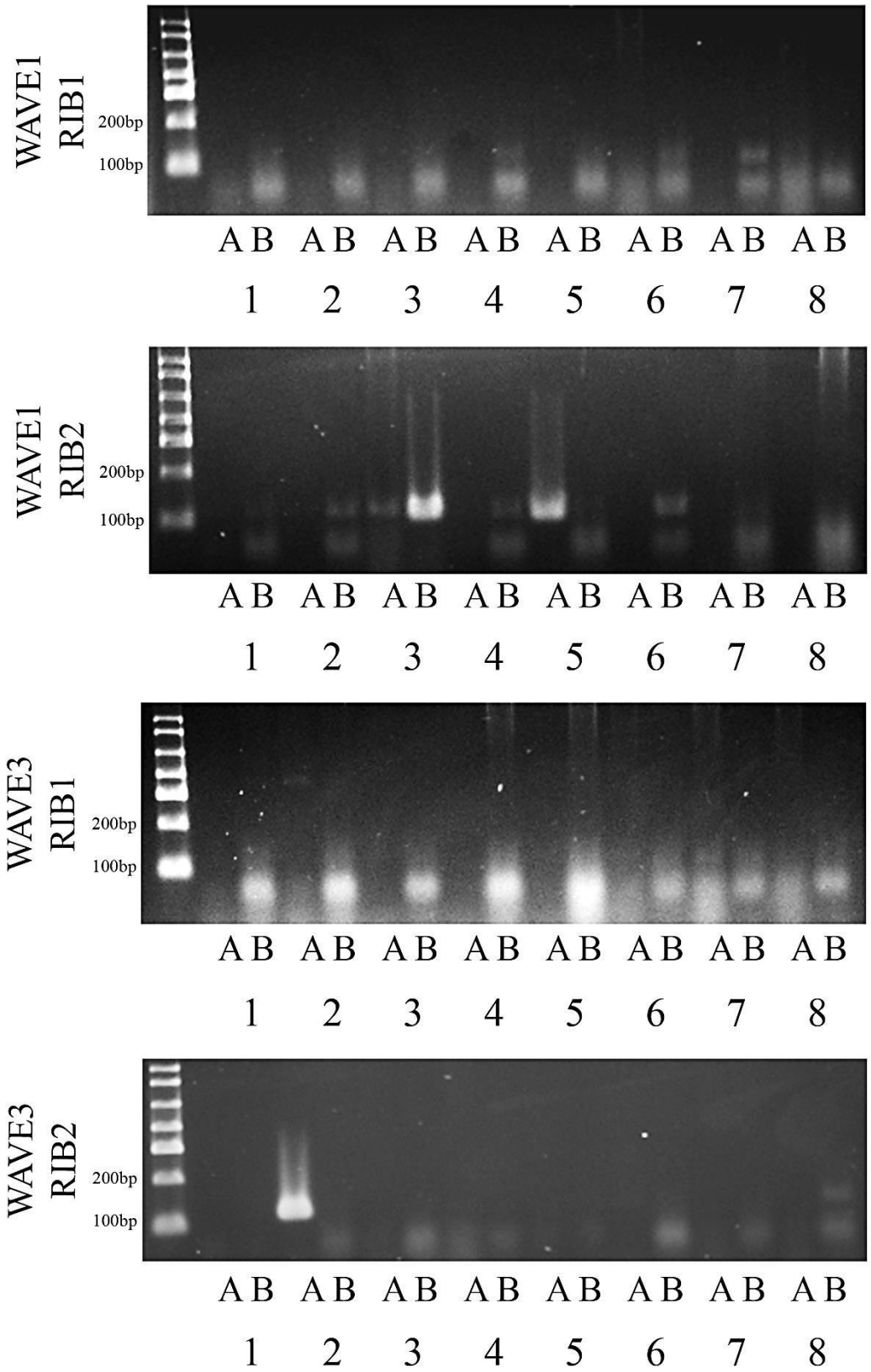

Figure 3.2 Plasmid insertion and orientation analysis of the ribozyme transgenes into the pEF6 plasmid vector. Colonies picked for orientation analysis are labelled 1 to 8. Correct orientation checks with a T7F and RbBMR reaction are labelled B whilst a T7F and RbToP reaction tested for incorrect orientation and is labelled A. A 140bp band present for either reaction A or B provides an indication of insert orientation into the plasmid vector.

3.3.2 Confirmation of WAVE 1 and WAVE 3 knockdown in PC-3 cells at the mRNA level with polymerase chain reaction (PCR) and quantitative PCR (Q-PCR)

The results of the expression analysis and knockdown verification at the mRNA level are shown in Figures 3.3 and 3.4. WAVE1 and 3 expression is similar for PC-3 WT and the control cell line PC-3 pEF6 when using both conventional and quantitative/real time PCR (Q-PCR). Using conventional PCR, PC-3 cells transfected with either ribozyme 1 or 2 targeting WAVE1 were shown to have a reduced WAVE1 mRNA expression level. The expression levels of WAVE3 were also seen to be lower in PC-3 cells transfected with either WAVE3 specific ribozyme 1 or 2. The expression analysis was performed in parallel with that of the housekeeping gene, GAPDH (glyceraldehyde 3-phosphate dehydrogenase) as a control to ensure that the band intensity seen in the agarose gel following staining reflected expression level differences and not differences in cDNA starting quantities. Expression analysis of the cDNA samples showed no change in GAPDH expression level. Additionally, a negative control was set up with cDNA substituted for water to help indicate any contamination. PCR of all PC-3 cDNA samples revealed no sign of DNA contamination in the primers or PCR water used as suggested by the lack of PCR product band when using WAVE1, WAVE3 or GAPDH primers. The knockdown of WAVE1 or 3 was quantitatively analysed by Q-PCR which focused on cell lines transfected with ribozyme 2 targeting WAVE1 (W1R2) and ribozyme 1 specific for WAVE3 (W3R1) which were the cell lines used in subsequent experiments. Expression analysis using this method was undertaken in parallel with the housekeeping gene, GAPDH to normalise the values obtained for WAVE1 and 3. Additionally, standards of known transcript level were simultaneously amplified

alongside these experiments which allowed a calculation of the expression level in the samples being analysed. Q-PCR experiments were repeated at least three times. This method also revealed a knockdown in mRNA expression of WAVE1 in PC-3 cells transfected with W1R2 and WAVE3 with W3R1.

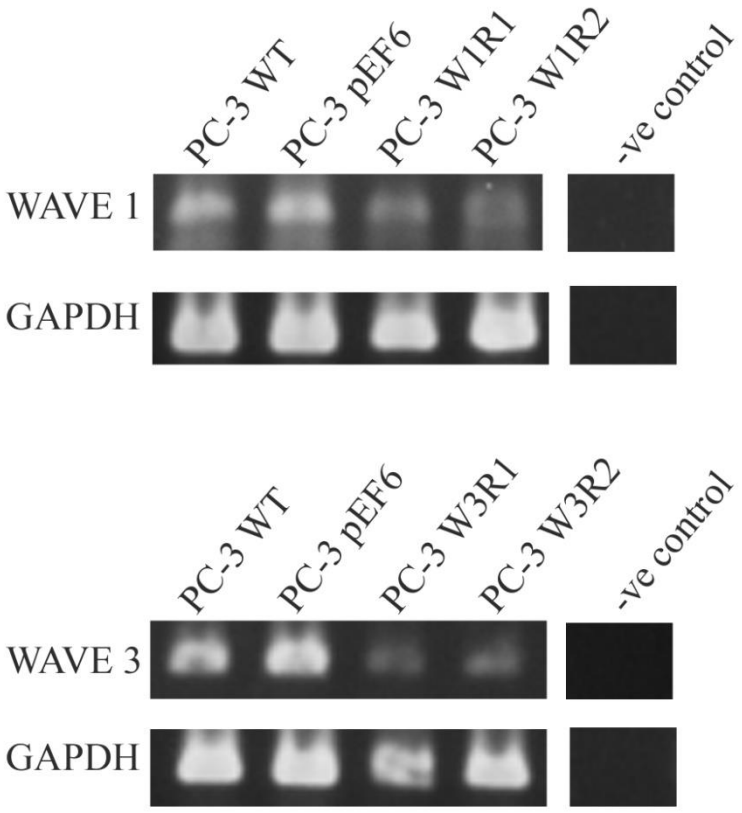

Figure 3.3 Expression analysis of WAVE1 and WAVE3 following targeted ribozyme transgene transfection of PC-3 wild type cells. The expression of both WAVE1 and 3 was shown to be knocked down at the mRNA level following transfection by either ribozyme 1 or 2.

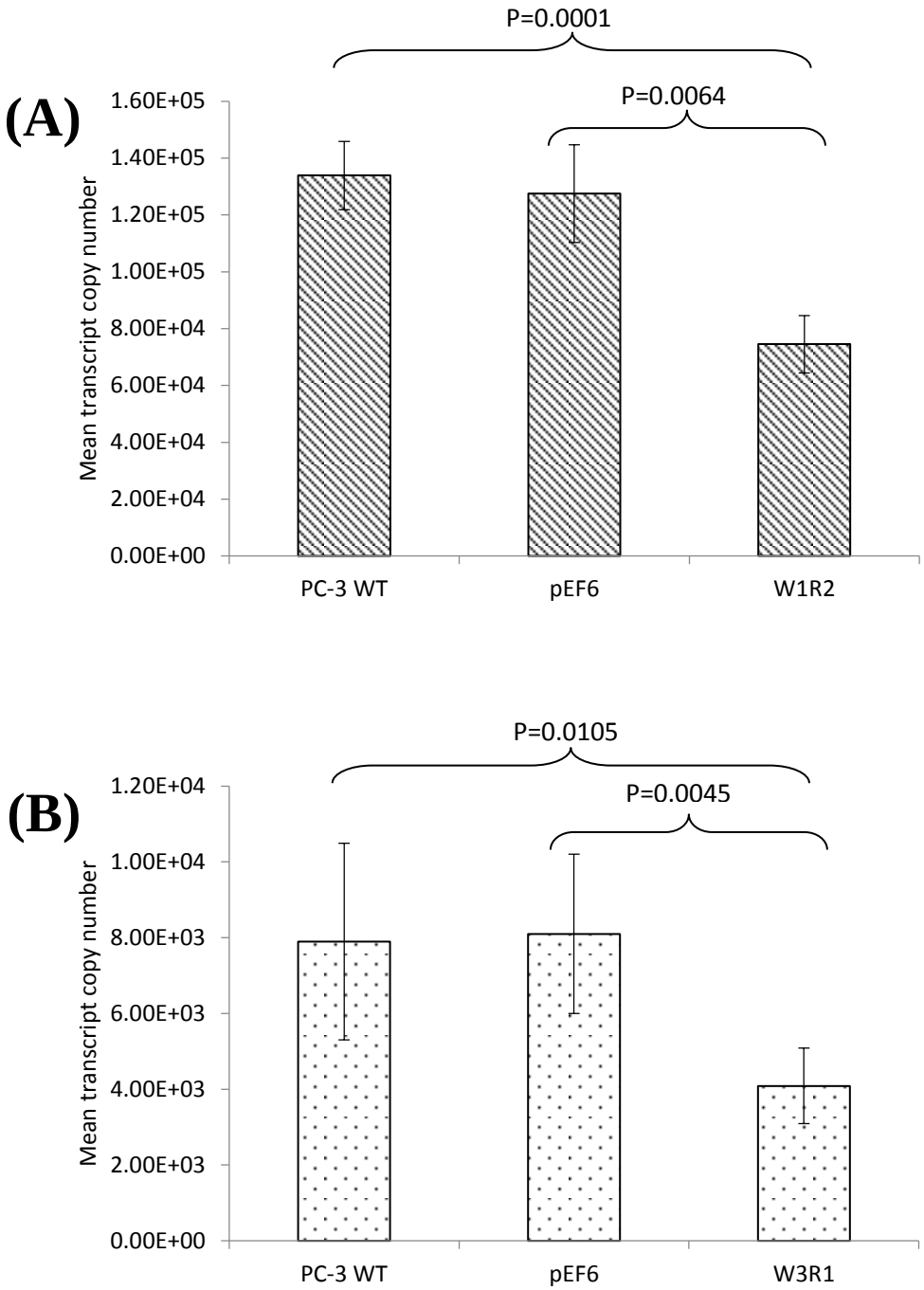

Figure 3.4 WAVE1 and 3 knockdown confirmed at the mRNA level using Q-PCR. (A) WAVE 1 expression knockdown in PC-3 cells transfected with WAVE1 ribozyme 2 (W1R2) compared to both wild type (WT) and pEF6 control cell lines. (B) WAVE3 expression knockdown in PC-3 cells transfected with WAVE3 ribozyme 1 (W3R1) compared to both wild type (WT) and pEF6 control cell lines. Expression levels of WAVE1 and 3 were normalised against the housekeeping gene, GAPDH. Experiments were repeated at least three times.

3.3.3 Confirmation of WAVE 1 and WAVE 3 knockdown in PC-3 cells at the protein level with Western blotting

Western blotting was used to determine protein expression levels of WAVE1 and 3 in wild type control and ribozyme transfected PC-3 cells and verify protein knockdown as shown in Figure 3.5. Whilst WAVE1 protein expression was observed to be at similar levels for wild type and pEF6 PC-3 cells, the band intensity for protein derived from PC-3 cells transfected with WAVE1 ribozyme 1 was also seen to be at similar band intensity to these control counterparts. Even so, WAVE1 knockdown was observed in PC-3 cells transfected with ribozyme 2, indicated by weak band intensity relative to the wild type and pEF6 controls. WAVE3 protein expression was also seen to be reduced in PC-3 W3R1 cells in comparison to PC-3 WT and pEF6 controls. Protein expression levels for the housekeeping gene GAPDH were also analysed to ensure that any differences in band intensity for WAVE (in comparison to wild type and pEF6 to ribozyme transfected cells) were due to differences in expression level as opposed to initial starting protein quantities.

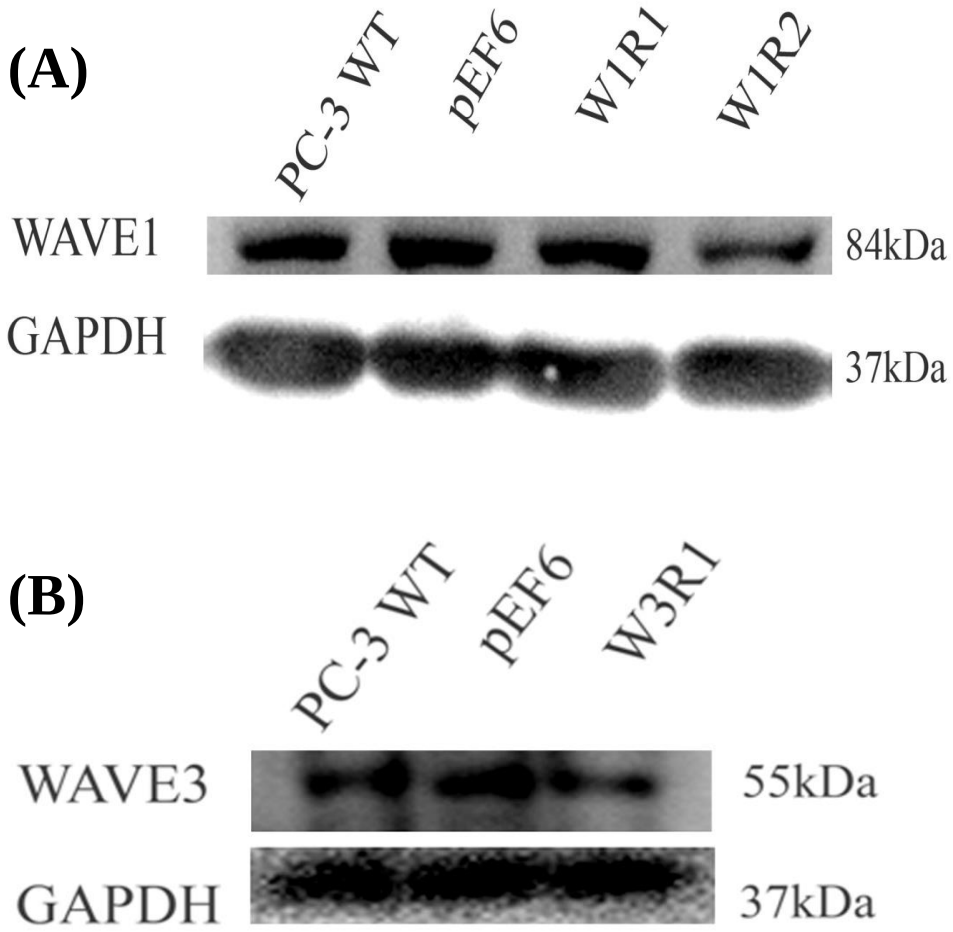

Figure 3.5 Protein expression analysis of WAVE1 and WAVE3 following targeted ribozyme transgene transfection of PC-3 wild type cells. (A) Band intensity for PC-3 cells transfected with the ribozyme transgene 1 targeting WAVE1 (W1R1) was not dissimilar to the protein bands corresponding to wild type (WT) and pEF6. However, PC-3 cells carrying the WAVE1 ribozyme transgene 2 (W1R2) clearly show WAVE1 expression knockdown at the protein level. Protein expression for GAPDH is consistent for both control and transfected cell lines. (B) Protein expression analysis was carried out on PC-3 cells transfected with ribozyme 1 specific for WAVE3 expression knockdown (W3R1). Band intensity for WAVE3 expression is seen to be fainter in W3R1 compared to wild type and pEF6 control cells. GAPDH protein expression is observed to be consistent overall in control and transfected PC-3 cells.

3.3.4 WAVE 1 or WAVE 3 knockdown reduces cell growth rate in the PC-3 cell line

Wild type PC-3 cells were incubated in parallel with the control equivalent PC-3 pEF6 and the WAVE 1 and WAVE 3 knockdown counterparts. Seeding the cells in three separate plates allowed them to be fixed after 24, 72 and 120 hours.

As described in Chapter 2, these cell lines were examined after 120 hours of incubation using an *in vitro* cell growth assay; the results are displayed in Figure 3.6. As no significant differences were discerned when comparing the growth rates of wild type and pEF6 cells, pEF6 cells were subsequently used as the control cell line for comparing the effects of WAVE1 or 3 knockdown in PC-3 cells. The effects on proliferation for cells exhibiting either of the two ribozymes targeting WAVE1 were found to be similar, therefore future experiments focused on using WAVE1 ribozyme 2 (W1R2). Similarly, the use of either of the two PC-3 cell lines transfected with either of the two available WAVE3 specific ribozymes revealed similar effects on cell growth, therefore WAVE3 ribozyme 1 (W3R1) was selected for future experiments in this study. These transgenes were also seen to give the best levels of knockdown of the respective WAVE proteins.

A significant decrease in cell growth rate was observed after 5 days of incubation when comparing the PC-3 pEF6 control cells to WAVE1 knockdown cells ($p>0.001$) (Figure 3.6A). A similar trend was observed in PC-3 cells exhibiting decreased WAVE3 expression. This decrease in cell growth potential for PC-3 cells exhibiting WAVE3 knockdown was more pronounced than that for WAVE1 knockdown ($p>0.001$) (Figure 3.6B).

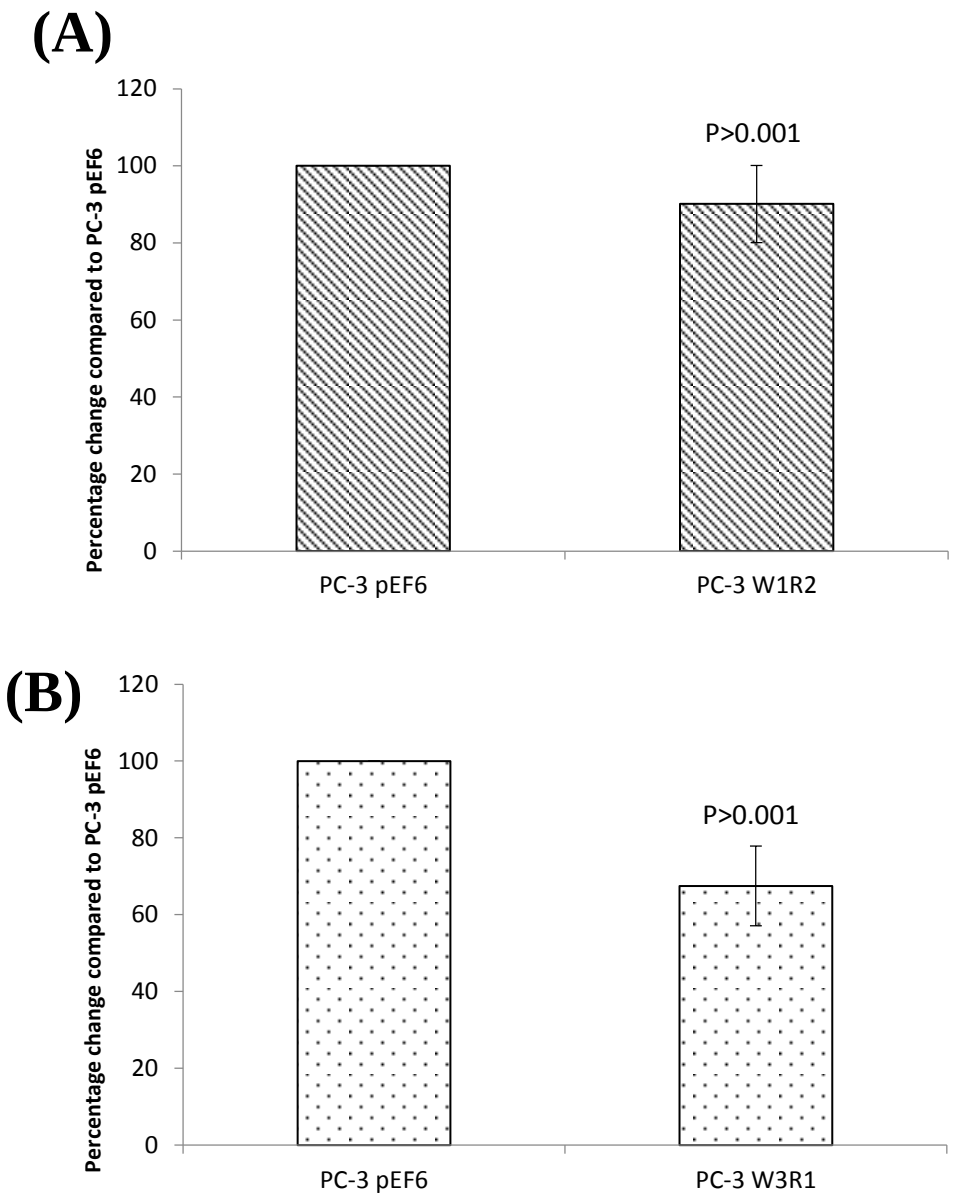

Figure 3.6 The effects of WAVE knockdown in the PC-3 cell line on cell growth over a 5 day incubation period. (A) WAVE1 knockdown was shown to have a significant inhibitory effect on cell growth when compared to the pEF6 control. Similarly, (B) WAVE3 knockdown also significantly reduced cell growth compared to pEF6 control cells. Shown are mean data from a minimum of three independent repeats, values represent percentage pEF6 control, error bars represent SEM. * represents $p<0.05$.

3.3.5 WAVE 3 knockdown decreases cell invasiveness in the PC-3 cell line

The invasive capacity of PC-3 cells was examined using an *in vitro* Matrigel invasion assay comparing wild type and pEF6 cells to PC-3 cells carrying either WAVE 1 (Figure 3.7) or WAVE 3 (Figure 3.8) ribozyme transgenes. The number of cells which had degraded the Matrigel and invaded through the pores of the insert was counted under the microscope allowing for calculation of the percentage change between the pEF6 control cells with either the WAVE1 or 3 knockdown cells. These values were collated to provide an overall appreciation of the effects of WAVE knockdown in the PC-3 cell line. When comparing the overall percentage change in cell invasiveness of WAVE1 knockdown cells to pEF6 controls, there appears to be a decrease in cell invasive ability which was found to be significant ($p<0.001$). However, the extent of this decrease was modest compared to the effects of WAVE3 knockdown in PC-3 cells compared to pEF6 controls where it was shown to potently inhibit cell invasion ($p<0.001$).

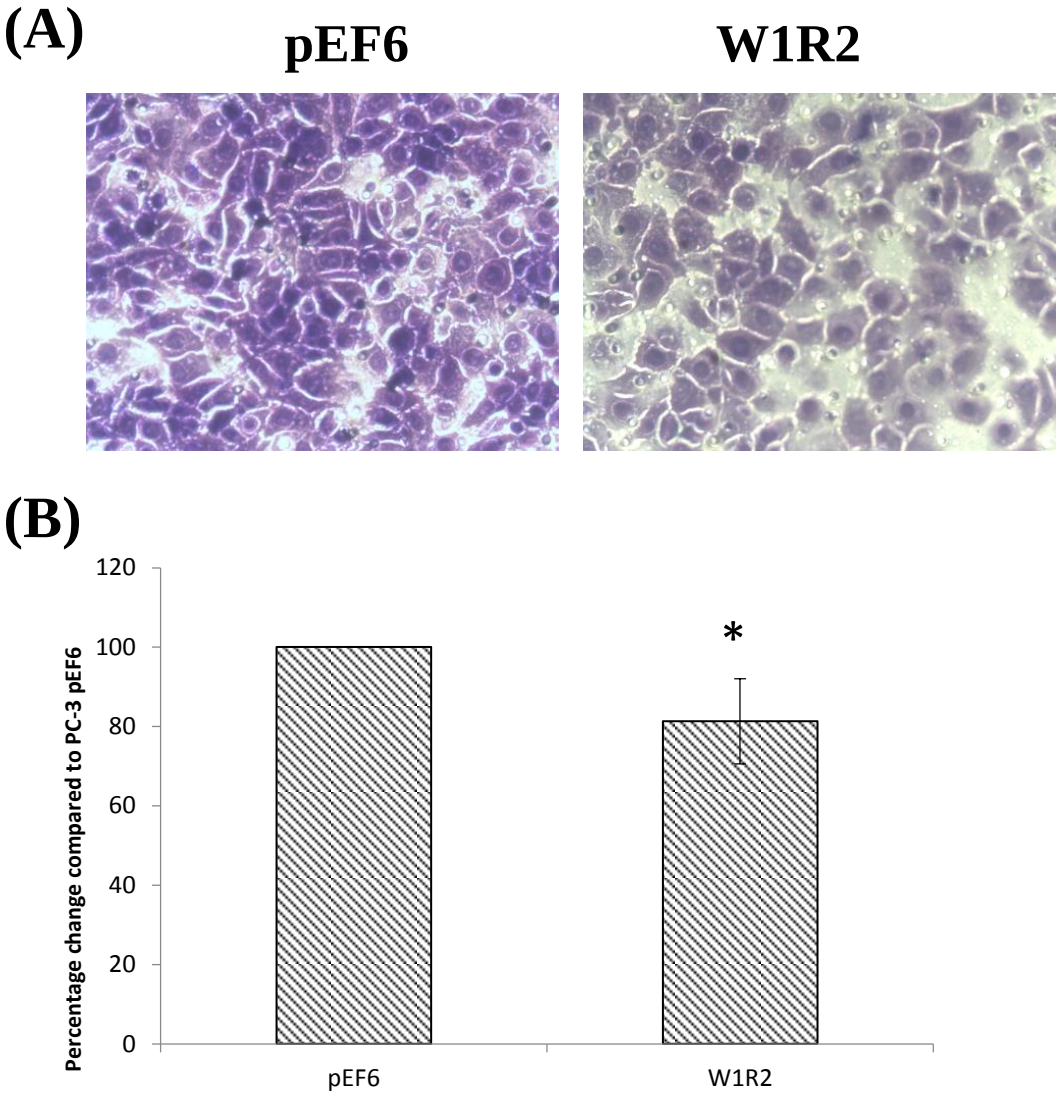

Figure 3.7 The cell invasion effects of WAVE1 knockdown in the PC-3 cell line A) Displayed above the graph is a representative image acquired under a microscope for its corresponding cell line in the cell invasion assay. B) WAVE1 knockdown was shown to significantly decrease cell invasion when compared to pEF6 control. Images acquired at 200X magnification. Shown are mean data from a minimum of three independent repeats, values represent percentage pEF6 control, error bars represent SEM. * represents $p < 0.05$.

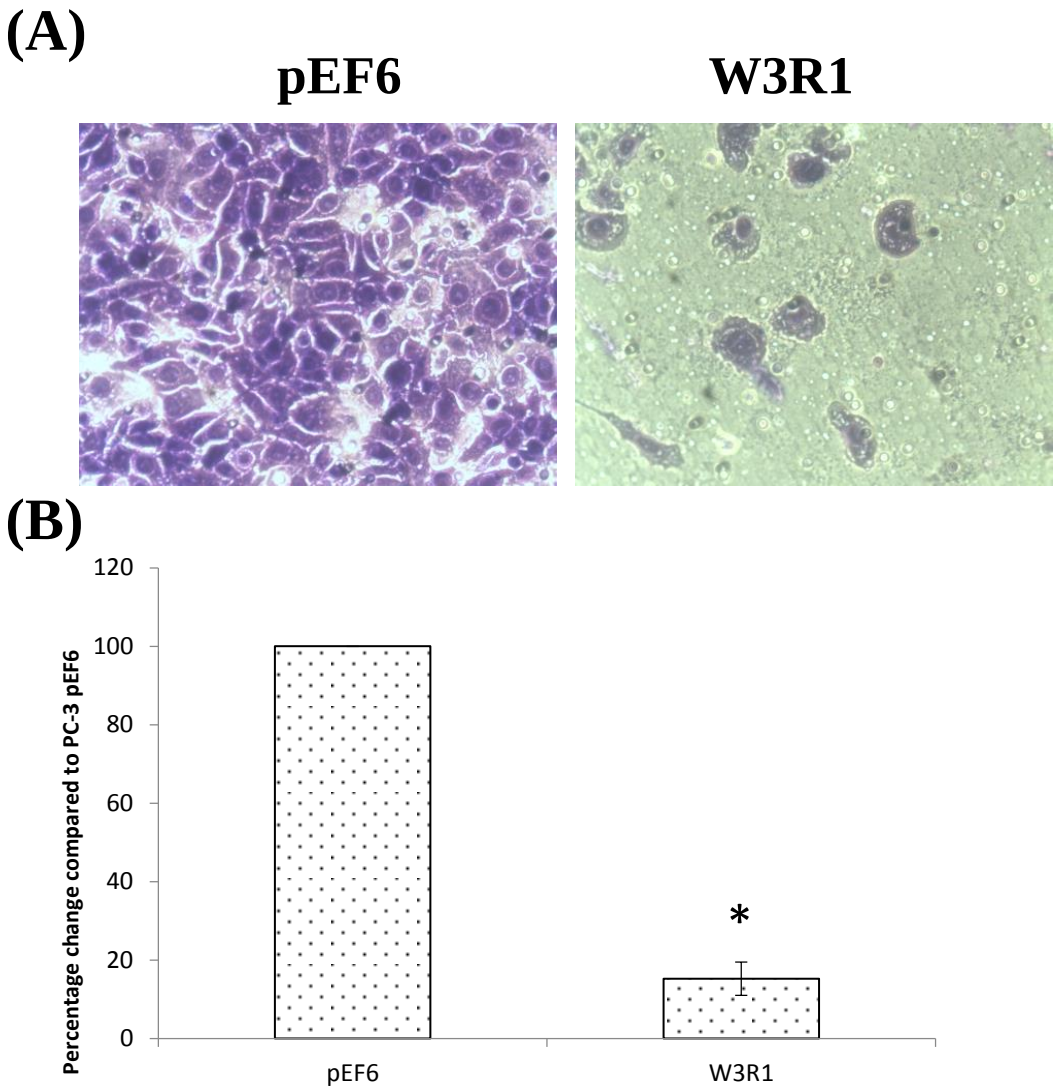

Figure 3.8 The cell invasion effects of WAVE3 knockdown in the PC-3 cell line A) Displayed above the graph is a representative image acquired under a microscope for its corresponding cell line in the cell invasion assay. B) WAVE3 knockdown was shown to significantly decrease cell invasion of PC-3 cells compared to the pEF6 control cell line. Images acquired at 200X magnification. Shown are mean data from a minimum of three independent repeats, values represent percentage pEF6 control, error bars represent SEM. * represents $p < 0.05$.

3.3.6 WAVE 1 or WAVE 3 knockdown does not influence cell adhesiveness in the PC-3 cell line

Cells were seeded on a Matrigel layer to mimic the substrate to which cells would typically adhere in an *in vivo* environment. After a 45 minute incubation period, the cells were examined under a microscope to compare the adherence of PC-3 pEF6 control cells to the WAVE 1 (Figure 3.9) and 3 (Figure 3.10) knockdown cells to this Matrigel layer. Overall, a non-significant increase in adhesion was observed in WAVE1 knockdown PC-3 cells whilst no changes were seen for WAVE3 knockdown cells ($p=1.00$; $p=0.712$).

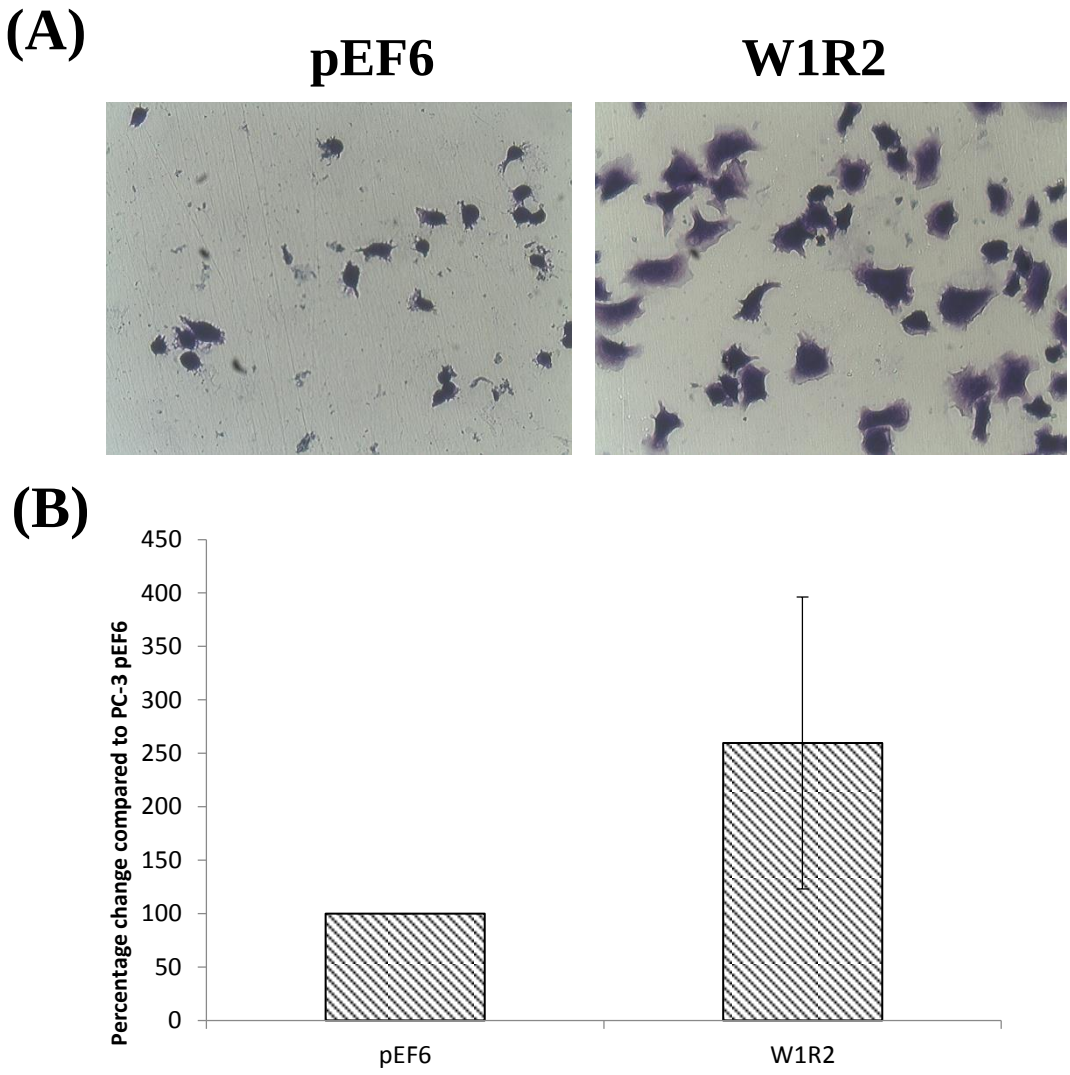

Figure 3.9 The effects of WAVE1 knockdown in the PC-3 cell line on cell adhesion. A) Displayed above the graph is a representative image acquired under a microscope for its corresponding cell line in the cell adhesion assay.B) Knockdown of WAVE1 expression revealed no significant effect on cell adhesion in PC-3 cells when compared to pEF6 control. Images acquired at 200X magnification. Shown are mean data from a minimum of three independent repeats, values represent percentage pEF6 control, error bars represent SEM.

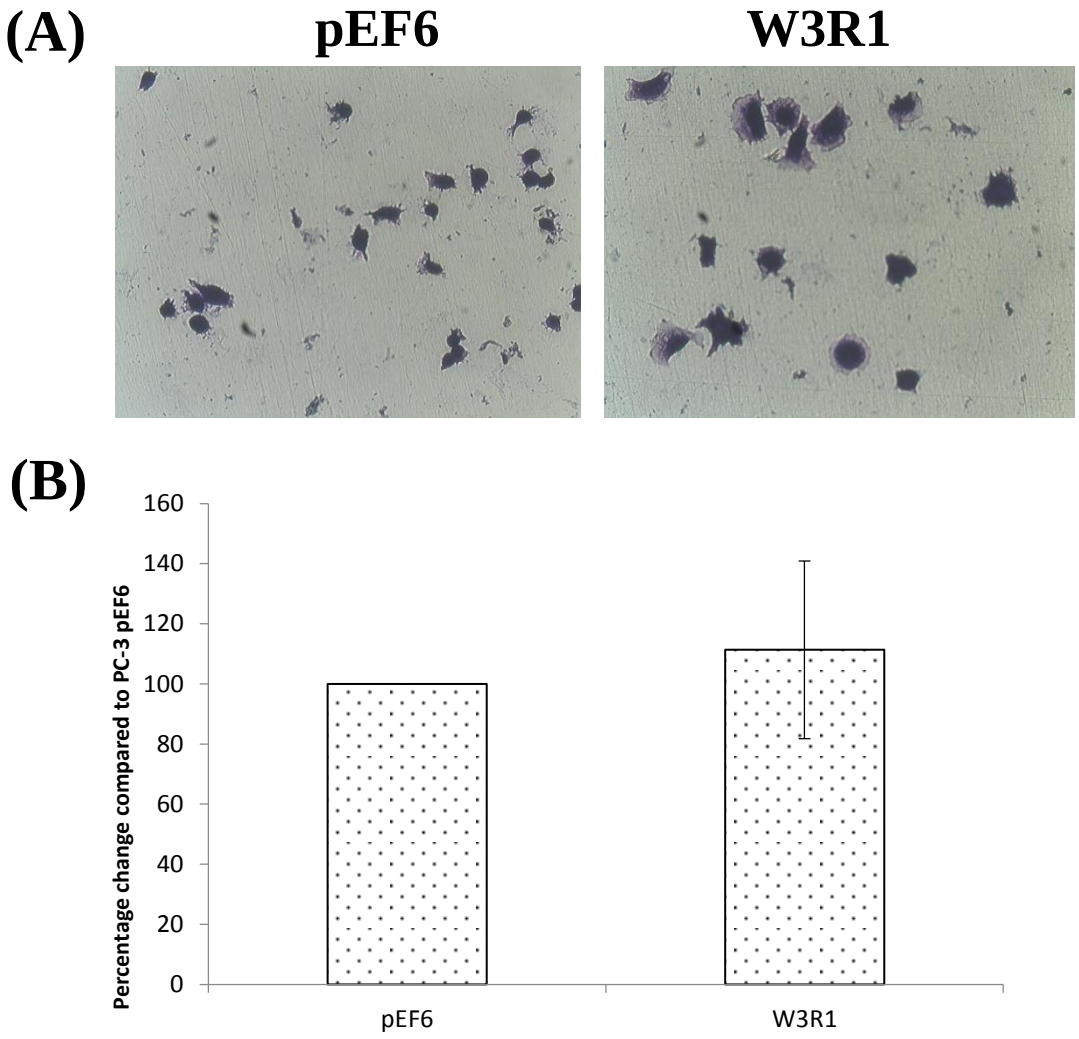

Figure 3.10 The effects of WAVE3 knockdown in the PC-3 cell line on cell adhesion. A) Displayed above the graph is a representative image acquired under a microscope for its corresponding cell line in the cell adhesion assay. B) Knockdown of WAVE3 expression revealed no significant effect on cell adhesion in PC-3 cells when compared to pEF6 controls. Images acquired at 200X magnification. Shown are mean data from a minimum of three independent repeats, values represent percentage pEF6 control, error bars represent SEM.

3.3.7 WAVE 3 knockdown is associated with decreased cell motility in the PC-3 cell line

A Cytodex-2 bead motility assay was used to examine the effects of WAVE 1 (Figure 3.11A) or WAVE 3 (Figure 3.11B) knockdown in PC-3 cells compared to the pEF6 control cell line. WAVE 3 suppression was found to decrease cell motility in the Cytodex-2 bead assay in PC-3 cells ($p<0.001$) relative to both wild type and pEF6 cells. However, the motility of PC-3 cell carrying the WAVE 1 ribozyme transgene was not found to be significantly altered ($p=0.474$).

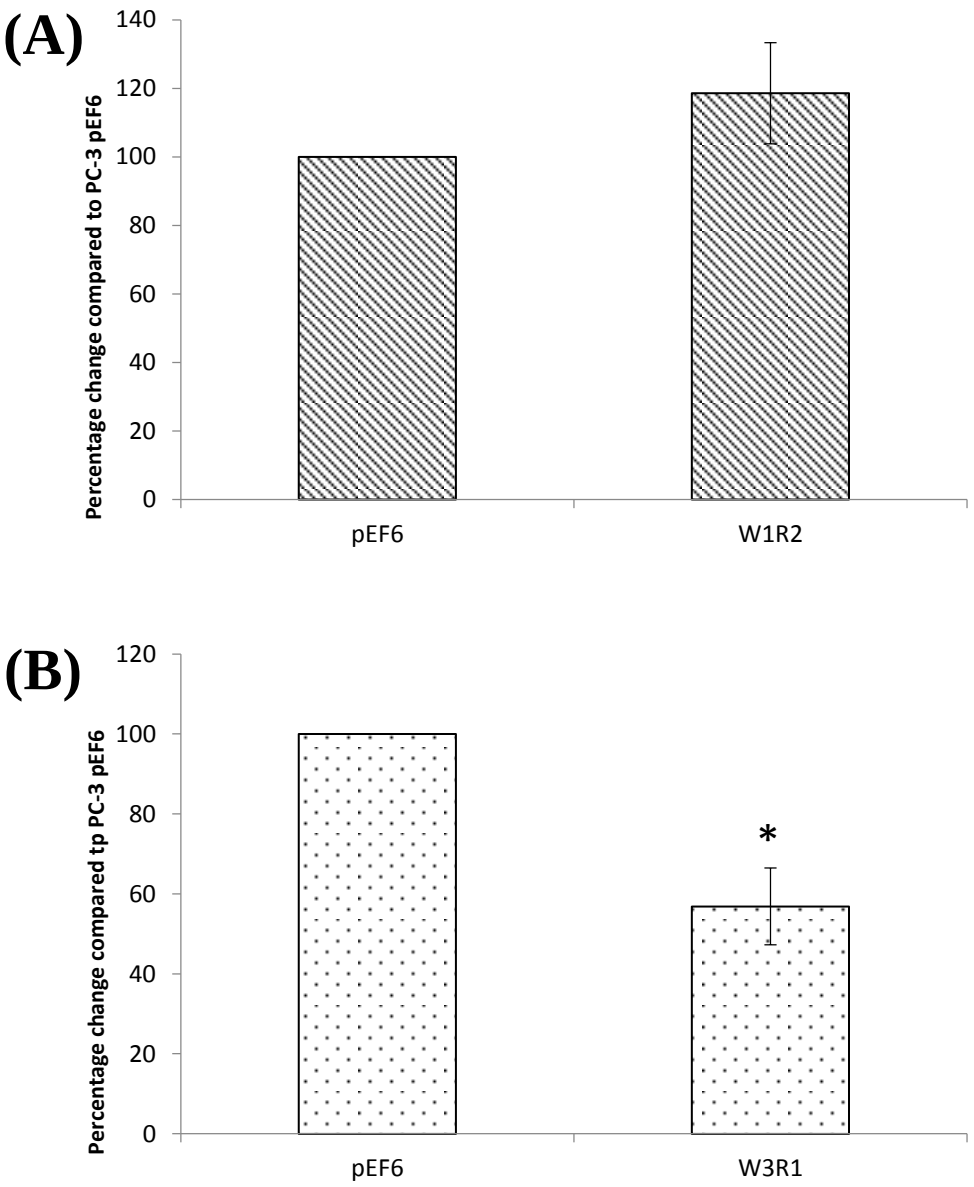

Figure 3.11 The effects of WAVE knockdown in the PC-3 cell line on cell motility. (A) PC-3 cells with WAVE1 knockdown show no significant change in cell motility whilst a significant decrease in the motile ability of cells was observed in WAVE3 knockdown cells compared to pEF6 control cells (B). Shown are mean data from a minimum of three independent repeats, values represent percentage pEF6 control, error bars represent SEM. * represents $p < 0.05$.

3.4 Discussion

Due to the partially known role of WAVE proteins in cell migration, it was a logical step to postulate a role for these proteins in cancer metastasis; a process associated with uncontrolled levels of cell migration. Indeed, expression levels of WAVE1 and WAVE3 have been found to be elevated in aggressive prostate cancer cell lines compared to epithelial prostate cell lines (Fernando *et al*, 2008a; Fernando *et al*, 2008b).

Transfection of wild type PC-3 with either of the two ribozyme transgenes designed to target WAVE1 (W1R1 and W1R2) resulted in the successful knockdown of the target gene at the mRNA level as demonstrated using PCR and Q-PCR techniques. However, only W1R2 showed knockdown at the protein level using Western blotting methods. Similarly, use of either of the two ribozymes available specifically for WAVE3 (W3R1 and W3R2) was also successful in achieving WAVE3 expression knockdown in PC-3 wild type cells at the mRNA level but protein knockdown was only evident for W3R1. Therefore, the PC-3 W1R2 and W3R1 cell line was used for subsequent experiments. It is important to bear in mind the potentiality for heterogeneous cell populations to be generated this way which may affect expression levels of WAVE isoforms and possibly the data collected, however, the aims of WAVE knockdown were to determine overall effect on cell function.

Additionally, wild type PC-3 cells were transfected with the empty vector, pEF6, to generate a PC-3 pEF6 control cell line. Similarly, mRNA and protein expression levels were deduced for wild type and pEF6 cell lines using PCR and Western blotting, respectively. This control confirmed that any decrease of WAVE 1 or 3 expression in WAVE ribozyme transfected cells was attributable to specific gene targeting as opposed to artefacts arising from the process of gene manipulation

through plasmid transfection. With this in mind, the PC-3 pEF6 cell line was used as a control for comparison in subsequent experiments.

Changes in the cellular properties investigated (growth, invasion, adhesion and motility) were calculated as a percentage change compared to the pEF6 control cell line. As a result of WAVE1 expression knockdown, the proliferative rate of PC-3 cells was reduced by approximately 15%. A similar trend was also observed for WAVE3 knockdown cells, although this significant reduction was seen to a much greater extent. Similarly, cell invasiveness was also significantly reduced in both WAVE1 and WAVE3 knockdown PC-3 cells compared to the pEF6 control cell line. WAVE1 and 3 knockdown resulted in a significant reduction in cell invasion which was much more pronounced with WAVE3 knockdown when compared to pEF6 cells. Assays carried out to determine the effects of WAVE knockdown on cell adhesion revealed an overall increase in adhesiveness following WAVE1 knockdown, however, the values obtained from this assay were widely distributed, thus yielding a very large standard error resulting in the conclusion that the overall change in adhesiveness was insignificant. When analysing the consequences of WAVE knockdown on cell motility in PC-3 cells, it was found that a decrease in WAVE1 expression resulted in a moderate increase in cell motility, which did not reach significance. In contrast, WAVE3 knockdown was shown to very significantly reduce the motility of PC-3 cells.

These functional assays revealed similar roles for WAVE1 and 3 in PC-3 cells with particular regard to cell growth and cell invasion where both traits were suppressed following WAVE1 or 3 knockdown. Even so, the extent of trait suppression differed between the WAVE members as the WAVE3 knockdown was observed to suppress proliferative and invasive ability to a greater extent than WAVE1 knockdown when

compared to PC-3 pEF6 control cells. Although WAVE1 knockdown was seen to promote adhesiveness, these changes were not significant; as for WAVE3 knockdown, cell adhesion was not found to be altered. Some of the findings described here such as the cell invasion experiments concur with those outlined by Fernando *et al* (2008; 2010), however, there were some conflicting results.

The findings outlined here and the studies published by Fernando *et al* (2008; 2010) describe a reduction in cell proliferation as a result of WAVE1 knockdown. Similarly both studies demonstrate a suppressed proliferative potential of PC-3 cells following WAVE3 knockdown. Fernando *et al* showed this change to be very moderate and was not found to be significant whereas in contrast WAVE3 knockdown in PC-3 potently decreased proliferation by approximately 35% and was found to be statistically significant.

The discrepancy between these two studies is possibly due to the different statistical tests used and the number of independent repeats used. Five independent repeats were tested using ANOVA by Fernando *et al* whilst in this present study Mann-Whitney test was used to analyse at least nine independent experiments, thus making it a more robust experiment. Furthermore, the results presented here agree with those published by an independent research group which observed a reduction in cell proliferation with a decrease in WAVE3 expression. In addition to these *in vitro* experiments, the same group discovered a significant reduction of tumour growth rate within *in vivo* experiments (Teng *et al*., 2010).

As mentioned previously, the effects on cell migration were investigated using a Cytodex motility bead assay. Whilst WAVE3 knockdown was shown to significantly repress cell motility, this was not observed for PC-3 cells exhibiting WAVE1

knockdown. This is a surprising result as the involvement of the WAVE proteins during cell migration is well established (Fernando *et al.,* 2009).

Investigations of the above mentioned cell properties show how WAVE1 and 3 display both similar and dissimilar effects on cell function when their expression is knocked down in the metastatic prostate cancer cell line, PC-3. Such findings suggest that they are potentially involved in both common and distinct signalling pathways in facilitating cell motility and that they have an effect on proliferation and invasion, two traits over which they are less attributed to having influence. The contrasting observations of WAVE knockdown on motility may suggest that their roles in the cell are not entirely genetically redundant. Whilst WAVE1 and 3 share the same protein domains fundamental to their functional roles in the cell, an alignment of their protein sequences reveal only 49.7% identity (Pearson *et al,* 1997). With these two proteins sharing a relatively low similarity in protein sequence, it can be postulated that any divergence could translate into different traits due to the ability to regulate or be regulated by different protein partners and thus potentially influence different signalling pathways.

Originally, both PC-3 and DU-145 cell lines were used as these are androgen-independent cells and are popular models of metastatic prostate cancer. However, cell function assays with DU-145 showed considerable spread of data and were therefore not included in this study.

The findings of this chapter indicate the potential for the WAVE1 and 3 to influence the PC-3 prostate cancer cell line and thus further implicate these proteins in the processes of cell metastasis and cancer progression. Future chapters will aim to explore further the mechanistic action of these proteins.

Chapter 4

The association between WAVE 1 and 3 and the Arp2/3 complex in the PC-3 cell line

4.1 Introduction

Coordinating the dynamic process of cell migration requires numerous diverse networks of proteins and complexes which interact within a complicated signalling cascade. Instigation of this signalling pathway begins with an exchange of GDP for GTP in the Rho GTPase cycle which occurs in response to upstream signals. This message is conveyed to targets downstream of activated Rho GTPase and thus triggers a sequence of protein interactions including WAVE activation which induces conformational changes in the Arp2/3 complex (Kobayashi *et al*., 1998; Machesky and Insall., 1998; Miki *et al.*, 1998). These steps promote actin polymerisation at the cell leading edge and form a rudimentary principle underpinning cell migration. Although this order of events and its associated cell function is well defined, it is still not clear whether auxiliary proteins are involved in this complex mechanism and ultimately what these collaborating proteins are.

Increasing evidence points towards an association between WAVE and human cancer. As described in Chapter 1, the general trend suggests elevated levels of WAVE to be linked with more aggressive cancer traits such as increased invasive and motile abilities as seen in both *in vitro* and *in vivo* assays (Fernando *et al,* 2008; Fernando *et al,* 2010; Teng *et al,* 2010). Furthermore, this trend appears to be of clinical importance as shown by the observation of aberrant WAVE expression levels in cancers that have progressed to a more advanced stage (Semba *et al*., 2006; Iwaya *et al*., 2007; Yang *et al*., 2006; Sossey-Alaoui *et al.*, 2007).

Whilst the research interests of this project are focused towards the role of WAVE in prostate cancer metastasis, the metastatic potential of cancer cells is not solely limited to their motile ability but also their capacity to proliferate and establish secondary tumours. Furthermore, cancer metastasis is also dependent on the ability

of tumour cells to resist apoptosis and induce angiogenesis. With a comprehension of how multi-layered cancer metastasis can be, being able to define WAVE interacting proteins in this signalling cascade would allow a greater appreciation of the mechanism.

Actin polymerisation as a driver of cell migration is dependent on the Arp2/3 complex and is unable to elicit this function without stimulation by its nucleation promoting factors (NPF) (Higgs and Pollard, 1999). As previously mentioned, the WAVE proteins are well defined NPFs of Arp2/3 (Goley and Welch, 2006). Although WAVE is only functional when coordinated with four additional components to comprise the WAVE regulatory complex (WRC) (Eden *et al.*, 2002), it is unclear whether actin polymerisation occurs in response to the interaction of solely Arp2/3 and WRC or whether additional proteins are required. Also, as humans exhibit three WAVE isoforms, WAVE1, 2 and 3; it would be interesting to investigate whether any functional redundancy exists in this signalling pathway and whether different WAVE isoforms require the interplay of different proteins or if the different WAVE proteins regulate different downstream targets.

The protein domains of WAVE are integral to their ability to interact with Arp2/3 and their association with the other four subunits that comprise the WAVE regulatory complex (Eden *et al.*, 2002; Takenawa and Suetsugu., 2007). Whilst the domains of WAVE proteins do not appear to confer the ability of the protein to phosphorylate downstream targets, the effects of WAVE knockdown on the phosphorylation state of Arp2 and 3 were investigated. As a result, it was hoped that this would reveal insight into the molecular consequences of WAVE knockdown and whether other cell migration pathways directly or indirectly interplay with WAVE.

With this in mind, the initial section of this chapter describes work to firstly determine the effect on Arp 2 and 3 expression in response to the knockdown of WAVE 1 or 3 expression in the metastatic prostate cancer cell line, PC-3. Following this, the cell function assays described previously in Chapter 3 were utilised to investigate the effects of a small protein inhibitor specifically targeting the Arp2/3 complex. These findings were compared to experiments outlined in Chapter 3 to permit a comparison between PC-3 control cells and WAVE knockdown cells with and without Arp2/3 inhibitor treatment. Additionally, the effects of WAVE knockdown on Arp2 and 3 protein phosphorylation in PC-3 cells were analysed. Consequently, this would allow a better understanding of the mode of action of WAVE in the context of prostate cancer metastasis.

Given the well documented relationship between WAVE and the Arp2/3 complex and their contributory role in actin polymerisation, it would plausible to predict similar functional effects when comparing WAVE knockdown and Arp2/3 inhibition.

4.2 Methods and materials

4.2.1 Cell lines

PC-3 cells were cultured and maintained as described in Section 2.2.4.

4.2.2 Synthesis of complementary DNA and RT-PCR

Complementary DNA was generated as described in Section 3.2.3, whilst the same RT-PCR techniques were used to determine expression levels of Arp2 and 3 using primers designed specifically for these genes. These primer sequences are shown in Chapter 2, Table 2.3. RT-PCR was also run in parallel to the housekeeping gene GAPDH to allow a validation of cDNA quality and enable a demonstration of normalised expression levels of the cDNA within the separate cell lines.

4.2.3 *In vitro* cell growth assay

The method for the cell growth assay is described in Section 2.6.1. When setting up the inhibitor treatment groups of the same cell lines to target Arp2/3, the small molecule inhibitor, CK-0944636 (Sigma-Aldrich, Dorset, UK), was used at a concentration of 200nM (inhibitor concentration based on cytotoxic assays performed within the laboratory). This small molecule inhibitor blocks the Arp2 and Arp3 subunits of the Arp2/3 complex moving into close proximity and therefore into a conformation that activates the protein complex, the basic principle behind actin polymerisation. The molecular structure of CK-0944636 is shown in Figure 4.1.

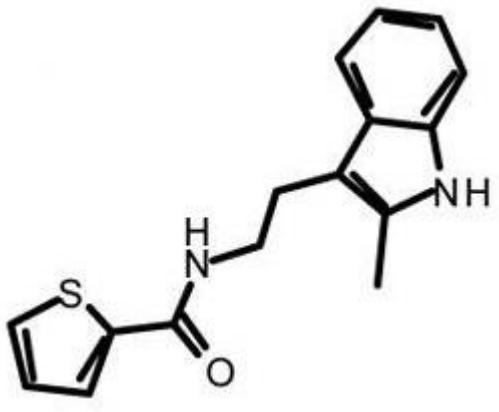

Figure 4.1 Molecular structure of the Arp2/3 inhibitor CK-0944636 (image taken from Nolen *et al*, 2009)

4.2.4 *In vitro* cell Matrigel invasion assay

The preparation of the cell invasion assay is outlined in Section 2.6.2. For the treatment groups, the inhibitor and the corresponding concentration used is described in Section 4.2.3.

4.2.5 *In vitro* cell motility assay

The preparation of the cell motility assay is outlined in Section 2.6.4. For the treatment groups, the inhibitor and the corresponding concentration used is described in Section 4.2.3.

4.2.6 Protein extraction, SDS-PAGE and Western blotting

To study proteins in their native, non-denatured form, lysis buffer with SDS substituted for NP-40 detergent was used to extract protein from control and WAVE knockdown PC-3 cells. Protein quantification allowed standardisation of the samples to ensure consistent loading of total protein. The protocol followed is outlined in Section 2.5.

4.2.7 Immunoprecipitation

The procedure for the immunoprecipitation of proteins and appropriate antibodies used is described in Section 2.3.3. To set up a positive control when analysing protein tyrosine phosphorylation, wild type PC-3 cells were cultured until 60-80% confluent. Medium was aspirated for the washing of cells with BSS then aspirated for the addition of 10mM sodium orthovanadate in 5ml serum free medium and hydrogen peroxide to make the final concentration 0.8%. After 10 minutes, this was aspirated for subsequent protein extraction outlined in Section 2.5.1.

4.2.8 Confocal microscopy

The confocal microscopy procedure is outlined in Section 2.7 and the primary and secondary antibodies used are shown in Tables 2.4 and 2.6, respectively.

4.3 Results

4.3.1 Expression analysis of Arp2 and Arp3 in WAVE1 and WAVE3 knockdown PC-3 cells

Overall, expression levels of both Arp2 and 3 in the wild type and pEF6 control PC-3 cells were observed to be similar. PC-3 cells shown to exhibit either WAVE1 or 3 knockdown displayed no significant change in Arp2 or 3 expression. As expected, expression levels of GAPDH are seen to remain similar across all PC-3 cell lines analysed. The negative control, which substituted cDNA by PCR water, revealed no signs of contamination. The results of the expression analysis utilising PCR are shown in Figure 4.2.

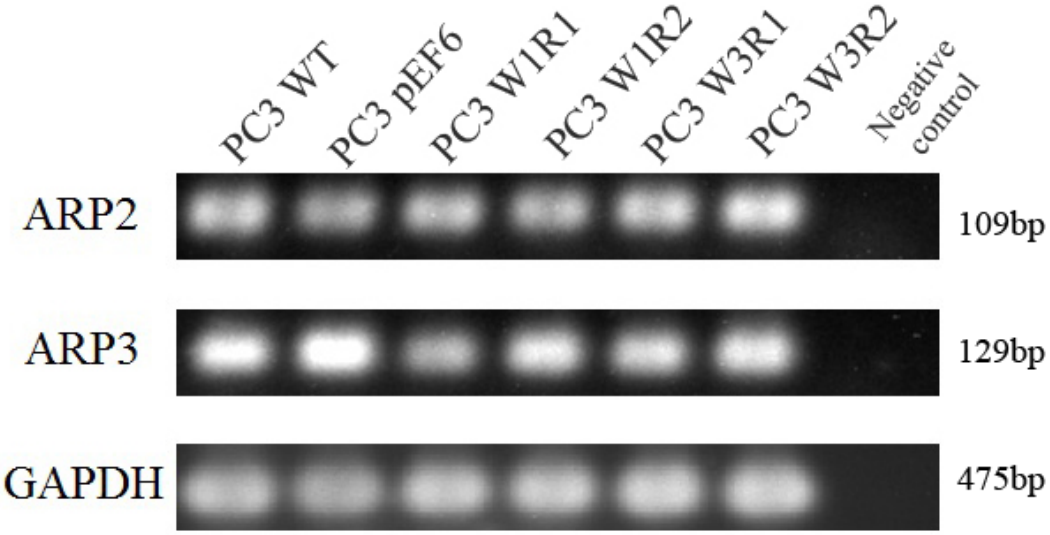

Figure 4.2 Arp2 and 3 mRNA expression analysis following knockdown of either WAVE 1 or 3 revealed no significant effect on levels of Arp2 or 3 expressed in PC-3 cells. GAPDH expression remained unaffected regardless of WAVE1 or 3 knockdown whilst the negative control revealed no signs of contamination.

4.3.2 Arp inhibitor treatment affects cell growth in WAVE knockdown PC-3 cells but shows little effect on pEF6 control cells

Treatment of pEF6 control PC-3 cells with an Arp2/3 inhibitor, CK-0944636 resulted in no significant change in cell growth ($p=0.109$). Treatment of PC-3 cells which had been shown to exhibit WAVE1 knockdown with the same Arp2/3 inhibitor showed a non-significant decrease in cell growth compared to the untreated PC-3 W1R2 cells ($p=0.182$). WAVE3 knockdown PC-3 cells showed a significant reduction in cell growth with Arp inhibitor treatment compared to cells without Arp inhibition ($p=0.045$). These cell growth results are displayed in Figure in 4.3.

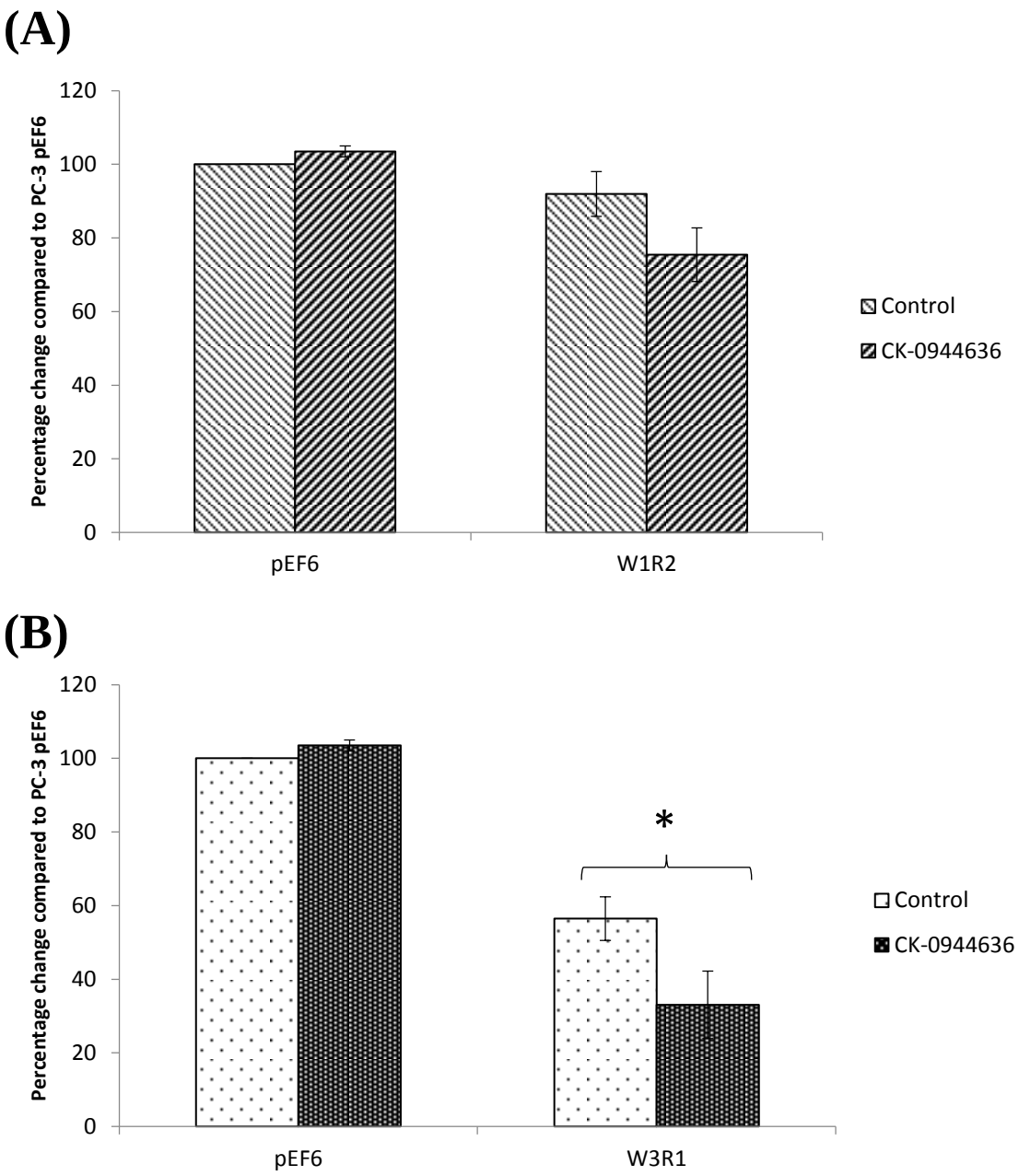

Figure 4.3 Arp2/3 inhibitor treatment showed little effect on cell growth in pEF6 control PC-3 cells however a moderate decrease in cell growth was observed in WAVE1 knockdown cells (A) whilst this treatment showed a greater reduction of cell growth in WAVE3 knockdown cells (B). Shown are mean data from a minimum of three independent repeats, values represent percentage change to pEF6 cells without treatment (control). Error bars represent SEM. * represents $p < 0.05$.

4.3.3 Arp2/3 inhibitor treatment affects cell invasion in PC-3 cells with WAVE1 knockdown but not with WAVE3 knockdown

The number of cells which invaded the Matrigel layer of the invasion insert after 72 hours of incubation was compared between those with and those without Arp2/3 inhibitor treatment. This comparison revealed a moderate decrease in cell invasion in pEF6 control PC-3 cells in response to Arp2/3 inhibitor treatment compared to untreated PC-3 pEF6 cells ($p=0.214$). No significant change in cell invasiveness was observed in WAVE3 knockdown cells following treatment with the Arp2/3 inhibitor, CK-0944636 compared to untreated PC-3 W3R1 cells ($p=0.652$) (shown in Figure 4.5). When examining the data for PC-3 cells showing WAVE1 knockdown, an overall increase in invaded cells was observed in cells treated with the Arp2/3 inhibitor relative to no treatment. However, this change was not found to be significant ($p=0.216$). These cell invasion results are displayed in Figure in 4.4.

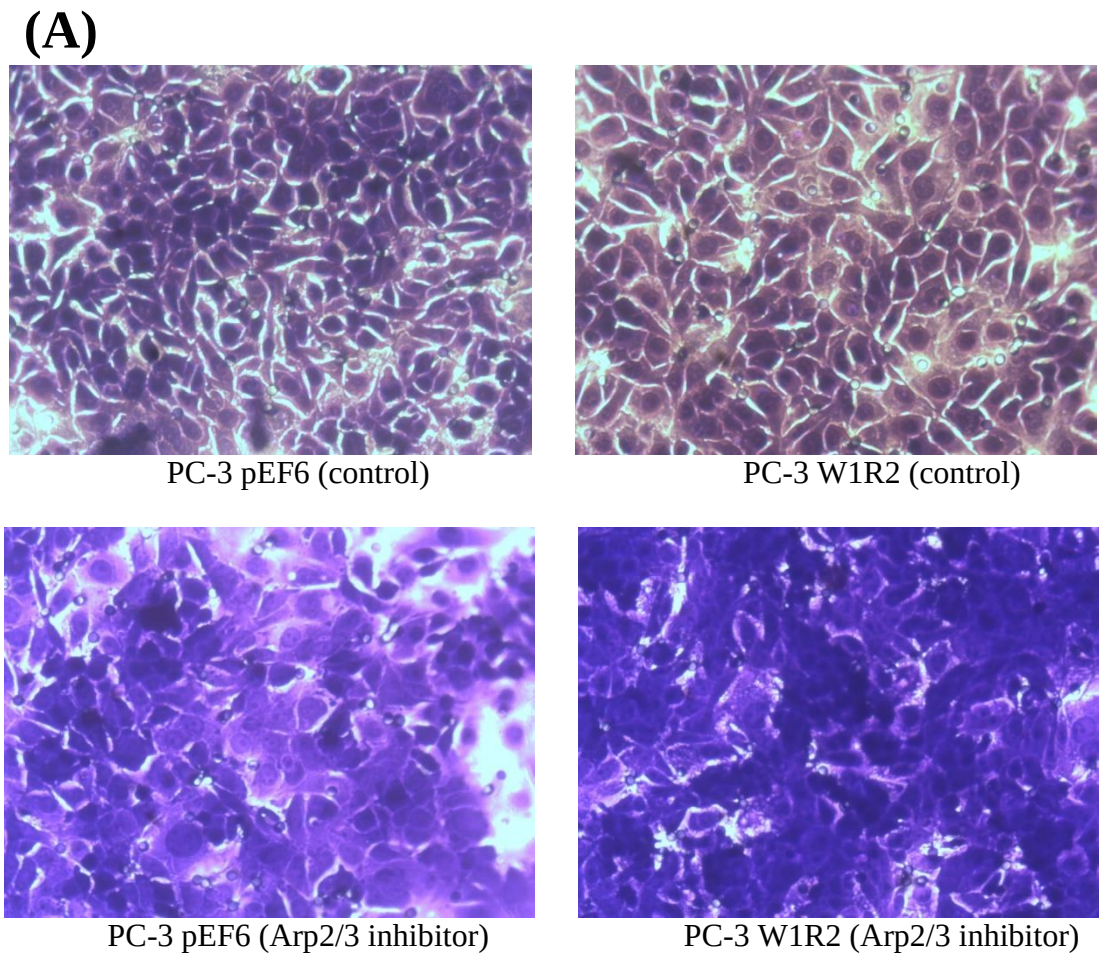

Figure 4.4 Arp2/3 inhibitor treatment showed a small reduction in cell invasion in the pEF6 control cell line. In contrast, an increase in cell invasion was observed in WAVE1 knockdown (W1R2) PC-3 cells following Arp2/3 inhibitor treatment. Figure 4.4A displays representative images acquired for PC-3 pEF6 and W1R2 cells with/without Arp2/3 inhibitor treatment. Images were acquired from at least three independent experiments where cells were counted to calculate percentage change in cell invasion compared to PC-3 pEF6 cells without Arp2/3 inhibitor treatment (shown in Figure 4.4B). Images acquired at 200X magnification. Shown are mean data with error bars representing SEM.

(A)

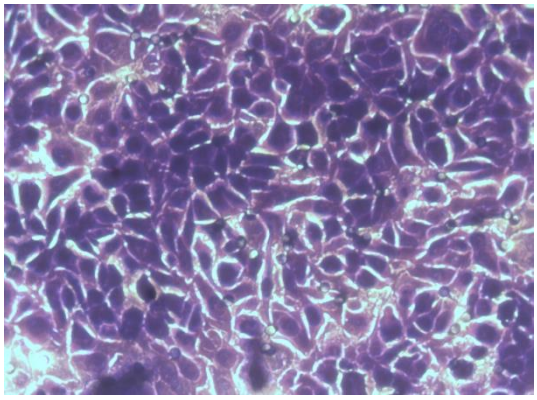

PC-3 pEF6 (control)

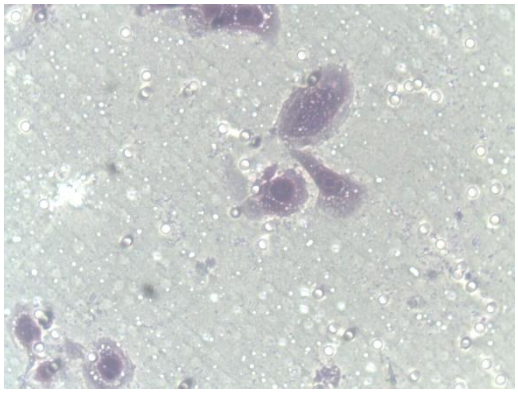

PC-3 W3R1 (control)

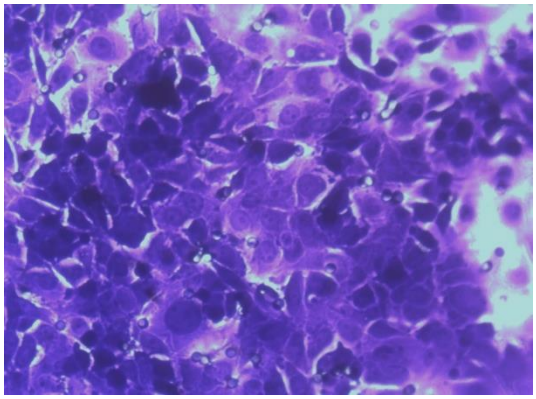

PC-3 pEF6 (Arp2/3 inhibitor)

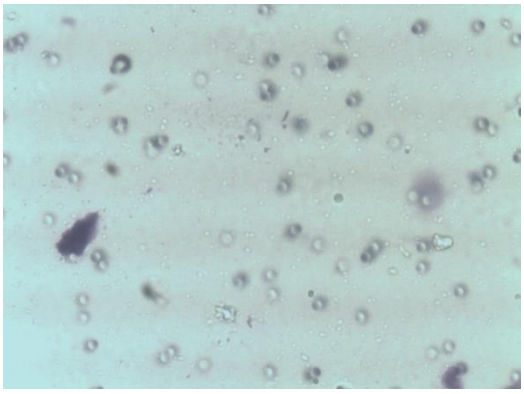

PC-3 W3R1 (Arp2/3 inhibitor)

(B)

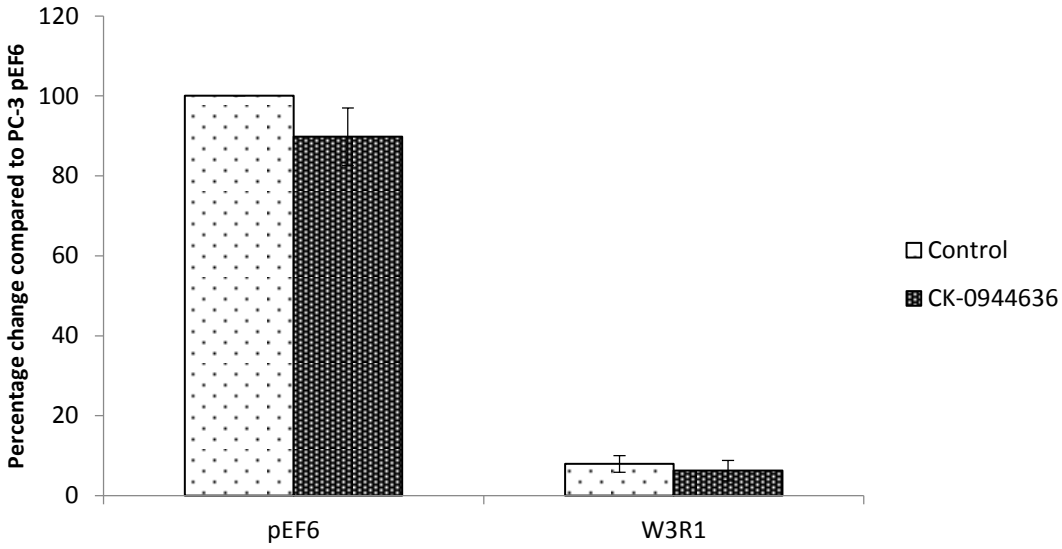

Figure 4.5 Arp2/3 inhibitor treatment showed a small reduction in cell invasion in the pEF6 control cell line whilst the same but non-significant trend was also seen for WAVE3 knockdown (W3R1) PC-3 cells. Figure 4.5A displays representative images acquired for PC-3 pEF6 and W3R1 cells with/without Arp2/3 inhibitor treatment. Images were acquired from at least three independent experiments where cells were counted to calculate percentage change in cell invasion compared to PC-3 pEF6 cells without Arp2/3 inhibitor treatment (shown in Figure 4.5B). Images acquired at 200X magnification. Shown are mean data with error bars representing SEM.

4.3.4 Arp2/3 inhibitor treatment increases cell motility in PC-3 cells

An overall trend of increased cell motility was observed with a four hour treatment of the Arp2/3 inhibitor. PC-3 pEF6 cells as well as both W1 and W3 knockdown cells appeared to be more motile following treatment with the Arp2/3 inhibitor. However, this increase in motile ability was only significant in pEF6 control cells ($p<0.001$) whilst it was not found to be significant for either WAVE1 or WAVE3 knockdown cells when compared to the untreated equivalent cell lines ($p=0.078$; $p=0.421$, respectively). These cell motility results are displayed in Figure in 4.6.

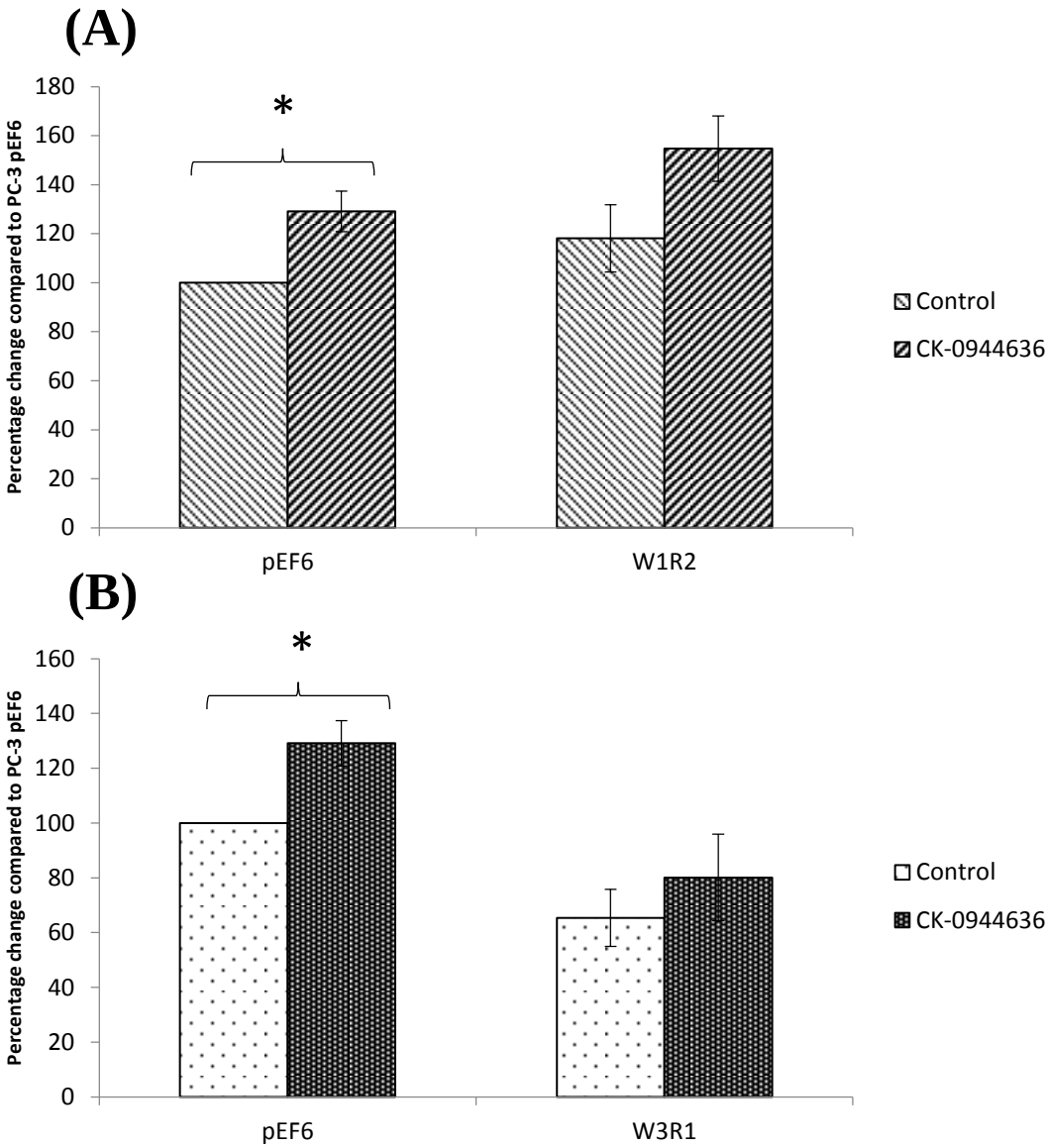

Figure 4.6 Arp2/3 inhibitor treatment increased cell motility in pEF6 control, WAVE1 (A) and WAVE3 (B) knockdown PC-3 cells. However, this increase was found to be insignificant for PC-3 W1R2 and W3R1 cell lines. Shown are mean data from a minimum of three independent repeats, values represent percentage change to pEF6 cells without treatment. Error bars represent SEM. * represents $p < 0.05$.

4.3.5 ARP2 co-localises with WAVE1 and 3 in PC-3 cells

Confocal microscopy approaches were employed to further investigate the relationship between WAVE and ARP proteins in the PC-3 cell line. Firstly, WAVE1 and 3 proteins were probed with a FITC-conjugated antibody which fluoresces green whilst ARP2 was probed with a TRITC-conjugated antibody and fluoresces red. The acquired images revealed co-localisation of WAVE1 and ARP2 to the perimeter of the cell lamellipodia of PC-3 pEF6 cells (refer to Figure 4.7A), however, this was less prominent in PC-3 WAVE1 knockdown cells (W1R2) (refer to Figure 4.7B). Furthermore, lamellipodia of pEF6 cells encompassed a larger area than W1R2 cells.

Similarly, analysis of WAVE3 and ARP2 protein location in PC-3 pEF6 cells revealed co-localisation of these proteins to the lamellipodia edge (refer to Figure 4.8A). In contrast, WAVE3 knockdown cells (W3R1) demonstrated a lack of WAVE3 and ARP2 co-localisation (refer to Figure 4.8B). Moreover, the lamellipodia of PC-3 W3R1 cells were also less pronounced than those of pEF6 cells.

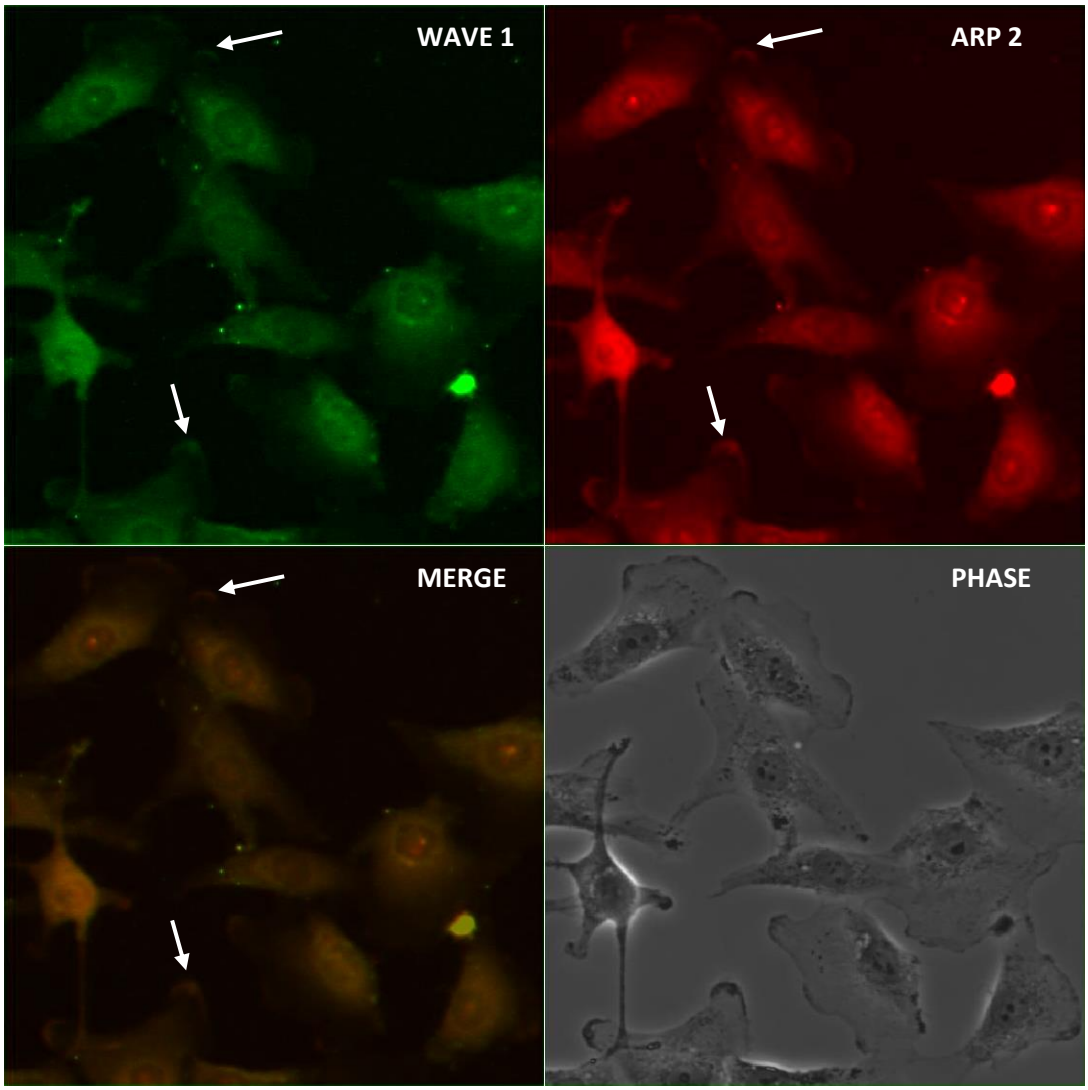

Figure 4.7A Confocal microscopy images of PC-3 pEF6 cells stained for WAVE1 (FITC) and ARP2 (TRITC) reveal co-localisation of these proteins (represented by arrows). Also shown are FITC and TRITC merged images (MERGE) and the phase contrast image (PHASE). Representative images shown. Images acquired at 600X magnification.

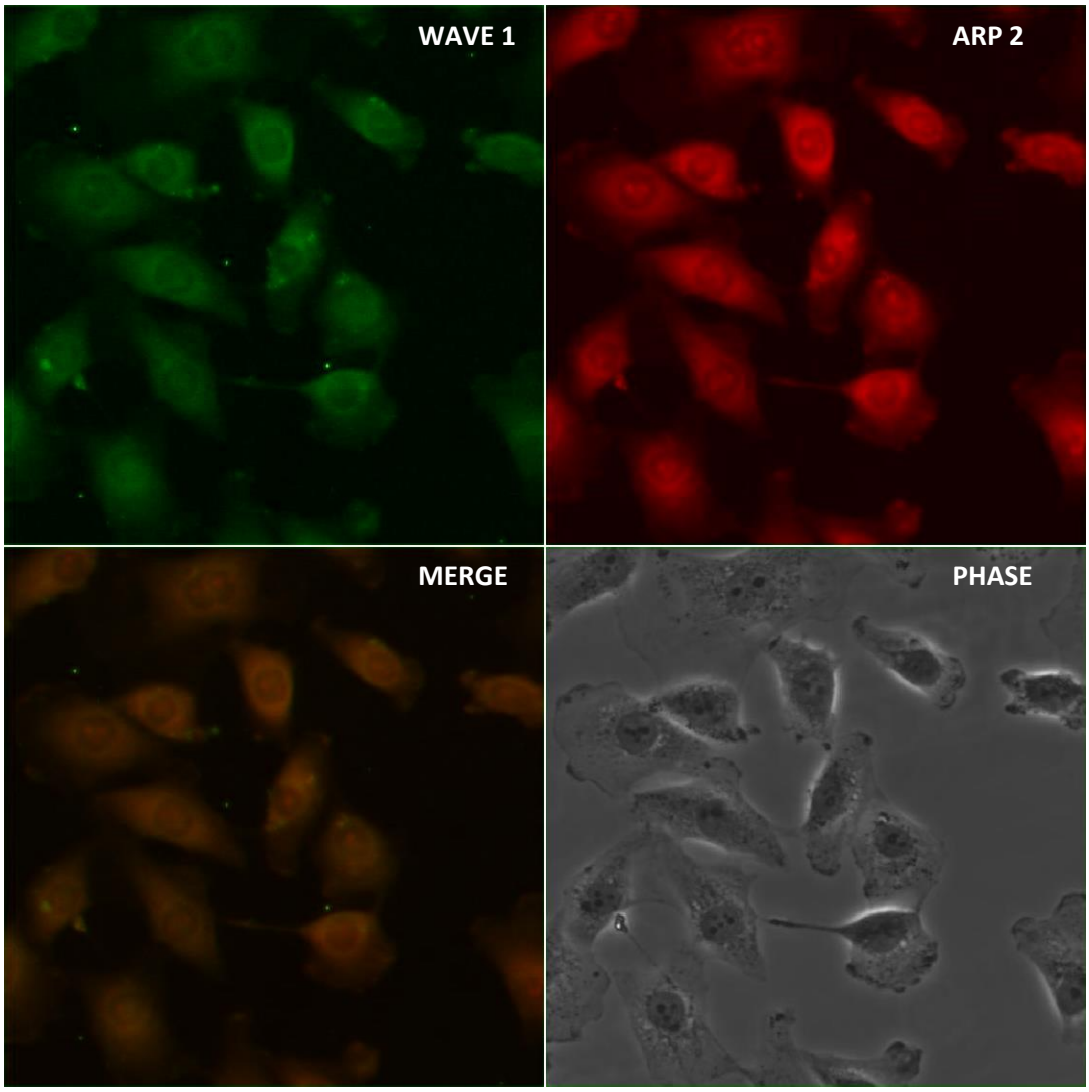

Figure 4.7B Confocal microscopy images of PC-3 W1R2 cells stained for WAVE1 (FITC) and ARP2 (TRITC). Also shown are FITC and TRITC merged images (MERGE) and the phase contrast image (PHASE). Representative images shown. Images acquired at 600X magnification.

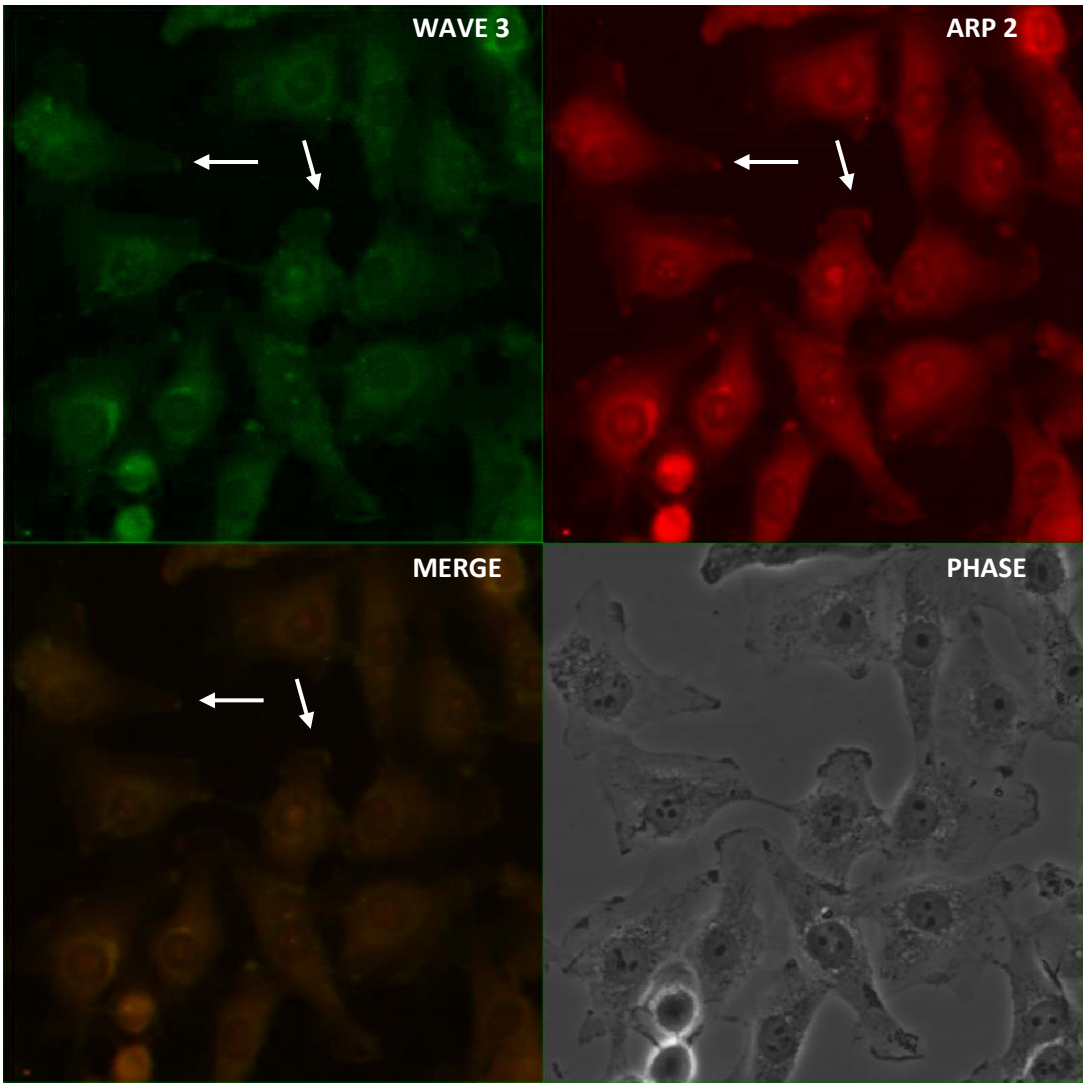

Figure 4.8A Confocal microscopy images of PC-3 pEF6 cells stained for WAVE3 (FITC) and ARP2 (TRITC) reveal co-localisation of these proteins (represented by arrows). Also shown are FITC and TRITC merged images (MERGE) and the phase contrast image (PHASE). Representative images shown. Images acquired at 600X magnification.

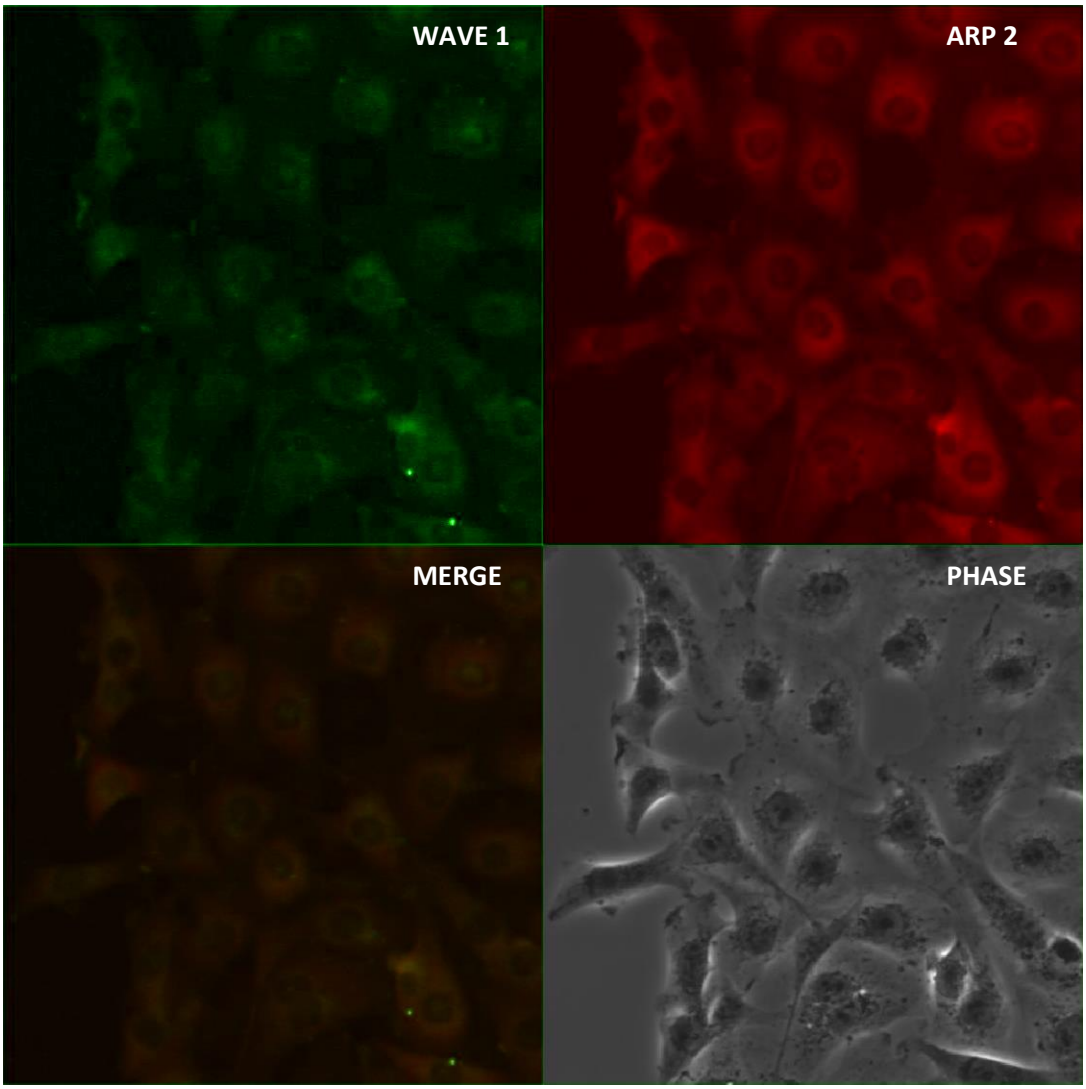

Figure 4.8B Confocal microscopy images of PC-3 W3R1 cells stained for WAVE3 (FITC) and ARP2 (TRITC). Also shown are FITC and TRITC merged images (MERGE) and the phase contrast image (PHASE). Representative images shown. Images acquired at 600X magnification.

4.3.6 WAVE3 knockdown increases ARP2 tyrosine phosphorylation in PC-3 cells

Proteins were immunoprecipitated with the anti-phosphotyrosine antibody, PY20 and subsequently probed with ARP2 and 3 antibodies. This approach revealed a higher level of tyrosine phosphorylation of ARP2 in PC-3 cells exhibiting WAVE3 knockdown relative to wild type and pEF6 control cells (Figure 4.9A). Levels of ARP2 tyrosine phosphorylation in WAVE3 knockdown cells were comparable to the positive control. In contrast, PC-3 cells expressing lower levels of WAVE1 were found to have similar ARP2 tyrosine phosphorylation levels as the wild type and pEF6 control cells. Similar levels of ARP2 protein were observed in the raw lysate for all PC-3 protein samples and levels of GAPDH protein were consistent in all samples probed.

Using the same techniques revealed no changes in ARP3 tyrosine phosphorylation levels following WAVE1 or 3 knockdown in PC-3 cells as the intensity of the bands were observed to be similar. Moreover, the ARP3 tyrosine phosphorylation levels of PC-3 wild type, pEF6 control, WAVE1 and 3 knockdown were seen to be lower than the positive control. Overall, ARP3 and GAPDH protein levels were demonstrated to be the same in the cell lysates examined (Figure 4.9B).

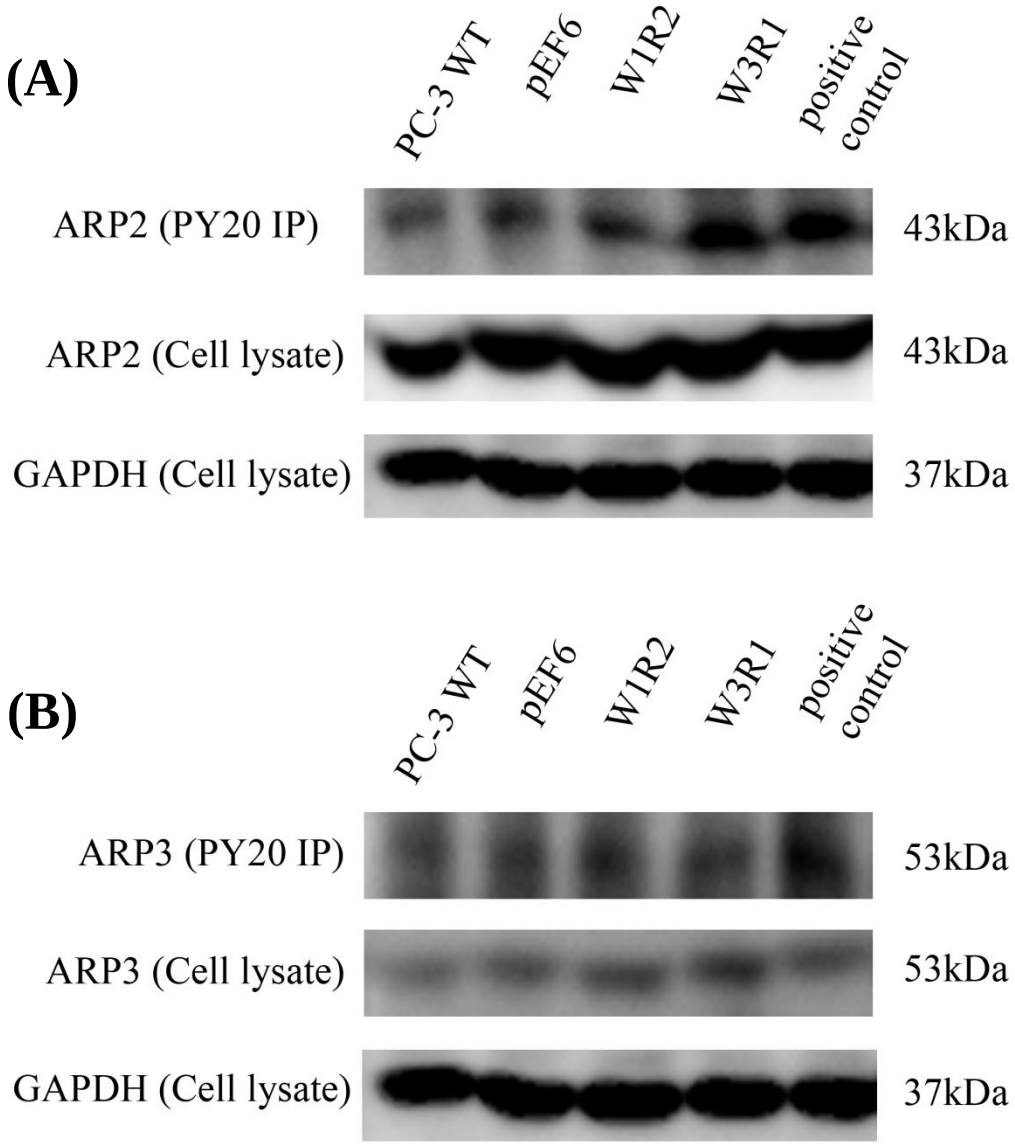

Figure 4.9 Proteins immunoprecipitated with the anti-phosphotyrosine antibody, PY20, revealed increased tyrosine phosophorylation of ARP2 in WAVE3 knockdown (W3R1) PC-3 cells. This was similar to levels in the positive control. Wild type (WT) and pEF6 control PC-3 cells showed similar levels of tyrosine phosphorylation which were comparable with levels observed for WAVE1 knockdown (W1R2) PC-3 cells. ARP2 and GAPDH levels in the cell lysate were observed to be the same in all protein samples (A). The same approaches revealed no changes in tyrosine phosphorylation when comparing protein extracted from PC-3 WT and pEF6 to either W1R2 or W3R1 cells. Levels of ARP3 and GAPDH are similar in these protein samples (B).

4.4 Discussion

The mechanism of Arp2/3 complex activation by WAVE proteins for driving actin polymerisation is well established. WAVE induces the integral subunits of this complex, Arp2 and Arp3, into a conformation which resembles an actin nucleation seed (actin dimer), which is essential for actin polymerisation and the resulting cellular function, cell migration (Higgs and Pollard, 1999). The finding of aberrant WAVE expression and elevated Arp2 levels associated with some metastatic human cancers (Kurisu *et al.*, 2005; Iwaya *et al*., 2007; Sossey-Alaoui *et al.*, 2007) are not surprising considering their role in cell motility. When unregulated, cell motility is known to benefit the spread of aggressive cancer to both local and distant sites. Accordingly, by studying the possible mechanism underlying the relationship between WAVE and the Arp2/3 complex further, it was hoped that this would enable a better understanding of how their association contributes to metastatic prostate cancer.

In the current study, expression analysis in control and WAVE knockdown PC-3 cells revealed WAVE1 or 3 expression knockdown had no significant effect on Arp2 or 3 expression. This implies that the regulation of WAVE1 and 3 expression could be independent to Arp2 and 3 expression. Whilst Figure 4.2 appears to show a slightly higher Arp3 expression in PC-3 pEF6, this difference is minor and not reflected in ARP3 protein expression as shown for the cell lysate in Figure 4.9B. Therefore, the role of WAVE1 and 3 in this actin polymerisation pathway is to regulate Arp2/3 activation and not the expression of its protein subunits.

An investigation into the effects of WAVE1 and 3 expression knockdown was found to have implications on the proliferative and invasive ability of PC-3 cells whilst motility was affected by WAVE3 downregulation (as outlined in Chapter 3). With

these WAVE knockdown PC-3 cell lines established, the relationship between WAVE1 and 3 and the Arp2/3 complex, in the context of these cell functions, was explored with the use of a small molecule inhibitor (CK-0944636) targeting the Arp2/3 complex. Treatment of PC-3 pEF6 control cells with the Arp inhibitor was found to have little effect on cell growth; this is in contrast to the findings of significant suppression of cell proliferation in PC-3 cells with WAVE3 knockdown whereas these inhibitory effects were modest in WAVE1 knockdown cells. Whilst pEF6 cells appear to be unaffected by Arp inhibition, it is interesting to find that the response when replicated in both WAVE1 and 3 knockdown cells is a dramatic drop in levels of growth ($p=0.016$ for both W1R2 and W3R1 when compared to treated pEF6 cells). It would appear that coupling WAVE knockdown and Arp inhibition achieves the most dramatic inhibitory effects on cell proliferation in PC-3 cells with WAVE3 knockdown and Arp inhibition producing the most pronounced effect ($p=0.045$) compared to WAVE1 ($p=0.182$). These observations suggest both WAVE1 and 3 and Arp2/3 play a role in cell growth although the influence of WAVE on proliferation is greater than the Arp2/3 complex. These findings highlight a complexity to the cell proliferation pathway which extends beyond WAVE and Arp2/3 and involves auxiliary proteins (proposed in Figure 4.10). As the treatment of pEF6 cells with the Arp2/3 inhibitor show little change in cell growth, this implies WAVE may target downstream proteins in a pathway independent of Arp2/3 to regulate proliferation of PC-3 cells. Furthermore, it is likely that the Arp2/3 complex is influenced by an upstream regulator separate to WAVE as inhibition of Arp2/3 activity reduces cell proliferation further when coupled to WAVE knockdown. This upstream protein could be WASP and/or N-WASP as they are both known activators of the Arp2/3 complex (Machesky and Insall., 1998).

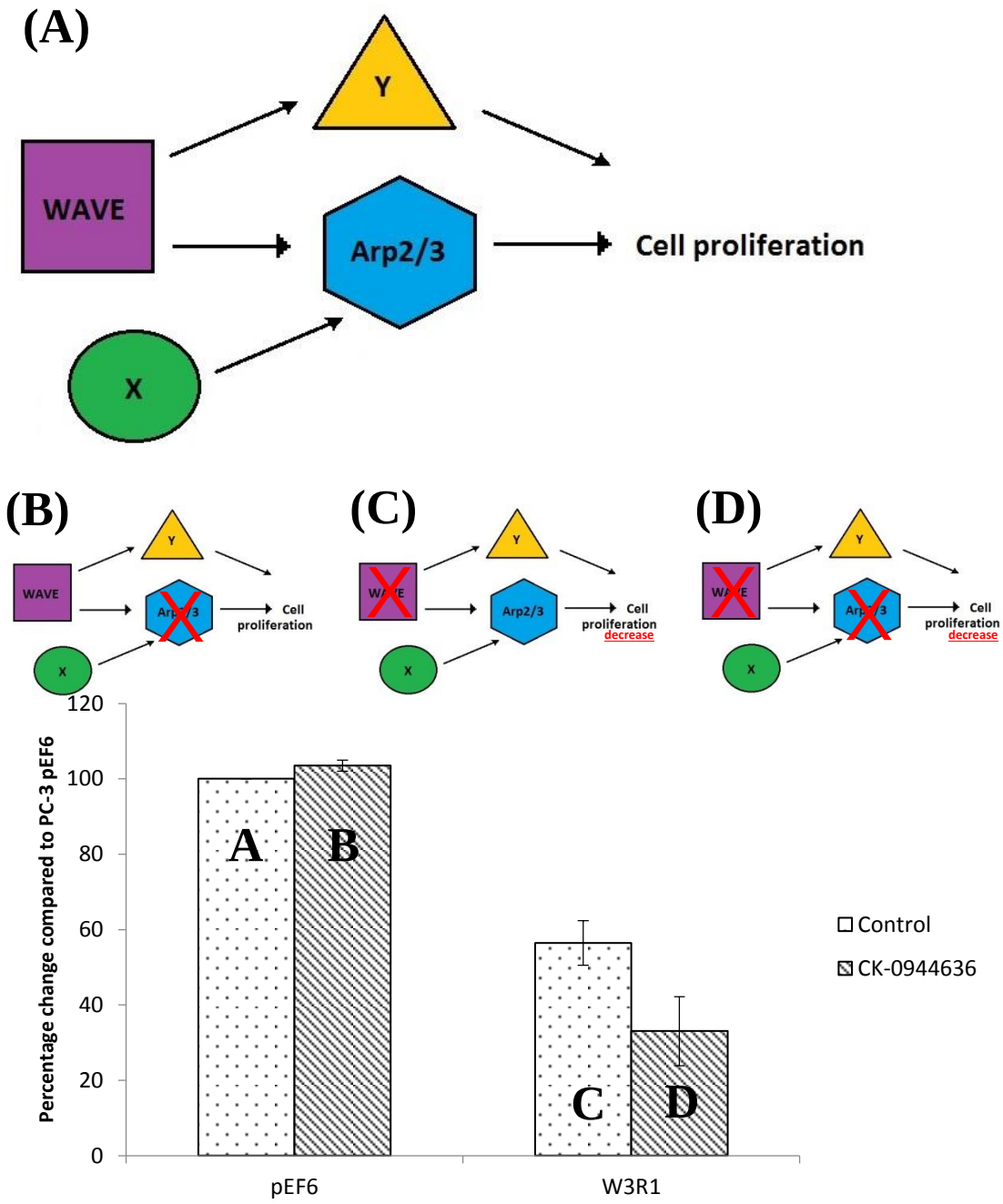

Figure 4.10 Hypothesised WAVE-Arp2/3 cell proliferation pathway. (A) WAVE regulates downstream targets including Arp2/3 and others yet unidentified. Both influence cell proliferation. Other proteins besides WAVE regulate Arp2/3. This diagram depicts the hypothesised cell growth signalling in pEF6 cells without Arp inhibitor treatment (B) pEF6 cells with Arp inhibitor has no effect on cell growth due to an independent pathway to Arp2/3 (C) Arp2/3 is unable to be activated by WAVE in WAVE knockdown cells but is stimulated by unidentified upstream proteins, but overall cell growth is reduced (D) Both WAVE and Arp2/3 are out of action in WAVE knockdown cells treated with Arp2/3 inhibitor. Cell growth is greatly suppressed. Figure 4.3B depicting WAVE3 knockdown was used to represent hypothetical cell proliferation signalling involving Arp2/3 for WAVE1 and 3.

Cell invasion showed a moderate decrease in pEF6 cells treated with Arp2/3 inhibitor and very little effect in WAVE3 knockdown cells. On the contrary, the suppressed cell invasive effect which was observed in response to WAVE1 knockdown was seen to be rescued by Arp inhibitor treatment to levels comparable with untreated pEF6 cells. This was a very surprising effect which highlights a distinction between WAVE1 and 3 functions. It would not be unreasonable to interpret these contrasting effects of Arp2/3 inhibitor treatment, when comparing WAVE1 and 3 knockdown cells, as a consequence of specific and different functions served by these two proteins in the cell.

Although cell invasion was significantly suppressed with WAVE1 knockdown, when Arp2/3 complex activity was blocked with Arp2/3 inhibitor treatment, these repressed levels of cell invasion were rescued to levels similar to those observed in pEF6 control cells without Arp inhibitor treatment. Whilst WAVE1 or 3 knockdown is shown to suppress the ability for PC-3 cells to invade the Matrigel layer in the *in vitro* invasion assay, it is apparent that an independent mechanism is utilised by WAVE1 during cell invasion to that used by WAVE3. The ability of cancer cells to invade into the surrounding tissue requires deconstruction of the extracellular matrix (ECM) and is facilitated by matrix metalloproteases (MMPs) which have the ability to degrade components of the ECM (Deryugina and Quigley., 2006). An association between WAVE3 and various MMPs in cell invasion and motility has been proposed as a contributory factor to cancer metastasis (Sossey-Alaoui *et al.*, 2005; 2009; Zhang *et al.,* 2012). These studies focused on elucidating the relationship between WAVE3 and MMP expression and in particular how the former affected the latter in addition to exploring their co-expression in colorectal cancer tissues. Whilst this link has been established, the mechanism that underlies this WAVE3-dependent MMP

regulation is not well understood. It would be interesting to investigate the signalling cascade which links these proteins together and to discover what other proteins interplay along this pathway and additionally their function. In doing so, it would be interesting to see where the Arp2/3 complex lies in the pathway and whether it is involved with a signalling cascade that controls WAVE1 directed cell invasion and not that regulated by WAVE3. Alternatively, it may be the case that Arp2/3 is indeed involved with WAVE3 controlled cell invasion but there may be an inclusion of auxiliary proteins adding an extra dimension of complexity to this hypothetical MMP-WAVE3-Arp2/3 cell invasion pathway.

Cell invasion is dependent on the ability of the cell to migrate; repressing actin polymerisation by inhibiting Arp2/3 would hinder cell motility and likewise, downregulating WAVE1 expression would also produce this outcome due to the requirement of WAVE1 to activate Arp2/3. Indeed, these effects were found to be the case, however, coupling Arp2/3 inhibition and WAVE1 knockdown together was found to rescue this suppressed effect to yield levels of cell invasion similar to pEF6 control cells. This interesting observation could be explained by the fact that WAVE3 is still functional in WAVE1 knockdown cells. Although Arp2/3 activity is inhibited, WAVE3 is able to regulate MMPs which can digest the Matrigel layer of the *in vitro* invasion insert. As this is the first hurdle to be overcome by cancer cells in the metastatic cascade, it makes it possible for alternative cell motility signalling pathways to come into play. However, the effects of Arp2/3 inhibition in WAVE1 knockdown cells were not seen for WAVE3 knockdown cells. This would imply that whilst WAVE3 could be responsible for the invasiveness of WAVE1 knockdown cells through its interaction with MMPs, WAVE1 does not have the same ability to

regulate MMPs in WAVE3 knockdown cells and is therefore unable to rescue suppressed cell invasiveness seen with WAVE3 knockdown and Arp2/3 inhibition.

Alternative cell motility signalling pathways could also explain the observation that PC-3 cells exhibited increased motile abilities with Arp2/3 inhibitor treatment regardless of whether WAVE was knocked down or not and regardless of which WAVE was targeted. These alternative signalling cascades would have to be independent of WAVE as the increased motility trend is seen in both control and WAVE knockdown cells. The increase in cell motility would have to be attributed to these alternative signalling pathways which are not Arp2/3 dependent but are possibly regulated to a certain degree by Arp2/3. It could be postulated that the role of Arp2/3 is to drive cell motility via actin polymerisation whilst regulating it to an appropriate level by suppressing these alternative cell motility pathways.

Previous studies have highlighted the clinical importance of WAVE and ARP proteins in human cancer. These studies demonstrated the co-expression of ARP2 and WAVE2 in lung adenocarcinoma sections and their co-localisation in colon cancer cell lines metastasis (Semba *et al*, 2006; Iwaya *et al*, 2007). Immunofluorescence analysis of PC-3 pEF6 cells in this study demonstrated the co-localisation of ARP2 with both WAVE1 and 3 to the outer boundaries of the cell lamellipodia. Proteins responsible for actin polymerisation are commonly recruited to these cell protrusions to cope with the dynamic nature of cytoskeleton remodelling to facilitate cell migration (Insall and Machesky, 2009). The co-localisation of ARP2 with both WAVE1 and 3 at the PC-3 pEF6 cell edge corresponds with previous findings. The PC-3 cell line was derived from a patient presenting aggressive metastatic prostate cancer and the finding that these proteins, known for their role in cell migration by co-localising at the cell edge, is unsurprising. Furthermore, the

observation of a reduced area encompassed by the cell in WAVE1 or 3 knockdown cells implies a suppressed ability of the cell to generate cell protrusions. Coupling this observation with reduced ARP2/WAVE co-localisation implies that, by knocking down WAVE1 or 3 expression, these proteins are unable to activate the Arp2/3 complex to stimulate actin polymerisation.

The regulatory role of WAVE to stimulate Arp2/3 activity has been well established, however, as the *in vitro* cell models have demonstrated, this relationship is not as linear as: Rho GTPase → WAVE → Arp2/3 → cell function. Experiments described in this chapter hint at the action of auxiliary proteins adding a layer of complexity to pathways which impact on cell growth, invasion and motility. Protein tyrosine kinases are integral to regulating intracellular signalling transduction pathways. Their activity influences several cellular properties including proliferation and survival. With such an essential role in the cell, it is unsurprising to find deregulated cell traits such as uncontrolled growth attributed to aberrant tyrosine kinase activity in human cancer (Blume-Jensen and Hunter, 2001). A knockdown in WAVE3 expression was shown to increase levels of tyrosine phosphorylation of Arp2 in PC-3 cells whilst WAVE1 knockdown was found to show no change. These observations suggest WAVE3 functions upstream of a protein regulator of a tyrosine kinase which is able to target Arp2 of the Arp2/3 complex. At present, five sites of tyrosine phosphorylation have been identified in Arp2: Y22, Y72, Y91, Y225 and Y378. The majority of these modifications are associated with different manifestations of leukaemia and lymphoma (Phosphosite). However, the cell functional consequences from the phosphorylation of these tyrosine residues have not been investigated. Whilst it is uncertain in this study which tyrosine residues are phosphorylated, it is

evident that WAVE3 knockdown has an influence on the phosphorylation of tyrosine residues in Arp2 which may affect its activity.

The effects of WAVE1 and 3 knockdown coupled with Arp2/3 inhibitor treatment has revealed their influence on several cell traits. Whilst some of the trends observed were shared by both WAVEs investigated (cell growth and motility), the intriguing finding that Arp2/3 inhibitor treatment was able to rescue the suppressed cell invasive properties in response to WAVE1 knockdown was not found to be the same with WAVE3 knockdown. Additionally, WAVE3 knockdown was shown to affect Arp2 tyrosine phosphorylation whilst WAVE1 did not. Overall, the *in vitro* cell experiments described along with the phospho-immunoprecipitation approaches, emphasise both shared and distinct roles for WAVE1 and 3 in PC-3 cells. More importantly, the use of a small protein inhibitor targeting the Arp2/3 complex highlights the relationship between WAVE1 and 3 with Arp2/3 involving a multiplex and elaborate network of proteins. Ideally, future work will aim to identify these collaborating proteins. However, the work presented here has revealed additional paths which show that WAVE1 and 3 are able to regulate Arp2/3 and its consequential effect on cell properties. Moreover, it would be interesting to explore the interaction between WAVE and MMP in future work.

Chapter 5

Investigating the association between WAVE 1 and 3 and ROCK-I and II in the PC-3 cell line

5.1 Introduction

A series of dynamic protein interactions upstream of the actin polymerisation stimulator, Arp2/3 complex, drives the formation of cell protrusions at the cell leading edge to drive cell migration (Schafer *et al.,* 1998). The Arp2/3 complex requires stimulation by members of the WASP proteins which themselves need to be activated by members of the Rho GTPases (Kim *et al.,* 2000; Kobayashi *et al.,* 1998). The extensive contribution of this GTPase family to cell function is attributed to the diversity of family members in addition to the vast number of upstream and downstream regulators.

Rho-associated protein kinase (ROCK) is involved in influencing cell motility and has been identified as a downstream effector of one of the main Rho GTPase isoforms, RhoA . These protein serine/threonine kinases of approximately 160kDa consist of two mammalian isoforms, ROCK-I and II (as shown in Figure 5.1). The amino-acid sequences of these ROCK isoforms are highly homologous (approximately 65%) with 92% identity at the kinase domains. The ROCK kinase domain resides at the amino-terminus with the Rho binding domain (RBD), pleckstrin homology (PH) domain and internal cysteine-rich region/domain (CRD) found at the carboxyl-terminus. Separating these functional domains is a region predicted to be a coiled-coil-forming region (Riento and Ridley, 2003).

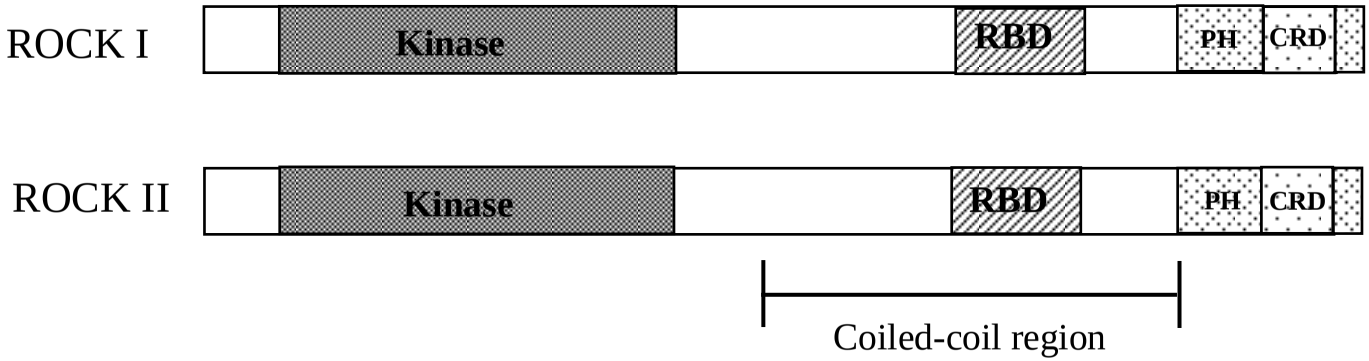

Figure 5.1 The structure of ROCK- I and -II mammalian proteins share overall 65% identity. The kinase domain at the amino-terminus is separated from the Rho-binding domain (RBD), pleckstrin homology (PH) domain and internal cysteine-rich region/domain (CRD) by a predicted coiled-coil-forming domain (Image taken from Riento and Ridley, 2003).

The role of ROCK proteins is to relay signals to multiple targets influencing focal adhesion, actomyosin contractility as well as actin nucleation and polymerisation (Lee *et al*., 2010; Kimura *et al*., 1996; Ohashi *et al*., 2000). With its contribution weighted towards an involvement with actin filament dynamics, ROCK regulates the morphology and movement of cells through cytoskeletal remodelling. Due to the ability of the RBD and PH domains to bind with the amino-terminus, this is an intramolecular mechanism exists which inhibits ROCK kinase activity (Chen *et al.,* 2002). However, activated Rho is able to interact with the RBD and relieve the inhibitory effects of carboxyl-terminal binding to the amino-terminal allowing ROCK to phosphorylate its downstream substrates. Of particular relevance to cell migration is the signalling cascade downstream of ROCK which regulates LIM domain kinase (LIMK) (Sumi *et al.*,2001). ROCK phosphorylates specific threonine residues of LIMK which enhances the ability of LIMK to phosphorylate cofilin. Doing so suppresses the ability of cofilin to dissociate and sever actin filaments at the pointed end. However when phosphorylated by LIM kinase this function is suppressed and thus stabilises filamentous actin (Arber *et al*., 1998).

Through its association with many mechanisms, including those that govern actin filament maintenance and cell motility regulation, it is apparent that ROCK has an essential role in the cell (Amano *et al*., 2010). The relationship between the ROCK and WAVE isoforms was investigated due to their important contributions to cell migration and to elucidate their significance in relation to prostate cancer metastasis. As WAVE and ROCK both play an important role in actin filament dynamics to drive cell motility through separate mechanistic approaches, coupling WAVE knockdown with ROCK inhibition should see a decrease in cell traits such as cell migration which is a contributory feature in cell metastasis.

5.2 Methods and materials

5.2.1 Cell lines

PC-3 cells were cultured and maintained as outlined in Section 2.2.4.

5.2.2 Synthesis of complementary DNA and RT-PCR

Complementary DNA was generated as described in Section 2.4 whilst the same RT-PCR techniques were used to determine expression levels of ROCK-I and II using primers designed specifically for these genes. These primer sequences are shown Table 2.3 (Chapter 2). RT-PCR was also run in parallel to the housekeeping gene GAPDH to allow a validation of cDNA quality and enable a demonstration of normalised expression levels of the cDNA within the separate cell lines.

5.2.3 *In vitro* cell growth assay

The preparation of the cell growth assay is outlined in Section 2.6.1. The small molecule inhibitor, Y-27632 (dihydrochloride monohydrate) (sc-3536, Santa-Cruz, USA), targets both mammalian ROCK isoforms (ROCK-I and II) (Ishizaki *et al*., 2000). Y-27632 was used for inhibitor treatment groups at a concentration of 100nM (inhibitor concentration based on cytotoxic assays performed within the laboratory) (Mediero *et al*, 2008*).* Y-27632 is a selective inhibitor which acts as an ATP-competitive inhibitor of ROCK. The molecular structure of Y-27632 is shown in Figure 5.2.

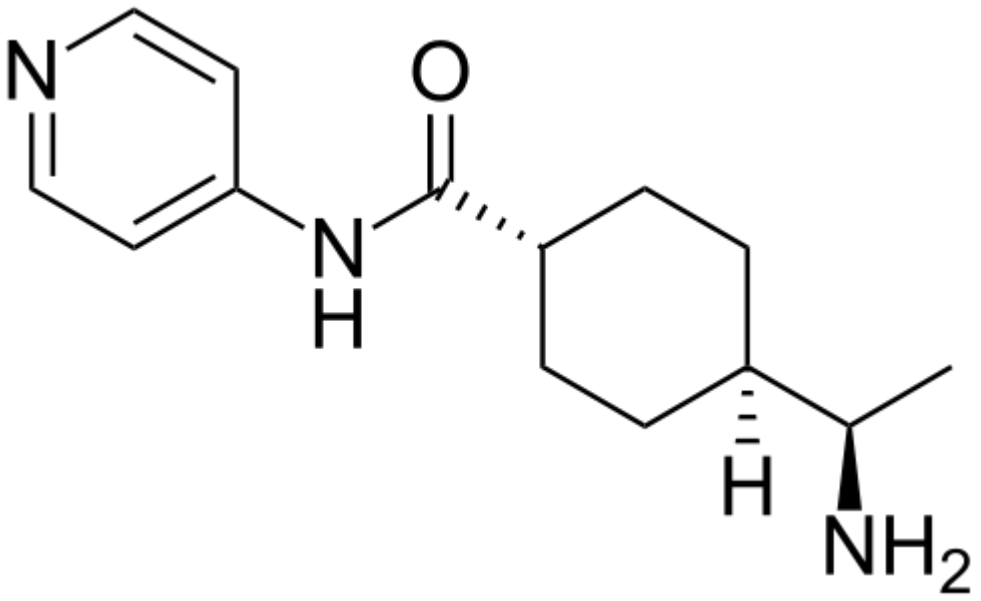

Figure 5.2 Molecular structure of the ROCK inhibitor Y-27632 dihydrochloride monohydrate (image taken from Sigma-Aldrich)

5.2.4 *In vitro* cell Matrigel invasion assay

The preparation of the cell invasion assay as outlined in Section 2.6.2. For the treatment groups, the inhibitor and the corresponding concentration used is described in Section 5.2.3.

5.2.5 *In vitro* cell motility assay

The preparation of the cell motility assay is outlined in Section 2.6.4. For the treatment groups, the inhibitor and the corresponding concentration used are described in Section 5.2.3.

5.2.6 Protein extraction, SDS-PAGE and Western blotting

To study proteins in their native, non-denatured form, lysis buffer with SDS substituted for NP-40 detergent was used to extract protein from control and WAVE knockdown PC-3 cells. Protein quantification allowed standardisation of the samples to ensure consistent loading of total protein. The protocol followed is outlined in Section 2.5.

5.2.7 Immunoprecipitation

The procedure for the immunoprecipitation of proteins with the antibody of choice is described in Section 2.3.3. To set up a positive control when analysing protein tyrosine phosphorylation, wild type PC-3 cells were cultured until 60-80% confluent. Medium was aspirated for the washing of cells with BSS then aspirated for the addition of 10mM sodium orthovanadate in 5ml serum free medium and hydrogen peroxide to make the final concentration 0.8%. After 10 minutes, this was aspirated for subsequent protein extraction outlined in Section 2.5.1.

5.2.8 Confocal microscopy

The confocal microscopy procedure is outlined in Section 2.7 and the primary and secondary antibodies used are shown in Tables 2.4 and 2.6, respectively.

5.3 Results

5.3.1 Expression analysis of ROCK-I and ROCK-II in WAVE1 and WAVE3 knockdown PC-3 cells

ROCK-I and II mRNA expression was investigated in PC-3 cell lines using conventional PCR; the results of this analysis are shown in Figure 5.3. A comparison of both ROCK-I and II expression between the wild type and pEF6 control cells with their equivalents following either WAVE 1 or 3 expression knockdown show no change in expression levels. Likewise, GAPDH expression levels are seen to be consistent across the cell lines tested which indicates no bias due to sample loading. The use of negative control ROCK-I, II and GAPDH primer sets indicates no contamination; although a weak band for ROCK-I can be observed, this is unlikely to be due to contaminants in any of the reagents as the band size is dissimilar, and therefore may be due to background noise.

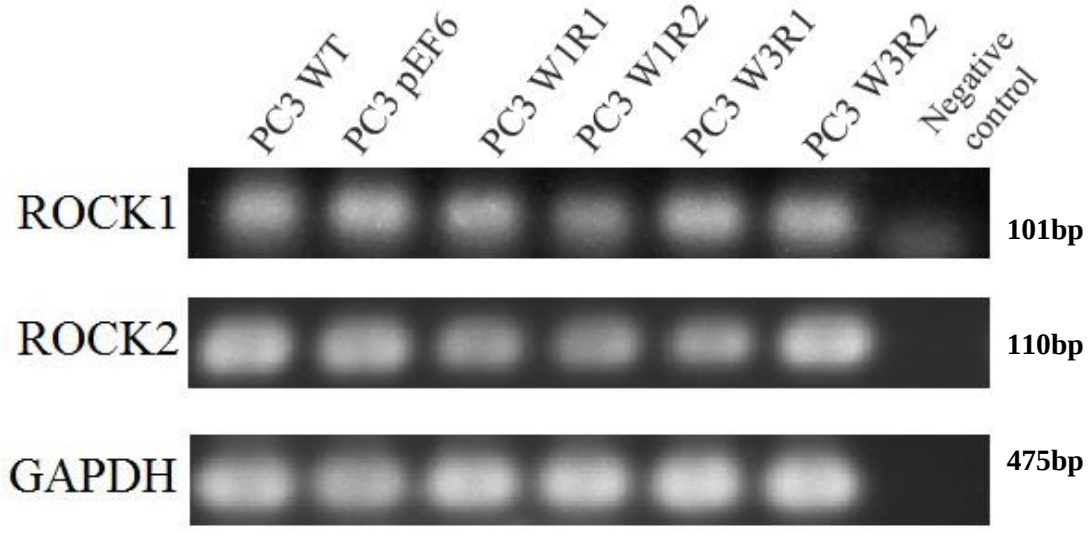

Figure 5.3 ROCK-I and II expression analysis in PC-3 cells comparing wild type, pEF6 control, WAVE1 and 3 knockdown cells demonstrate consistent expression levels. Analysis of the same cell lines found consistent GAPDH expression throughout the samples. Negative controls revealed no obvious signs of contamination.

5.3.2 Impact of ROCK inhibitor treatment on cell growth

As mRNA expression analysis revealed no obvious differences between wild type and pEF6 control PC-3 cells along with similar observations in *in vitro* cell function assays, pEF6 cells were used for subsequent experiments to compare the effects of WAVE knockdown with and without ROCK inhibitor treatment.

After a period of 120 hours, treatment with the broad range ROCK inhibitor, Y-27632, was seen to moderately increase cell growth in the PC-3 pEF6 control cell line compared to untreated pEF6 cells. However, this change was observed to be non-significant ($p=0.476$). A similar trend of increased cell growth was also observed for PC-3 cells exhibiting reduced WAVE1 expression with ROCK inhibitor treatment compared to untreated PC-3 W1R2 cells. This change was also observed to be non-significant ($p=0.755$). Unlike the moderate increase in cell growth for pEF6 and W1R2 with ROCK inhibition, there was no overall change in cell growth in WAVE3 knockdown cells following ROCK inhibition ($p=0.710$). The results from these findings are shown in Figure 5.4.

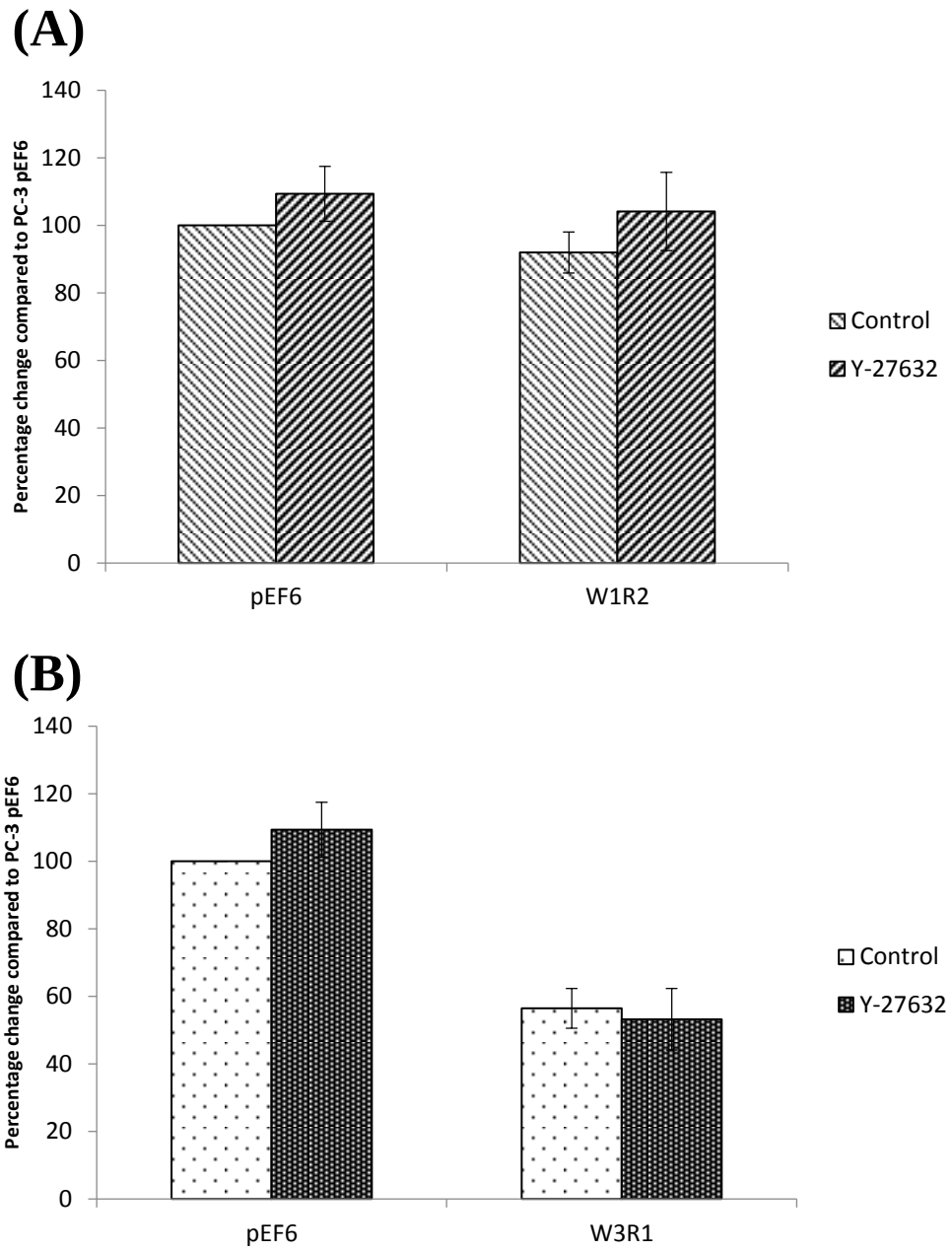

Figure 5.4 ROCK inhibition showed a moderate cell growth increase in both pEF6 and WAVE1 knockdown (W1R2) cells (A). WAVE3 knockdown (W3R1) cells showed little change in cell growth levels when treated with the ROCK inhibitor, Y-27632 (B). Shown are mean data from a minimum of three independent repeats, values represent percentage change to pEF6 cells without treatment (control). Error bars represent SEM.

5.3.3 Impact of ROCK inhibitor treatment on cell invasion

Following an incubation period of 72 hours, the number of PC-3 pEF6 control cells which had invaded the Matrigel layer of the *in vitro* invasion assays was lower when treated with the ROCK inhibitor, Y-27632, when compared to pEF6 cells without treatment (p=0.093). In contrast, PC-3 cells exhibiting WAVE1 knockdown showed an overall increase in the number of invaded cells with ROCK inhibition although this was not significant when compared to untreated PC-3 W1R2 cells (p=0.365) (refer to Figure 5.5). ROCK inhibitor treatment of WAVE3 knockdown PC-3 cells was not observed to influence cell invasion when compared to untreated W3R1 cells (p=0.490) (see to Figure 5.6).

(A)

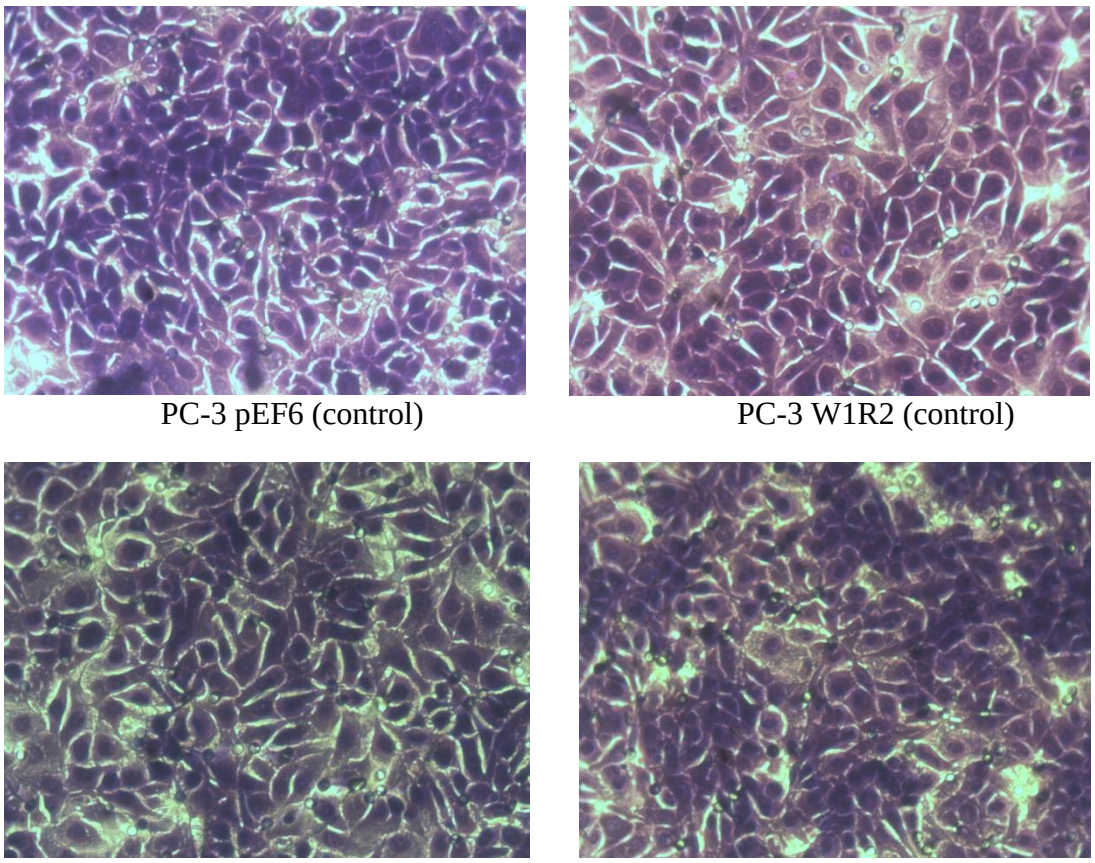

(B)

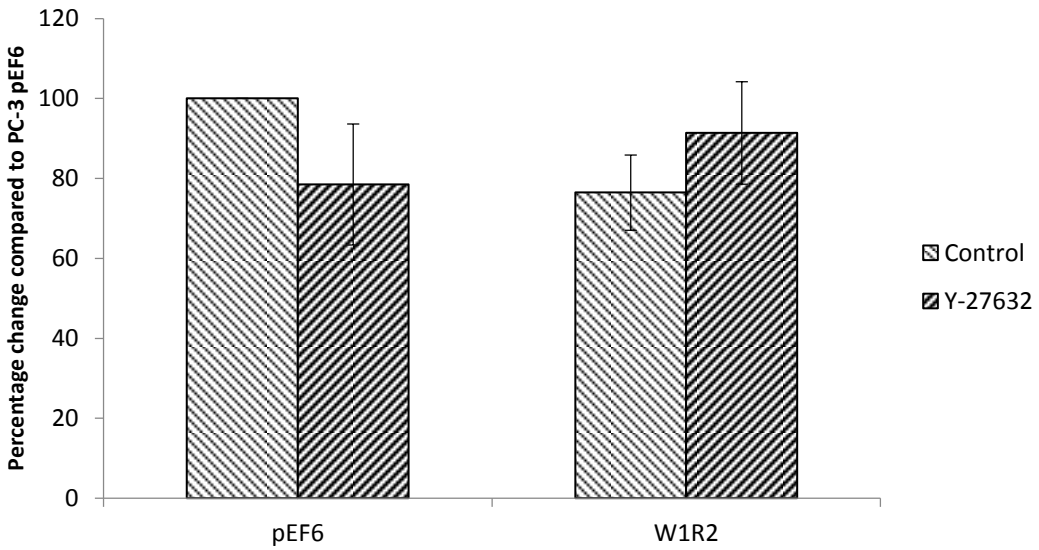

Figure 5.5 ROCK inhibitor treatment reduced cell invasion of pEF6 control cells whilst it increased the invasiveness of PC-3 cells with WAVE1 knockdown. A) Representative images acquired for PC-3 pEF6 and W1R2 cells without ROCK inhibitor treatment (control) and with. Images were acquired from at least three independent experiments. B) Cells were counted to calculate percentage change in cell invasion compared to PC-3 pEF6 cells without ROCK inhibitor treatment. Images acquired at 200X magnification. Shown are mean data with error bars representing SEM.

(A)

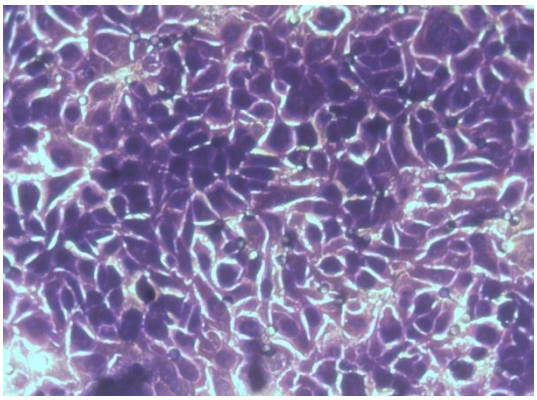

PC-3 pEF6 (control)

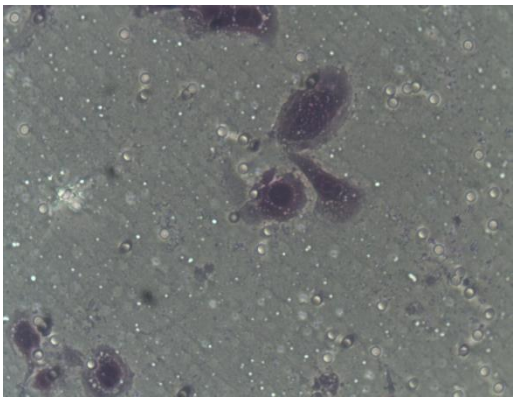

PC-3 W3R1 (control)

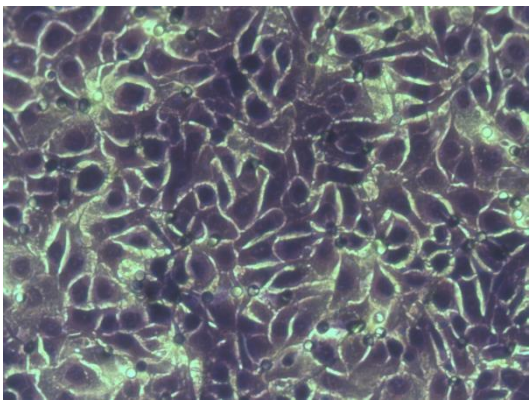

PC-3 pEF6 (ROCK inhibitor)

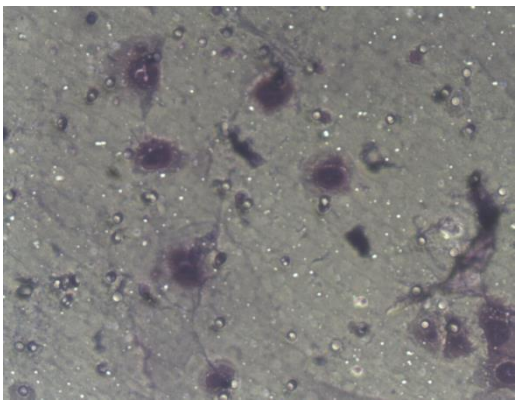

PC-3 W3R1 (ROCK inhibitor)

(B)

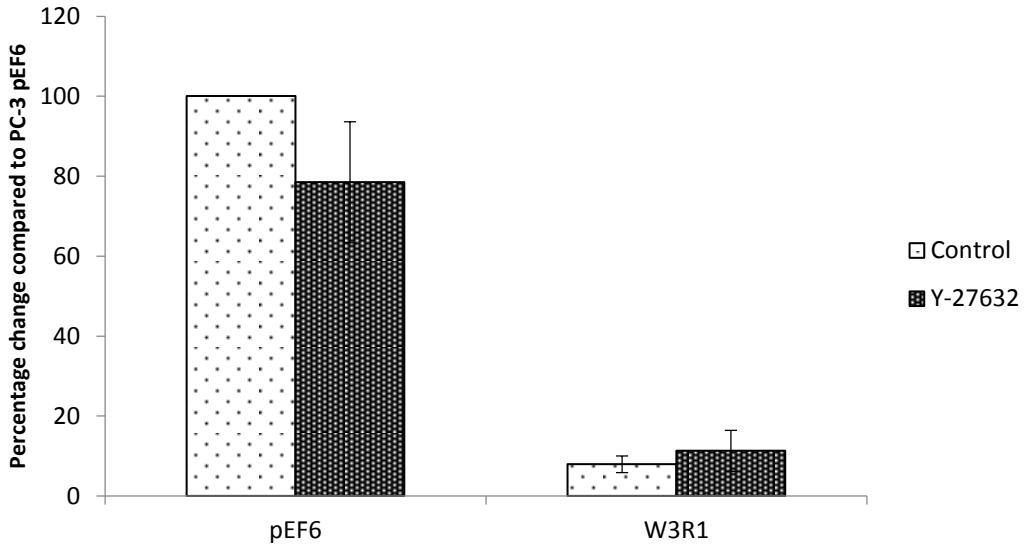

Figure 5.6 ROCK inhibitor treatment reduced cell invasion of pEF6 control cells but had little effect on WAVE3 knockdown cells. A) Representative images acquired for PC-3 pEF6 and W3R1 cells without ROCK inhibitor treatment (control) and with. Images were acquired from at least three independent experiments. B) Cells were counted to calculate percentage change in cell invasion compared to PC-3 pEF6 cells without ROCK inhibitor treatment. Images acquired at 200X magnification. Shown are mean data with error bars representing SEM.

5.3.4 Impact of ROCK inhibitor treatment on cell motility

The motile abilities of pEF6 control PC-3 cells were found to be significantly upregulated in response to the ROCK inhibitor, Y-27632 compared to their untreated equivalents ($p<0.001$). A similar trend of increased cell motility was also observed for both WAVE1 and 3 knockdown PC-3 cells with ROCK inhibitor treatment, however, this did not reach significance when compared to untreated equivalents ($p=0.489$; $p=0.151$, respectively). These results are shown in Figure 5.7.

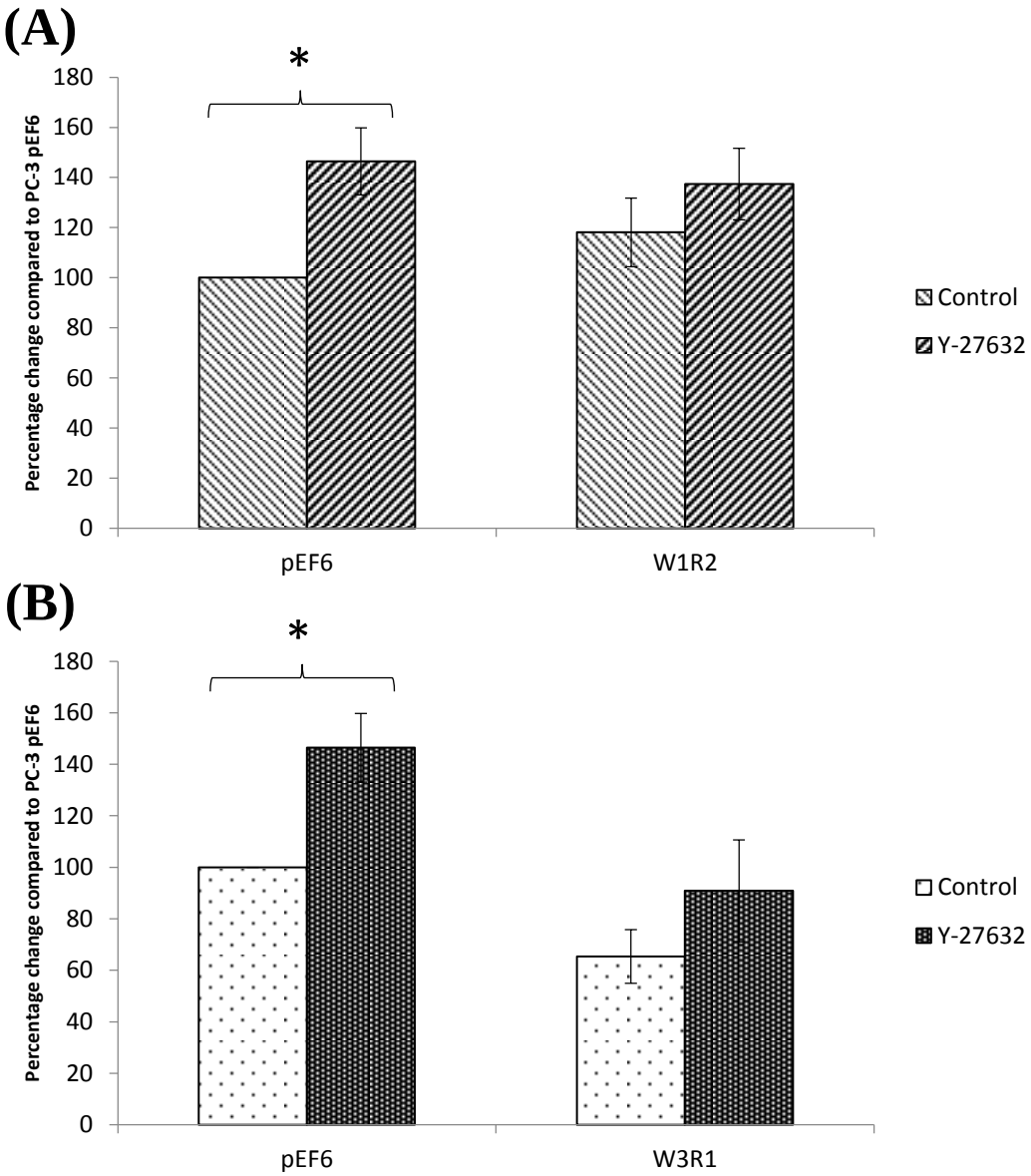

Figure 5.7 ROCK inhibitor treatment increases cell motility in pEF6 control, WAVE1 (A) and WAVE3 (B) knockdown PC-3 cells. Shown are mean data from a minimum of three independent repeats, values represent percentage change to pEF6 cells without treatment. Error bars represent SEM.

5.3.5 ROCK I co-localisation with WAVE1 and 3 in PC-3 cells

The relationship between the WAVE and ROCK protein family was explored using immunofluorescence and confocal microscope techniques. A FITC-conjugated antibody was used to probe WAVE1 or 3 in the PC-3 cell lines, pEF6, W1R2 (WAVE1 knockdown) and W3R1 (WAVE3 knockdown) whilst a TRITC-conjugated antibody was used to probe ROCK-I. The outermost boundaries of pEF6 cells showed moderate ROCK-I and WAVE1 co-localisation (refer to Figure 5.8A). There was no evidence of these proteins co-localising at the edge of the cell lamellipodia in W1R2 cells (refer to Figure 5.8B). Reduced WAVE1 in these confocal images also reconfirms its knockdown in PC-3 W1R2 cells compared to pEF6 controls. Notably, the cell morphology of PC-3 cells is distinctly altered with WAVE1 knockdown as implied by the lack of cell protrusions generated in the W1R2 cell line compared to pEF6 cells.

ROCK-I and WAVE3 showed very little co-localisation to the cell perimeter in PC-3 pEF6 cells whilst W3R1 cells show no co-localisation of these proteins (refer to Figures 5.9A and B, respectively). Similarly, the finding of reduced WAVE3 in PC-3 W3R1 under confocal analysis supports WAVE3 knockdown in this cell line compared to pEF6 cells. Much like the effects of WAVE1 knockdown in PC-3 cells, PC-3 W3R1 cells appear to lack the ability to form broad flat sheets which is characteristic of lamellipodia generation. It is also difficult to discern the outline of W1R2 and W3R1 cells when analysing FITC and TRITC images compared to the phase contrast images. This suggests that knocking down WAVE1 or 3 affects not only the localisation of ROCK-I to the outermost fringes of the cell but also to areas of the cytoplasm towards the main body of the cell.

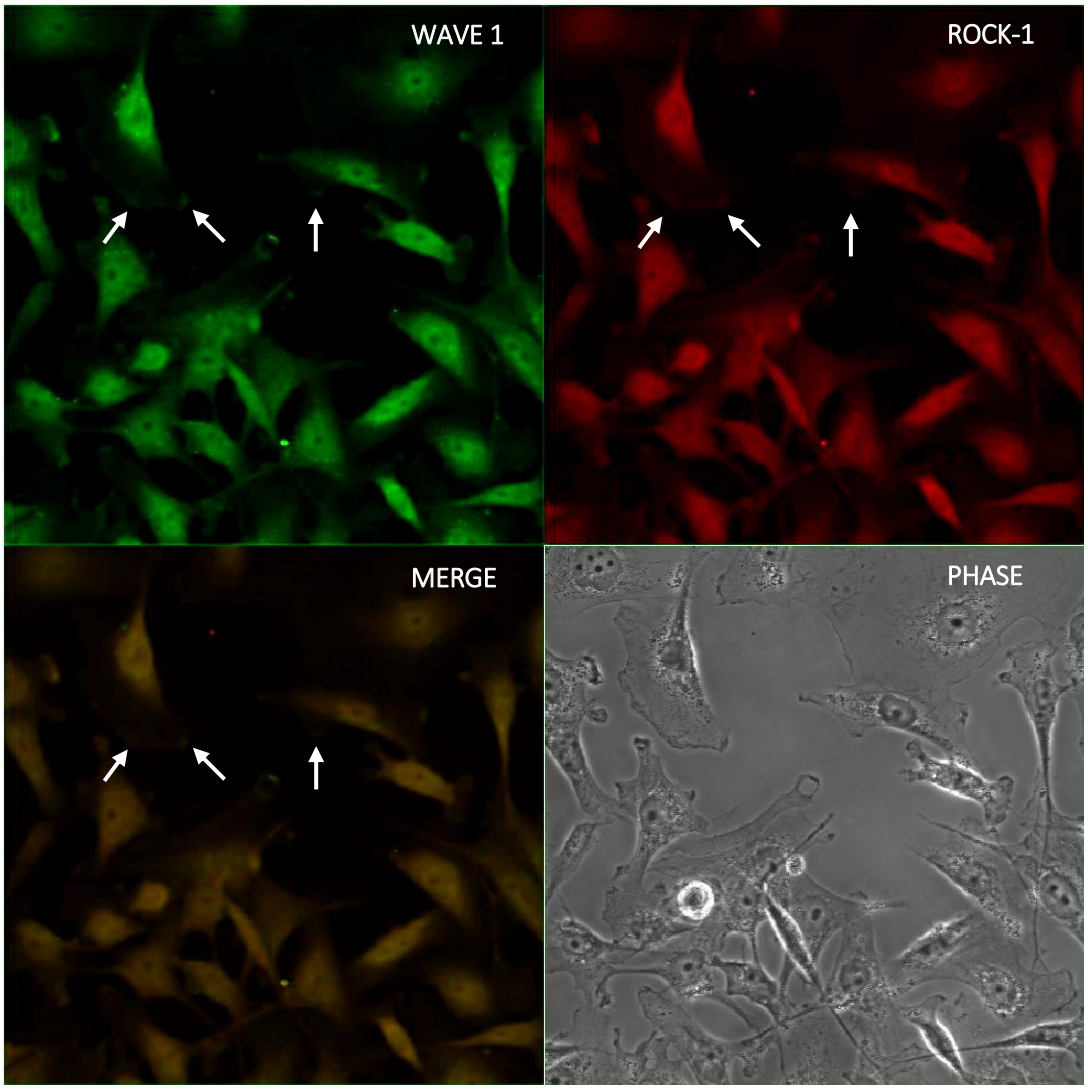

Figure 5.8A Confocal microscopy images of PC-3 pEF6 cells stained for WAVE1 (FITC) and ROCK-I (TRITC) reveal co-localisation of these proteins (represented by arrows). Also shown are FITC and TRITC merged images (MERGE) and the phase contrast image (PHASE). Representative images are shown. Images acquired at 600X magnification.

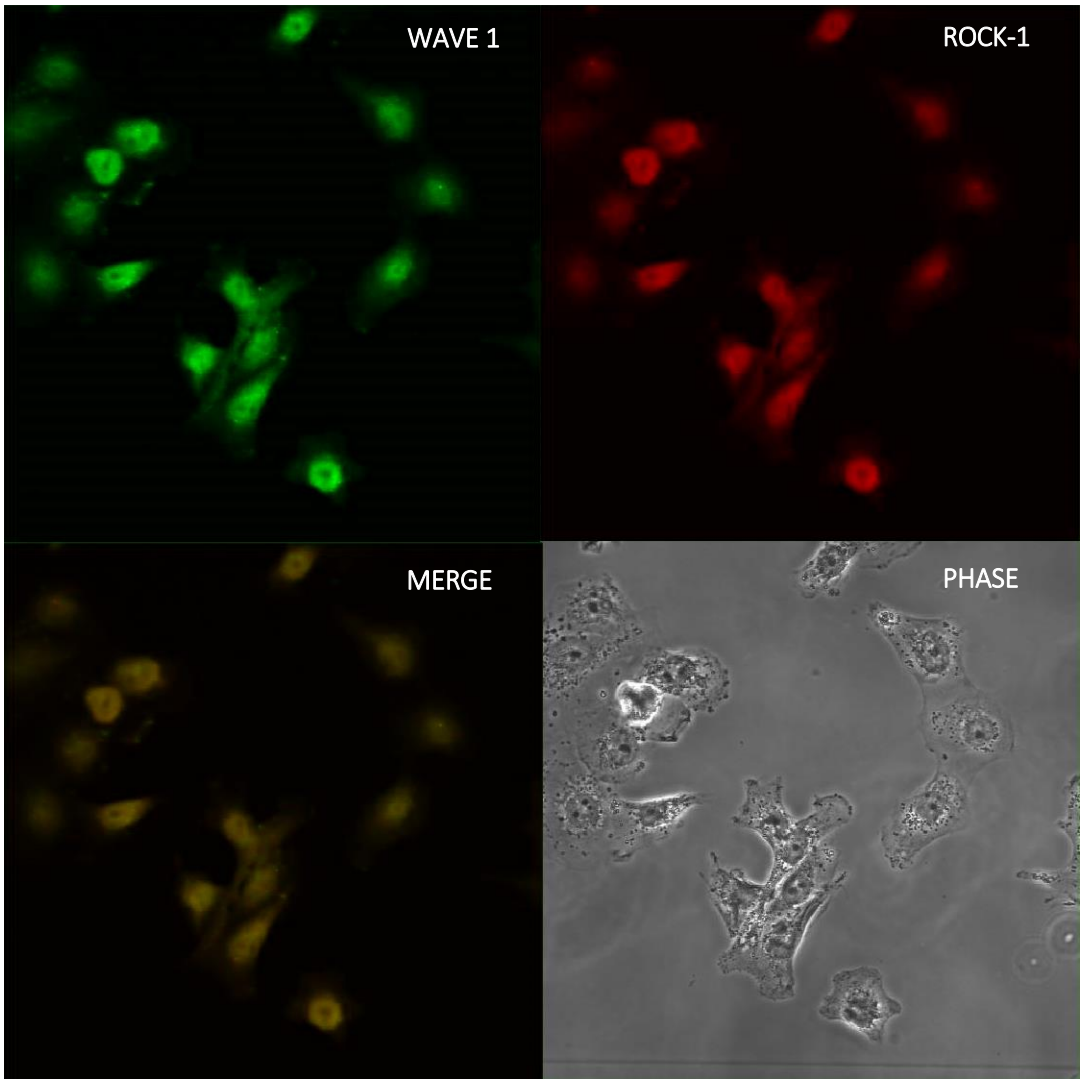

Figure 5.8B Confocal microscopy images of PC-3 W1R2 cells stained for WAVE1 (FITC) and ROCK-I (TRITC). Also shown are FITC and TRITC merged images (MERGE) and the phase contrast image (PHASE). Representative images are shown. Images acquired at 600X magnification.

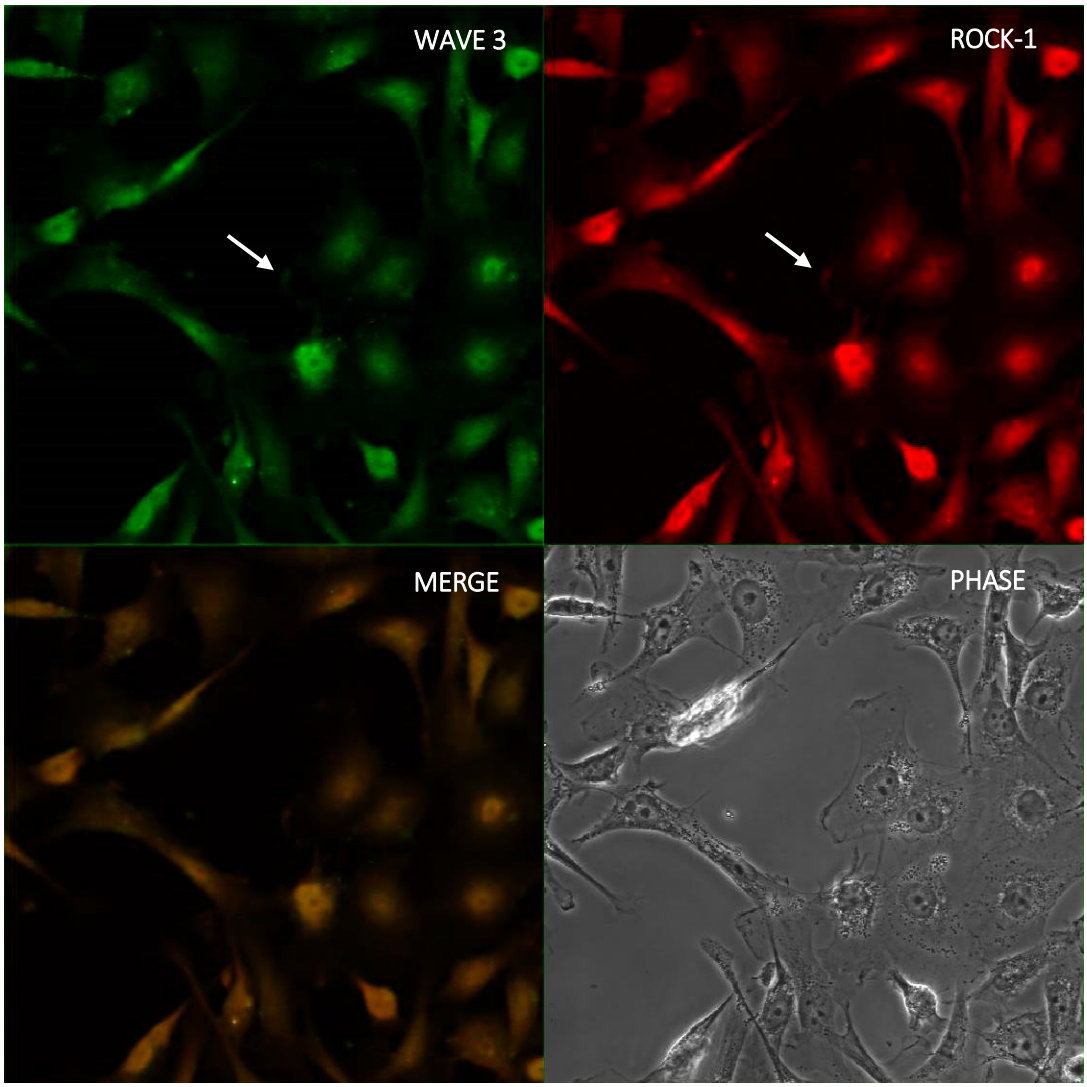

Figure 5.9A Confocal microscopy images of PC-3 pEF6 cells stained for WAVE3 (FITC) and ROCK-I (TRITC) reveal some co-localisation of these proteins (represented by arrow). Also shown are FITC and TRITC merged images (MERGE) and the phase contrast image (PHASE). Representative images are shown. Images acquired at 600X magnification.

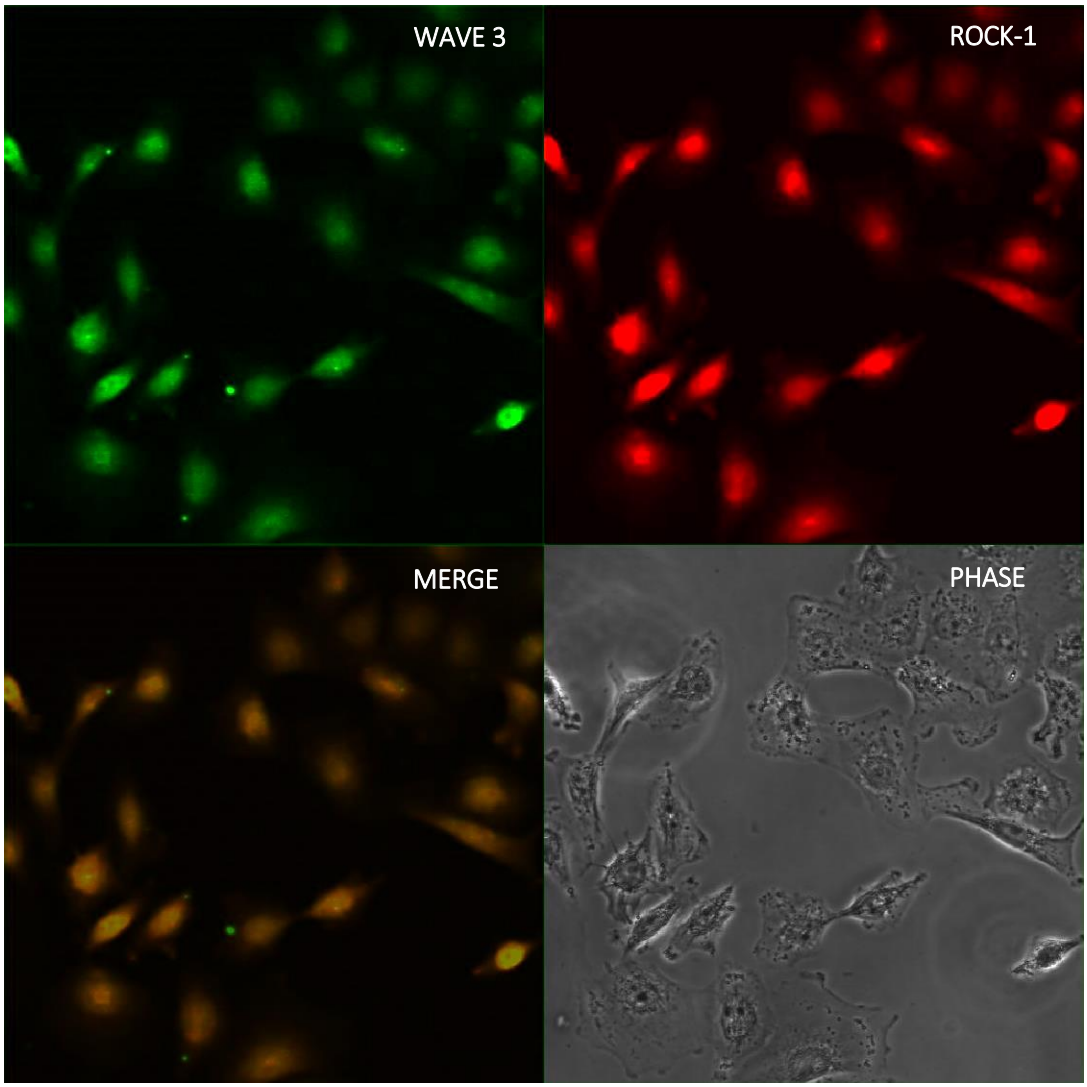

Figure 5.9B Confocal microscopy images of PC-3 W1R2 cells stained for WAVE3 (FITC) and ROCK-I (TRITC). Also shown are FITC and TRITC merged images (MERGE) and the phase contrast image (PHASE). Representative images are shown. Images acquired at 600X magnification.

5.3.6 WAVE1 knockdown increases ROCK-II tyrosine phosphorylation in PC-3 cells

Protein extracted from PC-3 cells with a NP-40 based lysis buffer was immunoprecipitated with a phosphotyrosine antibody (PY99) following standardisation. These immunoprecipitated proteins were separated by SDS-PAGE then transferred to a nitrocellulose membrane for probing with either ROCK-I or II primary antibodies. Using these techniques demonstrated no change in ROCK-I tyrosine phosphorylation in W1R2 or W3R1 cells relative to wild type or pEF6 cells and showed levels lower than positive control (refer to Figure 5.10A). However, a higher level of ROCK-II tyrosine phosphorylation was observed in WAVE1 knockdown PC-3 cells compared to either wild type or pEF6 control PC-3 cells. Levels of ROCK-II tyrosine phosphorylation in PC-3 cells demonstrating WAVE 1 knockdown were comparable to the positive control used. Levels of tyrosine phosphorylation of ROCK-II protein also appeared to be moderately higher in WAVE3 knockdown PC-3 cells compared to wild type and pEF6 cells although this was lower than levels seen for the positive control. (Figure 5.10B). Total ROCK-II protein levels (labelled as 'Raw lysate') appear marginally higher in wild type and pEF6 cells compared to WAVE1 and 3 knockdown PC-3 cells as well as the positive control used. GAPDH protein levels were consistent in all samples probed.

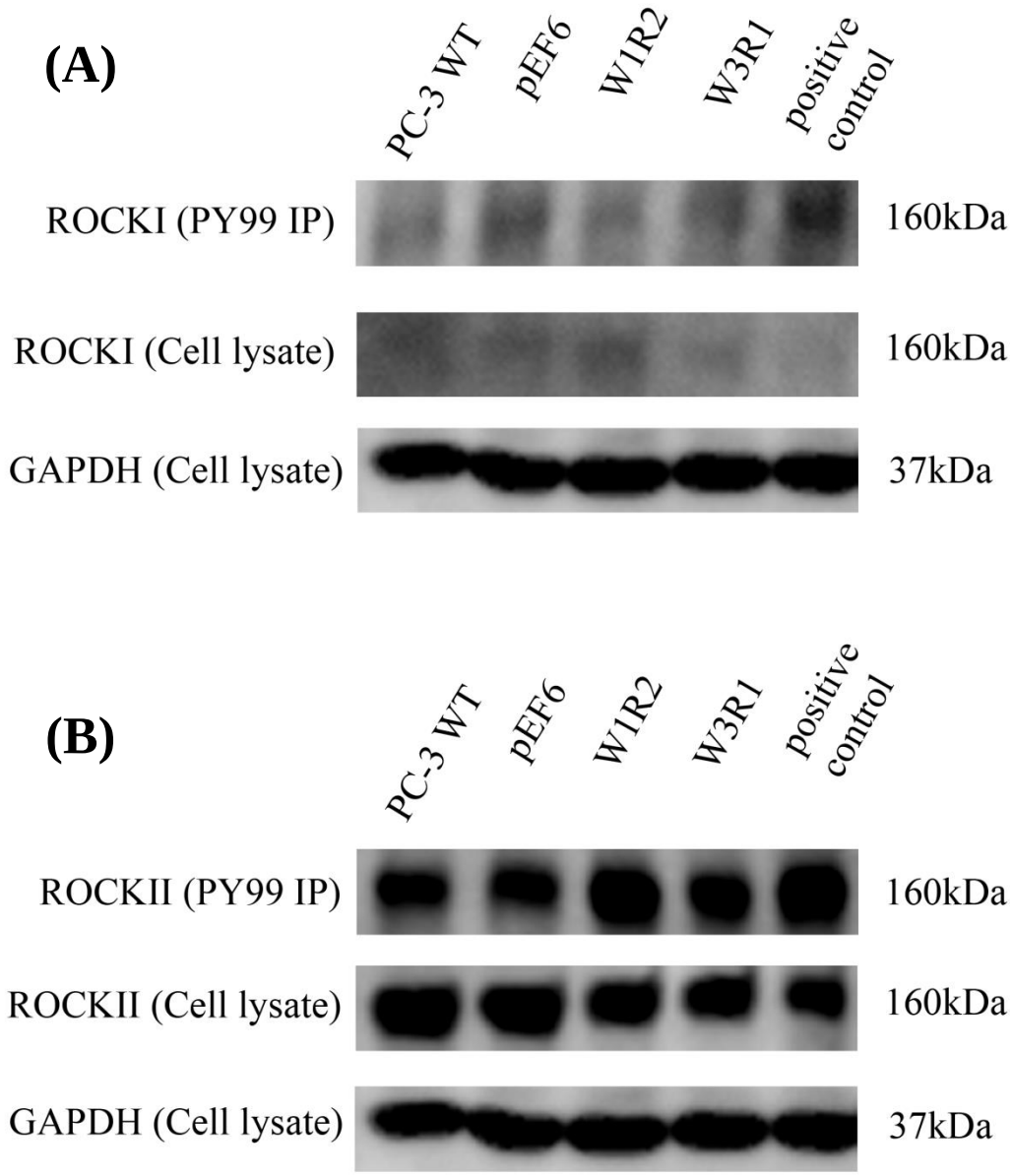

Figure 5.10 ROCK-I and II tyrosine phosphorylation status in PC-3 cells in response to WAVE1 or 3 knockdown. A) Proteins immunoprecipitated with a phospho-tyrosine antibody (PY99) revealed no change in ROCK-1 tyrosine phosphorylation following WAVE1 or 3 knockdown. B) Increased tyrosine phosophorylation of ROCK-II in WAVE1 knockdown (W1R2) PC-3 cells. Levels of tyrosine phosphorylation also appeared slightly higher with WAVE1 knockdown compared to wild type and pEF6 control cells. Wild type and pEF6 cells showed similar levels of tyrosine phosphorylation. Representative images are shown.

5.4 Discussion

Cancer progression is driven by multistep events including aberrations in cell invasion and metastasis. Remodelling of the actin cytoskeleton can alter cell adhesion, invasion and migration thus advancing cells through epithelial-mesenchymal or mesenchymal-epithelial transition ultimately contributing to the metastasis of cancer cells (Rubin *et al.,* 2001; Cavallaro and Christofori., 2004). A plethora of proteins are involved in actin polymerisation/depolymerisation, capping and bundling of actin filaments which help to coordinate actin cytoskeletal dynamics (Ayscough, 1998). A main driver of actin cytoskeletal remodelling is the Rho GTPase family of which the most prominent members are Rho, Rac and Cdc42 (Nobes and Hall, 1995). The ability of the Rho GTPase family to elicit so many cell functions is due to the vast number of downstream effectors. ROCK is a downstream target of Rho GTPase whilst members of the WASP family are targeted by Rac and Cdc42 (WAVE and WASP, respectively) (Kobayashi *et al*., 1998; Miki *et al*, 1998). Following activation by Rho GTPases, ROCK and WASP/WAVE are able to relay this signal by targeting their own downstream proteins. As previously stated, WASP/WAVE stimulates the Arp2/3 complex which is then able to accelerate actin polymerisation (Higgs and Pollard., 1999). Both ROCK isoforms are also able to influence actin cytoskeleton remodelling as well as regulate cell migration through interaction with a number of protein targets (Riento and Ridley, 2003).

It is unsurprising that aberrations in the expression and activity of ROCK-I and II have been linked to several human cancers. Gene mutations which relieve the autoinhibitory state of these ROCK isoforms have been linked with increased kinase activity in addition to having been identified in several human cancer genomes

(Greenman *et al*, 2007). Increased ROCK-I and II protein levels were demonstrated in human breast cancer whilst elevated ROCK-I expression was correlated with increased tumour grade (Lane *et al,* 2008), whilst conditionally activated ROCK demonstrated enhanced tumour dissemination and angiogenesis (Croft *et al*, 2004). As ROCK and the WASP/WAVE proteins have an influence on cell migration through their role in actin cytoskeletal dynamics, a trait which is implicated in human cancer, the relationship between these two protein groups and their pathways was investigated.

Expression analysis of control and WAVE knockdown PC-3 cells revealed no effect on either ROCKI or II mRNA level in response to reduced WAVE1 or 3 expression. These observations indicate that WAVE1 and 3 are not involved in a pathway that regulates the transcript expression of ROCK-I and II. Therefore it is postulated that there is not expected to be a signalling cascade downstream of WAVE1 or 3 that controls ROCK-I and II expression.

As described in Chapter 3, *in vitro* cell function assays revealed a role for WAVE1 and 3 in cell growth and invasion, whilst only WAVE3 was found to influence cell motility. To gain an understanding of the association between WAVE and ROCK in relation to prostate cancer metastasis, the *in vitro* experiments described here were coupled with experiments using the ROCK inhibitor, Y-27632 to determine its effect on cell function. The treatment of pEF6 control PC-3 cells with a ROCK inhibitor was shown to increase cell growth. However, this change was found to be very moderate and not significant ($p=0.476$). The same trend was displayed in PC-3 cells exhibiting WAVE1 knockdown ($p=0.755$). For WAVE3 knockdown cells, no change in cell growth was observed ($p=0.710$).

These findings are perplexing as treatment with the ROCK inhibitor, Y-27632 has been previously shown to reduce cell proliferation in a glioblastoma cell line (Zohrabian *et al,* 2009). Despite this, a study that demonstrated ROCK inhibitor treatment to suppress actin polymerisation also inhibited apoptosis in the metastatic prostate cancer cell line, DU-145 (Papadopoulou *et al,* 2008). Given the Y-27632 treatment of PC-3 cell lines displayed increased cell growth in pEF6 and W1R2 cells, this could in part be explained by apoptosis inhibition. However, as Figure 5.4 shows, this does not explain why ROCK inhibition in WAVE3 knockdown PC-3 cells moderately suppresses cell proliferation. The *LDOC1* (Leucine Zipper, Down Regulated in Cancer 1) gene encodes a protein able to bind directly to the verprolin homology domain of WAVE3 and has been characterised as an inducer of cell apoptosis. However, WAVE3 expression promotes translocation of LDOC1 thus inhibiting LDOC1-induced apoptosis (Mizutani *et al*, 2005). WAVE3 knockdown may prevent its ability to negatively regulate LDOC1 and therefore promote apoptosis. This not only helps to explain how WAVE3 knockdown results in a decrease in cell growth but also the differing effects of WAVE1 and 3 in response to ROCK inhibition. As WAVE3 is still active in pEF6 and W1R2 cells, it is still able to negatively regulate LDOC1-induced apoptosis. Whilst ROCK inhibition has been linked with inhibited apoptosis and WAVE3 knockdown with promoted apoptosis, when coupled together this showed little change compared to cells without ROCK inhibitor treatment. This would suggest that WAVE3 regulates apoptosis in a pathway upstream of ROCK-regulated apoptosis. Future work examining apoptosis in WAVE1 and 3 knockdown cells with and without ROCK inhibition is required to fully understand this phenomenon.

ROCK inhibitor treatment of pEF6 control PC-3 cells was shown to reduce the number of invaded cells through the Matrigel layer compared to cells without ROCK inhibition. Whilst this finding was not quite found to be significant (p=0.093), this contrasted to the effects of ROCK inhibitor treatment in WAVE1 knockdown cells which was shown to increase cell invasion in relation to cells without treatment (p=0.365). PC-3 cells exhibiting WAVE3 knockdown was not found to have an effect on cell invasion when treated with the ROCK inhibitor, Y-27632 (p=0.490). In the previous chapter, it was postulated that the regulation of matrix metalloproteinases by WAVE3 was responsible for increased cell invasion in WAVE1 knockdown PC-3 cells treated with the Arp2/3 inhibitor, CK-0944636. However, the finding that human articular chondrocytes cultured in the presence of Y-27632 suppressed MMP-3 expression would contradict this (Furumatsu *et al*, 2013). It would appear that proteins belonging to ROCK or WAVE subgroups have a role in cell invasion through their MMP regulatory role (Vishnubhotla *et al.,* 2007; Sossey-Alaoui K *et al.,* 2005). However, the contradictory finding of increased invasion when coupling WAVE1 knockdown with ROCK inhibition could be explained by the cells still retaining functional WAVE3, with the ability to regulate MMPs. It would be interesting to hypothesise a feedback mechanism whereby the regulation of MMPs by WAVE3 or other upstream proteins is upregulated in response to suppression of both WAVE1 and ROCK activity. It is of note that WAVE knockdown or ROCK inhibition suppresses the quantity of invaded cells. However, WAVE1 knockdown and ROCK inhibition together results in increased cell number suggesting that there is an association between these two proteins with regards to control of cell invasion.

The role of ROCK-I and -II in cell migration is well defined (Riento and Ridley, 2003), yet treatment with the ROCK inhibitor, Y-27632, was demonstrated to elevate cell motility in pEF6 control and WAVE1 or 3 knockdown PC-3 cells. Whilst this seemingly contradictory effect of ROCK inhibition is surprising, other studies have also demonstrated conflicting effects of ROCK inhibition on cell invasion which is dependent on the microenvironment in which the cells were cultured (Vishnubhotla *et al*., 2012). Reasons underlying the increased motile ability may stem from the finding that ROCK-I knockdown results in decreased cell adhesion in keratinocytes cultured on fibronectin (Lock and Hotchin., 2009). This loss of adhesion will affect the ability of the cell to remain stably attached within its microenvironment and may facilitate cell motility. This fact may explain increased cell motility in both control and WAVE knockdown PC-3 cells when subjected to ROCK inhibition. The finding that this trend is observed in all of these PC-3 cell lines also suggests that the increased cell motility effect is not WAVE1 or 3 dependent.

An additional theory which may explain the elevated cell motility results has been mentioned in the previous chapter whereby alternative signalling cascades with a role in cell migration may become activated when ROCK is inhibited. Signalling cascades which cooperate to induce a cell function are integral to a physiologically healthy cell, however, if conditionally activated this can lead to the progression of cancer traits. It was hypothesised that signalling cascades with a role in cell motility not only drive this function but also regulate other cell migration pathways. As discussed in the previous chapter, it was indicated that the trend towards increased cell motility observed with the treatment of cells with an Arp2/3 inhibitor was as a result of alternative cell migration pathways i.e. ROCK-I and II. It may be postulated

therefore that the ability of the cell to migrate in the absence of ROCK function is driven by Arp2/3 or other unrelated pathways.

A key role of ROCK in the cell lies with its ability to regulate actin cytoskeletal dynamics through the phosphorylation of LIMK serine/threonine residues to drive cell migration. Even so, ROCK is not the sole effector that links Rho GTPases to cytoskeletal reorganisation through LIMK. Rac and Cdc42 are able to activate p21-activated kinase 1 (PAK1) which in turn is able to target a number of downstream proteins including LIMK. Phosphorylation of LIMK1 at threonine residue 508 was shown to increase its kinase activity targeted at cofilin with the effect of stabilising actin filament assembly (Edwards *et al.*, 1999). This is a possible pathway utilised by the cell to facilitate actin cytoskeletal dynamics which is LIMK dependent but ROCK independent (shown in Figure 5.11). The *in vitro* experiments outlining the impact of WAVE knockdown and ROCK inhibition implicate little association between these two groups of proteins. However, there appeared to be differing effects of ROCK inhibitor treatment on cell invasion depending on whether PC-3 cells exhibited WAVE knockdown and which WAVE (1 or 3) was knocked down. These findings seem to suggest a role for WAVE and ROCK in cell invasion as well as a potential relationship between these two protein groups.

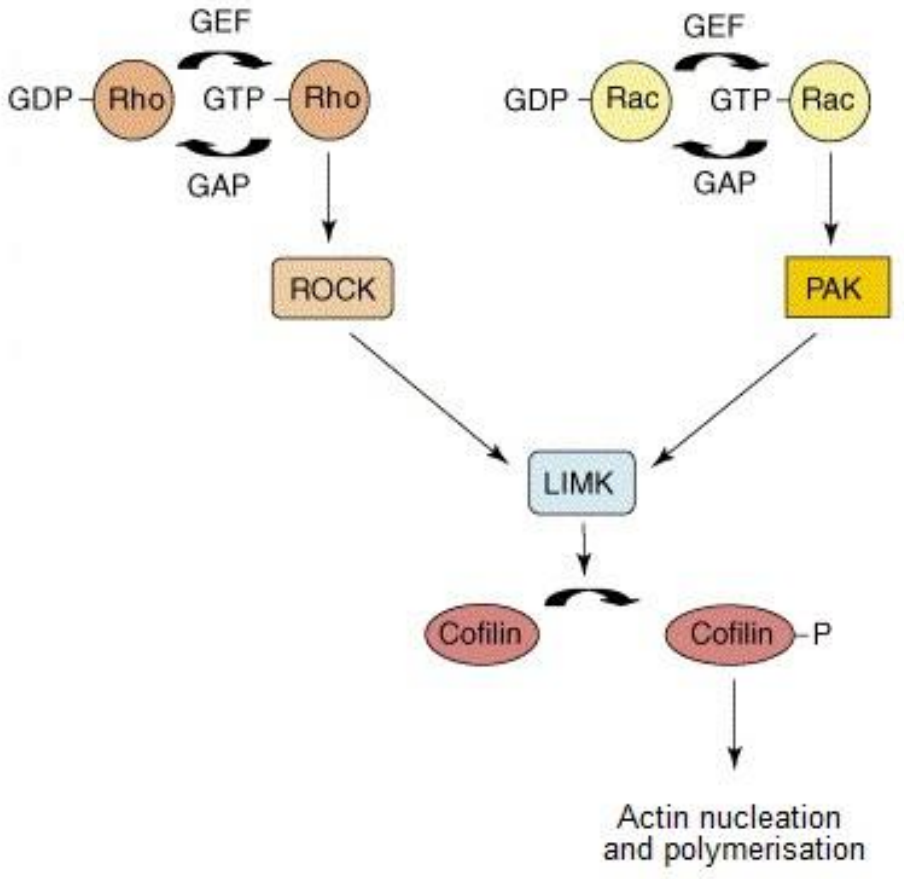

Figure 5.11 LIM domain kinase (LIMK) phosphorylation by Rho-associated protein kinase (ROCK) and p21-activated kinase (PAK). ROCK and PAK are activated by Rho and Rac, respectively. LIMK phosphorlation in turn leads to phosphorylation of cofilin which suppresses its actin filament depolymerising activity and thus promotes actin filament stability and polymerisation (Adapted from Ridley, 2006)

The relationship between WAVE and ROCK was further hinted at with the observation of some specific co-localisation of ROCK-I with WAVE1 and 3 to the outer perimeter of PC-3 cells which was not evident with either WAVE1 or 3 knockdown. Interestingly, the immunofluorescent images also implied a role for WAVE1 and 3 to localise ROCK-I to general cytoplasmic areas of the cell as suggested by the lack of ROCK-I in these areas in WAVE1 or 3 knockdown PC-3 cells (W1R2 and W3R1, respectively). There was a distinct lack of lamellipodia in W1R2 and W3R1 cells which greatly altered the cell's morphology compared to pEF6 cells. The finding that knockdown of either WAVE1 or 3 in PC-3 cells had a profound effect on lamellipodia generation suggests that this process and ROCK-I localisation in the cell is reliant on both of these proteins.

These observations imply the ability of WAVE1 and 3 to influence ROCK-I localisation and to an extent, function, in the cell. This could in part explain the insignificant findings in the *in vitro* cell assays when comparing the effects on cell function with and without the ROCK inhibitor, Y-27632. When coupling a WAVE knockdown cell line with Y-27632, it is possible that ROCK activity is already suppressed due to its localisation in the cell being hampered by the absence of WAVE1 and 3. Even so, this does still leave the finding of increased cell motility with Y-27632 a puzzling observation. However, these immunofluorescence and confocal microscopy approaches have highlighted some interesting findings on the relationship between the WAVE and ROCK-I protein family in PC-3 cells.

Increased levels of ROCK-II tyrosine phosphorylation were observed in PC-3 cells following WAVE1 knockdown compared to wild type and pEF6 control cells, both of which were at similar levels. Elevated ROCK-II tyrosine phosphorylation levels in

WAVE1 knockdown of PC-3 cells were comparable to those seen in the positive control used. At present, six tyrosine phosphorylation sites have been identified in ROCKII: Y256, Y692, Y722, Y936, Y1232 and Y1319. Little is known about the functional consequences of tyrosine phosphorylation at these sites apart from Y722 which has been linked to disease tissue originating from gastric cancer, acute myelogenous leukemia, lung cancer and neuroblastoma (Phosphosite). Tyrosine phosphorylation at this site reduces RhoA binding to ROCKII which is important for focal adhesion dynamics. Increased cell adhesion of a myeloid leukemia cell line was observed with tyrosine phosphorylation at this site (Lee and Chang, 2008).

PC-3 cells exhibiting WAVE1 knockdown were demonstrated to exhibit reduced cell invasiveness as well as increased tyrosine phosphorylation of ROCK-II. Given the link between phosphorylation at specific tyrosine residues with increased cell adhesion, it seems that these findings are conflicting. However, it is important to emphasise that the tyrosine phosphorylation findings outlined in this chapter do not specify which particular residues are being targeted. Furthermore, it is worth noting that the roles of ROCK-I and -II in the cell are subtly different. Whilst ROCK-I is involved in destabilising the actin cytoskeleton and cell detachment; ROCK-II is essential for stabilising the actin cytoskeleton and cell adhesion (Shi *et al,* 2013). Although the functional consequence of phosphorylation at Y722 was deliberated in the case of ROCK-II, there is no evidence of a homologous site in ROCK-I being subjected to phosphorylation. This highlights a distinction between these two ROCK isoforms which emphasizes their functionally non-redundant roles in the cell. Despite these points, it is very interesting to note that whilst WAVE1 knockdown was shown to decrease cell invasion and increase tyrosine phosphorylation, ROCK inhibition in these cells was shown to moderately rescue these suppressed cell invasion effects.

Ideally, further work would investigate the tyrosine phosphorylation levels in WAVE1 knockdown cells compared to those treated with the ROCK inhibitor, Y-27632. This would allow an insight into whether there exists an association between post-translational modification and functional consequence to the cell.

Chapter 6

WAVE 1 and 3 and N-WASP in the PC-3 cell line

6.1 Introduction

Actin polymerisation is the driving force underlying cell migration and is initiated through a multitude of mechanisms including the pathway that utilises the Arp2/3 complex. Besides the stimulation of this complex by the WAVE protein subgroup, other nucleation promoting factors include the related proteins, WASP and N-WASP (Kurisu and Takenawa., 2009). The ability of these proteins to initiate actin polymerisation is attributed to the presence of specific protein domains at the carboxy-terminal. Known collectively as the VCA region, this is comprised of the verprolin homology domain, the cofilin homology domain and the acidic region; together they confer the ability of the protein to bind to and activate the Arp2/3 complex (Kurisu and Takenawa, 2009). Although the VCA region is a defining characteristic of WASP and WAVE proteins, the presence of different domains located at the amino-terminal places these proteins into two distinct subgroups (refer to Figure 6.1).

The presence of the WASP homology 1/Ena-VASP homology 1 (WH1/EVH1) domain and GTPase binding domain (GBD) in WASP and N-WASP but absent from WAVE1, 2 and 3 is one obvious distinction between these proteins which is a prime defining factor that makes the role of these proteins subtly different. Having a WH1/EVH1 domain in WASP and N-WASP allows these proteins to bind with members of the WASP-interacting protein (WIP) family which includes WIP, CR16 (corticosteroids and regional expression-16), and WICH/WIRE (WIP- and CR14-homologous protein/WIP-related) in mammals (Antón *et al*, 2007; Ho *et al*, 2001; Kato *et al*, 2002). The functional importance of this protein domain is emphasized by the finding that the vast majority of missense mutations are located in regions that encode the WH1 domain with the potential to interfere with WIP interaction.

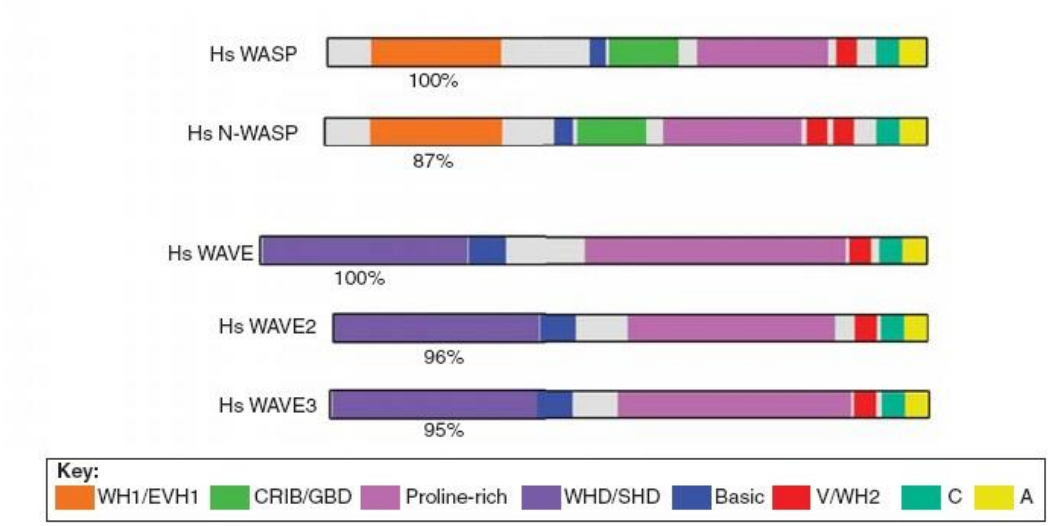

Figure 6.1 The protein structure of the WASP and WAVE proteins in *homo sapiens.* The percentage displayed under the WH1/EVH1 and WHD/SHD represent the amino acid similarity of these domains between the WASP and WAVE subgroup, respectively. WH1/EVH1: WASP homology 1/Ena-VASP homology 1; CRIB/GBD: Cdc42 and Rac interactive binding domain/GTPase binding domain; WHD/SHD: WAVE homology domain/Scar homology domain; V/WH2: verprolin homology domain/WASP homology 2; C: cofilin homology; A: acidic region (Image adapted from Kurisu and Takenawa, 2009).

Whilst specific Rho GTPases are associated with the generation of particular actin-rich formations at the cell leading edge, it is apparent that these effects are in fact mediated through WASP and WAVE proteins (Hall, 1998; Kurisu and Takenawa; 2009). It is reasonable to link the presence or absence of WH1/EVH1 in WASP and WAVE proteins, respectively, with the formation of filopodia or lamellipodia, respectively. Whilst WASP proteins have been show to stimulate actin filament bundling, targeting these effects to the cell leading edge is driven by WIP proteins and together they influence filopodia formation (Martinez-Quiles *et al.,* 2001). Moreover, the generation of invadopodia and podosomes resulting in cell migratory and matrix degradation effects has also been attributed to WIP and WASP proteins (García *et al.,* 2012). In contrast, WAVE proteins lack a WH1/EVH1 domain and therefore do not allow direct interaction with proteins such as members of the WIP protein family.

Also specific to WASP and N-WASP is the GBD which is responsible for Cdc42 interaction and alleviation of WASP proteins from their intrinsically inactivate state (Kim *et al,* 2000). Whilst the WASP and N-WASP proteins are able to bind directly with multiple proteins partners through their WH1/EVH1 and GBD domains, these functional domains are absent in the WAVE proteins. Instead, WAVE proteins elicit their cell motility properties indirectly through the pentameric formation of the WAVE regulatory complex (WRC) which is comprised of four additional proteins: Sra1, Nap1, HSPC300 and Abi2. The lack of a GBD domain in WAVE is overcome by the ability of Rac to bind with the Sra1 subunit which recruits WAVE to the cell membrane and drives lamellipodia formation (Soto *et al*., 2002). Furthermore, the WHD (WAVE homology domain) in WAVE proteins, which is absent in WASP proteins, has been found to associate with Abi2 and HSPC300 and has been

suggested to contribute to WRC formation (Gautreau *et al,* 2004). The close association of the five proteins in the WRC, where each has the potential to bind with multiple binding partners, implicates the complex with several signalling pathways in which WAVE may interplay either directly or indirectly.

In addition to the obvious structural variations between WASP and WAVE, the ability for specific Rho GTPases to activate these proteins may also account for the different actin formations generated at the cell leading edge. As mentioned previously, the cellular functions associated with Rho GTPases are not only vast but also diverse (Jaffe and Hall., 2005). This is attributed to the numerous protein interactions involving each Rho GTPase. Due to the elaborate nature of actin cytoskeleton maintenance, contemporaneous stimulation of proteins involved in different signalling pathways by Rho GTPases may have the potential to influence actin filament dynamics through mechanisms alternative to those that involve WASP/WAVE. Despite both WASP and WAVE proteins stimulating Arp2/3 through their VCA regions, the association of these proteins with specific binding partners and the possibility of alternative signalling pathways via the different Rho GTPases could be responsible for their physiologically specific roles in the cell.

Although WASP and WAVE are characterised by their ability to activate Arp2/3, it is apparent that they do not function independently of each other during cell migration. Previous studies have demonstrated the suppressive effects of WAVE expression knockdown on invasive and motility ability in breast and prostate cancer cells (Sossey-Alaoui *et al.*,2007; Fernando *et al.,* 2008). Interestingly, a similar study presented contrasting results with the loss of WRC activity in epithelial cells (Tang *et al.*, 2013). Depletion of WRC activity was found to correlate with an increase in N-WASP recruitment to the leading edges of cells to drive 3D cell migration. A loss of

WRC subunits also correlated with an increase in focal adhesion kinase (FAK) expression, a protein involved in cell adhesion and a known driver of cancer cell invasion (Brunton and Frame, 2008). Furthermore, the ability of FAK to phosphorylate N-WASP, a process that enhances N-WASP function and recruitment to the cell leading edge was also demonstrated. This study emphasises the intricate nature of mechanisms that regulate cell migration and highlights an important synergy between WASP and WAVE proteins.

Cancer metastasis is a common characteristic of aggressive and advanced stage cancer and is often associated with uncontrolled cell migration. With integral roles in cell migration, it is not surprising that several members of the WASP protein family have been implicated in a number of human cancers as both prognostic indicators and therapeutic targets (Matrin *et al.,* 2011; Kurisu *et al.,* 2005; Iwaya *et al.,* 2007; Sossey-Alaoui *et al.,* 2007). Given this link with cancer and their roles as nucleating promoting factors of Arp2/3, it would be interesting to investigate the relationship between the WASP and WAVE protein subgroups and ascertain any role for their association in prostate cancer metastasis. As both WAVE and N-WASP proteins interact with the Arp2/3 complex to activate it in a similar manner, it would be logical to predict that WAVE knockdown will show comparable effects on cell traits to N-WASP inhibition whilst a these cell characteristics may shown to be effected to a greater extent when coupling both WAVE knockdown and N-WASP inhibition.

6.2 Methods and materials

6.2.1 Cell lines

PC-3 cells were cultured and maintained as outlined in Section 2.2.4.

6.2.2 Synthesis of complementary DNA and RT-PCR

Complementary DNA was generated as described in the Section 2.4 whilst the same RT-PCR techniques were used to determine expression levels of N-WASP using primers designed specifically for this gene. The forward and reverse primer sequences are shown Table 2.3 (Chapter 2). RT-PCR was also run in parallel with the housekeeping gene GAPDH to allow a validation of cDNA quality and enable a demonstration of normalised expression levels of the cDNA within the separate cell lines.

6.2.3 *In vitro* cell growth assay

The preparation of the cell growth assay is outlined in Section 2.6.1. When setting up the inhibitor treatment groups of the same cell lines to target N-WASP, the small molecule inhibitor, Wiskostatin, was used at a concentration of 100nM (inhibitor concentration based on cytotoxic assays performed within the laboratory). This small molecule inhibitor interacts with the regulatory GTPase binding domain of N-WASP thus preventing Arp2/3 activation. The molecular structure of Wiskostatin (681525 1MG) from Calbiochem, Merck Millipore (Darmstadt, Germany) is shown in Figure 6.2 (Peterson *et al,* 2004).

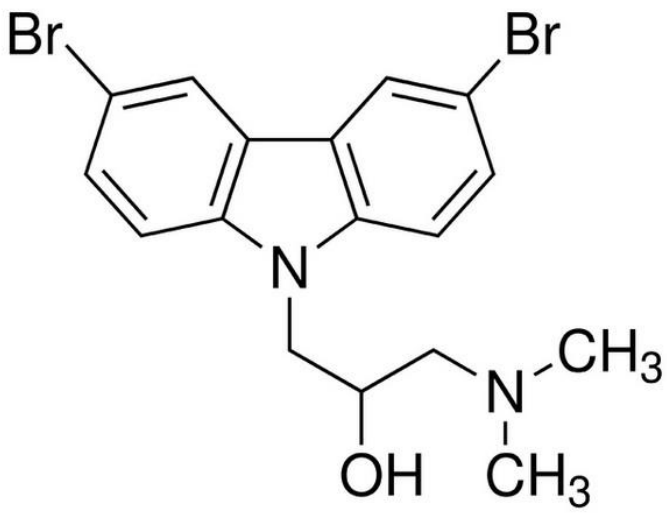

Figure 6.2 Molecular structure of the N-WASP inhibitor, Wiskostatin (image taken from Sigma Aldrich)

6.2.4 *In vitro* cell Matrigel invasion assay

The preparation of the cell invasion assay is outlined in Section 2.6.2. For the treatment groups, the inhibitor and the corresponding concentration used is described in Section 6.2.3.

6.2.5 *In vitro* cell motility assay

The preparation of the cell motility assay is outlined in Section 2.6.4. For the treatment groups, the inhibitor and the corresponding concentration used is described in Section 6.2.3.

6.2.6 Protein extraction, SDS-PAGE and Western blotting

Protein was extracted from control and WAVE knockdown PC-3 cells using a SDS-free lysis buffer (NP-40 based). Protein quantification allowed standardisation of the samples to ensure consistent loading of total protein. The protocol followed is outlined in Section 2.5.

6.2.7 Immunoprecipitation

The procedure for the immunoprecipitation of proteins with the antibody of choice is described in Section 2.3.3. To set up a positive control when analysing protein tyrosine phosphorylation, wild type PC-3 cells were cultured until 60-80% confluent. Medium was aspirated for the washing of cells with BSS then aspirated for the addition of 10mM sodium orthovanadate in 5ml serum free medium and hydrogen peroxide to make the final concentration 0.8%. After 10 minutes, this was aspirated for subsequent protein extraction outlined in Section 2.5.1.

6.2.8 Confocal microscopy

The confocal microscopy procedure is outlined in Section 2.7 and the primary and secondary antibodies used are shown in Chapter 2, Tables 2.4 and 2.6, respectively.

6.3 Results

6.3.1 Expression analysis of N-WASP in WAVE1 and WAVE3 knockdown PC-3 cells

The mRNA levels of N-WASP were analysed to gain an insight as to whether WAVE 1 or 3 knockdown in PC-3 cells would affect its expression. Knockdown of WAVE 1 or 3 expression was not observed to affect N-WASP expression as indicated by the similar band intensity of both wild type and pEF6 PC-3 samples in WAVE 1 and 3 knockdown samples. Expression levels of GAPDH were also observed to be at consistent levels across the PC-3 cell derived samples thus indicating consistent loading of samples. The negative control used in this analysis was a substitution of cDNA in polymerase chain reaction for PCR water. As no bands were detected for negative controls, this indicated no sign of contamination. This expression analysis is shown in Figure 6.3.

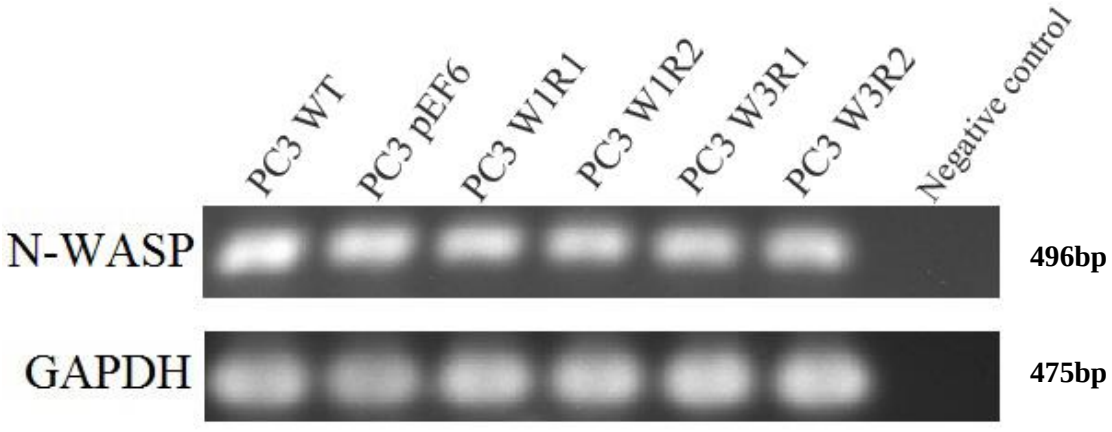

Figure 6.3 N-WASP mRNA expression analysis following knockdown of either WAVE 1 or 3 revealed no significant effect on levels of N-WASP expressed in PC-3 cells. GAPDH expression remained unaffected regardless of WAVE1 or 3 knockdown whilst the negative control revealed no signs of contamination.

6.3.2 Impact of N-WASP inhibitor treatment on PC-3 cell growth

PC-3 cells were treated with the N-WASP inhibitor, Wiskostatin to compare its effect on cell growth to cells without Wiskostatin treatment. In pEF6 control PC-3 cells, cell growth was observed to be upregulated in reponse to N-WASP inhibition ($p<0.001$). Similarly, WAVE3 knockdown cells treated with the N-WASP inhibitor were found to increase cell growth compared to cells without inhibitor treatment, however, this was not found to be statistically significant ($p=0.143$). In contrast, a marginal decrease in cell growth was demonstrated in WAVE1 knockdown PC-3 cells when treated with Wiskostatin, however, this change was not found to be statistically significant ($p=0.589$) (refer to Figure 6.4).

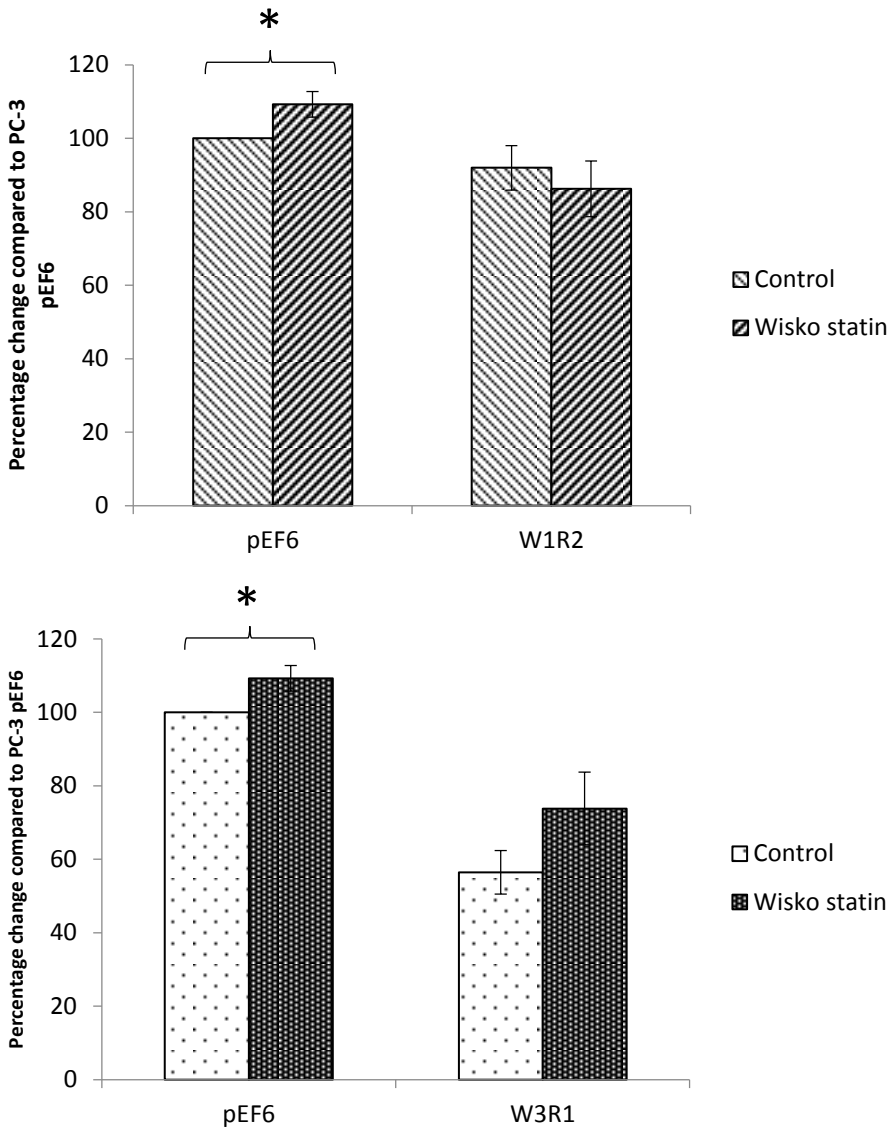

Figure 6.4 N-WASP inhibition showed cell growth increase in PC-3 pEF6 control whilst WAVE1 knockdown PC-3 cells (W1R2) showed a decrease (A). PC-3 cells exhibiting WAVE3 knockdown showed cell growth increase in response to the N-WASP inhibitor, Wiskostatin (B). Shown are mean data from a minimum of three independent repeats, values represent percentage change to pEF6 control cells without treatment (control). Error bars represent SEM. * represents $p < 0.05$.

6.3.3 Impact of N-WASP inhibitor treatment on cell invasion

Cell invasion was compared in PC-3 cell lines with and without the N-WASP inhibitor, Wiskostatin. A very moderate decrease in cell invasiveness was seen in pEF6 control PC-3 cells when treated with Wiskostatin relative to untreated cells, whilst N-WASP inhibitor treatment was shown to moderately increase cell invasivon in WAVE1 knockdown PC-3 cells. However, these cell invasion changes following N-WASP inhibitor were found to be insignificant in both pEF6 and WAVE1 knockdown PC-3 cells compared to their untreated equivalents ($p=0.497$; $p=0.586$, respectively) (refer to Figure 6.5).

Wiskostatin treatment of PC-3 cell exhibiting WAVE3 knockdown was shown to have no overall effect on cell invasion ($p=0.985$) (refer to Figure 6.6).

(A)

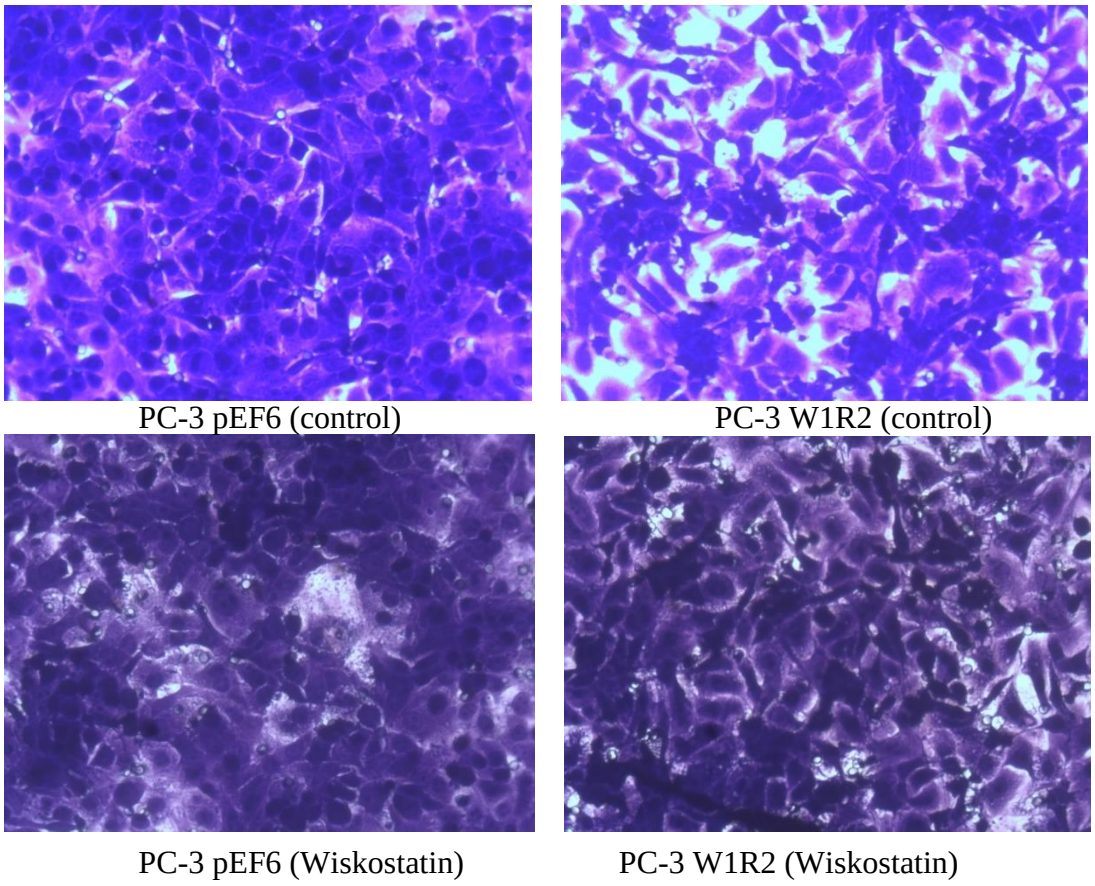

(B)

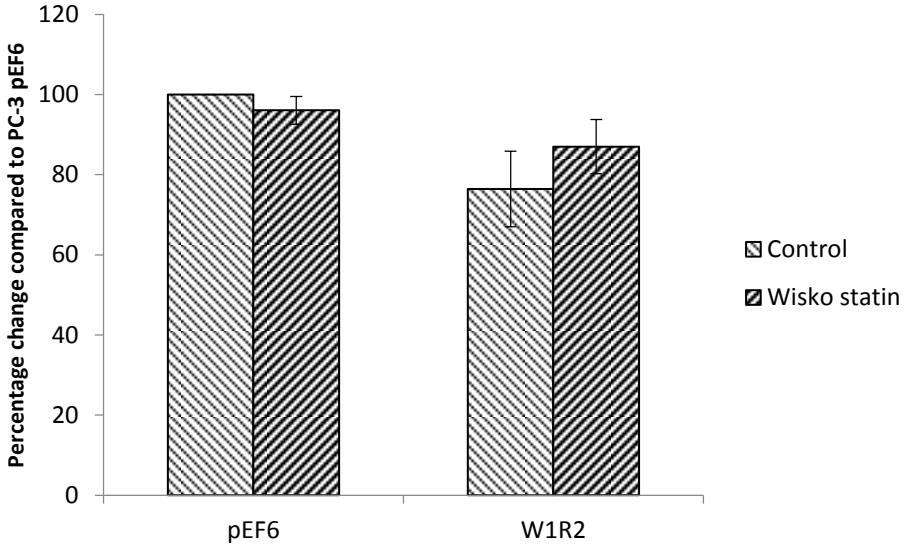

Figure 6.5 N-WASP inhibitor treatment reduced cell invasion of pEF6 control cells whilst it increases the invasiveness of PC-3 cells with WAVE1 knockdown. A) Representative images acquired for PC-3 pEF6 and W1R2 cells without N-WASP inhibitor treatment (control) and with (Wiskostatin). Images were acquired from at least three independent experiments. B) Cells were counted to calculate percentage change in cell invasion compared to PC-3 pEF6 cells without N-WASP inhibitor treatment. Images acquired at 200X magnification. Shown are mean data with error bars representing SEM.

(A)

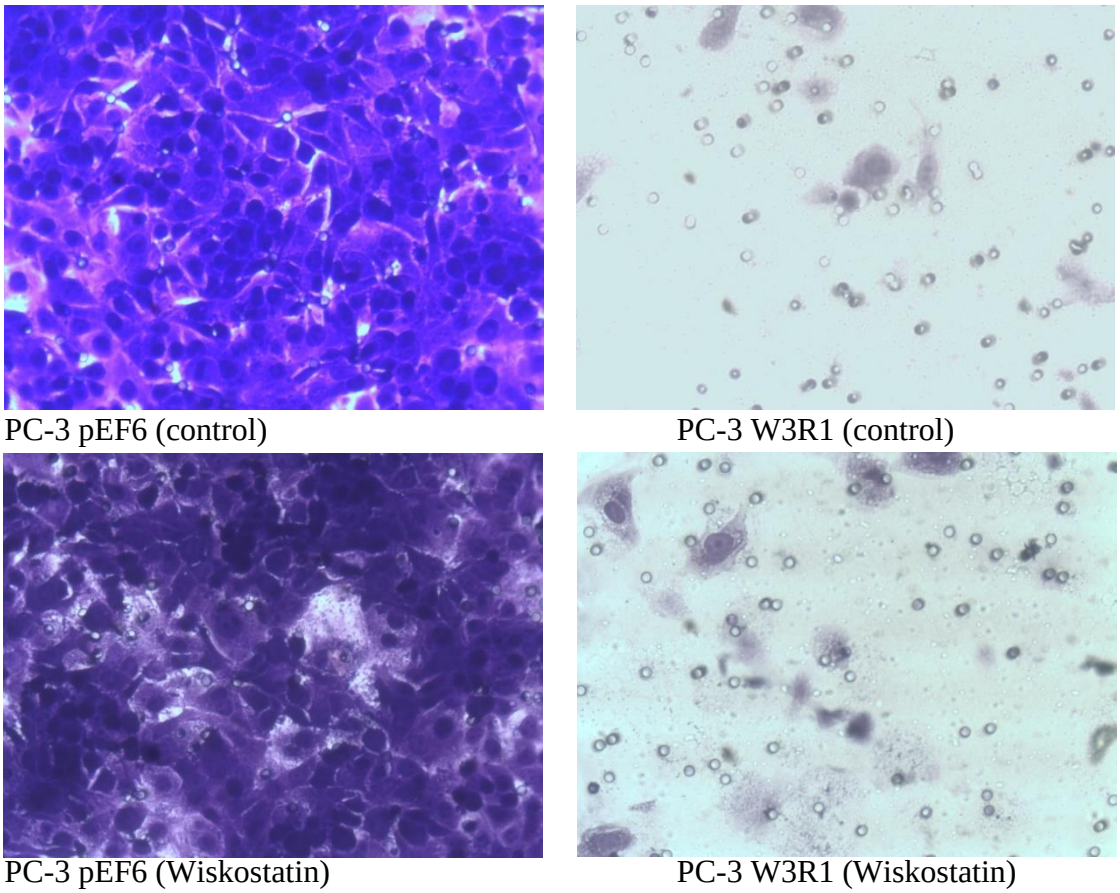

(B)

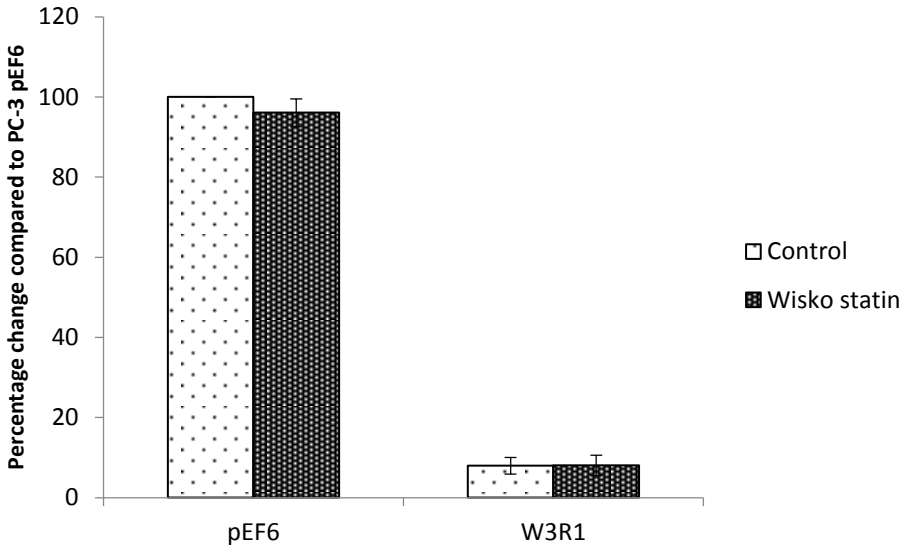

Figure 6.6 N-WASP inhibitor treatment marginally reduced cell invasion of pEF6 control cells but had little effect on WAVE3 knockdown cells. A) Representative images acquired for PC-3 pEF6 and W3R1 cells without N-WASP inhibitor treatment (control) and with (Wiskostatin). Images were acquired from at least three independent experiments. B) Cells were counted to calculate percentage change in cell invasion compared to PC-3 pEF6 cells without N-WASP inhibitor treatment. Images acquired at 200X magnification. Shown are mean data with error bars representing SEM.

6.3.4 Impact of N-WASP inhibitor treatment on cell motility

Treatment of PC-3 pEF6 cells with Wiskostatin was found to significantly increase cell motility when compared to untreated cells ($p=0.012$). An overall trend of increased cell motility was also observed for WAVE1 knockdown PC-3 cells following treatment with Wiskostatin, although this was not found to be significant when compared to untreated PC-3 W1R2 cells ($p=0.71$). Inhibition of N-WASP in WAVE3 knockdown PC-3 cells was not shown to affect cell motility compared W3R1 without N-WASP inhibition ($p=0.89$).

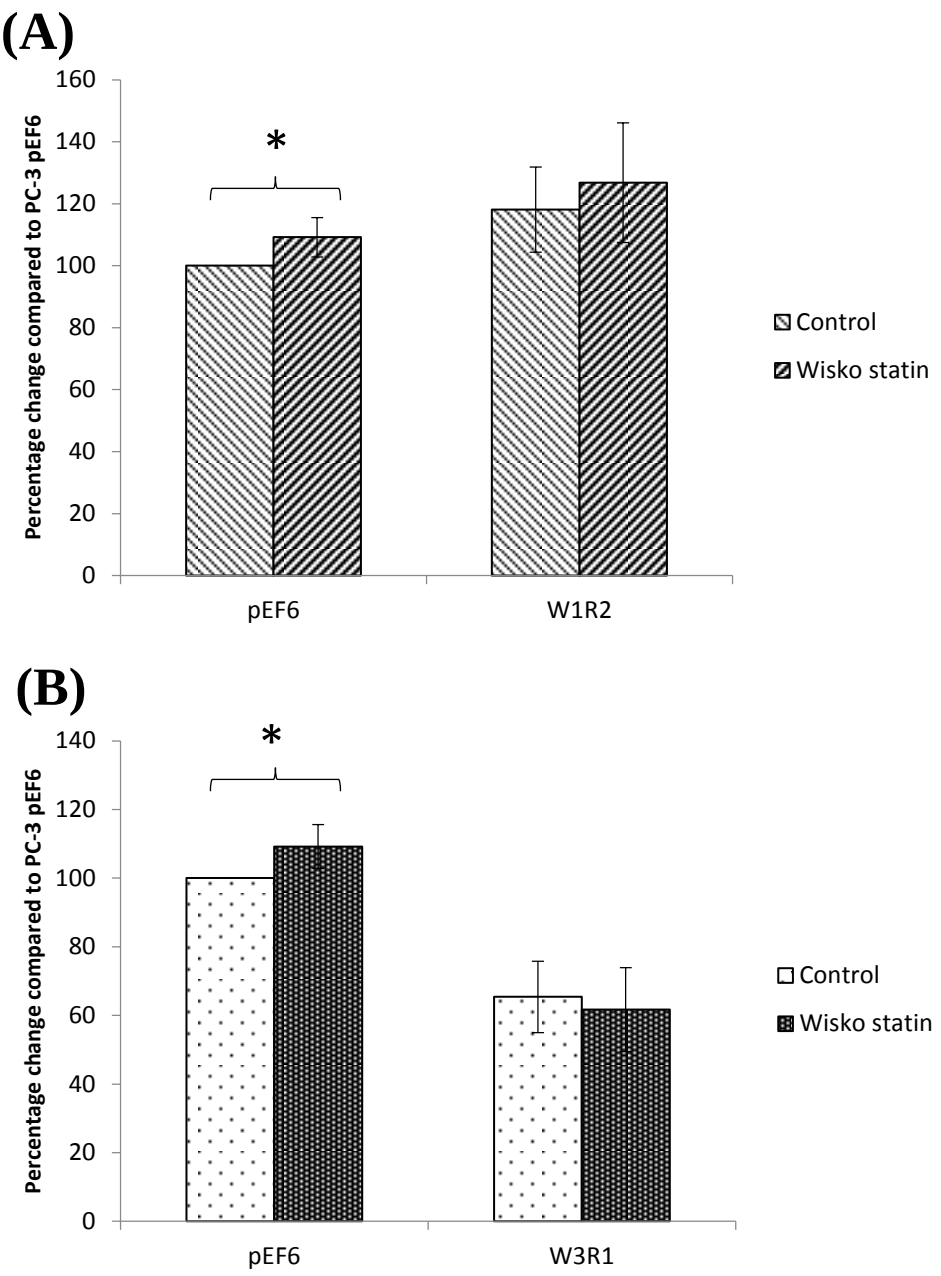

Figure 6.7 Wiskostatin treatment moderately increased cell motility in PC-3 pEF6 control and WAVE1 knockdown cells (A). On the contrary, little effect on cell motility was observed in WAVE3 knockdown cells with N-WASP inhibition (B). Shown are mean data from a minimum of three independent repeats, values represent percentage change to pEF6 cells without treatment. Error bars represent SEM. * represents $p < 0.05$.

6.3.5 WAVE knockdown has no impact on N-WASP tyrosine phosphorylation

Protein extracted from PC-3 cells with a NP-40 based lysis buffer was immunoprecipitated with a phosphotyrosine antibody (PY20) following standardisation. These immunoprecipitated proteins were separated by SDS-PAGE then transferred to a nitrocellulose membrane for probing with N-WASP antibody. As Figure 6.8 shows, there appears to be no obvious changes in N-WASP tyrosine phosphorylation levels in PC-3 cells following either WAVE 1 or WAVE 3 knockdown (W1R2 and W3R1, respectively). Notably, levels of tyrosine phosphorylation in the majority of protein samples were comparable to the positive control. On the whole, similar levels of N-WASP protein were observed in the cell lysate for the PC-3 protein samples analysed. Consistent levels of GAPDH were observed in all samples probed.

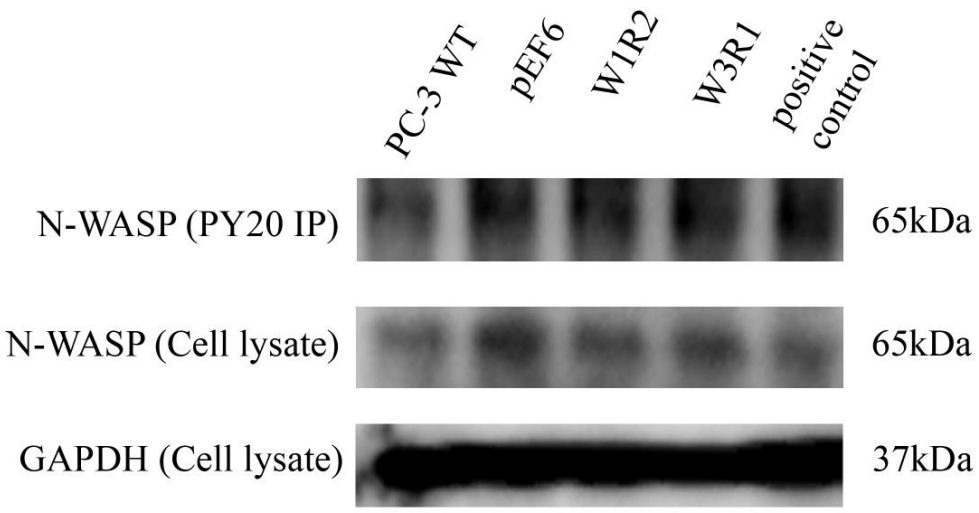

Figure 6.8 Protein immunoprecipitated with the anti-phosphotyrosine antibody PY20 revealed no changes in phosphorylated tyrosine levels of N-WASP protein in PC-3 cells. Even so, levels of tyrosine phosphorylation in these protein samples were similar to the positive control.

6.4 Discussion

Dynamic remodelling of the actin cytoskeleton is a major driving force underlying cell migration. The ability of monomeric actin to form filamentous actin which comprises the cytoskeleton is stimulated by the Arp2/3 complex. Actin polymerisation requires activation of the Arp2/3 complex by nucleation promoting factors which include members of the WASP family; WASP and WAVE proteins (Higgs and Pollard, 1999).

The association of WASP and WAVE proteins with Arp2/3 is analogous; both have the consequence of influencing cell migration. Even though the role of WASP proteins in the cell is similar to that served by the WAVEs, these subgroups can be characterised by their ability to generate physiologically distinct cell protrusions at the cell leading edge (Ridley, 2011). Their specific roles in the cell are defined by the ability of WASP and N-WASP to drive filopodia formation and WAVE1, 2 and 3 with the generation of lamellipodia; both of which are an integral mechanism that facilitates cell motility. Despite serving analogous roles in the cell, WRC activity has been demonstrated to affect the recruitment and therefore the function of N-WASP at the cell leading edge and was shown to effect cell migration and invasion (Tang *et al,* 2013). The ability of WASP and WAVE to generate different cell formations and the implication that each may influence the activity of the other suggest that these two protein subgroups are not functionally redundant.

Disrupting WRC activity was shown to effect cell migration and invasion with evidence of N-WASP being a contributing factor. Since the implication is that there is signalling between these related protein groups and given the association of their aberrant expression and/or activity with several human cancers, the aim of this

section of the project was to analyse the relationship between WAVE1 and 3 with N-WASP in metastatic prostate cancer cells.

N-WASP expression was analysed in the metastatic prostate cancer cell line, PC-3 following successful WAVE1 or 3 knockdown. A comparison of WAVE1 or 3 knockdown cells with wild type or pEF6 control cells revealed no change in N-WASP expression. This could suggest that WAVE1 or 3 does not regulate N-WASP expression and the expression of these two protein subgroups are regulated independently of each other.

The *in vitro* function assays outlined in Chapter 3 revealed a decrease in cell growth in both WAVE1 and 3 knockdown PC-3 cells compared to pEF6 control cells. For this section of the study, the same experiments were coupled with the N-WASP inhibitor, Wiskostatin. In doing so, it was hoped that this would provide insight into the relationship between WAVE1 and 3 with N-WASP during the process of cell growth, invasion and motility. Treating pEF6 cells with the N-WASP inhibitor, Wiskostatin was demonstrated to moderately increase cell growth with a similar trend observed with WAVE3 knockdown cells when compared to untreated equivalent cells ($p<0.001$ and $p=0.143$, respectively). In contrast, N-WASP inhibition was seen to further decrease cell growth in WAVE1 knockdown PC-3 cells, however this was not found to be statistically significant ($p=0.589$). The different cell growth response to Wiskostatin in PC-3 cells exhibiting WAVE1 and WAVE3 knockdown highlighted functional differences in these cells and emphasised distinctive roles for these proteins in the cell. Whilst either WAVE1 or 3 knockdown in PC-3 cells was shown to decrease cell growth, coupling WAVE1 knockdown with N-WASP inhibition was shown to decrease growth further, whereas the opposite was observed in either PC-3 pEF6 or WAVE3 knockdown cells with Wiskostatin

treatment. These findings may implicate that N-WASP activity inhibition reduces cell growth only when cells are also exhibiting a knockdown in WAVE1 activity. It is of interest to note that Wiskostatin treatment of pEF6 control cells showed a similar trend of increased cell growth as Wiskostatin treatment of WAVE3 knockdown cells. Having discussed the relationship between WAVE1 and N-WASP in the context of growth in PC-3 cells is it reasonable to suggest that WAVE1 is still functional in pEF6 and W3R1 cells. In a hypothesised signalling cascade, cell growth is increased despite N-WASP inhibition as it results in a feedback loop that involves WAVE1. This theory is not too dissimilar to the findings previously described where the depletion of WRC activity resulted in the unexpected finding of increased cell motility which was dependent on N-WASP activity (Tang *et al,* 2013).

As described in Chapter 3, the knockdown of either WAVE1 or 3 was shown to potently decrease cell invasiveness (Figure 3.7). However, the treatment of PC-3 pEF6 control cells with Wiskostatin was shown to have very little effect on cell invasion. This implies that the role of WAVE1 and 3 in cell invasion is more important than that of N-WASP. Interestingly, when W1R2 cells were treated with Wiskostatin, the effects of decreased cell invasion seen with WAVE1 knockdown were moderately alleviated. However, this was not observed for cells exhibiting WAVE3 knockdown coupled with N-WASP inhibition. Whist this demonstrates fundamental differences between WAVE1 and 3, it also emphasises a relationship between N-WASP and WAVE1 which is not so apparent with WAVE3 in cell invasion. To reiterate the points made in Chapter 4, MMPs have a cardinal role in cell invasion due to their ability to digest components of the ECM. Much work has demonstrated a regulatory role for WAVE3 with MMPs, therefore, whilst PC-3

W1R2 cells lack functional WAVE1, WAVE3 is still active and able to promote MMP activity.

Cell motility was found to be greatly decreased with WAVE3 knockdown in PC-3 cells when compared to pEF6 control cells. On the other hand, a moderate increase in the motile abilities of PC-3 cells was observed with WAVE1 knockdown, although this was found to be statistically insignificant (refer to Chapter 3, Section 3.3.7). The small molecule inhibitior, Wiskostatin was used to inhibit N-WASP in PC-3 cells to investigate the relationship with WAVE1 or 3 in cell motility. Wiskostatin treatment of pEF6 control cells showed a moderate increase in cell motility which was similar to the effects of N-WASP inhibition in WAVE1 knockdown cells, however, this was found to be non-significant. On the contrary, PC-3 cells exhibiting WAVE3 knockdown showed very little change in cell motility in response to N-WASP inhibition. It is interesting to note that the effects of WAVE knockdown on PC-3 cell motility appeared to be moderately enhanced by N-WASP inhibition with Wiskostatin treatment (i.e. WAVE1 knockdown increased cell motility, when coupled with N-WASP inhibition, cell motility was increased further. WAVE3 knockdown decreased cell motility, whilst combining with N-WASP inhibition decreased cell motility further). Despite differing effects of WAVE1 or 3 knockdown, these observations suggest a regulatory role of N-WASP with both WAVE1 and 3 in facilitating cell motility.

As Figures 6.3 and 6.8 demonstrate, neither WAVE1 nor 3 knockdown was shown to affect N-WASP mRNA and protein expression. However, it has previously been reported that N-WASP activity can be influenced by WAVE (Tang *et al,* 2013). Due to the important regulatory role played by tyrosine kinases in signalling transduction pathways, it is unsurprising that abnormal tyrosine kinase activity is implicated in

several human cancers (Blume-Jensen and Hunter, 2001). Due to the complex network of protein interactions that could be involved in moderating N-WASP activity, the effects of WAVE knockdown on N-WASP tyrosine phosphorylation levels was investigated in PC-3 cells to understand the regulatory relationship between these proteins. Immunoprecipitation approaches revealed no change in tyrosine phosphorylation levels of N-WASP in PC-3 cells following WAVE1 or 3 knockdown. N-WASP tyrosine phosphorylation was observed to be at similar levels in PC-3 wild type, pEF6 control, WAVE1 and 3 knockdown cells; interestingly, these levels were also similar to the positive control that was run in parallel. Although previous studies implicate a regulatory relationship between WAVE and N-WASP, the findings outlined here suggest tyrosine phosphorylation is not part of the mechanism utilised by WAVE1 or 3 to moderate N-WASP activity. Furthermore, there is an implication that levels of N-WASP tyrosine phosphorylation are intrinsically high in PC-3 cells as a comparison to positive control showed similar levels. Currently there are two tyrosine phosphorylation sites identified for N-WASP: Y175 and Y256. Whilst the former has been linked to gastric cancer, the latter residue site has been characterised in bladder, gastric, breast and lung cancer tissue. Furthermore, tyrosine phosphorylation at this site has been linked to altered cell adhesion and cytoskeletal reorganisation (Phosphosite).

Treating PC-3 cells with Wiskostatin resulted in contrasting cell growth, invasion and motility effects when comparing those cells exhibiting WAVE1 or 3 knockdown. The main point emphasised by these observations is that these two proteins play particular roles in the cell, but while this is the case, it is also apparent that with the knockdown of a specific WAVE activity, the other WAVE protein is still functional. As previously mentioned, Wiskostatin was used at a concentration of 100nM and

was based on cytotoxic assays performed in the lab. Although these cell function assays show intruging results for Wiskostatin in this study, other studies used this small molecule inhibitor at concentrations varying from 10 to 50µM (Guerriero and Weisz, 2007). However, Wiskostatin at concentrations above 10µM was linked with an irreversible dose-dependent drop in cellular ATP levels with the potential to affect cell function. If given the opportunity, this study would be repeated with Wiskostatin at a higher concentration than 100nM to confirm the results presented here.

Whilst the N-WASP tyrosine phosphorylation levels of WAVE1 or 3 knockdown cells were observed to remain the same as wild type and pEF6 controls, these levels were also at similar levels as the positive control. Given that the phosphorylation of a particular tyrosine residue is linked with altered cell adhesion, in retrospect, it would possibly have been useful to have included cell adhesion assays in this study. However, what this current work conveys is that whilst WASP and WAVE proteins work at the same level by relaying messages from Rho GTPases to the Asp2/3 complex, their roles in the cell are not interchangeable. In fact, the findings from the *in vitro* studies outlined here suggest the influence of auxiliary proteins from additional signalling pathways that work alongside WASP and WAVE to impact cell growth, invasion and motility. Given the role of both N-WASP and WAVE1 and 3 in cytoskeletal dynamics, the inclusion of confocal approaches would be a sensible step to progress the findings outlined here.

Chapter 7

General discussion

Cancer metastasis is a complex process governed by a multitude of possible aberrations in normal molecular machinery of the cell. Whilst cell migration is an integral process which facilitates many physiologically important processes, when uncontrolled it is major contributor to cancer metastasis (Lambrechts *et al*., 2004). Dynamic remodelling of the actin filament network, the major constituent of the cytoskeleton, enables cells to migrate. The ability of the Arp2/3 complex to stimulate rapid actin polymerisation defines this protein complex as an integral cell migration mechanism (Schafer *et al.,* 1998; Higgs and Pollard., 1999).

The clinical importance of WASP Verprolin homologous proteins (WAVE) was first demonstrated in a ganglioneuroblastoma case study (Sossey-Alaoui *et al*., 2002). A flourish of research has since stemmed from this work which has highlighted significant links between this protein family and human cancer. Identifying their influence on actin polymerisation through their interaction with the Arp2/3 complex has helped to shed light on how abnormal function in the cell can have potential clinical implications manifesting as cancer metastasis. This point has been extensively emphasised by findings that the increased expression and/or activity of particular WAVE proteins was associated with several human cancers (Kurisu *et al*., 2005, Sossey-Alaoui *et al.*, 2007). Furthermore, a trend of higher WAVE expression was linked with cancers that had progressed to a more advanced stage and/or with those which had metastasised (Iwaya *et al*., 2007). The expression of WAVE1 and 3 was demonstrated to be higher in metastatic prostate tissue compared to normal epithelial tissue. The clinical importance of these proteins was further emphasised when it was found that several metastatic traits were suppressed with the knockdown of WAVE1 or 3 expression in metastatic prostate cancer cells (Fernando *et al*., 2008; Fernando *et al*., 2010).

7.1 The role of WAVE1 and 3 in PC-3 cell proliferation

Cell growth data from the present study demonstrated WAVE1 or 3 knockdown has the ability to suppress cell growth and suggests a role for these proteins in cell proliferation. Whilst work by Fernando *et al,* concurred with the effects of WAVE1 knockdown on cell growth data presented here, WAVE3 knockdown was not previously shown to have any effect (Fernando *et al*., 2008; Fernando *et al*., 2010). However, the integrity of the results described here is supported by the role of WAVE3 as a negative regulator of LDOC1-induced apoptosis (Mizutani *et al*, 2005). Apoptosis through this pathway is promoted with reduced WAVE3 expression and therefore successful knockdown of WAVE3 would see a decrease in viable cells.

Arp2/3 inhibition was observed to decrease cell growth furthermore in both WAVE1 or 3 knockdown cells whilst showing little effect in pEF6 cells. This implies that both WAVE1 and 3 interact with Arp2/3 but have additional signalling partners to drive cell proliferation (see Figure 4.10). Whilst targeting Arp2/3 with the inhibitor CK-0944636 suggests analogous roles for both WAVE proteins in cell proliferation, experiments using Y-27632 to target ROCK activity dispelled this theory. Cell growth was observed to increase with ROCK inhibition in pEF6 and W1R2 cells whilst having little effect in W3R1 cells. Previous findings suggest that ROCK inhibition has been linked to suppressed apoptosis (Papadopoulou *et al,* 2008). The data presented here is not wholly surprising since it highlighted significant cell growth differences in response to ROCK inhibition when comparing PC-3 cells exhibiting WAVE1 or 3 knockdown. As previously mentioned, the ability of WAVE3 to suppress apoptosis through LDOC1 mediates an understanding of these observations and emphasises the complex signalling networks that are influenced by WAVE proteins.

Functional differences between WAVE 1 and 3 were further reiterated in cell growth experiments coupled with the N-WASP inhibitor, Wiskostatin. Targeting N-WASP in pEF6 cells increased cell growth which was a trend also seen in PC-3 W3R1 cells. In contrast, Wiskostatin reduced cell growth in W1R2 cells. It is difficult to ascertain whether N-WASP regulates cell proliferation through WAVE1 and 3 or vice versa, however, as it has been postulated that WAVE3 can influence apoptosis as a separate mechanism to its relationship with Arp2/3 to drive cell proliferation, it is possible that N-WASP has a role in apoptosis. There is no literature that makes this link, however, disruption of the *WASP* gene, a related member of N-WASP, has been shown to impair apoptosis (Sato *et al*, 2012). If this were also a mechanism utilised by N-WASP, its inhibition would suppress apoptosis and therefore an increase in cell growth. However, given the different ways WAVE1 and 3 knockdown cells responded to Wiskostatin, it is apparent that these WAVE proteins interact differently with N-WASP.

7.2 The role of WAVE1 and 3 in PC-3 cell invasion

Knockdown of either WAVE1 or 3 expression in PC-3 cells was demonstrated to decrease cell invasion as described and agrees with findings outlined in previous studies (Fernando *et al*., 2008; Fernando *et al*., 2010). Interestingly, experiments coupling these findings with small molecule inhibitors targeting either ARP2/3, ROCK-I/II or N-WASP all showed similar results; increased cell invasion in WAVE1 knockdown cells and very little effect in WAVE3 knockdown cells.

The ability for WAVE proteins to promote actin polymerisation can help to explain why knockdown of their expression sees a suppression of PC-3 cell invasion.

Moreover, the regulatory role of WAVE3 on matrix metalloprotease (MMP) activity is well known and offers an explanation for the dramatic cell invasion decrease in WAVE3 knockdown cells compared to PC-3 cells exhibiting WAVE1 knockdown (Sossey-Alaoui K *et al.,* 2005; 2009; Zhang Y *et al.,* 2012). Due to the specificity of ribozyme transfection, PC-3 cells targeted with WAVE1 ribozyme would still exhibit functional WAVE3, able to promote MMP activity. It is not entirely clear whether the increased cell invasion changes in W1R2 cells following CK-0944636, Y-27632 and Wiskostatin treatment is due to a regulatory role for ARP, ROCK and N-WASP proteins on MMP activity. Findings that Y-27632 suppressed MMP-3 expression in human articular chondrocytes would contradict this (Furumatsu *et al*, 2013), however, it is important to consider that this may not reflect cell invasion signalling in metastatic prostate cancer cell lines.

Although there is no literature describing a link between MMPs with either the Arp2/3 complex or N-WASP, these proteins may have a cell invasion regulatory role through pathways independently of MMPs. Loss of WRC has been found to upregulate N-WASP activity and cell invasiveness (Tang *et al,* 2013). N-WASP activity is proposed to be upregulated by Focal Adhesion Kinase (FAK) in response to abolished WRC activity. As FAK has a role in matrix attachment and degradation, it is possible to hypothesise that despite N-WASP inhibition with Wiskostatin treatment, WAVE1 knockdown simulates loss of WRC activity and promotes FAK activity. With a role in matrix degradation, FAK enables functional WAVE3 to drive the invasion of PC-3 cells.

7.3 The role of WAVE1 and 3 in cell motility

The role of both WAVE 1 and 3 in cell proliferation, invasion and migration is well established (Zhang *et al,* 2013; Fernando *et al,* 2010; Teng *et al,* 2013). The cell motility data presented here which shows a decrease with WAVE3 knockdown is unsurprising, however, the motility increase observed when targeting WAVE1 expression in PC-3 cells is puzzling. It is possible that WAVE3 plays a bigger regulatory role in cell motility relative to WAVE1 and therefore limiting its expression will produce a more pronounced change in cell motility (see Figure 3.9). As for the cell motility increase with WAVE1 knockdown, it is possible that knocking down WAVE1 expression upregulates WAVE3 activity through an unknown mechanism that is intrinsically buffered by WAVE1 by the cell.

Inhibitors targeting proteins known to play a role in cell migration were paired with these cell motility assays. Treatment with CK-0944636, Y-27632 or Wiskostatin to target Arp2/3, ROCK and N-WASP, respectively was shown to increase cell motility in PC-3 pEF6, W1R2 and W3R1 cells. The one exception seen was with Wiskostatin treatment of WAVE3 knockdown cells which had very little effect on cell motility. It is not clear whether the similar cell motility trend demonstrated in all the cells treated with CK-0944636, Y-27632 or Wiskostatin is indeed a true result of the inhibitors used or whether the Cytodex bead assay is suitable for this application. Despite an overall increase in cell motility observed, as Figures 4.6, 5.7 and 6.7 show, the error bars representing standard error of the mean show a relatively large spread of data. To validate the data presented here, alternative assays would need to be used including wound healing assays and those utilised by different research groups (Teng *et al,* 2013; Zhang *et al,* 2013). Furthermore, increasing evidence suggests that signalling pathways that drive two dimensional (2D) migration differ to those that

govern motility in three dimensional (3D) microenvironments; these different modes of migration have been demonstrated for the same cell line and were found to be dependent on physical properties of the extracellular matrix (Petrie and Yamada, 2012; Giri *et al,* 2013). Therefore, an analysis of WAVE proteins using a 3D cell migration model would simulate the microenvironment faced by metastatic prostate cancer cells.

7.4 WAVE1 and 3 co-localisation with other cell motility proteins in PC-3 cells

Confocal microscopy approaches demonstrated that both WAVE1 and 3 co-localise with both ARP 2 and ROCK-I to the boundaries of PC-3 cells as seen in pEF6 control cells. A distinct reduction of WAVE1 was apparent in WAVE1 knockdown cells in both the cell edges and the cytoplasmic areas. Likewise, WAVE3 knockdown cells also showed a decrease in WAVE3 protein in PC-3 cells. In parallel, ARP2 and ROCK-I was also less distinguishable in both WAVE1 and 3 knockdown cells. These findings suggest co-localisation of WAVE1 and 3 with ARP2 and ROCK-I in PC-3 cells and in particular to the outermost fringes of the cell which are discernable as flat broad sheets extending out from the cell which is a characteristic of lamellipodia. The reduced prominence of these cell protrusions following WAVE1 or 3 knockdown alter the overall morphology of the cell and suggest an important role for WAVE1 and 3 in generating such cell formations.

These findings suggest ARP2 associates closely with WAVE1 and 3 in PC-3 cells, particularly to the cell edge. Similarly, WAVE1 and 3 appear to influence the localisation of ROCK-I in this cell line. This highlights an important relationship between WAVE and Arp2/3 in addition to a relationship between WAVE and ROCK

in the PC- 3 cell line. Ultimately, the relationship between ARP3 and ROCK-II with WAVE1 and 3 will have to be explored in order to gain a complete picture of the relationship between these protein networks and their significance in metastatic prostate cancer cells. Co-immunoprecipitation approaches would allow a better understanding of the protein relationship between WAVE proteins with ARP and ROCK proteins.

7.5 Effects of WAVE1 and 3 knockdown on protein tyrosine phosphorylation levels of cell motility related proteins in PC-3 cells

Protein tyrosine phosphorylation plays an essential role in many cell functions including cell proliferation and survival. Protein tyrosine kinases are key regulators of tyrosine phosphorylation and their dysregulated expression and/or activity have been implicated as a potential contributor to cancer development. Whilst the present study did not focus on the expression or activity of particular protein tyrosine kinases, levels of tyrosine phosphorylation in the proteins of interest were examined in response to WAVE1 or 3 knockdown. In doing so, PC-3 cells exhibiting WAVE3 knockdown were observed to show elevated levels of ARP2 tyrosine phosphorylation. Phosphosite database searches revealed five potential sites of tyrosine phosphorylation in the ARP2 protein that have been linked to several forms of leukaemia and lymphoma (Gu TL *et al*, 2010; Weber C *et al*, 2012). However, there is no literature that explains the functional significance of tyrosine phosphorylation in either ARP2 or 3.

Additionally, increased ROCK-II tyrosine phosphorylation levels were observed in WAVE1 knockdown PC-3 cells. Several tyrosine residues of ROCK-II were

identified to be phosphorylated with one site, Y722, being associated with disease tissue including those originating from gastric and lung cancer. Functionally, Y722 phosphorylation of ROCK-II has been linked with its reduced binding to RhoA and is important for focal adhesion dynamics; this was demonstrated in a myeloid leukemia cell line (Lee and Chang, 2008). Whilst the data here does not signify which specific tyrosine residues are targeted, an overall picture of tyrosine phosphorylation in ARP2 and ROCK-II is presented for the PC-3 cell line and may be of importance in understanding prostate cancer metastasis.

7.6 Future work

This study has provided an insight into the functional importance of WAVE1 and 3 and their implications in prostate cancer cell lines derived from metastases. It is clear that these proteins govern cell proliferation, invasion and motility through complex signalling networks which are not well defined. *In vitro* experiments coupling PC-3 cells exhibiting WAVE1 or 3 knockdown with specific protein inhibitors have indicated a role for Arp2/3, ROCK-I/II and N-WASP with WAVE1 and 3 in cell growth and invasion. However, the relationship between the WAVE proteins with these proteins of interest is not clear and requires further work. Immunopreciptation approaches exploring phosphorylated tyrosine levels highlighted potential regulatory relationships between WAVE3 with ARP2 and WAVE1 with ROCK-II. The functional significance of these findings will need to be explored in detail. It is clear that further investigation into the relationship between WAVE1 and 3 with ARP2/3, ROCK-I/II and N-WASP in prostate cancer metastasis is essential. Future work is required in the following areas to clarify some of the question raised by this thesis:

1) Growth: In addition to the assay outlined to investigate cell proliferation in PC-3 cells, pairing this with an apoptosis and cell cycle assay would provide another insight into the cell growth effects of WAVE1 and 3. As WAVE3 and LDOC1 have been linked in apoptosis, the significance of this mechanism could be explored in prostate cancer metastasis. Also, alternative approaches could be employed to determine cell number such as the colourimetric based MTT assay to assess viable cells. Furthermore, as FAK plays a role in cell migration and its function as a molecular scaffold, it is worth exploring its relationship with WAVE especially due to the finding that WRC regulates N-WASP through FAK.

2) Invasion: As WAVE3 is known as a regulator of MMPs and has a role in cell invasion, it would be useful to establish whether ARP2/3, ROCK-I/II and N-WASP have a role in moderating their activity and whether this mechanism involves either WAVE1 or 3.

3) Motility: A 3D cell migration model to mimic the microenvironment faced by prostate cancer cells would provide an insight into signalling pathways that may differ to those used by cells during 2D cell migration

4) Generation of dual WAVE1 and 3 knockdown cell lines to further explore the redundancy of two molecules and compare results to those described in this study

5) As the experiments described in this study were *in vitro* assays, the use of *in vivo* models would allow a better indication of the therapeutic implications of WAVE1 and 3 in prostate cancer metastasis.

6) The use of inhibitors to target ARP2/3, ROCK-I/II and N-WASP in WAVE knockdown cells and an investigation into its effects on tyrosine phosphorylation

lead to some interesting findings. However, co-immunoprecipitation approaches would provide an insight into interactions between these proteins.

7) Due to the regulatory role of WAVE, N-WASP, ARP2/3 and ROCK in actin filament dynamics, confocal techniques and live cell motion tracking imaging would be ideal to investigate the effects on cell morphology and motility following WAVE1 or 3 knockdown and the use of the small protein inhibitors, CK-0944636, Y-27632 or Wiskostatin.

Chapter 8

References

Abdel-Ghany M., Cheng HC., Elble RC., Pauli, BU. 2002. Focal adhesion kinase activated by β_4 integrin ligation to mCLCA1 mediates early metastatic growth. J Biol Chem 277(37) pp.34391-400

Ablin, R,J., 1997. A retrospective and prospective overview of prostate-specific antigen. J Cancer Res Clin Oncol 123(11-12) pp.583-94

Abraham MT., Kuriakose MA., Sacks PG., Yee H., Chiriboga L., Bearer EL., Delacure MD., 2001. Motility-related proteins as markers for head and neck-squamous cell cancer. Laryngoscope 111(7) pp.1285-9

Adams, J., Cheng, L., 2011. Lymph node-positive prostate cancer: current issues, emerging technology and impact on clinical outcome. Expert Rev Anticancer Ther 11(9) pp.1457-69

Aiuti A., Tavian M., Cipponi A., Ficara F., Zappone E., Hoxie J., Peault B., Bordignon C.,1999. Expresion of CXCR4, the receptor for stromal cell-derived factor-1 on fetal and adult human lympho-hematopoietic progenitors. Eur J Immunol 29(6) pp.1823-31

Ali A, Nguyen DP, Tewari A., 2013. Robot assisted laparoscopic prostatectomy in 2013. Minerva Chir Oct;68(5) pp.499-512

Al-Mehdi AB., Tozawa K., Fisher, AB., Shientag L., Lee A., Muschel RJ. 2000. Intravascular origin of metastasis from the proliferation of endothelium-attached tumour cells: a new model for metastasis. Nat Med 6(1) pp.100-102

Amano M, Nakayama M, Kaibuchi K., Rho-kinase/ROCK: A key regulator of the cytoskeleton and cell polarity. Cytoskeleton 67(9):545-54

American Joint Committee on Cancer, 7th Edition, American Cancer Society, 2009

Antón IM, Jones GE, Wandosell F, Geha R, Ramesh N., 2007. WASP-interacting protein (WIP): working in polymerisation and much more. Trends Cell Biol 17(11) pp.555-62

Arber S, Barbayannis FA, Hanser H, Schneider C, Stanyon CA, Bernard O, Caroni P., 1998. Regulation of actin dynamics through phosphorylation of cofilin by LIM-kinase. Nature 393(6687):805-9

Ardern H., Sandilands E., Machesky LM., Timpson P., Frame MC., Brunton VG., 2006. Src-dependent phosphorylation of Scar1 promotes its association with the Arp2/3 complex. Cell Motil Cytoskeleton 63(1) pp.6-13

Armstrong, B., Doll,R ., 1975. Environmental factors and cancer incidence and mortality in different countries, with special reference to dietary practices. Int J Cancer 15(4) pp.617-31

Ayscough KR., 1998. In vivo functions of actin-binding proteins. Curr Opin Cell Biol 10(1):102-11

Bellovin DI., Simpson KJ., Danilov T., Maynard E., Rimm DL., Oettgen P., Mercurio AM., 2006. Reciprocal regulation of RhoA and RhoC characterises the EMT and identifies RhoC as a prognostic marker of colon carcinoma. Oncogene 25(5) pp.6959-67

Binks M, Jones GE, Brickell PM, Kinnon C, Katz DR, Thrasher AJ., 1998. Intrinsic dendritic cell abnormalities in Wiskott-Aldrich syndrome. Eur J Immunol 28(10) pp.3259-67

Blessing CA, Ugrinova GT, Goodson HV., 2004. Actin and ARPS: action in the nucleus. Trends Cell Biol 14(8) pp.435-42

Blume-Jensen P, Hunter T., 2001. Oncogenic kinase signalling. Nature 411(6835) pp.355-65

Borley, N., Feneley, M,R., 2009. Prostate cancer: diagnosis and staging. Asian J Androl 11(1) pp.74-80

Brown MD., Hart CA., Gazi E., Bagley S., Clarke NW., 2006. Promotion of prostatic metastatic migration towards human bone marrow stoma by Omega 6 and its inhibition by Omega 3 PUFAs. Br J Cancer 94(6) pp.842-53

Brunton VG, Frame MC., 2008. Src and focal adhesion kinase as therapeutic targets in cancer. Curr Opin Pharmacol 8(4) pp.427-32

Bryden AA., Hoyland JA., Freemont AJ., Clarke NW., Schembri Wismayer D., George NJ., 2002. E-cadherin and beta-catenin are down-regulated in prostatic bone metastases. BJU Int 89(4) pp.400-3

Bubendorf L., Schöpfer A., Wagner U., Sauter G., Moch H., Willi N., Gasser TC., Mihatsch MJ., 2000. Metastatic patterns of prostate cancer: an autopsy study of 1,589 patients. Hum Pathol 31(5) pp.578-83

Burns S, Thrasher AJ, Blundell MP, Machesky L, Jones GE., 2001. Configuration of human dendritic cell cytoskeleton by Rho GTPases, the WAS protein, and differentiation. Blood 98(4) pp.1142-9

Bussemakers MJ., Van Bokhoven A., Tomita K., Jansen CF., Schalken JA., 2000. Complex cadherin expression in human prostate cancer cells. Int J Cancer 85(3) pp.446-50

Carlier MF, Pantaloni D., 1986. Direct evidence for ADP-Pi-F-actin as the major intermediate in ATP-actin polymerization. Rate of dissociation of Pi from actin filaments. Biochemistry 25(24):7789-92

Carlier MF, Pantaloni D, Evans JA, Lambooy PK, Korn ED, Webb MR., 1988. The hydrolysis of ATP that accompanies actin polymerization is essentially irreversible. FEBS Lett 235(1-2):211-4

Carlier MF, Nioche P, Broutin-L'Hermite I, Boujemaa R, Le Clainche C, Egile C, Garbay C, Ducruix A, Sansonetti P, Pantaloni D., 2000. GRB2 links signaling to actin assembly by enhancing interaction of neural Wiskott-Aldrich syndrome protein (N-WASp) with actin-related protein (ARP2/3) complex. J Biol Chem 275(29) pp.21946-52

Carpten J, Nupponen N, Isaacs S, Sood R, Robbins C, Xu J, Faruque M, Moses T, Ewing C, Gillanders E, Hu P, Bujnovszky P, Makalowska I, Baffoe-Bonnie A, Faith D, Smith J, Stephan D, Wiley K, Brownstein M, Gildea D, Kelly B, Jenkins R, Hostetter G, Matikainen M, Schleutker J, Klinger K, Connors T, Xiang Y, Wang Z, De Marzo A, Papadopoulos N, Kallioniemi OP, Burk R, Meyers D, Grönberg H, Meltzer P, Silverman R, Bailey-Wilson J, Walsh P, Isaacs W, Trent J,. 2002. Germline mutations in the ribonuclease L gene in families showing linkage with HPC1. Nat Genet 30(2) pp.181-4

Castro E, Eeles R., 2012. The role of BRCA1 and BRCA2 in prostate cancer. Asian J Androl 14(3):409-14

Cavallaro U, Christofori G. 2004. Cell adhesion and signalling by cadherins and Ig-CAMs in cancer. Nat Rev Cancer 4(2) pp.118-32

Chaffer CL., Weinberg RA. 2011. A perspective on cancer cell metastasis. Science 331(6024) pp.1559-64

Chambers AF., Groom AC., MacDonald IC. 2002. Dissemination and growth of cancer cells in metastatic sites. Nat Rev Cancer 2(8) pp.563-72

Chen XQ, Tan I, Ng CH, Hall C, Lim L, Leung T., 2002. Characterization of RhoA-binding kinase ROKalpha implication of the pleckstrin homology domain in ROKalpha function using region-specific antibodies. J Biol Chem 277(15)pp.12680-8

Chen, Z., Borek, D., Padrick, S.B., Gomez, T.S., Metlagel, Z., Ismail, A.M., Umetani, J., Billadeau, D.D., Otwinowski, Z., Rosen, M.K. 2010. Structure and control of the actin regulatory WAVE complex. Nature 468(7323) pp. 533-538

Cher, M,L., 2001. Mechanisms governing bone metastasis in prostate cancer. Curr Opin Urol 11(5) pp.483-8

Cho YJ, Zhang B, Kaartinen V, Haataja L, de Curtis I, Groffen J, Heisterkamp N., 2005. Generation of rac3 null mutant mice: role of Rac3 in Bcr/Abl-caused lymphoblastic leukemia. Mol Cell Biol 25(13) pp.5777-85

Clark EA., Golub TR., Lander ES., Hynes RO., 2000. Genomic analysis of metastasis reveals an essential role for RhoC. Nature 406(6795) pp.532-5

Clarke NW, Hart CA, Brown MD, 2009. Molecular mechanism of metastasis in prostate cancer. Asian J Androl 11(1) pp.57-67

Cory GO, Cramer R, Blanchoin L, Ridley AJ., 2003. Phosphorylation of the WASP-VCA domain increases its affinity for the Arp2/3 complex and enhances actin polymerization by WASP. Mol Cell 11(5)pp.1229-39

Cory GO, Garg R, Cramer R, Ridley AJ., 2002. Phosphorylation of tyrosine 291 enhances the ability of WASp to stimulate actin polymerization and filopodium formation. Wiskott-Aldrich Syndrome protein. J Biol Chem 277(47) pp.45115-21

Cress AE., Rabinovitz I., Zhu W., Nagle RB., 1995. The alpha 6 beta 1 and alpha 6 beta 4 integrins in human prostate cancer progression. Cancer Metastasis Rev 14(3) pp.219-28

Croft DR, Sahai E, Mavria G, Li S, Tsai J, Lee WM, Marshall CJ, Olson MF., 2004. Conditional ROCK activation in vivo induces tumor cell dissemination and angiogenesis. Cancer Res 64(24):8994-9001

Croft DR, Olson MF., 2006. The Rho GTPase effector ROCK regulates cyclin A, cyclin D1, and p27Kip1 levels by distinct mechanisms. Mol Cell Biol 26(12):4612-27

D'Amico AV, Whittington R, Malkowicz SB, Schultz D, Blank K, Broderick GA, Tomaszewski JE, Renshaw AA, Kaplan I, Beard CJ, Wein A., 1998. Biochemical outcome after radical prostatectomy, external beam radiation therapy, or interstitial radiation therapy for clinically localized prostate cancer. JAMA 280(11) :969-74

Davidson AJ, Insall RH, 2011. Actin-based motility: WAVE regulatory complex structure reopens old SCARs. Curr Biol 21(2) pp.R66-8

Davies G, Martin TA, Ye L, Lewis-Russell JM, Mason MD, Jiang WG., 2008. Phospholipase-C gamma-1 (PLCgamma-1) is critical in hepatocyte growth factor induced in vitro invasion and migration without affecting the growth of prostate cancer cells. Urol Oncol 26(4) pp.386-91

Davies SP, Reddy H, Caivano M, Cohen P., 2000. Specificity and mechanism of action of some commonly used protein kinase inhibitors. Biochem 351(Pt 1) pp.95-105

de la Fuente MA, Sasahara Y, Calamito M, Antón IM, Elkhal A, Gallego MD, Suresh K, Siminovitch K, Ochs HD, Anderson KC, Rosen FS, Geha RS, Ramesh N, 2007. WIP is a chaperone for Wiskott-Aldrich syndrome protein (WASP). Proc Natl Acad Sci USA 104(3) pp.926-31

DeChello, L, M., Greorio, D,I., Samociuk, H., 2006. Race-specific geography of prostate cancer incidence. Int J Health Geogr 18(5) pp.59

DeMarzo, A,M., Nelson, W,G., Isaacs, W,B., Epstein, J,I., 2003. Pathological and molecular aspects of prostate cancer. Lancet 15;361(9361) pp.955-64

Deryugina EI, Quigley JP., 2006. Matrix metalloproteinases and tumour metastasis. Cancer Metastasis Rev 25(1) pp.9-34

Desgrosellier JS and Cheresh DA., 2010. Integrins in cancer: biological implications and therapeutic opportunities. Nat Rev Cancer 10(1) pp.9-22

Denmeade SR and Isaacs JT., 2002. A history of prostate cancer treatment. Nat Rev Cancer 2 pp.389-396

Derry, J.M., Ochs, H.D., Francke, U. 1994. Isolation of a novel gene mutated in Wiskott-Alrich syndrome. Cell 78(4)pp. 635-644

Dreckhahn, D., Pollard, T.D. 1986. Elongation of actin filaments is a diffusion-limited reaction at the barbed end and is accelerated by inert macromolecules. J Biol Chem. 261(27) pp.12754-12758.

Eden S., Rohatgi R., Podtelejnikov AV., Mann M., Kirschner MW., 2002. Mechanism of regulation of WAVE1-induced actin nucleation by Rac1 and Nck. Nature 418(6899) pp.790-3

Edwards DC, Sanders LC, Bokoch GM, Gill GN., 1999. Activation of LIM-kinase by Pak1 couples Rac/Cdc42 GTPase signalling to actin cytoskeletal dynamics. Nat Cell Biol 1(5) pp.253-9

Ellerbroek, S,M., Wennerberg, K., Burridge, K., 2003. Serine phosphorylation negatively regulates RhoA in vivo. J Biol Chem 278(21) pp.19023-31

Escudero-Esparza A, Jiang WG, Martin TA., 2012. Claudin-5 is involved in breast cancer cell motility through the N-WASP and ROCK singalling pathways. J Exp Clin Cancer Res 4;31:43

Etienne-Manneville, S., Hall, A., 2002. Rho GTPases in cell biology. Nature 420(6916) pp.629-35

Feldman BJ., Feldman D., 2001. The development of androgen-independent prostate cancer. Nat Rev Cancer 1(1) pp.34-45

Fernando HS., Davies SR., Chhabra A., Watkins G., Douglas-Jones A., Kynaston HG., Mansel RE., Jiang WG., 2007. Expression of the WASP verprolin-homologues (WAVE members) in human breast cancer. Oncology 73(5-6) pp.376-383

Fernando HS, Sanders AJ, Kynaston HG, Jiang WG., 2008. WAVE1 is associated with invasiveness and growth of prostate cancer cells. J Urol 180(4) pp.1515-21

Fernando HS., Kynaston HG., Jiang WG., 2009. WASP and WAVE proteins: Vital intrinsic regulators of cell motility and their role in cancer (Review). Int J Mol Med 23(2) pp.141-8

Fernando HS, Sanders AJ, Kynaston HG, Jiang WG., 2010. WAVE3 is associated with invasiveness in prostate cancer cells. Urol Oncol 28(3) pp.320-7

Fidler I., 1970. Metastasis: Quantitative Analysis of Distribution and Fate or Tumour Emboli Labeled With ^{123}I-5-Iodo-2'-deoxyuridine 2,3. J. Natl. Cancer Inst. 45(4), pp.773-82

Fidler IJ., 2003. The pathogenesis of cancer metastasis: the 'seed and soil' hypothesis revisited. Nat Rev Cancer 3(6) pp.453-8

Fritz G, Just I, Kaina B., 1999. Rho GTPases are over-expressed in human tumors. Int J Cancer. 81(5) pp.682-7

Fukuoka M, Suetsugu S, Miki H, Fukami K, Endo T, Takenawa T., 2001. A novel neural Wiskott-Aldrich syndrome protein (N-WASP) binding protein, WISH, induces Arp2/3 complex activation independent of Cdc42. J Cell Biol 152(3) pp.471-82

Furumatsu T, Matsumoto-Ogawa E, Tanaka T, Lu Z, Ozaki T., 2013. ROCK inhibition enhances aggrecan deposition and suppresses matrix metalloproteinase-3 production in human articular chondrocytes. Connect Tissue Res

Gao D., Vahdat LT., Wong S., Chang JC., Mittal V. 2012. Microenvironment regulation of epithelial-mesenchymal transitions in cancer. Cancer Res 72(19) pp.4883-9

García E, Jones GE, Machesky LM, Antón IM., 2012. WIP: WASP-interacting proteins at invadopodia and podosomes. Eur J Cell Biol 91(11-12) pp.869-77

Gautreau A, Ho HY, Li J, Steen H, Gygi SP, Kirschner MW., 2004. Purification and architecture of the ubiquitous Wave complex. Proc Natl Acad Sci U S A 101(13) pp.4379-83

Gavrilov D., Kenzior O., Evans M., Calaluce R., Folk WR., 2001. Expression of urokinase plasminogen activator and receptor in conjunction with the ets family and AP-1 complex transcription factors in high grade prostate cancers. Eur J Cancer 37(8) pp.1033-40

Giri A, Bajpai S, Trenton N, Jayatilaka H, Longmore GD, Wirtz D., 2013. The Arp2/3 complex mediates multigeneration dendritic protrusions for efficient 3-dimensional cancer cell migration. FASEB J 27(10)pp.4089-99

Gleason, D,F., Mellinger, G,T., 1974. Prediction of prognosis for prostatic adenocarcinoma by combined histological grading and clinical staging. J Urol 111(1) pp.58-64

Gleason, D,F., 1992. Histological grading of prostate cancer: a perspective. Hum Pathol 23(3) pp.273-9

Gligorijevic B, Wyckoff J, Yamaguchi H, Wang Y, Roussos ET, Condeelis J., 2012. N-WASP-mediated invadopodium formation is involved in intravasation and lung metastasis of mammary tumors. J Cell Sci 125(Pt 3) pp.724-34

Goel HL., Breen M., Zhang J., Das I., Aznavoorian-Cheshire S., Greenberg NM., Elgavish A., Languino LR., 2005. B1A integrin expression is required for type 1 insulin-like growth factor receptor mitogenic and transforming activites and localization to focal contacts. Cancer Res 65(15) pp.6692-700

Goel HL., Li J., Kogan S., Languino LR., 2008. Integrins in prostate cancer progression. Endocr Relat Cancer 15(3) pp.657-64

Goel HL., Alam N., Johnson IN., Languino LR., 2009. Integrin signalling aberrations in prostate cancer. 1(3) pp.221-220

Goley ED, Welch MD., 2006. The ARP2/3 complex:
an actin nucleator comes of age. Nat Rev Mol Cell Biol 7(10) pp.713-26

Gómez del Pulgar T., Benitah SA., Valerón PF., Espina C., Lacal JC., 2005. Rho GTPase expression in tumourigenesis: evidence for a significant risk. Bioessays 27(6) pp.602-13

Gralow, J,R., Biermann, J,S., Farook,i A., Fornier, M,N., Gagel, R,F., Kumar, R,N., Shapiro, C,L., Shields, A., Smith, M,R., Srinivas, S., Van Poznak, C,H., 2009. NCCN Task Force Report: Bone Health in Cancer Care. J Natl Compr Canc Netw Suppl 3:S1-32; quiz S33-5

Greenman C, Stephens P, Smith R et al., 2007. Patterns of somatic mutation in human cancer genomes. Nature 446(7132):153-8

Grönberg H., 2003. Prostate cancer epidemiology. Lancet. 361 pp.859-864

Guinamard R, Aspenström P, Fougereau M, Chavrier P, Guillemot JC., 1998. Tyrosine phosphorylation of the Wiskott-Aldrich syndrome protein by Lyn and Btk is regulated by CDC42. FEBS Lett 434(3) pp.431-6

Gupta GP, Massaqué J. 2006. Cancer metastasis: building a framework. Cell 127(4) pp.679-95

Hall A., 1998. Rho GTPases and the actin cytoskeleton. Science 279(5350) pp.509-14

Harris TJ, Tepass U., 2010. Adherens junctions: from molecules to morphogenesis. Nat Rev Mol Cell Biol 11(7) pp.502-14

Hart CA., Brown M., Bagley S., Sharrard M., Clarke NW., 2005. Invasive characteristics of human prostatic epithelial cells: understanding the metastatic process. Br J Cancer 92(3) pp.503-12

Hart, M,J., Maru, Y., Leonard, D., Witte, O,N., Evans, T., Cerione, R,A., 1992. A GDP dissociation inhibitor that serves as a GTPase inhibitor for the Ras-like protein CDC42Hs. Science 258(5083) pp.812-5

Hartwig, J.H. et al. 1995. Thrombin receptor ligation and activated Rac uncap filament barbed ends through phosphoinositide synthesis in permeabilized platelets. Cell 82, 643-653

Haythorn MR, Ablin RJ., 2001. Prostate-specific antigen testing across the spectrum of prostate cancer. Biomark Med 5(4):515-26

Higgs HN, Pollard TD., 1999. Regulation of actin polymerisation by Arp2/3 and WASp/Scar proteins. J Biol Chem 274(46) pp.32531-4

Higgs HN, Pollard TD., 2000. Activation by Cdc42 and PIP(2) of Wiskott-Aldrich syndrome protein (WASp) stimulates actin nucleation by Arp2/3 complex. J Cell Biol. 150(6), pp. 1311-1320

Ho HY, Rohatgi R, Ma L, Kirschner MW., 2001. CR16 forms a complex with N-WASP in brain and is a novel member of a conserved proline-rich actin-binding protein family. Proc Natl Acad Sci USA 98(20) pp.11306-11

Hossein NM., Boyd DD., Hollas WJ., Mazar A., Henkin J., Chung LW., 1991. Involvement of urokinase and its receptor in the invasiveness of human prostatic carcinoma cell lines. Cancer Commun 3(8) pp.255-64

Huang M., Prendergast GC., 2006. RhoB in cancer suppression. Histol Histopathol 21(2) pp.213-8

Huggins, C; Hodges,C,V., 1941. Studies on prostate cancer. 1. The effect of castration, estrogen and of androgen injection on serum phosphatases in metastatic carcinoma of the prostate. Cancer Res 1 pp.293-297

Humprey, P,A., 2004. Gleason grading and prognostic factors in carcinoma of the prostate. Mol Pathol 17(3) pp.292-306

Hwang SL., Hong YR., Sy WD., Lieu AS., Lin CL., Lee KS., Howng SL., 2004. Rac1 gene mutations in human brain tumours. Eur J Surg Oncol. 30(1) pp.68-72

Ichetovkin I, Grant W, Condeelis J. 2002. Cofilin produces newly polymerized actin filaments that are preferred for dendritic nucleation by the Arp2/3 complex. Curr Biol. 12, 79-84

Imai K., Nonoyama S, Ochs HD., 2003. WASP (Wiskott-Aldrich syndrome protein) gene mutations and phenotype. Curr Opin Allergy Clin Immunol 3(6) pp.427-36

Insall RH[1], Machesky LM., 2009. Actin dynamics at the leading edge: from simple machinery to complex networks. Dev Cell 17(3) pp.310-22

Ishizaki T, Uehata M, Tamechiuka I, Keel J, Nomomura K, Maekawa M, Narumiya S., 2000. Pharmacological properties of Y-27632, a specific inhibitor of rho-associated kinases. Mol Pharmacol 57(5):976-83

Iwaya K., Oikawa K., Semba S., Tsuchiya B., Mukai Y., Otsubo T., Nagao T., Izumi M., Kuroda M., Domoto H., Mukai K., 2007. Correlation between liver metastasis of the colocalization of actin-related protein 2 and 3 complex and WAVE2 in colorectal carcinoma. Cancer Sci 98(7) pp.992-999.

Jacob K., Webber M., Benayahu D., Kleinman HK., 1999. Ostenectin promotes prostate cancer cell migration and invasion: a possible mechanism for metastasis to bone. Cancer Res 59(17) pp.4453-7

Jośko J, Mazurek M., 2004. Transcription factors having impact on vascular endothelial growth factor (VEGF) gene expression in angiogenesis. Med Sci Monit 10(4) pp.RA89-98

Joyce JA., Pollard JW. 2008. Microenvironment regulation of metastasis. Nat Rev Cancer 9(4) pp.2239-52

Kallergi G, Konstantinidis G, Markomanolaki H, Papadaki MA, Mavroudis D, Stournaras C, Georgoulias V, Agelaki S., 2013. Apoptotic Circulating Tumor Cells (CTCs) in early and metastatic breast cancer patients. Mol Cancer Ther 18

Kato M, Miki H, Kurita S, Endo T, Nakagawa H, Miyamoto S, Takenawa T., 2002. WICH,a novel verprolin homology domain containing protein that functions

cooperatively with N-WASP in actin-microspike formation. Biochem Biophys Res Commun 291(1) pp.41-7

Katoh, K., Kano, Y., Noda, Y., 2011 Rho-associated kinase-dependent contraction of stress fibres and the organization of focal adhesions. J R Soc Interface 8(56) pp.305-11

Kawada K[1], Hasegawa S, Murakami T, Itatani Y, Hosogi H, Sonoshita M, Kitamura T, Fujishita T, Iwamoto M, Matsumoto T, Matsusue R, Hida K, Akiyama G, Okoshi K, Yamada M, Kawamura J, Taketo MM, Sakai Y., 2011. Molecular mechanisms of liver metastasis. Int J Clin Oncol 16(5) pp.464-72

Kessler B, Albertson P., 2003. The natural history of prostate cancer. Urol Clin North Am 30 pp.219-6

Khan, N., Adhami, V, M., Mukhtar, H., 2009. Green tea polyphenols in chemopreventation of prostate cancer: preclinical and clinical studies. Nutr Cancer 61(6) pp.836-41

Kim AS, Kakalis LT, Abdul-Manan N, Liu GA, Rosen MK., 2000. Autoinhibition and activation mechanisms of the Wiskott-Aldrich syndrome protein. Nature 404(6774) pp.151-8

Kim Y., Sung JY., Ceglia I., Lee KW., Ahn JH., Halford JM., Kim AM., Kwak SP., Park JB., Ho Ryu S., Schenck A., Bardoni B., Scott JD., Nairn AC., Greengard P., 2006. Phosphorylation of WAVE1 regulates actin polymerization and dendritic spine morphology. Nature 442(7104) pp.814-7

Kim H., He Y., Yang I., Zeng Y., Kim Y., Seo YW., Murnane MJ., Jung C., Lee JH., Min JJ., Kwon DD., Kim KK., Lu Q., Kim K., 2012. δ-Catenin promotes E-

cadherin processing and activates β-catenin-mediated signalling: Implications on human prostate cancer progression. Biochim Biophys Acta 1822(4) pp.509-21

Kim, J., 2008. Protective effects of Asian dietary items on cancers – soy and ginseng. Asian Pac J Cancer Prev 9(4) pp.543-8

Kimura K, Ito M, Amano M, Chihara K, Fukata Y, Nakafuku M, Yamamori B, Feng J, Nakano T, Okawa K, Iwamatsu A, Kaibuchi K., 1996. Regulation of myosin phosphatase by Rho and Rho-associated kinase (Rho-kinase). Science 273(5272):245-8

Kobayashi K, Kuroda S, Fukata M, Nakamura T, Nagase T, Nomura N, Matsuura Y, Yoshida-Kubomura N, Iwamatsu A, Kaibuchi K., 1998. p140Sra-1 (specifically Rac1-associated protein) is a novel specific target for Rac1 small GTPase. J Biol Chem 273(1):291-5

Koronakis V., Hume PJ., Humphreys D., Liu T., Hørning O., Jensen ON., McGhie EJ., 2011. WAVE regulatory complex activaton by cooperating GTPases Arf and Rac1. Proc Natl Acad Sci USA 108(35) pp.14449-54

Kurisu S., Suetsugu S., Yamazaki D., Yamaguchi H., Takenawa T., 2005. Rac-WAVE2 signalling is involved in the invasive and metastatic phenotypes of murine melanoma cells. Oncogene 24(8) pp.1309-19

Kurisu,S., Takenawa, T. 2009. The WASP and WAVE family proteins. Genome Biol 10(6):226

Lambrechts, A., Troys, V., Ampe, C. 2004. The actin cytoskeleton in normal and pathological cell motility. Int J Biochem Cell Biol 36(10) pp. 1890-1909

Lane J, Martin TA, Watkins G, Mansel RE, Jiang WG., 2008. The expression and prognostic value of ROCK I and ROCK II and their role in human breast cancer. Int J Oncol 33(3):585-93

Langley RR., Fidler IJ. The seed and soil hypothesis revisited – the role of tumor-stroma interactions in metastasis to different organs. Intl J Cancer 128(11) pp.2527-35

Lauffenburger DA, Horwitz AF, 1996. Cell Migration: A physically integrated molecular process 84(3) pp.359-69

Lecouvet FE, Geukens D, Stainier A, Jamar F, Jamart J, d'Othée BJ, Therasse P, Vande Berg B, Tombal B., 2007. Magnetic resonance imaging of the axial skeleton for detecting bone metastases in patients with high-risk prostate cancer: diagnostic and cost-effectiveness and comparison with current detection strategies. J Clin Oncol 25(22)pp.3281-7

Lee HH, Chang ZF., 2008. Regulation of RhoA-dependent ROCKII activation by Shp2. J Cell Biol 181(6) pp.999-1012

Lee HH, Tien SC, Jou TS, Chang YC, Jhong JG, Chang ZF., 2010. Src-dependent phosphorylation of ROCK participates in regulation of focal adhesion dynamics. J Cell Sci 123(Pt 19):3368-77

Lehr JE., Pienta KJ., 1998. Preferential adhesion of prostate cancer cells to a human bone marrow endothelial cell line. J Natl Cancer Inst 90(2) pp.118-23

Leng Y., Zhang J., Badour K., Arpaia E., Freeman S., Cheung P., Siu M., Siminovitch K., 2005. Abelson-interactor-1 promotes WAVE2 membrane

translocation and Abelson-mediated tyrosine phosphorylation required for WAVE2 activation. Proc Natl Acad Sci USA 102(4) pp.1098-103

Leonard D, Hart MJ, Platko JV, Eva A, Henzel W, Evans T, Cerione RA., 1992. The identification and characterization of a GDP-dissociation inhibitor (GDI) for the CDC42Hs protein. J Biol Chem 267(32):22860-8

Li Y., Cozzi PJ., 2007. Targeting uPA/uPAR in prostate cancer. Cancer Treat Rev 33(6) pp.521-7

Liang SL, Quirk D, Zhou A, 2006. Rnase L: its biological roles and regulation. IUBMB Life 58(9) pp.508-14

Lichtinghagen R., Musholt PB., Lein M., Römer A., Rudolph B., Kristiansen G., Hauptomann S., Schnorr D., Loening SA., Jung K., 2002. Different mRNA and protein expression of matrix metalloproteinases 2 and 9 and tissue inhibitor of metalloproteinases 1 in benign and malignant prostate tissue. Eur Urol 42(4) pp.398-406

Liotta LA., 1986. Tumor invasion and metastases--role of the extracellular matrix: Rhoads Memorial Award lecture. Cancer Res 46(1) pp.1-7

Lock FE, Hotchin NA., 2009. Distinct roles for ROCK1 and ROCK2 in the regulation of keratinocyte differentiation. PLoS One 4(12):e8190

Lokeshwar BL., Selzer MG., Block NL., Gunja-Smith Z., 1993. Secretion of matrix metalloproteinases and their inhibitors (tissue inhibitor of metalloproteinases) by human prostate in explants cultures: reduced tissue inhibitor of metalloproteinases secretion by malignant tissues. Cancer Res 53(19) pp.4493-8

Lozano E., Betson M., Braga VM., 2003. Tumour progression: Small GTPases and loss of cell-cell adhesion. Bioessays 25(5) pp.452-63

Ma L., Teruya-Feldstein J., Weinberg RA., 2007. Tumour invasion and metastasis intiated by micro-RNA-10b in breast cancer. Nature 449(7163) pp.682-8

Machesky LM, Insall RH., 1998. Scar1 and the related Wiskott-Aldrich syndrome protein, WASP, regulate the actin cytoskeleton through the Arp2/3 complex. Curr Biol 8(25) pp.1347-56.

Machesky LM, Gould KL., 1999. The Arp2/3 complex: a multifunctional actin organizer. Current Opinion on Cell Biology. 11(1) pp.117-21

Machesky LM, Mullins RD, Higgs HN, Kaiser DA, Blanchoin L, May RC, Hall ME, Pollard TD., 1999. Scar, a WASp-related protein, activates nucleation of actin filaments by the Arp2/3 complex. Proc Natl Acad Sci USA 96(7) pp.3739-44

Makridakis NM, Ross RK, Pike MC, Crocitto LE, Kolonel LN, Pearce CL, Henderson BE, Reichardt JK., 1999. Association of mis-sense substitution in SRD5A2 gene with prostate cancer in African-American and Hispanic men in Los Angeles, USA. Lancet 354(9183):975-8

Manes T., Zheng DQ., Tognin S., Woodard AS., Marchisio PC., Languino LR., 2003. $\alpha_v\beta_3$ integrin expression upregulates cdc2, which modulates cell migration. J Cell Biol 161(4) pp.817-826

Martin TA, Pereira G, Watkins G, Mansel RE, Jiang WG., 2008. N-WASP is a putative tumour suppressor in breast cancer cells, in vitro and in vivo, and is associated with clinical outcome in patients with breast cancer. Clin Exp Metastasis 25(2) pp.97-108

Martinez-Quiles N, Rohatgi R, Antón IM, Medina M, Saville SP, Miki H, Yamaguchi H, Takenawa T, Hartwig JH, Geha RS, Ramesh N., 2001. WIP regulates N-WASP-mediated actin polymerization and filopodium formation. Nat Cell Biol 3(5) pp.484-91

Mattila PK, Lappalainen P, 2008. Filopodia: molecular architecture and cellular functions. Nat Rev Mol Cell Biol 9(6) pp.446-54

McNeal, J, E., 1988. Normal histology of the prostate. American Journal of Surgical Pathology 12, 619 – 633

Mediero A, Guzmán-Aranquez A, Crooke A, Peral A, Pintor J., 2008. Corneal re-epithelialization stimulated by diadenosine polyphosphates recruits RhoA/ROCK and ERK1/2 pathways. Invest Ophthalmol Vis Sci 49(11): 4982-92

Merajver SD., Usmani SZ., 2005. Multifaceted role of Rho proteins in angiogenesis. J Mammary Gland Biol Neoplasia 10(4) pp.291-8

Miki H., Miura K., Takenawa T., 1996. N-WASP, a novel actin-depolymerizing protein, regulates the cortical cytoskeletal rearrangement in a PIP2-dependent manner downstream of tyrosine kinases. EMBO J 15(19) pp.5326-35

Miki H., Suetsugu S., Takenawa T., 1998. WAVE, a novel WASP-family protein involved in actin reorganization induced by Rac. EMBO J 17(23) pp.6932-41

Miki H, Yamaguchi H, Suetsugu S, Takenawa T, 2000. IRSp53 is an essential intermediate between Rac and WAVE in the regulation of membrane ruffling. Nature 408(6813) pp.732-5

Mira JP., Benard V., Groffen J., Sanders LC., Knaus UG., 2000. Endogenous, hyperactive Rac3 controls proliferation of breast cancer cells by a p21-activated kinase-dependent pathway. Proc Natl Acad Sci U S A 97(1) pp.185-9

Mizutani K[1], Koike D, Suetsugu S, Takenawa T., 2005. WAVE3 functions as a negative regulator of LDOC1. J Biochem 138(5) pp. 639-46

Mohan, R., Schellhammer, P,F., 2011. Treatment options for localised prostate cancer. Am Fam Physician 84(4) pp.413-20

Monroe KR, Yu MC, Kolonel LN, et al. Evidence of an X-linked or recessive genetic component to prostate cancer risk. Nat Med 1995; 1: 827–29.

Montague R., Hart CA., George NJ., Ramani VA., Brown MD., Clarke NW., 2004. Differential inhibition of invasion and proliferation by bisphosphonates: anti-metastatic potential of Zoledronic acid in prostate cancer. Eur Urol 46(3)pp.389-401

Mulhbacher J, St-Pierre P, Lafontaine DA., 2010. Therapeutic applications of ribozymes and riboswitches. Curr Opin Pharmacol 10(5):551-6

Mullins RD, Heuser JA, Pollard TD., 1998. The interaction of Arp2/3 complex with actin: nucleation, high affinity pointed end capping, and formation of branching networks of filaments. Proc Natl Acad Sci USA 95(11):6181-6

Nabha SM., dos Santos EB., Yamamoto HA., Belizi A., Doug Z., Heng H., Saliganan A., Sabbota A., Bonfil RD., Cher ML., 2008. Bone marrow stromal cells enhance prostate cancer cell invasion through type I collagen in an MMP-12 dependent manner. Int J Cancer 122(11) pp.2482-90

Nagakawa O., Murakami K., Yamaura T., Fujiuchi Y., Murata J., Fuse H., Saiki I., 2000. Expression of membrane-type 1 matrix metalloproteinase (MT1-MMP) on prostate cancer cell lines. Cancer Lett 155(2) pp.173-9

Nakanishi H., Orita S., Kaibuchi K., Miura K., Miki H., Takenawa T., Takai Y., 1994. Kinetic properties of Ash/Grb2-interacting GDP/GTP exchange protein. Biochem Biophys Res Commun 198(3) pp.1255-61

Narain, V., Cher, M,L., Wood, D,P., 2002. Prostate cancer diagnosis, staging and survival. Cancer Metastasis Rev 21(1) pp.17-27

Nesbitt S., Nesbit A., Helfrich M., Horton M. Biochemical characterization of human osteoclast integrins. Osteoclasts express alpha v beta 3, alpha 2 beta 1, and alpha v beta 1 integrins. J Biol Chem 268(22) pp.16737-45

Nobes CD, Hall A., 1995. Rho, rac, and cdc42 GTPases regulate the assembly of multimolecular focal complexes associated with actin stress fibers, lamellipodia, and filopodia. Cell 81(1) pp.53-62

Nolen BJ, Tomasevic N, Russell A, Pierce DW, Jia Z, McCormick CD, Hartman J, Sakowicz R, Pollard TD., 2009. Characterization of two classes of small molecule inhibitors of Arp2/3 complex. Nature 460(7258):1031-4

Oesterling, J, E., Jacobsen, S, J., Chute, C, G., Guess, H, A., Girman, C, J., Panser, L, A., Lieber, M, M., 1993. Serum prostate-specific antigen in a community-based population of healthy men. Establishment of age-specific reference ranges. JAMA 270(7) pp.860-4

Ohashi K, Nagata K, Maekawa M, Ishizaki T, Narumiya S, Mizuno K., 2000. Rho-associated kinase ROCK activates LIM-kinase 1 by phosphorylation at threonine 508 within the activation loop. J Biol Chem 275(5):3577-82

Oikawa T., Yamaguchi H., Itoh T., Kato M., Ijuin T., Yamazaki D., Suetsugu S., Takenawa T., 2004. PtdIns(3,4,5)P3 binding is necessary for WAVE2-induced formation of lamellipodia. Nat Cell Biol 6(5) pp.420-6

Olofsson, B., 1999. Rho guanine dissociation inhibitors: pivotal molecules in cellular signalling. Cell Signal 11(8) pp.545-54

Orange JS, Stone KD, Turvey SE, Krzewski K., 2004. The Wiskott-Aldrich syndrome. Cell Mol Life Sci 61(18) pp.2361-85

Otsubo T, Iwaya K, Mukai Y, Mizokami Y, Serizawa H, Matsuoka T, Mukai K., 2004. Involvement of Arp2/3 complex in the process of colorectal carcinogenesis. Mod Pathol 17(4):461-7

Paget S., 1889. The distribution of secondary growths in cancer of the breast. The Lancet 133(3421) pp.571-3

Palmer, T,D., Ashby, W,J., Lewis, J,D., Zijlstra, A., 2011. Targeting tumour cell motility to prevent metastasis. Adv Drug Deliv Rev 63(8) pp.568-81

Papadopoulou N[1], Charalampopoulos I, Alevizopoulos K, Gravanis A, Stournaras C., 2008. Rho/ROCK/actin signaling regulates membrane androgen receptor induced apoptosis in prostate cancer cells. Exp Cell Res 314(17) pp. 3162-74

Parri, M., Chiarugi, P., 2010. Rac and Rho GTPases in cancer cell motility control. Cell Commun Signal 8:23

Payne, H., Mason, M., 2011. Androgen deprivation therapy as adjuvant/neoadjuvant to radiotherapy for high-risk localised and locally advanced prostate cancer: recent developments. Br J Cancer 105(11) pp.1628-34

Pearson WR, Wood T, Zhang Z, Miller W., 1997. Comparison of DNA sequences with protein sequences. Genomics 46(1):24-36

Peled A., Petit I., Kollet O., Magid M., Ponomaryov T., Byk T., Nagler A., Ben-Hur H., Many A., Shultz L., Lider O., Alon R., Zipori D., Lapidot T., 1999. Dependence of human stem cell engraftment and repopulation of NOD/SCID mice on CXCR4. Science 283(5403) pp.845-8

Peterson JR, Bickford LC, Morgan D, Kim AS, Ouerfelli O, Kirschner MW, Rosen MK., 2004. Chemical inhibition of N-WASP by stabilization of a native autoinhibited conformation. Nat Struct Mol Biol 11(8)pp.747-55

Petrie RJ[1], Yamada KM., 2012. At the leading edge of three-dimensional cell migration. J Cell Sci 125(Pt 24) pp.5917-26

Pollard, T,D., 1986. Rate constants for the reactions of ATP- and ADP-actin with the ends of actin filaments. J Cell Biol 103(6 Pt 2) pp.2747-54

Pollard TD, Beltzner CC., 2002. Structure and function of the Arp2/3 complex. Curr Opin Struct Biol 12(6) pp.768-74

Pollard TD, Blanchoin L, Mullins RD., 2000. Molecular mechanisms controlling actin filament dynamics in nonmuscle cells. Annu Rev Biophys Biomol Struct 29:545-76

Pollard TD, Borisy GG., 2003. Cellular motility driven by assembly and disassembly of actin filaments. Cell 112(4):453-65

Potosky AL, Miller BA, Albertson PC, Kramer BS., 1995. The role of increasing detection in the rising incidence of prostate cancer. Journal of the American Medical Association. 273(7) pp. 548-52

Powell IJ: Prostate cancer in the African American: is this a different disease? Semin Urol Oncol 1998, 16(4):221-226.

Prehoda, K, E., Scoot, J, A., Mullins, R, D., Lim, W, A. 2000. Integration of multiple signals through cooperative regulation of the N-WASP-Arp2/3 complex. Science 290(5492), pp.801-806.

Quinn, M., Babb, P., 2002. Patterns and trends in prostate cancer incidence, survival, prevalence and mortality. Part I: international comparisons. BJU Int 90(2) pp.162-73

Ragde, H., Grado, G,L., Nadir, B., Elgamal, A,A., 2000. Modern prostate brachytherapy. CA Cancer J Clin. 50(6) pp.380-93

Rajan R., Vanderslice R., Kapur S., Lynch J., Thompson R., Djakiew D., 1996. Epidermal growth factor (EGF) promotes chemomigration of a human prostate tumour cell line, and EGF immunoreactive proteins are present at sites of metastasis in the stroma of lymph nodes and medullary bone. Prostate 28(1) pp.1-9

Ramesh, N., Anton, I. M., Hartwig, J.H. and Geha, R.S. 1997. WIP, a protein associated with Wiskott-Aldrich syndrome protein, induces actin polymerisation and redistribution in lymphoid cells. Proc Natl Acad Sci USA. 94, pp.14671-14676

Rauhala HE, Teppo S, Niemelä S, Kallioniemi A., 2013. Silencing of the ARP2/3 complex disturbs pancreatic cancer cell migration. Anticancer Res 33(1):45-52

Ridley, A,J., Allen, W,E., Peppelenbosch, M., Jones, G,E., 1999. Rho family proteins and cell migration. Biochem Soc Symp 65 pp.111-23

Ridley, A,J., Schwartz, M,A., Burridge, K., Firtel, R,A., Ginsberg, M,H., Borisy, G., Parsons, J,T., Horwitz, A,R., 2003. Cell migration: integrating signals from front to back. Science 302(5651) pp.1704-9

Ridley, AJ., 2006. Rho GTPases and actin dynamics in membrane protrusions and vesicle traffricking. Trends Cell Biol 16(10) pp.522-529

Ridley, A.J. 2011. Life at the leading edge. Cell 145(7) pp.1012-1022

Riento K, Ridley AJ., 2003. Rocks: multifunctional kinases in cell behaviour. Nat Rev Mol Cell Biol 4(6):446-56

Ritchie CK., Andrews LR., Thomas KG., Tindall DJ., Fitzpatrick LA., 1997. The effects of growth factors associated with osteoblasts on prostate carcinoma proliferation and chemotaxis: implications for the development of metastatic disease. Endocrinology 138(3) pp.1145-50

Rivero-Lezcano OM., Marcilla A., Sameshima JH., Robbins KC., 1995. Wiskott-Aldrich syndrome protein physically associates with Nck through Src homology 3 domains. Mol Cell Biol 15(10) pp.5725-31

Rohatgi R, Ho HY, Kirschner MW. 2000. Mechanism of N-WASP activation by CDC42 and phosphatidylinositol 4, 5-bisphosphate. J Cell Biol. 150(6) 1299-1310

Rohatgi R, Nollau P, Ho HY, Kirschner MW, Mayer BJ., 2001. Nck and phosphatidylinositol 4,5-bisphosphate synergistically activate actin polymerization through the N-WASP-Arp2/3 pathway. J Biol Chem 276(28)pp.26448-52

Romanov VI., Goligorsky MS., 1999. RGD-recognizing integrins mediate interactions of human prostate carcinoma cells with endothelial cells in vitro. Prostate 39(2) pp.108-18

Roy, A,K., Chatterjee,B., 1995. Androgen action. Crit Rev Eukaryot Gene Expr 5(2) pp.157-76

Rubin MA, Mucci NRm Figurski J, Fecko A, Pienta KJ, Day ML., 2001. E-cadherin expression in prostate cnacer: a broad survey using high-density tissue microarray technology. Human Pathol 32, pp.690-697

Sanchez AM, Flamini MI, Baldacci C, Goglia L, Genazzani AR, Simoncini T., 2010. Estrogen receptor-alpha promotes breast cancer cell motility and invasion via focal adhesion kinase and N-WASP. Mol Endocrinol 24(11) pp.2114-25

Scardino PT, Weaver R, Hudson MA., 1992. Early detection of prostate cancer. Hum Pathol 23(3):211-22

Schafer DA, Welch MD, Machesky LM, Bridgman PC, Meyer SM, Cooper JA. Visualization and molecular analysis of actin assembly in living cells. J Cell Biol 1998; 143(7):1919-30.

Schalken, J,A., van Leenders, G., Cellular and molecular biology of the prostate: stem cell biology Urology 62(5 Suppl 1) pp.11-20

Schmidt, A., Hall, A., 2002. Guanine nucleotide exchange factors for Rho GTPases: turning on the switch. Genes Dev 16(13) pp.1587-609

Schleutker J., 2012. Polymorphisms in androgen signaling pathway predisposing to prostate cancer. Mol Cell Endocrinol 360(1-2):25-37

Schulz WA., Burchardt M., Cronauer MV. 2003. Molecular biology of prostate cancer. Molecular human reproduction 9(8) pp.437-448

Semba S., Iawaya K., Matsubayashi J., Serizawa H., Kataba H., Hirano T., Kato H., Matsuoka T., Mukai K., 2006. Coexpression of Actin-Related Protein 2 and Wiskott-Aldrich Syndrome Family Verproline-Homologous Protein 2 in Adenocarcinoma of the lung. 12(8) pp.2449-54

Setlur, S,R., Chen, C,X., Hossain, R,R., Ha, J,S., Van Doren, V,E., Stenzel, B., Steiner, E., Oldridge, D., Kitabayashi, N., Banerjee, S., Chen, J.Y., Schäfer, G., Horninger, W., Lee, C., Rubin, M,A., Klocker, H., Demichelis, F., 2010. Genetic variation of genes involved in dihydrotestosterone metabolism and the risk of prostate cancer. Cancer Epidemiol Biomarkers Prev 19(1) pp.229-39

Shaw LC, Skold A, Wong F, Petters R, Hauswirth WW, Lewin AS., 2001. An allele-specific hammerhead ribozyme gene therapy for a porcine model of autosomal dominant retinitis pigmentosa. Mol Vis 26;7 :6-13

Shen MM, Abate-Shen C. 2010. Molecular genetics of prostate cancer: new prospects for old challenges. Genes Dev. 14(19) pp.2410-34

Shi J, Surma M, Zhang L, Wei L., 2013. Dissecting the roles of ROCK isoforms in stress-induced cell detachment. Cell Cycle 12(10) pp.1492-500

Shimizu H., Ross RK., Bernstein L.,Yatani R., Henderson BE., Mack TM.Cancers of the prostate and breast among Japanese and white immigrants in Los Angeles County. Br J Cancer 1991;63: 963–6

Sim, H, G., Cheng, C, W., 2005. Changing demography of prostate cancer in Asia. Eur J Cancer 41(6) pp.834-45

Smith JR, Freije D, Carpten JD, et al. Major susceptibility locus for prostate cancer on chromosome 1 suggested by a genome-wide search. Science 1996; 274: 1371–74.

Spigelman, S,S., McNeal, J,E., Freiha, F,S., Stamey, T,A., 1986. Rectal examination in volume determination of carcinoma of the prostate: clinical and anatomical correlations. J Urol 136(6):1228-30

Sossey-Alaoui K, Su G, Malaj E, Roe B, Cowell JK., 2002. WAVE3, an actin-polymerization gene, is truncated and inactivated as a result of a constitutional t(1;13)(q21;q12) chromosome translocation in a patient with ganglioneuroblastoma. Oncogene 21(38):5967-74

Sossey-Alaoui K., Li X., Ranalli TA., Cowell JK., 2005. WAVE3-mediated cell migration and lamellipodia formation are regulated downstream of phosphatidylinositol 3-kinase. J Biol Chem 280(23) pp.21748-55

Sossey-Alaoui K, Ranalli TA, Li X, Bakin AV, Cowell JK., 2005. WAVE3 promotes cell motility and invasion through the regulation of MMP-1, MMP-3, and MMP-9 expression. Exp Cell Res 308(1) pp.135-45

Sossey-Alaoui K., Li X., Cowell JK., 2007. c-Abl-mediated phosphorylation of WAVE3 is required or lamellipodia formation and cell migration. J Biol Chem 282(36) pp.26257-65

Sossey-Alaoui K., Safina A., Li Xiurong., Vaughan MM., Hicks DG., Bakin AV., Cowell JK., 2007. Down-regulation of WAVE3, a Metastasis Promoter Gene, Inhibits Invasion and Metastasis of Breast Cancer Cells. Am J Pathol 170(6) pp.2112-21

Soto MC, Qadota H, Kasuya K, Inoue M, Tsuboi D, Mello CC, Kaibuchi K., 2002. The GEX-2 and GEX-3 proteins are required for tissue morphogenesis and cell migrations in C.elegans. Genes Dev 16(5) pp.620-32

Steffen A., Rottner K., Ehinger J., Innocenti M., Scita G., Wehland J., Stradal TE., 2004. Sra-1 and Nap1 link Rac to actin assembly driving lamellipodia formation. EMBO J 23(4) pp.749-59

Stricker, H, J., 2001. Luteinizing hormone-releasing hormone antagonists in prostate cancer. Urology. 58(2 Suppl 1) pp.24-7

Suetsugu, S., Miki, H., Takenawa, T., 1999. Identification of two human WAVE/SCAR homologues as general actin regulatory molecules which associate with the Arp2/3 complex. Biochem Biophys Res Commun 260(1) pp.296-302

Suetsugu S, Hattori M, Miki H, Tezuka T, Yamamoto T, Mikoshiba K, Takenawa T., 2002. Sustained activation of N-WASP through phosphorylation is essential for neurite extension. Dev Cell 3(5) pp.645-58

Suetsugu S, Kurisu S, Oikawa T, Yamazaki D, Oda A, Takenawa T, 2006. Optimization of WAVE2 complex-induced actin polymerization by membrane-bound IRSp53, PIP(3), and Rac. J Cell Biol 173(4) pp.571-85

Sullivan KE, Mullen CA, Blaese RM, Winkelstein JA., 1994. A multiinstitutional survey of the Wiskott-Aldrich syndrome. J Pediatr 125(6 Pt 1) pp.876-85

Sumi T, Matsumoto K, Nakamura T., 2001. Specific activation of LIM kinase 2 via phosphorylation of threonine 505 by ROCK, a Rho-dependent protein kinase. J Biol Chem 276(1)pp.670-6

Sun YX., Wang J., Shelburne CS., Lopatin DE., Chinnaiyan AM., Rubin MA., Pienta KJ., Taichman RS., 2003. Expression of CXCR4 and CXCL12 (SDF-1) in human prostate cancers (PCa) in vivo. J Cell Biochem 89(3) pp.462-73

Tabatabaei S[1], Saylor PJ, Coen J, Dahl DM, 2011. Prostate cancer imaging: what surgeons, radiation oncologists, and medical oncologists want to know. AJR Am J Roentgenol 196(6):1263-6

Taichman RS., Cooper C., Keller ET., Pienta KJ., Taichman NS., McCauley LK., 2002. Use of the stromal cell-derived factor-1/CXCR4 pathway in prostate cancer metastasis to bone. Cancer Res 62(6) 1832-7

Tang H, Li A, Bi J, Veltman DM, Zech T, Spence HJ, Yu X, Timpson P, Insall RH, Frame MC, Machesky LM., 2013.
Loss of Scar/WAVE complex promotes N-WASP- and FAK-dependent invasion. Curr Biol 23(2)pp:107-17

Teng Y., Ren MQ., Cheney R., Sharma S., Cowell JK., 2010. Inactivation of the WASF3 gene in prostate cancer cells leads to suppression of tumorigenicity and metastases. Br J Cancer 103(7) pp.1066-75

Thrasher, A.J. 2009. New insights into the biology of Wiskott-Aldrich syndrome (WAS). American Society of Hemotology pp. 132-138

Tokuda Y., Satoh Y., Fujiyama C/. Toda S., Sugihara H., Masaki Z., 2003. Prostate cancer cell growth is modulated by adipocyte-cancer cell interaction. BJU Int 91(7) pp.716-20

Tominaga S. Cancer incidence inJapanese in Japan, Hawaii, and western United States. Natl Cancer Inst Monogr1985; 69: 83–92

Torres R., Rosen MK., 2006. Protein-tyrosine kinase and GTPase signals cooperate to phosphorylate and activate Wiskott-Aldrich syndrome protein (WASP)/neuronal WASP. J Biol Chem 281(6) pp.3513-20

Trikha M., Raso E., Cai Y., Fazakas Z., Porter AT., Timar J., Honn KV., 1998. Role of αIIbβ3 integrin in prostate cancer metastasis. Prostate 35(3) pp.185-92

Turkbey B[1], Mena E, Aras O, Garvey B, Grant K, Choyke PL., 2013. Functional and molecular imaging: applications for diagnosis and staging of localised prostate cancer. Clin Oncol (R Coll Radiol) 25(8):451-60

Umbras R., Schalken JA., Aalders TW., Carter BS., Karthaus HF., Schaafasma HE., Debruyne FM., Isaacs WB., 1992. Expression of the cellular adhesion molecule E-cadherin is reduced or absent in high-grade prostate cancer. Cancer Res 52(18) pp.5104-9

van Hengel J, D'Hooge P, Hooghe B, Wu X, Libbrecht L, De Vos R, Quondamatteo F, Klempt M, Brakebusch C, van Roy F. Continuous cell injury promotes hepatic tumorigenesis in cdc42-deficient mouse liver. Gastroenterology 134(3) pp.781-92

van Zijl, F., Krupitza, G., Mikulits, W., 2011. Initial steps of metastasis: cell invasion and endothelial transmigration. Mutat Res 728(1-2) pp.23-34

Vega FM., Ridley AJ., 2008. Rho GTPases in cancer cell biology. FEBS Lett 582(14) pp.2093-101

Venkateswaran, V., Klotz, L, H., 2010. Diet and prostate cancer: mechanisms of action and implications for chemoprevention. Nat Rev Urol 7(8) pp.442-53

Vishnubhotla R, Sun S, Huq J, Bulic M, Ramesh A, Guzman G, Cho M, Glover SC., 2007. ROCK-II mediates colon cancer invasion via regulation of MMP-2 and MMP-13 at the site of invadopodia as revealed by multiphoton imaging. Lab Invest 87(11) pp.1149-58

Vishnubhotla R, Bharadwaj S, Sun S, Metlushko V, Glover SC., 2012. Treatment with Y-27632, a ROCK Inhibitor, Increases the Proinvasive Nature of SW620 Cells on 3D Collagen Type 1 Matrix. Int J Cell Biol 2012 Article ID 259142, 7 pages

Voura EB., Ramjeesingh RA., Montgomery AM., Siu CH. 2001. Involvement of integrin $\alpha_v\beta_3$ and cell adhesion molecule L1 in transendothelial migration of melanoma cells. Mol Biol Cell 12(9) pp.2699-710

Wallace TA, Prueitt RL, Yi M, Howe TM, Gillespie JW, Yfantis HG, Stephens RM, Caporaso NE, Loffredo CA, Ambs S., 2008. Tumor immunobiological

differences in prostate cancer between African-American and European-American men. Cancer Res 68(3):927-36

Wang W, Wyckoff JB, Goswami S, Wang Y, Sidani M, Segall JE, Condeelis JS., 2007. Coordinated regulation of pathways for enhanced cell motility and chemotaxis is conserved in rat and mouse mammary tumors. Cancer Res 67(8) pp:3505-11

Walsh, P,C., Lepor, H., Eggleston, J,C., 1983. Radical prostatectomy with preservation of sexual function: anatomical and pathological considerations. Prostate 4(5) pp.473-85

Webber MM., Waghray A., Bello D., 1995. Prostate-specific antigen, a serine protease, faciliatates human prostate cancer cell invasion. Clin Cancer Res 1(10) pp.108-94

Welch MD., DePace AH., Verma S., Iwanatsu A., Mitchison TJ., 1997. The human Arp2/3 complex is composed of evolutionarily conserved subunits and is localized to cellular regions of dynamic actin filament assembly. J Cell Biol 138(2) pp.375-84

Welch MD., 1999. The world according to Arp: regulation of actin nucleation by the Arp2/3 complex. Trends Cell Biol 9(11):423-7

Wheeler AP, Wells CM, Smith SD, Vega FM, Henderson RB, Tybulewicz VL, Ridley AJ., 2006. Rac1 and Rac2 regulate macrophage morphology but are not essential for migration. J Cell Sci 119(Pt 13)pp.2749-57

Whittemore AS, Wu AH, Kolonel LN, et al. Family history andprostate cancer risk in black, white, and Asian men in the UnitedStates and Canada. Am J Epidemiol 1995; 141: 732–40.

Wu X, Suetsugu S, Cooper LA, Takenawa T, Guan JL., 2004. Focal adhesion kinase regulation of N-WASP subcellular localization and function. J Biol Chem 279(10) pp.9565-76

Yamaguchi H., Miki H., Suetsugu S., Ma L., Kirschner MW., Takenawa T., 2000. Two tandem verprolin homology domains are necessary for a strong activation of Arp2/3 complex-induced actin polymerization and induction of microspike formation by N-WASP. Proc Natl Acad Sci USA 97(23) pp.12631-6

Yang LY., Tao YM., Ou DP., Wang W., Chang ZG., Wu F., 2006. Increased expression of Wiskott-Aldrich Syndrome protein family verprolin-homologous protein 2 correlated with poor prognosis of hepatocellular carcinoma. Clin Cancer Res 12(19) pp. 5673-79

Yokotsuka M, Iwaya K, Saito T, Pandiella A, Tsuboi R, Kohno N, Matsubara O, Mukai K., 2011. Overexpression of HER2 signaling to WAVE2-Arp2/3 complex activates MMP-independent migration in breast cancer. Breast Cancer Res Treat 126(2):311-8

Zhang Y., Guan XY.,Dong B., Zhao M., Wu JH., Tian XY., Hao CY., 2012. Expression of MMP-9 and WAVE3 in colorectal cancer and its relationship to clinicopathological features. J Cancer Res Clin Oncol 138(12) pp.2035-44

Zohrabian VM, Forzani B, Chau Z, Murali R, Jhanwar-Uniyal M., 2009. Rho/ROCK and MAPK signaling pathways are involved in glioblastoma cell migration and proliferation. Anticancer Res 29(1):119-23

Zolfaghari, A., Djakiew, D., 1996. Inhibition of chemomigration of a human prostatic carcinoma cell (TSU-pr1) line by inhibition of epidermal growth factor receptor function. Prostate 28(4):232-8

Zong, H., Kaibuchi, K., Quilliam, L,A., 2001. The insert region of RhoA is essential for Rho kinase activation and cellular transformation. Mol Cell Biol. 21(16) pp.5287-98

Electronic resources:

www.cancerresearchuk.org

www.genecards.org

www.nice.org.uk

www.uniprot.org

www,phosphosite.org